CHALMERS
UNIVERSITY OF TECHNOLOGY

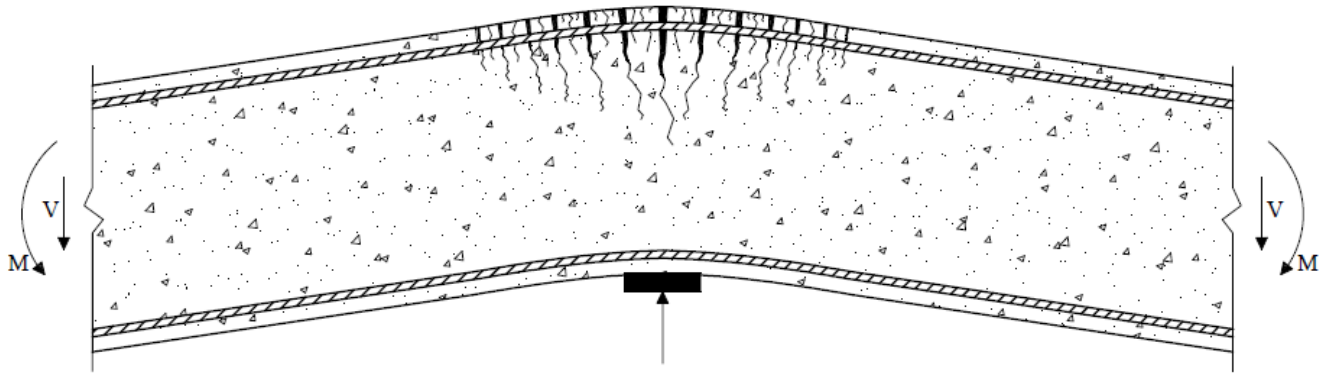

Residual load carrying capacity of overloaded reinforced concrete structures

Master's Thesis in the Master's Programme Structural Engineering and Building Technology

LINDA CEDERHOLM
EMELIE HALLERSTIG

Department of Civil and Environmental Engineering
Division of Structural Engineering
Concrete structures
CHALMERS UNIVERSITY OF TECHNOLOGY
Gothenburg, Sweden 2016
Master's Thesis BOMX02-16-32

MASTER'S THESIS BOMX02-16-32

Residual load carrying capacity of overloaded reinforced concrete structures

Master's Thesis in the Master's Programme Structural Engineering and Building Technology

LINDA CEDERHOLM

EMELIE HALLERSTIG

Department of Civil and Environmental Engineering
Division of Structural Engineering
Concrete structures
CHALMERS UNIVERSITY OF TECHNOLOGY
Göteborg, Sweden 2016

Residual load carrying capacity of overloaded reinforced concrete structures
Master's Thesis in the Master's Programme Structural Engineering and Building Technology

LINDA CEDERHOLM

EMELIE HALLERSTIG

Examensarbete BOMX02-16-32/ Institutionen för bygg- och miljöteknik,
Chalmers tekniska högskola 2016

Department of Civil and Environmental Engineering
Division of Structural Engineering
Concrete structures
Chalmers University of Technology
SE-412 96 Göteborg
Sweden
Telephone: + 46 (0)31-772 1000

Cover:
The cover picture presents cracking and formation of a plastic region over the middle support in a continuous beam.
Department of Civil and Environmental Engineering, Göteborg, Sweden, 2016

Residual load carrying capacity of overloaded reinforced concrete structures

Master's thesis in the Master's Programme Structural Engineering and Building Technology

LINDA CEDERHOLM
EMELIE HALLERSTIG
Department of Civil and Environmental Engineering
Division of Structural Engineering
Concrete structures
Chalmers University of Technology

ABSTRACT

The purpose of old building structures may change during their service life and as a consequence they need to be examined, changed and repaired. It also happened that existing structures have been damaged in the past by overloading or by high loads in combination with mistakes in execution or handling of the building. This results in a need to determine the current state of this structure and its remaining capacity. Symptoms that indicate a damaged structure are wide cracks and large deflections. The main purpose of this study was to examine whether these symptoms can be used in estimation of a past overloading and to assess the residual load carrying capacity. Moreover, a deeper understanding of the structural response during the process of overloading and unloading was aimed at.

As a basis for this study a two-span continuous beam subjected to a uniformly distributed and fixed load was selected. A general literature survey on forensic engineering and structural assessment was conducted. Moreover, an analytical analysis was carried out, which was divided into two parts. In Part 1 the response of the beam with regard to maximum deflection, moment distribution and plastic rotation was analysed for certain predefined load levels. Part 2 explained how a measured on site deflection may be used to estimate the magnitude of overloading. FE analysis was also conducted with the same beam properties and same loads that were used in Part 1 in the analytical analysis. Software TNO DIANA 9.6 was used for the numerical analysis and the program Mathcad for the analytical investigation.

The analyses of the studied beam showed that the plastic rotation over the middle support remained when the beam was subjected to a process of overloading and unloading. Also, a restraint moment appeared over the middle support while the beam was unloaded, which resulted in a change of moment distribution along the beam. When the beam again was loaded up to the same magnitude of overloading, the deflection was no longer limited by the plastic hinge developed over the middle support and the restraint moment disappeared. Thus, for the studied example the remaining capacity of the beam was not influenced by a temporary overloading that caused yielding of reinforcement in the middle support as long as load case was the same during the entire procedure. The investigation also resulted in a procedure for how a past overloading and the residual load carrying capacity can be estimated using measurements of the deflected shape of a beam.

Key words: Reinforced concrete, forensic engineering, structural assessment, overloading, deflection, crack width, plastic rotation, restraint moment

Resterande bärförmåga av överbelastade armerade betongkonstruktioner

Examensarbete inom masterprogrammet Structural Engineering and Building Technology

LINDA CEDERHOLM
EMELIE HALLERSTIG
Institutionen för bygg- och miljöteknik
Avdelningen för Konstruktionsteknik
Betongbyggnad
Chalmers tekniska högskola

SAMMANFATTNING

Ändamålet med gamla befintliga byggnader kan ändras med tiden och som en konsekvens av detta kan de behöva undersökas, förbättras och repareras. Det kan även hända att befintliga konstruktioner har blivit skadade på grund av överbelastning eller höga laster i kombination med misstag i samband med utförandet eller handhavandet av byggnaden. Detta resulterar i ett behov av att bedöma det aktuella skicket av konstruktionen och att fastställa den kvarvarande bärförmågan. Vida sprickor och stora nedböjningar kan vara tecken på att en konstruktion blivit överbelastad. Huvudsyftet med denna studie var att undersöka om det är möjligt att utifrån sådana kännetecken uppskatta en tidigare överbelastning och därefter utvärdera den kvarvarade bärförmågan. Därutöver var strävan att utveckla en mer djupgående förståelse för betongkonstruktioners verkningssätt vid på- och avlastning.

Undersökningen baserades på ett exempel i form av en fritt upplagd kontinuerlig balk på tre stöd med en jämnt utbredd och bunden last. En litteraturstudie gällande skadeutredning och tillståndsbestämning utfördes. Därefter utfördes en analytisk studie som delades upp i två delar. I del 1 analyserades betongbalken för förutbestämda belastningssteg och med hänsyn till maximal nedböjning, momentfördelning och plastisk rotation. I del 2 undersöktes hur man kan uppskatta storleken på en överbelastning utifrån uppmätt nedböjning hos en skadad betongbalk. En finit element analys utfördes på samma exempel som i den analytiska studien. Programmet TNO DIANA 9.6 användes för den numeriska analysen och programmet Mathcad användes för den analytiska undersökningen.

Analyserna på den studerade balken visade att den plastiska rotationen som uppkommer över mittstödet kvarstår när balken utsätts för ett förlopp med överbelastning och avlastning. Dessutom uppkommer ett tvångsmoment då balken avlastas, vilket resulterar i en förändring av momentfördelningen längs balken. När balken återigen belastas med samma last som den tidigare överbelastningen är nedböjningen inte längre påverkad av flytledens rotation och därmed försvinner tvångsmomentet. För det studerade exemplet påverkas inte balkens bärförmåga av en tillfällig överbelastning så länge som lastfördelningen var densamma. Inom projektet utarbetades även en metodik för hur en överbelastning och kvarvarande bärförmåga kan fastställas utifrån uppmätt nedböjning hos en befintlig konstruktion.

Nyckelord: Armerad betong, skadeutredning, tillståndsbestämning, överbelastning, nedböjning, sprickor, plastisk rotation, tvångsmoment

Contents

APPENDICES

Preface

In this work, the residual load carrying capacity of overloaded reinforced concrete structures was studied. A two-span continuous beam with uniformly fixed distributed load was analysed using literature survey, non-linear analytical and non-linear numerical analysis. The project was initiated and carried out at Norconsult AB in Gothenburg, Sweden from January to June 2016.

First of all, we would like to thank our supervisor Erik Skansebo, Norconsult AB for his support, advices and enthusiasm during our work. We would also like to thank the structural engineering team at Norconsult AB for a pleasant working atmosphere.

The thesis was in its essential part carried out in collaboration with the teachers from the Division of Structural Engineering at Chalmers University of Technology in Gothenburg, Sweden. We would like to thank Mario Plos for his advices and help in the initial parts of this work. Furthermore, we would like to express our special appreciation to our examiner Björn Engström, for his essential impact on this work, valuable discussions and comments. We also want to show our gratitude to Ignasi Fernandez Perez for his patience and great help with finite element modelling.

Göteborg, June 2016

Linda Cederholm & Emelie Hallerstig

Notations

Roman upper case letters

A_c	Area of gross concrete section
A_s	Sectional steel area
E_c	Modulus of elasticity of concrete
E_s	Modulus of elasticity of steel
EI_I	Flexural rigidity in state I
$EI_{II.sup}$	Stiffness of support section in state II
"EI_{sup}"	Stiffness of support section in state III
"EI_{span}"	Stiffness of span section in state III
$F_{c\,III}$	Resultant concrete force in state III
$F_{s,I}$	Resultant steel force in state I
$F_{s,II}$	Resultant steel force in state II
$F_{s\,III}$	Resultant steel force in state III
I_c	Moment of inertia for the gross concrete section
I_{II}	Moment of inertia of a cross section in state II
$I_{II.sup}$	Moment of inertia in state II for support section
$I_{II.span}$	Moment of inertia in state II for span section
M	Bending moment in cross section
$M_{1.x}$	Moment in section x in Phase 1
$M_{1.span}$	Maximum moment in span in Phase 1
$M_{1.sup}$	Moment in support B in Phase 1
$M_{2.x}$	Moment in section x in Phase 2
$M_{3.x}$	Moment in section x in Phase 3
$M_{3.span}$	Moment in span in Phase 3
$M_{3.sup}$	Moment in support B in Phase 3
$M_{4.x}$	Moment in section x in Phase 4
$M_{5.x}$	Moment in section x in Phase 5
M_{cr}	Cracking moment of cross section
$M_{R,B}$	Maximum moment capacity in support B
$M_{restraintsup}$	Restraint moment at support B
$M_{restraintspan}$	Restraint moment at span section
$M_{y.sup}$	Yielding moment of support section
$M_{u.sup}$	Ultimate moment of support section
$M_{u.span}$	Ultimate moment of span section

Roman lower case letters

b	Width of cross-section
d	Effective depth of cross-section
f	Deflection
$f_{1.span}$	Deflection in section x in Phase 1
$f_{2.span}$	Deflection in section x in Phase 2
$f_{3.span}$	Deflection in section x in Phase 3
$f_{4.span}$	Deflection in section x in Phase 4
$f_{5.span}$	Deflection in section x in Phase 5
f_c	Concrete compressive strength
f_{cm}	Mean concrete compressive strength
f_{ctm}	Mean concrete tensile strength
$f_{element}$	Deflection of one element in the beam model
f_{site}	Maximum deflection measured on site
f_y	Yield strength of steel
f_{yk}	Characteristic tensile strength of steel
h	Height of cross-section
$l_{element}$	Element length in the beam model
l_{pl}	Extension of a plastic region
k_λ	Modification factor for rotation capacity
q	Load
q_1	Load in Phase 1
q_2	Load in Phase 2
$q_{y.sup}$	Load that creates yielding of the support section
q_{ult}	Load that creates failure of a section
r	Radius of curvature
z	Sectional coordinate defined relative to the sectional centroid
x	Height of compressive zone
x_f	Distance from support A to the section with maximum deflection
x_{span}	Distance from support A to the section with maximum moment in span
x_y	Height of compressive zone when section starts to yield
x_u	Height of compressive zone when section fails
x_0	Distance from support A to the section with zero moment in the span after plastic redistribution
x_1	Coordinate along the beam to section where the plastic region starts
x_2	Coordinate along the beam to section where the plastic region ends

Greek lower case letters

α_s	Modular ratio in transformed concrete section
α_R	Stress block factor for stress block resultant
β_R	Stress block factor for location of stress block resultant
ε_c	Concrete strain
ε_{ctu}	Ultimate concrete tensile strain
ε_{cu}	Ultimate concrete compressive strain
ε_s	Steel strain
$\varepsilon_{cc.y.sup}$	Maximum concrete compressive strain in support section when yielding starts
ε_{suk}	Characteristic value of limit strain of steel
ε_y	Steel strain when yielding starts
ρ_c	Concrete density
θ_A	Rotation at support A
$\theta_{1.A}$	Rotation at support A in Phase 1
$\theta_{2.A}$	Rotation at support A in Phase 2
$\theta_{2.sup.left}$	Plastic rotation over the middle support B on its left side in Phase 2
$\theta_{3.A}$	Rotation at support A in Phase 3
$\theta_{3.sup.left}$	Plastic rotation over the middle support B on its left side in Phase 3
$\theta_{4.sup.left}$	Plastic rotation over the middle support B on its left side in Phase 4
$\theta_{5.A}$	Rotation at support A in Phase 5
$\theta_{5.sup.left}$	Plastic rotation over the middle support B on its left side in Phase 5
θ_{el}	Apparent rotation in the FE-model
θ_f	Plastic rotation of section in span
θ_s	Plastic rotation of section in support
θ_{pl}	Plastic rotation
$\theta_{pl,d}$	Design value of plastic rotation capacity
$\theta_{pl,d,f}$	Design value of plastic rotation capacity according to Figure 3.18
λ	Shear slenderness
ν	Poisson's ratio
$\sigma_{c.I}$	Stress of concrete in state I
$\sigma_{c.II}$	Stress of concrete in state II
$\sigma_{s.I}$	Stress of steel in state I
$\sigma_{s,II}$	Stress of steel in state II

Greek upper case letters

κ	Curvature
κ_1	Curvature in section x in Phase 1
$\kappa_{1,sup}$	Curvature for support section in cracked state in Phase 1
κ_2	Curvature in section x in Phase 2
$\kappa_{2.sup}$	Curvature for support section in Phase 2
κ_3	Curvature in section x in Phase 3
$\kappa_{3.sup}$	Curvature for support section in Phase 3
κ_4	Curvature in section x in Phase 4
$\kappa_{4.sup}$	Curvature for support section in Phase 4
κ_5	Curvature in section x in Phase 5
$\kappa_{5.sup}$	Curvature for support section in Phase 5
κ_{el}	Curvature of section before yielding is reached
κ_y	Curvature of section when yielding starts
$\kappa_{y.sup}$	Curvature of support section when yielding starts
κ_u	Curvature of section when it fails

1 Introduction

In this chapter the background of this research project is presented together with aim and objectives of the study and its limitations. The used research methods are presented and motivated. Finally, the outline of the report is explained.

1.1 Background

For many existing building structures there is a need to change the purpose of the building during the service life and the load carrying capacity can vary. Nowadays, many buildings are being rebuilt to provide other functions than originally designed for. However, the knowledge about the former usage is often incomplete, often due to insufficient documentation of the previous design and utilization, usage and handling. It also happens that building structures have been damaged in the past due to overloading or high loads in combination with mistakes in execution or handling. This may lead to uncertainties about the future use of the building and its residual load carrying capacity. Then the structure can be prevented to be reused for other purposes in the future.

One such case was recently encountered by Norconsult AB. A project concerning new loads on an existing column supported flat slab was to be carried out. However, during an inspection of the worksite a large amount of wide cracks was found, mainly around columns in the top of the slab. Such cracks are natural, however such wide cracks were unexpected.

Such observations in existing structures question the ability to expose the structure to specified loads in the future. The main issue is how to assess the cause of the observed damage in terms of past overloading? If so, how to estimate the remaining load carrying capacity? Can the observed orientation, localization and width of cracks give answer concerning the questionable remaining performance?

1.2 Aim and objectives

The aim of this study was to develop a methodology for how the influence of past overloading can be evaluated and how this can be taken into account when assessing the remaining load carrying capacity, structural performance and remaining service life.

To fulfil this aim a number of objectives was specified:

- Define how to consider previous overloading in the structural assessment,
- Identify what indicators can be used to verify that a structure has been overloaded in the past,
- Explain how temporary overloading and changes in structural response due to yielding and redistribution of moments will affect the remaining load carrying capacity.

1.3 Method

First of all, to be able to reach the aim and objectives, a literature survey was conducted. This covered study on assessment of existing reinforced concrete structures and study of the scientific field of forensic engineering. Also, problems related to cracking of reinforced concrete structures were analysed. Furthermore, a brief study was carried out on the typical structural response of reinforced concrete

beams under load increase. Specifically, the study focused on non-linear behaviour and development of plastic rotations. The study was also in its essential part based on discussions with supervisors and teachers at Chalmers University of Technology.

On the basis of the literature study and the discussions, an analytical non-linear analysis using beam theory was conducted. A two-span continuous beam was analysed to understand the structural behaviour of a simple type of structure when overloaded by a uniformly distributed load. The analysis was carried out in two parts. The purpose of Part 1 was to investigate the response of the beam when subjected to predefined load levels including overloading, unloading and loading to failure. Part 2 focused on the methodology of how to determine the magnitude of past overloading on the basis of observed damage.

An additional non-linear numerical analysis was conducted using finite element modelling and the software DIANA TNO. The non-linear analysis was checked by the analytical analysis to verify the validity of the model and also used as a comparison. It covered overloading of a two-span continuous beam and unloading back to normal service load, and then second overloading up to failure. Additionally, an analysis of a reference beam without overloading was conducted to compare the responses and capacities of beams with and without a past overloading.

The methodology used in this work was in its essential part based on discussions with supervisors and teachers at Chalmers University of Technology.

1.4 Limitations

This work contains a number of limitations. First of all, a simplification was introduced concerning time dependent effects. The long term effects were generally ignored in this work and considered only in Part 2 of the analytical analysis and then only to some extent.

Moreover, the tension stiffening effect was neglected in the analytical analysis due to its small effect on the results.

The residual load carrying capacity of overloaded concrete structures was analysed only in terms of bending moments acting on the structure and its sectional moment capacities. Shear forces, shear failures and anchorage failures were not considered in this work.

Furthermore, the proposed methodology for assessment of damaged structures is developed on the basis of discussions and literature survey. Neither real experiments of loaded beam, nor on-site measurements were carried out in this work.

Finally, the residual load carrying capacity was only checked in case of one-way action of two-span continuous beams with equal spans. Two-way action of a slab was not studied. Also, only the response under uniformly distributed, fixed load was studied in this work. No loads free in space, concentrated loads or dynamic loads were taken into account.

1.5 Outline

Chapter 2 contains general information about investigation of old and overloaded concrete structures, forensic engineering and structural assessment approach. Also, indicators which show that a structure was overloaded in the past are presented and the problem of cracking in reinforced concrete structures is explained.

In Chapter 3 the material and structural responses of a reinforced concrete beam are explained related to its uncracked, cracked and ultimate stages. Also the response of the beam in its plastic state is described.

In Chapter 4 the analytical analysis is presented, which also helps to understand the structural response of a beam under overloading. The method as well as the result from both Part 1 and Part 2 are presented and explained. Detailed calculations are presented in Appendix A and B.

Chapter 5 covers the FE modelling in the software DIANA TNO. The modelling choices are presented and the results described.

Chapter 6 contains an evaluation of the results gathered from the analytical and numerical analyses, as well as relevant information from the literature study. A discussion and explanation of the result can be found here.

In Chapter 7 the project is concluded and topics for further investigaton are suggested.

2 Evaluation of concrete structures

2.1 Introduction

Reinforced concrete is widely used as a structural material due to its long lifespan, although as all building materials it also has limited design service life. Once a reinforced concrete structure is approaching the end of its design service life, a decision has to be made whether the building should be demolished and replaced or rather repaired and strengthened. Due to rising importance of sustainability in built society, repair costs and increasing focus on waste recycling, it is preferable to bring structures back to their original performance (Urs et al. 2015).

Often refurbishment of existing buildings is not due to deterioration of the structure, but also other aspects, coming from economic reasons or a need of changing buildings function. It has been shown by a research in Oulu, Finland that only 17% of all the repairs that were done within one year, were generated by damage due to drastic change in buildings condition while many others due to change in the use of the building. Thus it may be concluded, that the design service life of a building is a period under which no unexpected changes in the building's condition should happen (Aikivuori et al. 1999).

Changes of a structure function may lead to changes in applied loads. It is essential then to determine whether the building can resist the new design loads and to estimate the remaining service life of the whole structure. Such assessment of residual service life includes investigation of current structure condition, which may be performed by non-destructive and destructive methods. Often, the very first determination of buildings condition relies on visual inspection (Urs et al. 2015).While noticing cracks at the face of structural components, rust stains, spalling or excessive deflection is quite easy, it is still very important but difficult to find reasons for their occurrence. Service life may be reduced by many various circumstances: mistakes in the design, errors in execution or by overloading the structure (Holický et al. 2013), (Banville 2008).

In order to find out what has caused any damage to a structure it is valuable to conduct a document survey. Specifications, plans, photographs, other structural documentation and even interviews may provide information about a building's history, sometimes very essential in finding the cause of the problem (Banville 2008).

2.2 Forensic engineering

A scientific field that is becoming more common in analysing possible reasons of damage is forensic engineering. It is an engineering methodology applied in case of damages in order to determine and interpret its probable reasons. While using this methodology, structures with insufficient functions are investigated using engineering expertise and knowledge in jurisprudence. To assess the cause and extent of the damage a forensic engineer studies the structure from an engineering perspective. However, to determine who is responsible for the damage, an understanding of business and practice is also needed. Since most structural deficiencies create disagreements and legal disputes, questions regarding what, where, when, how, why and who must be answered in order to state a correct cause or causes of the failure (Nguee 2006).

There are guidelines based on scientific principles for forensic investigations, but this is a relatively new discipline and in many cases an unfamiliar subject. Therefore the various recommendations may have conflicting requirements. In essence, the aim of the inspection is to;

- Assess the condition of the existing structure from before the damage was discovered,
- Assess what have happened in the structure after the damaged already occurred,
- Determine how consequences of the damage will affect the future,
- Search for proofs that either support or deny the hypotheses of causes,
- Apply engineering knowledge to relate the proofs into a reasonable scenario for the structure.

To determine the coherence of the steps listed above, technical skills and knowledge of legal procedures must be combined with logical thinking and ethical standards (Noon 2001).

Survey of older building structures can reveal unexpected problems which can cause complications. Also, reuse of existing structures and change in design criteria due to better knowledge of structural behaviour can make the structure insufficient (Campbell 2001). If damage occurs in these kinds of structures a forensic engineering investigation is required for insurance companies and owners. The investigation is also essential for the companies involved in the project in order to find out who is responsible and needs to pay for the structural problem. The magnitude of the deficiency decides how expansive the investigation will be, for instance when a building collapses litigation is needed, but for less catastrophic consequences it may be enough to state a cause and prescribe a remedy (Nguee 2006).

Forensic engineering is similar to root cause analysis and failure analysis, although these definitions divides the investigation into different parts. Failure analysis estimates how a specific structural component has failed, regarding material, design, production method and product usage. In a root cause analysis the system failure is investigated. This suggests how the procedure and managerial techniques were carried out in order to ensure that the damage do not reoccur in another construction project (Noon 2001).

A case when forensic engineering should have been used is the collapse of the Tacoma Narrows Bridge. This is an extreme case where the bridge swung and twisted under a speed of 40 miles/hour until it eventually collapsed. If the extensive resonance phenomenon and concrete cracking have been discovered earlier forensic investigation could have been carried out. The cause of the problem could then be estimated and repairing work could have prevented the bridge collapse. Instead the consequence was a large amount of cost and nearly death of humans (Greenberg 2015). A structural assessment could have been made in order to check adequacy for future use regarding structural stability, load-carrying capacity, serviceability, etc. of the existing bridge. The process of structural assessment of an existing structure is different compared with assessing a new building, something that needs to be considered during an inspection (Stuart 2012).

2.3 Structural assessment

2.3.1 Principle

Aging structures require systematic assessment in order to ensure their safety. However, despite the access to new structural design codes, an assessment of existing structures may not be conducted using these design requirements, considering the uncertainties of these two approaches. While using conditions for new structures to be built, the design is based on conservative assumptions, so that the results take into consideration material variations and the diversity of structures. Such approach in structural assessment might result in unnecessary refurbishment costs (Rücker et al. 2006).

Generally, structural assessment may be described as a process of reliability determination in consideration with current and future loads and a given time period. It may be initiated where there is a suspicion of insufficient resistance and structural performance or change of structure's function which result in a different load effects than originally assumed (Rücker et al. 2006).

Two main objectives in structural assessment can be distinguished, which are;

- It is only acceptable to use current valid design codes while assessing structural reliability, codes which were used during the design and construction process of the analysed structure may only be used as a guidance documents,
- Present data (materials characteristics, geometry, actions, structural behaviour) should be used in the assessment while previous documentation including drawings may be used as a guide (Holický et al. 2013).

Initially, condition appraisal should be used in load and capacity assessment. It provides information about defects that have occurred in the structure, possible reasons of the detected damages, their influence on performance of the structure and its remaining service life. It can be divided into two main steps: inspection and evaluation of conditions. The inspection should be conducted regularly and it should be carried out on various levels, from basic inspection when the structure is watched from the ground, through inspection where accessible parts of the structure are investigated to general inspection in presence of a structural engineer (Sustainable Bridges 2007a).

Simple assessment of a structure, which is based on studying previous calculations in consideration with regard to its load-carrying capacity, may sometimes not give a clear answer about the structure's condition. Then a more detailed assessment is to be conducted. The typical procedure of a detailed assessment is presented in Figure 2.1.

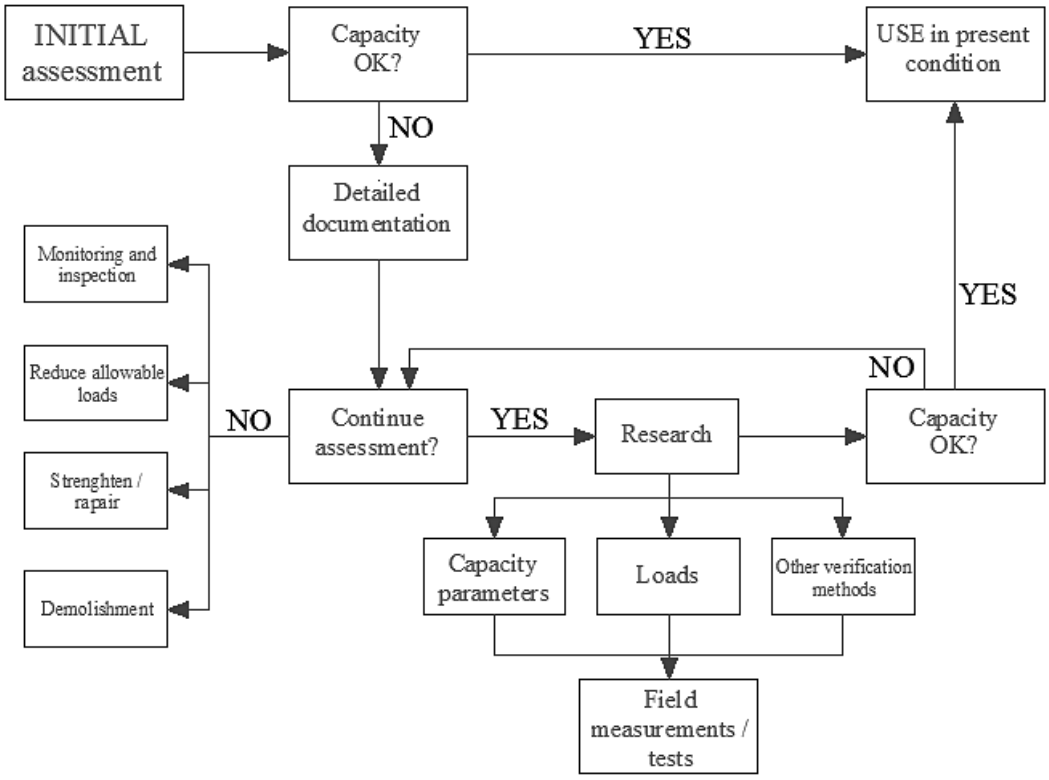

Figure 2.1 The typical procedure of structural assessment (Plos et al. 2004).

Valuable information may provide a special type of structural investigation named proof loading. Depending on which limit state is investigated, there exist different types of this test. In case of serviceability, proof load is applied and then verification is made whether the limit has been excited. In ultimate state the fact that the structure does not fail under applied loading is the verification, concerning the ultimate limit state (Rücker et al. 2006). Having a structural member proof loaded, load-bearing capacity, the performance of the structure or other load conditions may be concluded (Holický et al. 2013).

2.3.2 Damage detection

Many of the damages in structures can be avoided but if they occur, the cause is often not related to insufficient knowledge but rather lack of its application or wrong application. A defect may generally be described as an event that is not within acceptable standards. It could be assumed that nowadays many damages and their causes are well known and that there should be less building failures than in the past. However, that is not the case. Unfortunately, concerning cost reduction, need for innovation and lack of communication damages to buildings still occur (Douglas et al. 2007).

Often, it is not easy to determine cause of damage. It may happen that the access to a building's component is limited and that it is not possible to fully investigate the cause of the defect. Also, lack of information and knowledge about the structure's history may make the estimation of possible damage even more difficult. Drawings and specifications may be missing and the material suppliers are often unwilling to provide detailed information about the materials used. However, it is still important to study building's history and take into consideration pattern of the damage which may lead to its correct diagnosis, (Douglas et al. 2007).

If damage to the structure is detected through investigation, the evaluation of each type of damage should be conducted in consideration of;

- Defect type and what effect it has on safety and durability of the structural member,
- Effect of the damaged structural component on the whole structure with regard to safety and durability,
- Intensity of the defects,
- Area of damage occurrence and predicable propagation of the damage, (Sustainable Bridges 2007a).

The evaluation of damage may firstly be performed by simply using human senses. Discoloration, unnatural smell, unusual sound while e.g. using a hammer on the surface, roughness of surface or bitter taste, these are examples of possible signs of damage that can be discovered using human senses (Douglas et al. 2007).

Nevertheless, it is essential to detect and evaluate the possible damage properly. There are a few possible reasons leading to errors such as lack of knowledge, lack of accessibility, complex interaction, time limit or misleading signs and symptoms. Thus, a real cause of the problem may sometimes be not found (Douglas et al. 2007).

2.3.3 Residual life assessment

The assessment, inspection and maintenance plans are conducted to ensure performance of the structure during its remaining service life. The Residual Service Life (RSL) may be defined as a period of time, determined by the assessment, during which the structure will response as expected. The residual service life time is based on the client requirement together with socio-economic criteria. When the intended residual service life time is ended, a new assessment needs to be conducted. The RSL is determined separately for every case and it is usually longer than service life designed for a corresponding new building structure (Sustainable Bridges 2007b).

Practically, in order to predict what may happen to a structure, conceptual models are used. This includes applied load, load paths, displacements or failure that might occur. However, aging of a structure and its degradation are the main reasons for refurbishment or demolition and thus with economic consequences. It is important then to develop methodologies which would account for these aspects while planning, designing and managing existing structures (Sustainable Bridges 2007b).

2.3.4 Verification

To verify structural reliability of existing buildings it is very important to use valid codes (Holický et al. 2013). Since the commonly used Eurocodes are aimed to be used for design, they verify the assessment. General procedures and requirements for assessment of existing structure may be found in ISO 13822, a standardization used in reliability analyses, (Marková 2010). Also, a target reliability level needs to be determined. This should consider the requirement for structural performance, the intended service life and possible consequences of failure. Two methods may be used, either the partial factor method or the probability method (Holický et al. 2013).

The structural assessment with regard to failure under loading considers ultimate limit states, such as loss of equilibrium like overturning, failure of structural components, global or local instability, formation of a mechanism, unexpected change of structural system into a new one. Furthermore, structural defects that influence the usability of a

building structure may cause a need of serviceability assessment. This includes local damage leading to working life reduction, not allowed deformations resulting in decreased use efficiency, vibrations causing discomfort to people and improper appearance due to large cracks or discoloration. The two limit states may be evaluated due to various reasons, among which are concern about design and quality of the building, damage effects or increased in applied loads. In fact, structural assessment is the most often conducted with regard to increased design loads or change of use (Rücker et al. 2006).

Nowadays there exist even more advanced verification possibilities. One very common tool used in engineering is finite element method (FEM). This type of modelling allows conducting more realistic calculations, by using 2D- or 3D-elements instead of simple beam elements. Usually, analyses of structures are based on theory of elasticity for the check of acceptable response in the ultimate limit state as well as for the serviceability limit state. Also, linear elastic analysis is most often used in the modelling, mainly because it is the easiest variant, but also due to the fact that it provides better possibilities of handling loads. However, it may be needed to use non-linear FE analysis that considers that the material behaves in a more realistic way until collapse occurs. However, the difficulty with this method is that it is not that consistent with regard to safety demands, e.g. it is not obvious what kind of data should be used as input for various material parameters (Plos et al. 2004).

2.4 Overloading as a cause of failure

Structural failures may occur for many different reasons and in many varieties. However, regardless of the type of damage it needs to be checked regarding safety criteria since the consequences may be disastrous. Reasons for failures are for instance design errors, insufficient material properties, material deterioration, production error, defective maintenance, incorrect inspection, physical damage and overloading (Spellman & Bieber 2012).

A structural component is designed based on loads and then calculated according to Eurocodes requirements. If the design value of the load effect exceeds the design value of the capacity with regard to safety factors, overloading occurs, which eventually may lead to failure, either in shear, tension, fatigue, or flexure etc. (Interval 2012).

Unsuspected events by either human impacts or environmental influence can result in excessive loads effect on a structure that were not considered in the design from the beginning. Environmental actions can be external forces inducing overloading either locally or globally, for example earthquake, strong wind and heavy snow. If the building structure is reconfigured in order to meet the demands of a new, new structural components or increased imposed load can also expose the original structure for overload (Spellman & Bieber 2012).

Besides negligence and environmental impacts the most common causes of failures are temporary overloading and weakness at a critical section, due to variation in material properties for example. To reduce the probability of these kinds of failures, partial safety factors are used, which reduce the strength of the material and increase the load effect. In the design load the safety factor used with regard to dead weight is small due to the small possibility of an oversized structure. For the imposed load the partial safety factor is greater since this load is variable and more uncertain to its magnitude in extreme cases. If a structure is loaded above ultimate limit state it is

assumed to collapse, although if the serviceability limit state is exceeded cracks and deformations will occur. The difference between the limit states is that the deformations and crack width will more or less return to their original magnitudes, if the structure is only temporary overloaded (Wilby 1983). The importance is that the structure does not collapse for any possible load combination and to prevent this regularly inspection can be performed. If flexural and shear cracks over 0.3mm are discovered this may indicate overloading, which must be investigated by forensic engineering to establish the cause of the problem and prevent further damages (Gold & Martin 1999).

Often, construction overloading can be more severe than the one applied when the structure is already built. This can happen at early stages of construction and result in permanent cracks. Mostly precast members are subjected to such actions, but this might also happen to cast-in-situ components. That is why it is recommended to pay a special attention to the load handling, transport and unloading of precast concrete elements. Even inappropriate lifting accessories, the lifting itself and pace of a component landing may lead to overloading bigger than a couple of times the members mass (ACI Comittee 224 2007).

When a structural member with ductile behaviour is overloaded it starts to deform in a plastic mode and the load is transferred to other sections where capacity still remains. This is a favourable characteristic and in order to prevent a catastrophic collapse in accidental situations the following aspects are important; structural resistance, plastic redistribution of forces, energy absorption and dynamic strengthening. Under these circumstances a sudden fracture occurs to the structure due to overloading, as the case is for brittle behaviour. With ductile response some deformation of the member can be tolerated since the connecting ability still remains. How much more load an existing structure can manage before it reaches the ultimate limit state depends, among other parameters, on the age of the structure and its loading history (Acker et al. 2012).

2.5 Cracks

Presence of cracks in concrete structures is very common and it is not preventable. Although structures built up of concrete can be characterized by their high compressive strength and rigidity, they are not flexible when it comes to environmental or volume changes. Cracking of concrete can be understood as a first sign of distress in the material, but the damage of concrete may start even before crack formation (Bluey Technologies n.d.).

Generally, cracking occurs in concrete components while tensile stresses in a certain part of the member reach the concrete tensile strength. When this happens, the tensile forces are transferred mainly by reinforcement in this particular part. There are many various reasons leading to such increase of tensile stress. Nevertheless, cracking has not a damaging influence on a structure as long as the crack spacing and width are kept within the acceptable limits (Kattilakoski 2013).

It is essential to identify the type of crack when it is observed on concrete surface, what may help to understand their effect on structural performance (Bluey Technologies Pty Ltd). Generally, two main types of cracks can be distinguished:

- Structural cracks – considered to be more important with regard to the structural response,
- Non-structural cracks – important mainly due to aesthetic experience, are not influencing the structural response (Mehndi et al. 2014).

2.5.1 Causes of cracks

Cracking of concrete may be generated by various causes. In order to conduct refurbishment it is very important to identify the source of cracks correctly and select appropriate repair methods that take into account possible reasons. Otherwise, the repair is only temporary (ACI Comittee 224 2007). It is often possible to identify the probable reason of crack occurrence by looking at the crack location and crack pattern. Figure 2.2 below presents an overview of where and how various types of cracks are situated due to different formation mechanisms. The non-structural cracks are marked here with capital letters and the reader is referred to Table 2.1. This table contains explanation under which circumstances the non-structural cracks occur, where they are mostly situated and hypothesis of primary and secondary cause.

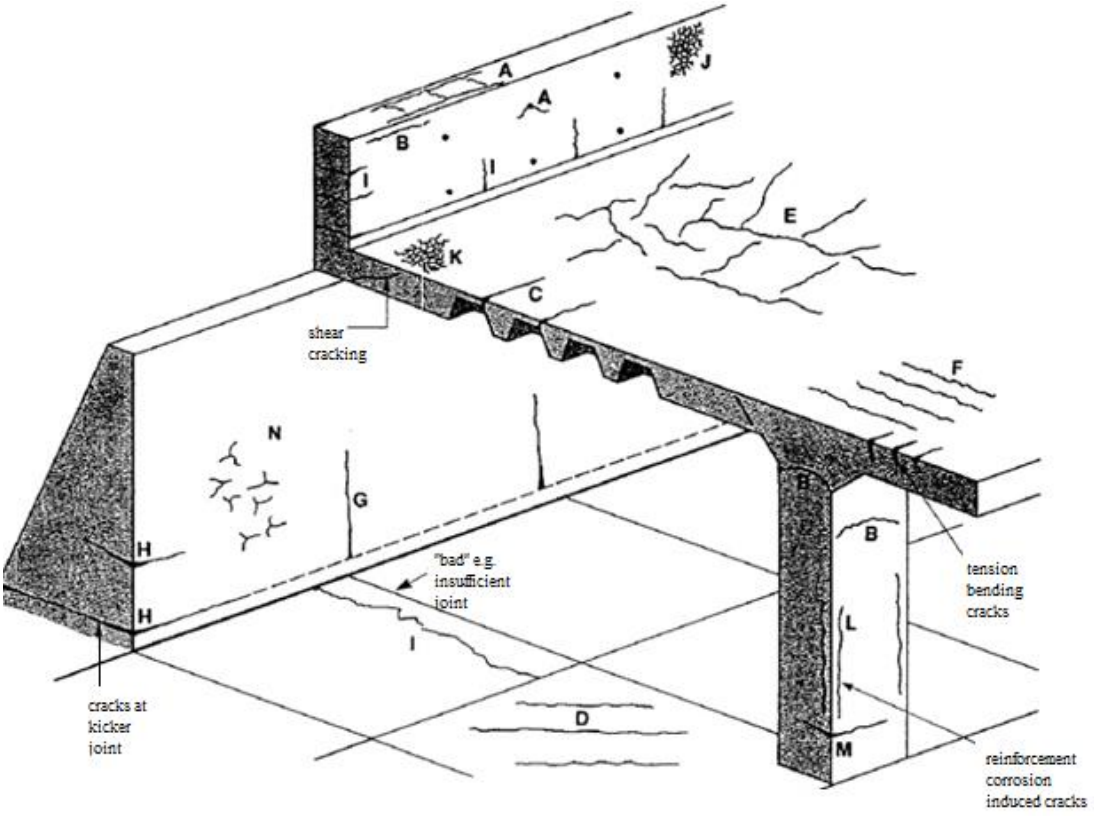

Figure 2.2 Crack patterns for non-structural cracks (Concrete Society 1992).

Table 2.1 Classification of non-structural cracks (Concrete Society 1992)

Type of cracking	Letter	Subdivision	Most common location	Primary cause	Secondary cause
Plastic settlement	A	Over reinforcement	Deep sections	Excess bleeding	Rapid early drying conditions
	B	Arching	Top of columns		
	C	Change of depth	Through and waffle slabs		

Plastic shrinkage	D	Diagonal	Roads and slabs	Rapid early drying	Low rate of bleeding
	E	Random	Reinforced concrete slabs		
	F	Over reinforcement	Reinforced concrete slabs	Ditto plus steel near surface	
Early thermal contraction	G	External restraint	Thick walls	Excess heat generation	Rapid cooling
	H	Internal restraint	Thick slabs	Excess temperature gradients	
Long term drying shrinkage	I	-	Thin slabs (and walls)	Insufficient joints	Excess shrinkage Insufficient curing
Crazing	J	Against formwork	"Fair laced" concrete	Impermeable formwork	Rich mixes Poor curing
	K	Floated concrete	Slabs	Over – trowelling	
Corrosion of reinforcement	L	Natural	Columns and beams	Lack of cover	Poor quality concrete
	M	Calcium chloride	Precast concrete	Excess calcium chloride	
Alkali-silica reaction	N	-	(Damp locations)	Reactive aggregate plus high alkali cement	

In addition, structural cracks occur often as vertical aligned pattern near the mid-span or as diagonals at the end-supports. Sometimes cracks caused by normal tensile forces, restraint or shrinkage may be misunderstood as cracks coming from overloading due to few examples of these patterns and because of too little experience. Thus it is difficult to estimate if a certain structure is really overloaded and long-term supervision is required (TSO 2007).

Flexural cracking usually appears within the middle third of the structure, besides for continuous structures where a more detailed study is required to estimate if the cause is bending stress. Shear cracking typically appears as inclined cracks from the end-support with an angle of 45 degrees. The widest crack can be expected close to the support and reinforcement has an influence on the crack direction. Torsional cracks have similarities with shear cracks besides that they start from the supports and propagate around the whole section, also with an approximate angle of 45 degrees (TSO 2007).

2.5.2 Observations

Visual observations on existing cracks, identification of their location and orientation are the first step in the evaluation process. Additionally, estimation of crack severity may be performed in a direct or indirect way.

A useful measure in crack evaluation process is crack width, which can be expressed by its characteristic or mean value. No further assessment of the crack is needed if it only covers the coating, but if any deeper propagation of the crack occurs its width can be estimated. An appropriate estimation of severity is easier made by grading the cracks according to different widths and furthermore divided into different environments. According to Table 2.2 the most severe category is III *(IAEA 2002).*

Table 2.2 Grades to assess severity of cracks (IAEA 2002).

Crack severity	Crack width, outdoor	Crack width, indoor
I	< 0.05 mm	< 0.2 mm
II	0.05 – 0.5 mm	0.2 – 1.0 mm
III	> 0.5 mm	> 1.0 mm

If the width of the crack is already categorized, a second survey is required in order to define crack pattern, age, location, depth and its cause (IAEA 2002). Nevertheless a judgement whether a crack is too large also depends on the climate, type of structure, reinforcement type and the type of crack. Other crack limitations than severity exists, for example the limit with regard to water tightness is 0.1 mm. For the same load effect and other conditions the crack width can vary in a magnitude of approximately 40%, which must be taken into account when only few cracks are measured (Suprenant & Basham 1993).

The estimation of crack severity may be conducted by plotting defects on a sketch and then mark out grids on the structural component's surface. Afterwards the width of visible cracks is measured by an instrument with accuracy of about 0.025mm, but a more simplified method is to measure the width by comparing a plastic card showing different line thicknesses. All displacements of the structure and other defects like wear, tear and rust on the reinforcement must also be documented (Mehndi et al. 2014). Another observation is to evaluate the crack as active or inactive, with regard to its changes of shape and increase of its width and depth. Inactive cracks have stopped in movement and a usual cause for this is temporary overloading. If a structure is regularly exposed to overloading, crack symptoms like changing thickness may indicate an active crack. Although an inactive crack caused by temporary overloading can change into active due to temperature changes (Suprenant & Basham 1993).

2.5.3 Testing

In uncertainty whether there are cracks or not, non-destructive testing can be performed on both new and old structures. However, in new buildings the method is conducted in order to check the material or the quality of the construction while after concrete hardening the test is conducted to check whether the structure is as it was designed. For an old building the tests are performed to assess whether the remaining capacity corresponds to what is expected. Often it is important to accomplish the assessment without destructive testing. In opposite to non-destructive testing, this destroys a part of the structure and therefore is more costly in terms of repair. As a result of the high costs only few tests are affordable to be performed and only at a small part of the structure, which can result in a misleading outcome (IAEA 2002).

Non-destructive tests are used to find internal cracks or voids which are not detected visually. For example knocking with a special hammer on the surface is an easy way to discover internal defects close to the top, since the difference in sound may indicate cracks. To detect and measure cracked regions many well developed equipment can be used. Some testing equipment estimates the crack depth while the observation from other tests informs about crack age, water-cement ratio and distribution of concrete components. In some cases it is difficult to detect cracks that belong to a group of cracks and instead misinterpret them as one large crack (Mehndi et al. 2014).

3 Response of reinforced concrete structure

3.1 Material response

3.1.1 Concrete

Concrete is a brittle material that cracks for a low tensile stress, as shown by the stress-strain relation in Figure 3.1.a. The main reason for this behaviour is the low tensile strength in the interface between aggregate and cement paste in comparison to how strong the paste is. This interface represents the weakest link in the material with regard to tension. The strength in compression is relatively high and the maximum stress depends on the strength class of the concrete. However, the ultimate strain ε_{cu} is normally assumed to be constant for all concrete classes between C12/16 and C50/60. An approximate estimation is that the compressive strength is ten times higher than the tensile strength, although the actual proportion depends on the capacity in compression (Lim 2013).

For tensile failure the relation between strain and stress is often assumed to be linear elastic until the maximum stress is reached and no plastic strains develop at that moment. In compression this relation is close to linear elastic up to a point where internal cracking has a significant influence. Beyond this point the stiffness decreases until a pronounced plastic response begins. When non-linear behaviour of reinforced concrete is presented, concrete is often expressed as elastic plastic in compression and elastic brittle in tension (Chen 2007). Figure 3.1.b describes how the strain and stress relation develops when the concrete is unloaded and then reloaded again (Lindelöf & Walhelm 2014).

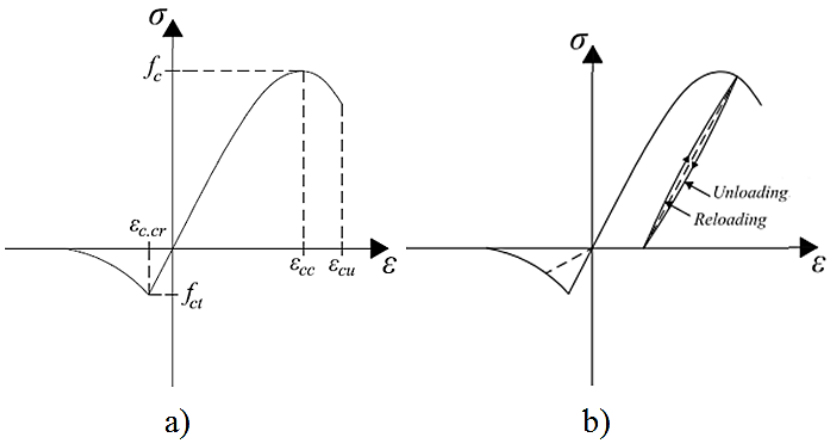

Figure 3.1 Stress-strain relationships for a) axially loaded plain concrete b) axially unloaded and reloaded plain concrete (Engström 2015).

3.1.2 Reinforcing steel

Hot-rolled reinforcing steel acts linear elastic until the yield stress is reached. Then the stress-strain relation shows a plastic plateau before strain hardening with large plastic deformation develops until a failure occurs. The stress-strain relation is assumed to be the same in both tension and compression and is shown in Figure 3.2.a. Another type of steel is cold worked steel and its stress-strain relation is shown in Figure 3.2.b. The difference between these two types of steel is that in cold worked steel the distinct yield limit is missing as well as the plastic plateau. Furthermore, the

strain for maximum stress is normally much smaller in cold worked steel. When non-linear behaviour of reinforced concrete is described, reinforcing steel is often characterised as elastic plastic in both compression and tension (Engström 2015). In Figure 3.2.c the stress and strain relationship for unloaded and then reloaded hot-rolled reinforcing steel is shown.

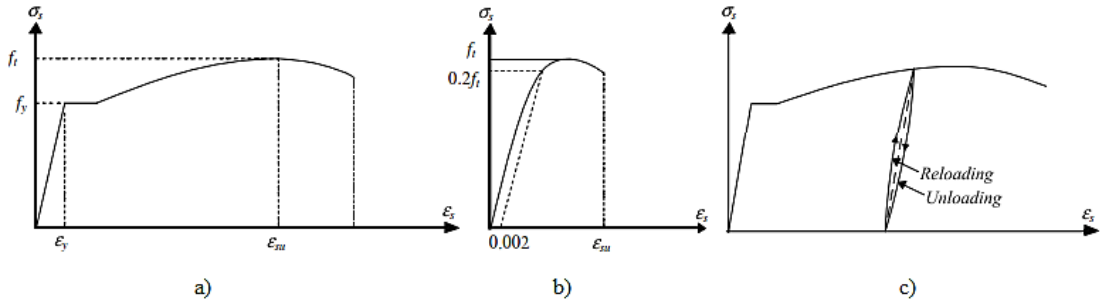

Figure 3.2 *Stress-strain relationships for a) hot-rolled reinforcing steel b) cold-worked reinforcing steel c) hot-rolled reinforcing steel that is unloaded and then reloaded again (Engström 2015),(Lim 2013).*

The reinforcing steel can be divided into different ductility classes depending on the ultimate strain and the ratio between the tensile strength and the yielding strength. The classification covers class A, B and C, where C is the most ductile reinforcing steel class (Engström 2015).

If a reinforced concrete structure is subjected to a load which is removed after a period of time the material response may be changed. If the load is removed from a reinforced bar before yielding is reached, the response at unloading follows the original linear elastic relation back to the origin. Therefore such material is called elastic and it returns to its original shape without any remaining deformation, as seen in Figure 3.3. As long as the material response is in the elastic range it can be exposed to cyclic unloading and reloading without significant impact on the behaviour (Johansson & Antona 2011).

If the steel is forced to deform much more, beyond yielding, the response at unloading depends on the original elasticity of the material and in a stress-strain graph the unloading follows a path that is parallel to the original branch when the load was applied. The typical behaviour is shown in Figure 3.3.c. The plastic strain between these two curves will remain even if the material is unloaded to zero. When the material is loaded into the plastic range the internal structure is changed and so are its properties (Johansson & Antona 2011).

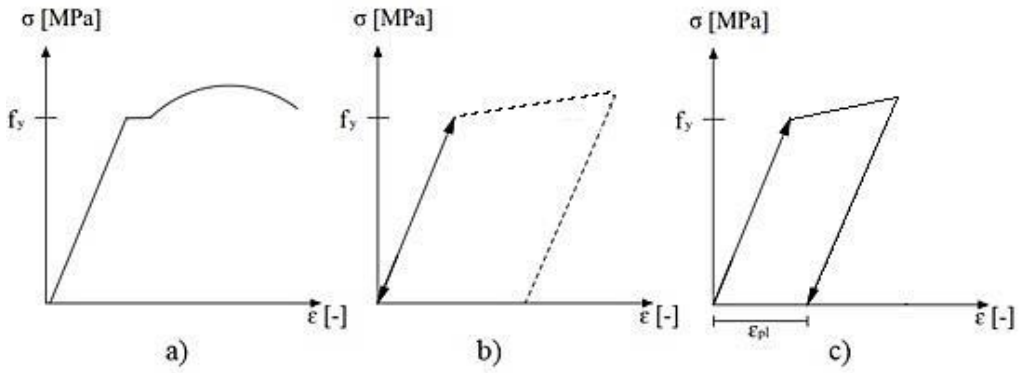

Figure 3.3 Material response of reinforcing steel in a stress-strain diagram, for a) typical behaviour b) unloaded and reloaded before yielding c) unloaded and reloaded after yielding.

3.1.3 Steel and concrete interaction

Reinforced concrete is a composite material where steel and concrete are bonded together and interact with each other. Forces are transferred between the materials resulting in shear stresses, which act at the steel-concrete interface. Such stresses are also called bond stresses and act within a length called transmission length. The transferred forces are different depending on the reinforcement bar type, which can be for example plain or deformed. In case of small tensile forces the bond depends on the adhesion. If the tensile force increases the adhesion decreases and the bond depends instead on the shear-key effect. This effect occurs when the surface of the reinforcement bar is rough. When the reinforcement bars are exposed to higher tensile forces, the shear stresses increases between the bars and the concrete which results in inclined tensile and compressive stresses in the concrete closest to the reinforcement bars (Engström 2011).

3.2 Response of reinforced concrete structures

3.2.1 Stages

The structural response of a reinforced concrete structure is highly depended on the material response as well as on the interaction between the steel and the concrete. When a structure is exposed to an increasing load its structural and material behaviour changes with consideration to four main stages. These stages correspond to uncracked concrete, cracked concrete, yielding of reinforcement and finally collapse of the structure. The first stage is when both the concrete and the reinforcement show linear response. When the load increases a critical section starts to crack and this is the start of the second stage. In this stage the reinforced concrete section cracks in flexure and the structural response and stiffness changes. This contributes to a non-linear behaviour and moment redistribution. When the beam is further loaded and the reinforcement begins to yield in the most critical section, plastic redistribution takes place.

The flexural response of reinforced concrete structures may be considered on two levels: sectional and global. The sectional response is characterised by the relation between bending moment and average curvature of a small region around a cross section. The global response, for instance the load-deflection relationship, depends on the summation of all sectional responses. It is generally assumed that strain varies

linearly across a section subjected to bending. The curvature κ is then given by the inclination of the strain distribution across the section (Lim 2013). This can be expressed as

$$\kappa = \frac{1}{r} = \frac{\varepsilon_S - \varepsilon_C}{d} \tag{3.1}$$

where: κ = Curvature
r = Radius of curvature
ε_S = Steel tensile strain
ε_C = Maximum concrete compressive strain
d = Effective depth of cross-section

The typical response of a reinforced concrete section and the described three main stages are indicated in Figure 3.4.

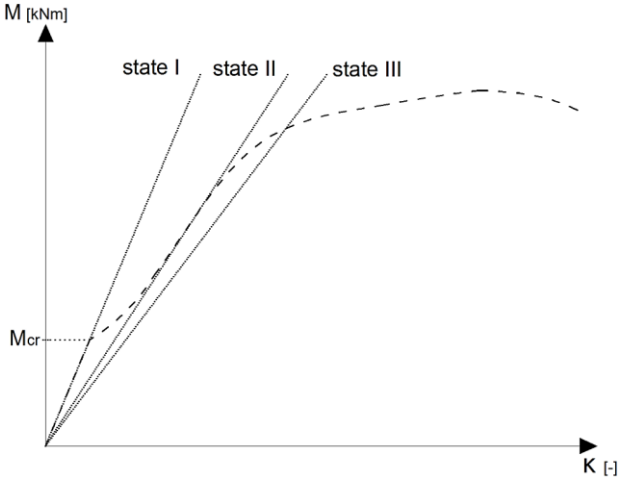

Figure 3.4 The typical response of a reinforced concrete section and the three main stages.

The moment-curvature relationship reveals the nonlinearity of reinforced concrete sections at three main modelling states, where state I is when the cross section is uncracked and state II when the section is cracked, but the materials are still practically linear elastic. State III is when significant plastic strain develops in steel, concrete or in both (Engström 2015).

3.2.2 Global deformation

The deformation of a structure depends on short term response and long term response. Effects that contribute to the long term deflection are shrinkage, creep and temperature. From all these influences, shrinkage is the most problematic. Restrained shrinkage can lead to time-dependent cracking and it also reduces the positive effect of tension stiffening. Existing cracks become gradually wider and in case of flexural members, a noticeable increase in deflection with time may be observed (Gilbert 2001).

In the service state all influences must be considered because the moment distribution is directly dependent on the curvature distribution. All factors that influence the curvature distribution along the structure also influence the moment distribution.

However, in the ultimate state any restraint moment disappears if there is sufficient plastic rotation capacity. Hence, the moment distribution is not influenced by restraining effects (Engström 2015).

A beam subjected to various actions has a particular moment distribution and a corresponding curvature distribution that results in a deflection. The deflection of a beam can generally be calculated as a summation of angels multiplied with lever arms. A principle of how the deflection in a section can be determined using the curvature distribution is presented in Figure 3.5 (Engström 2015).

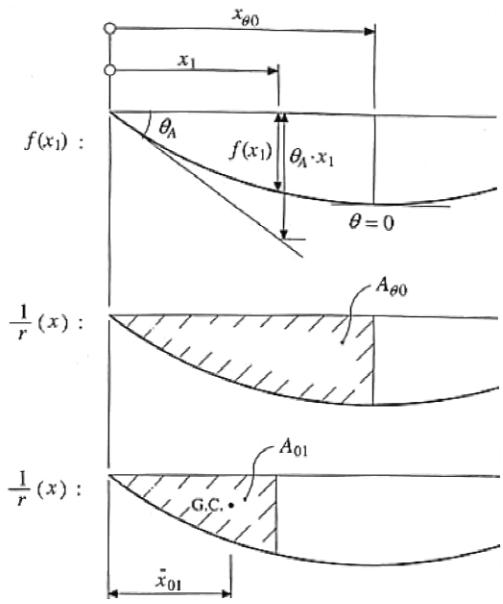

Figure 3.5 Relation between the deflection, support rotation and the curvature distribution (Engström 2015).

The deflection in the section x_1 can be calculated as

$$f(x_1) = \theta_A \cdot x_1 - \int_0^{x_1} \frac{1}{r}(x)(x_1 - x)dx \tag{3.2}$$

The parameters are defined in Figure 3.5. The integral in the expression above may be interpreted as the area between the support and the considered section x_1 multiplied by the average distance (Engström 2015).

3.3 Response of uncracked continuous beams

3.3.1 Global response

The sum of regional responses is the global response. Global response of a beam may be described by various parameters, such as relationship between the load and the deflection of a span or it can also be reflected by the relation between the load and the bending moment at an interior support.

When all sections in a beam are in uncracked state, their response is linear. This means that the relation between the moment and the curvature increases linearly. As the sum of sectional responses influences the global response, this response is also linear. This is for instance indicated by linear relation between applied load and deflection. When the response is linear, the reinforcement has a small influence on the beam response and its effect on the stiffness distribution can generally be neglected in

the analysis (Engström 2015), see Figure 3.6 to see a beam illustration when none of its sections is cracked.

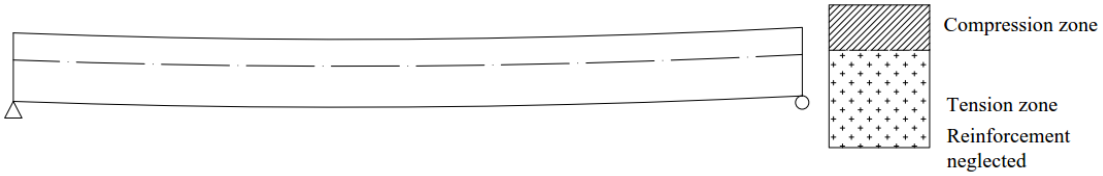

Figure 3.6 *A beam illustration without cracked sections and principle of analysis of an uncracked section.*

3.3.2 Sectional response

The sectional response in uncracked stage is analysed with consideration to linear material and structural response. The reinforced concrete section in state I is analysed using the modular ratio for steel and concrete, defined as

$$\alpha_s = \frac{E_s}{E_c} \tag{3.3}$$

where: α_s = Modular ratio
E_s = Modulus of elasticity for steel
E_c = Modulus of elasticity for concrete

In this state the concrete stresses can be calculated using the moment of inertia of the transformed concrete section

$$\sigma_c(z) = \frac{M}{I_c} z \tag{3.4}$$

where: σ_c = Stress of concrete in state I
M = Bending moment in cross section
I_c = Moment of inertia for concrete section in state I
z = Sectional coordinate defined relative to the sectional centroid

The steel stress is calculated using the modular ratio as

$$\sigma_{s,I} = \alpha_s \cdot \sigma_{c,I}(z_s) \tag{3.5}$$

where: z_s = Sectional coordinate defined relative to the layer of reinforcement bars

From the steel stress the resulting force in the tensile reinforcement is determined as

$$F_{s,I} = \sigma_{s,I} \cdot A_s \tag{3.6}$$

where: $F_{s,I}$ = Resultant steel force in state I
$\sigma_{s,I}$ = Stress of steel in state I
A_s = Sectional steel area

The principle of the sectional analysis in state I is shown in Figure 3.7.

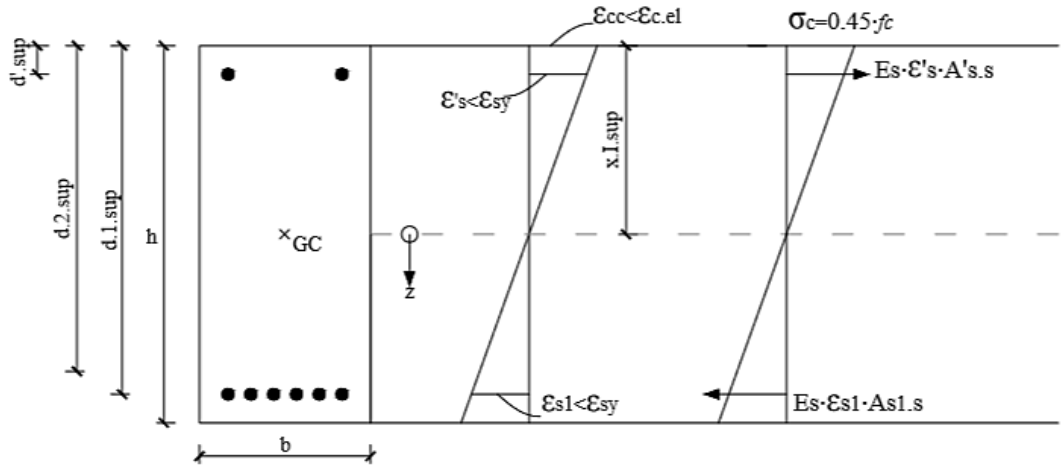

Figure 3.7 Principle of sectional analysis of reinforced concrete section in state I model.

In the uncracked stage, the response of the cross section is defined by the first part of the moment-curvature relation shown in Figure 3.8. This relation can be expressed according to equation (3.7).

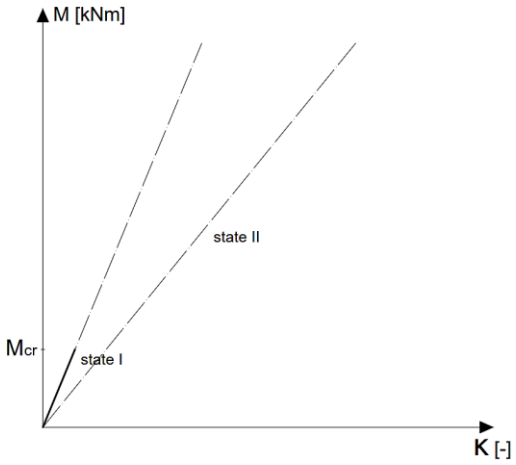

Figure 3.8 Simplified moment-curvature relationship of uncracked concrete section according to the state I model.

$$\kappa = \frac{1}{r} = \frac{M}{EI_I} \tag{3.7}$$

where:

r = Radius of curvature

EI_I = Flexural rigidity in state I

M = Bending moment in cross section

3.4 Response of cracked continuous beam

3.4.1 Global response

When the applied load reaches the magnitude of a load needed to develop cracks in a section, there will be a change in regional response, because the stiffness of a cracked section is much smaller in comparison to an uncracked one. The cracking happens since the maximum tensile stress in the section reaches the tensile strength f_{ct}. The reinforcing steel has significant influence on the stiffness in this state and the behaviour of cracked regions is mainly dependent on stiffness in state II. Since there are some sections with critical stresses in consideration with flexure in a continuous beam, the behaviour of these critical sections is important for the global response, see Figure 3.9 to see a beam illustration in its cracked state.

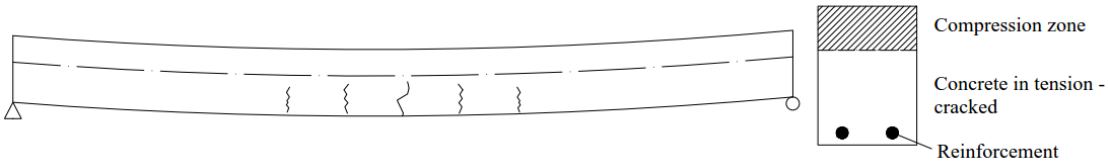

Figure 3.9 A beam illustration in cracked state and a principle of analysis of a cracked section.

Cracking of one of the critical sections has a drastic influence on the global response, resulting in a new stiffness distribution along the beam. Also, redistribution of moments will occur as stiffer regions attract forces. The moment in a cracked section will be smaller while it will be higher in the uncracked regions during application of the same load (Engström 2015).

If the applied load will increase further, more and more sections will crack and if the cracking is extensive, the beam can be considered as "fully cracked". Since normally the distribution and the amount of reinforcement placed in a beam varies along its length, the stiffness distribution in the cracked state will be quite different in comparison with the uncracked one. During cracking the moment distribution will adapt itself according to the new stiffness distribution.

The cracked state is also characterised by a phenomenon called "tension stiffening". Usually cracks appear in same distance from each other. As the parts in between the cracks will still remain uncracked, the uncracked concrete will help to distribute the forces transported by the reinforcing steel. This effect will be at its highest in the beginning of the cracking process. When more and more cracks appear, the effect of tension stiffening decreases. However, the stiffness of the uncracked parts in between the cracks is still closer to state II than to state I. The average steel strain of a small cracked region around one crack is in fact smaller than steel strain in flexural cracks. This results in overestimation of global deformations, if all sections are analysed with the sectional model for state II. The effect of tension stiffening has less importance in consideration with long term and repeated loading (Engström 2015).

The effect of tension stiffening is shown in Figure 3.10 and the dotted lines correspond to state I and state II.

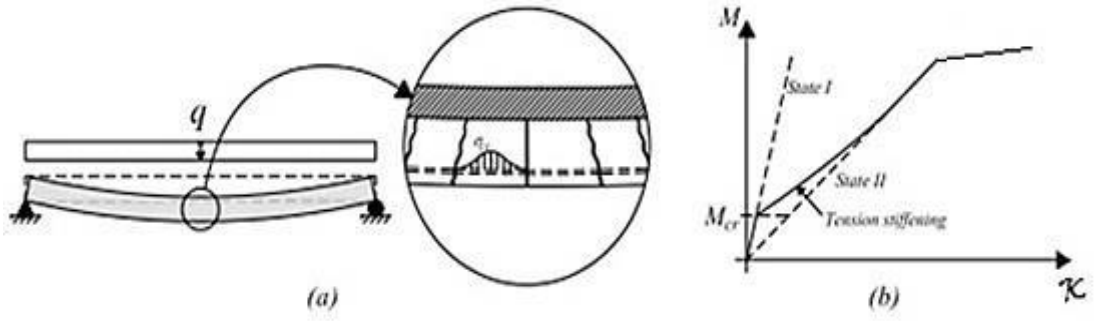

Figure 3.10 Influence of tension stiffening: (a) cracked beam (b) moment-curvature relationship with and without the effect of tension stiffening (Lindelöf & Walhelm 2014).

3.4.2 Sectional response

The analysis of a reinforced concrete section in state II is carried out by assuming linear elastic response for both steel and concrete, that steel and concrete has full interaction and that the concrete strain varies linearly across the section. Furthermore, concrete tensile stresses below the neutral axis are ignored. Hence the concrete stress can be expressed as

$$\sigma_{c,II}(z) = \frac{M}{I_{II}} \cdot z \tag{3.8}$$

where: $\sigma_{c,II}$ = Stress of concrete in state II

I_{II} = Moment of inertia of a cross section in state II

The steel stress is found as

$$\sigma_{s,II} = \alpha_s \cdot \sigma_{c,II}(z_s) \tag{3.9}$$

The resultant force in the tensile reinforcement can be expressed as

$$F_{s,II} = \sigma_{s,II} \cdot A_s \tag{3.10}$$

where: $F_{s,II}$ = Resultant steel force in state II

$\sigma_{s,II}$ = Stress of steel in state II

The principle of the sectional analysis in state II is shown in Figure 3.11.

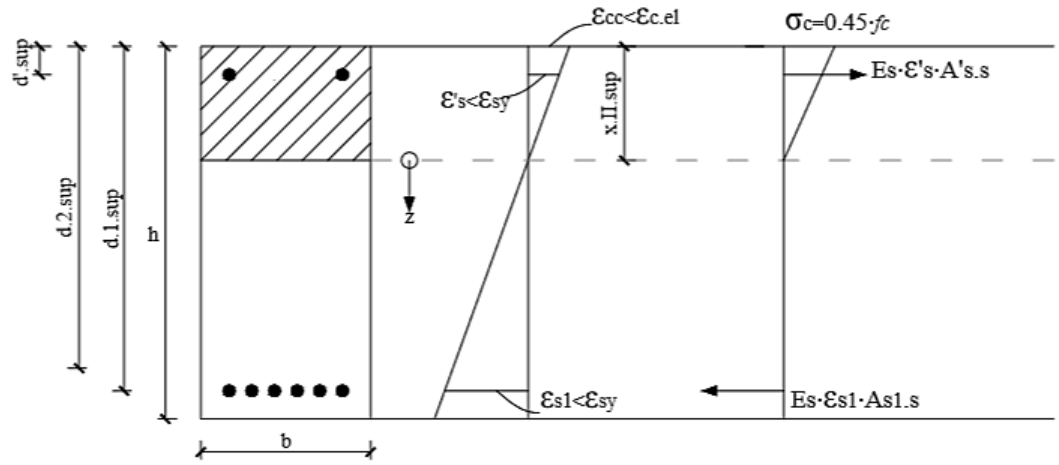

Figure 3.11 Principle of sectional analysis of reinforced concrete section in state II.

In the cracked stage, the response of the cross section is defined by the second branch in moment-curvature relation shown in Figure 3.12 and by expression (3.11).

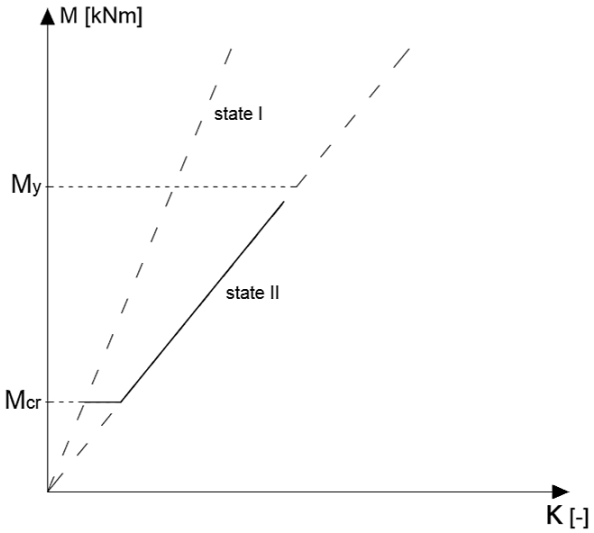

Figure 3.12 Simplified moment-curvature relationship of cracked concrete section according to state II model.

$$\kappa = \frac{1}{r} = \frac{M}{EI_{II}} \tag{3.11}$$

where: EI_{II} = Flexural rigidity in state II

3.5 Response in ultimate state

3.5.1 Global response

When formation of cracking is fully developed and the applied load is still increasing, the reinforcing steel will begin to yield in a section critical to flexure. If yielding in one section is reached, it does not mean that the capacity of the beam is exceeded. However, yielding of reinforcement in one section has a drastic impact on that region but also on the global response of the beam. If the load is further increasing, the

bending moment in this section can only increase slightly due to strain hardening of the reinforcing steel. Since other parts of the beam still have capacity left, this will result in redistribution of moments, called plastic redistribution. However, yielding of reinforcement also has another effect. Yielded steel will result in localisation of deformations, which means that the region where yielding is reached will deform much more in comparison to other parts of the beam, which still show linear behaviour. The shape of the deformed beam will thus not be continuous anymore, what will contribute to formation of a plastic region, threated often as a "plastic hinge" in the critical region (Engström 2015). See Figure 3.13 for a beam illustration in ultimate state and a principle of sectional analysis in ultimate state.

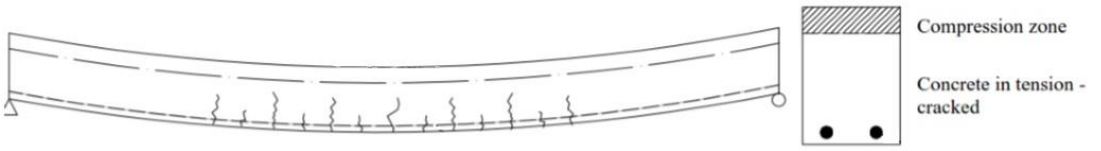

Figure 3.13 Beam response when a section is in ultimate state and the section in ultimate state.

With increase in load, one or more plastic region will develop. This will result in a failure of the beam either due to local failure of the already developed plastic region or by a formation of a new plastic hinge, what crates a collapse mechanism of the beam. Either the concrete or the steel ultimate strains has to be reached for a local failure of a plastic region to occur (Engström 2015).

3.5.2 Sectional response

When the concrete or reinforcing steel can no longer be considered to be linear elastic, the model for state II cannot be used any longer. In the sectional model for state III non-linear stress-strain relations are assumed for both concrete and steel and like in state II full interaction between concrete and steel is assumed and a linear strain distribution across the section. Furthermore, in cracked sections concrete tensile stresses are ignored below the neutral axis. The plastic capacity of the section is reached when yielding starts in the tensile reinforcement. The moment resistance can still increase slightly, while the sectional curvature increases, even if the steel force remains the same. This is because the height of the compressive zone decreases and, consequently, the internal level arm increases. At large deformations the tensile force can also increase in the reinforcement due to strain hardening. Sectional failure in bending is assumed when the ultimate strain is reached in either the concrete or the tensile reinforcement.

The compressive stresses are distributed across the compressive zone according to the non-linear stress-strain relationship. If the compressive zone is rectangular, the compressive resultant and its location can be expressed by stress block factors, see expression (3.12). The stress block factors depend on maximum compressive strain in the section and increase when the sectional curvature increases.

$$F_{c\,III} = \alpha_R(\varepsilon_{cc})\, f_c b x \tag{3.12}$$

where: $F_{c\,III}$ = Resultant concrete force

$\alpha_R(\varepsilon_{cc})$ = Stress block factor for stress block resultant

f_c = Concrete compressive strength

b = Width of compressive zone

x_{III} = Height of compressive zone

The resultant steel force is calculated by considering the actual steel stress that fulfils the equilibrium condition. The steel stress is dependent on the steel strain or on the stress at yielding according to

$$F_{s\,III} = \sigma_s A_s \tag{3.13}$$

where: $F_{s\,III}$ = Resultant steel force

σ_s = Steel stress, where:

$\sigma_s = \varepsilon_s \cdot E_s$ if $\varepsilon_s < \varepsilon_{sy}$

$\sigma_s = f_y$ if $\varepsilon_s \geq \varepsilon_{sy}$

Analysis in state III is shown in Figure 3.14.

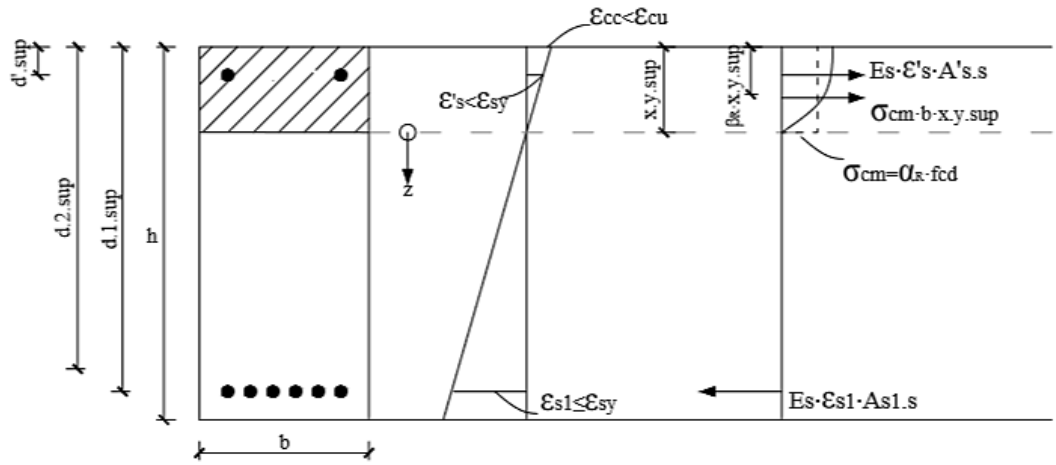

Figure 3.14 Principle of sectional analysis of reinforced concrete section in state III.

If the maximum concrete compressive strain reaches ultimate strain, the concrete stress block becomes fully developed. Then the stress block factors for concrete strength classes C12/16-C50/60 are α_R = 0.810 and β_R = 0.416.

In state III the response of the cross section may be defined by moment-curvature relation shown in Figure 3.15 and expression (3.14). Figure 3.15 indicates simplified moment-curvature relation in state III, without consideration of the effect of tension stiffening. Since there is already some plastic deformation in the concrete at the yielding load, the line that follows state II model starts to deviate from its path before yielding moment is reached. That is why a new line is introduced in this figure which represents state III. This line shows also the approximate stiffness used in the analysis when the reinforcement is yielding.

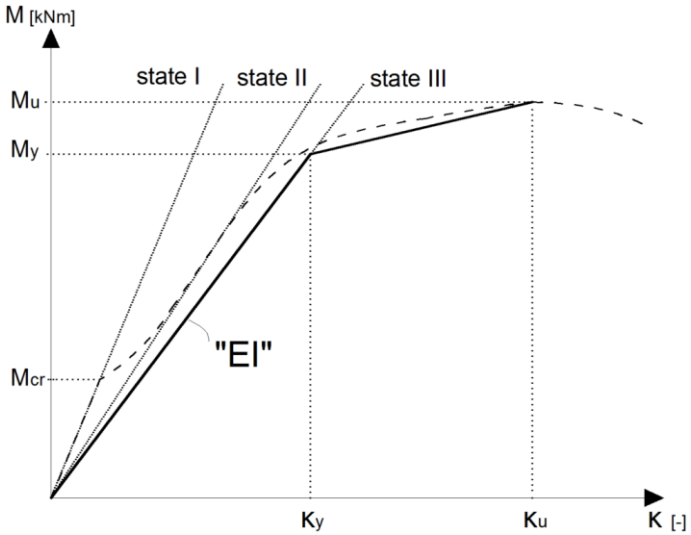

Figure 3.15 Simplified moment-curvature relationship of concrete section according to state III model with indicated stiffness used in analysis in state III. The dotted line indicates the calculated response according to state III model, while the solid line indicates the simplification implemented in the analysis.

The relation between strain and curvature in state III can be expressed as

$$\kappa = \frac{1}{r} = \frac{\varepsilon_c}{x_{III}} \tag{3.14}$$

As mentioned, Figure 3.15 also indicates how the stiffness in state III model is treated. The inclination of the line between zero moment and the yielding moment corresponds in approximate way to the flexural rigidity *"EI"* of the cross-section in ultimate state before yielding of this section starts. This average stiffness in ultimate state may be expressed as

$$"EI" = \frac{M_y}{\kappa_y} \tag{3.15}$$

The plastic deformation formed in concrete before yielding starts is the reason for the reduced stiffness *EI*. After yielding the moment-curvature relation is not linear as it is described by state II model. The yielding moment is reached after some plastification of concrete has occurred and this is why the stiffness at this moment must be lower than the stiffness corresponding to state II model, look at the meeting point of the yielding moment and its corresponding curvature in Figure 3.15. As it is shown in expression (3.15), the stiffness based on the state III model is calculated from the yielding moment and the curvature at yielding of the section. Despite the fact that the notation *EI* is generally used to describe flexural rigidity, in ultimate state it is a general parameter and it is not related to the modulus of elasticity of the materials or the moment of inertia in comparison to stiffness at uncracked and cracked state.

3.5.3 Plastic redistribution

Reinforced concrete beams have a non-linear response when the load increases due to cracking of concrete, yielding of steel and plastic deformation of concrete in compression. In statically indeterminate beams the non-linear response results in

moment redistribution between support regions and span regions. The moment redistribution takes place due to change of the stiffness distribution and it can be visualised by changed proportions of the moment diagram. When moment redistribution occurs due yielding of the steel, this is called plastic redistribution. If the tensile reinforcement starts to yield in a section, the moment cannot increase significantly in such section any more. However, deformation of this region can increase significantly due to yielding of the steel. In case of a two span continuous beam, a plastic region can in normal cases be assumed to form over the interior support. When the load increases, the moment in this section cannot increase, but since the yielding is not reached in the span yet, the span moment can still increase as shown in Figure 3.16. This plastic redistribution continues until the span moment reaches the moment capacity in these sections and at that time a collapse mechanism is formed.

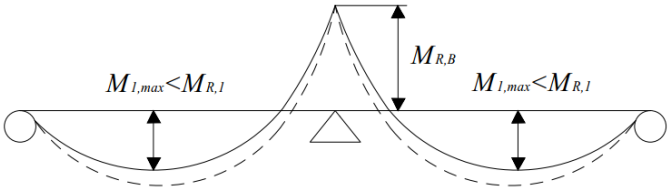

Figure 3.16 Moment redistribution due to yielding in the support section, when load increases[1].

The behaviour of a two span reinforced concrete beam can also be expressed by the relationships between load and moment in critical sections, as shown in Figure 3.17. Normally cracking starts over the support which decreases the stiffness in this section and as the load increases the span starts to crack as well. Stiffer regions attract forces which lead to redistribution of moments due to cracking. Further loading normally results in yielding over the support and consequently further loading results in plastic redistribution. The support moment then remains constant and the span moment increases until the span capacity is reached.

[1] Björn Engström (Professor, Chalmers University of Technology) Lecture 3-11-2015

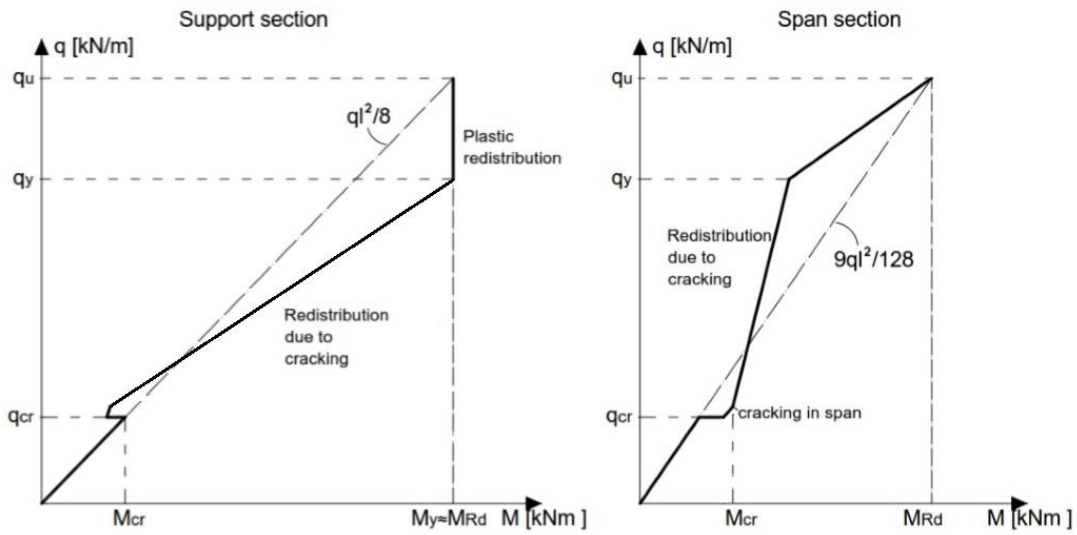

Figure 3.17 Moment-load relation for support and span sections when the load is increasing[1].

To allow for formation of a collapse mechanism, the plastic hinge needs a certain plastic deformation capacity. Otherwise the plastic redistribution will be interrupted by a premature failure in the plastic hinge. Since plastic redistribution may be an advantage for design in the ultimate limit state, it is important to remember that this phenomenon is not permitted in service state.

3.5.4 Plastic rotation

The plastic moment capacity of a section is reached when the reinforcement bars start to yield. In the region where this occurs the strain will then increase rapidly without any significant increase in stress. Due to this fact, a concentrated rotation develops in such region called a plastic hinge. Development of such plastic hinge may result in a collapse of the beam. The failure of a continuous beam can occur either by a local failure due to insufficient plastic rotation capacity of an already existing plastic region, local shear or anchorage failures, or globally by a new plastic hinge that turns the beam into a collapse mechanism, see Figure 3.18. In the figure the load increases stepwise from a state with elastic response with cracked sections (Figure 3.18.a) to a state where a plastic hinge over the support develops (Figure 3.18.b) and furthermore to a state with plastic hinges in the spans, what creates a collapse mechanism (Figure 3.18.c). In structural analysis, extended plastic regions are normally treated as concentrated plastic hinges. The need for plastic rotations depends on the elastic deformation of the beam, but cannot exceed the plastic rotation ability of these concentrated plastic regions. In the regions between the plastic hinges yielding is not reached yet and consequently the beam is here still assumed to have elastic response in the ultimate state (Engström 2015). The stiffness *EI* for these regions can be estimated approximately on the basis of the sectional model for state III, as explained in Section 3.5.2.

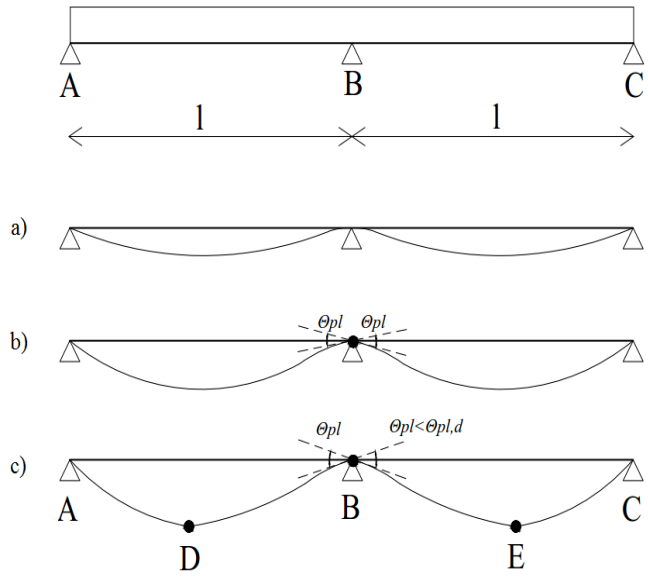

Figure 3.18 *Development of plastic hinges in the global model for analysis in ultimate state a) before yielding b) plastic redistribution with one plastic hinge over the support, plastic rotation develops c) plastic hinges also in the span, which leads to a failure mechanism and collapse (Engström 2015).*

A reinforced concrete beam demands a sufficient plastic rotation capacity of the plastic hinges in order to fail by formation of a collapse mechanism. Otherwise, a premature flexural failure occurs in the plastic hinge due to crushing of concrete or rupture of the reinforcement. For a real member the plastic rotation is a result of plastic deformations in plastic regions with an extension l_{pl}. The plastic rotation is determined by integrating the plastic curvature over the plastic region, according to equation (3.16) and the plastic region length is determined by equation (3.17).

$$\theta_{pl} = \int_{x_1}^{x_2} (\kappa - \kappa_y) dx \tag{3.16}$$

$$l_{pl} = x_2 - x_1 \tag{3.17}$$

where: l_{pl} = Extension of a plastic region in the beam model

x_1 = Coordinate along the beam to section where the plastic region starts

x_2 = Coordinate along the beam to section where the plastic region ends

The plastic rotation depends on both the curvature of the cross-sections involved and the extension of the plastic region. The influence of these factors appears from Figure 3.19 (Engström 2015).

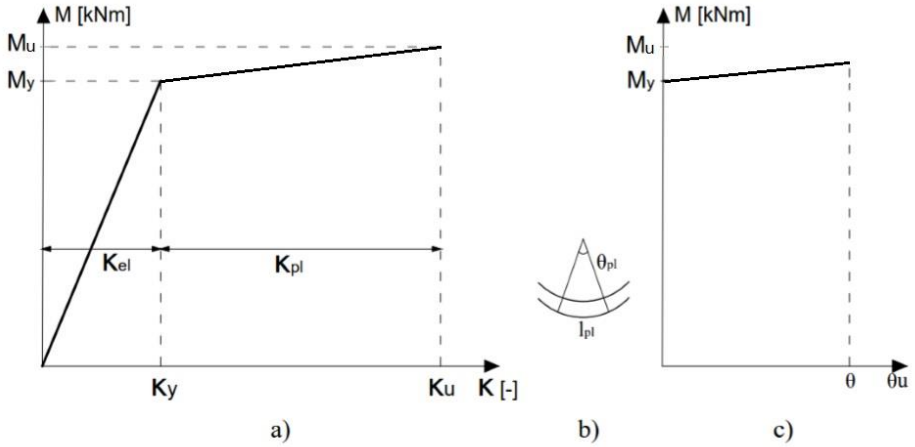

Figure 3.19 Factors influencing the plastic rotation is l_{pl} and κ a) plastic curvature κ b) extension of the plastic region, l_{pl} c) plastic rotation developed over l_{pl}.

A method to estimate the plastic rotation capacity of a reinforced concrete section is given by Eurocode 2 (CEN 2004) and shown in Figure 3.20. Here the design value of the plastic rotation is presented as a function of the x_u/d-ratio, the ductility class of the reinforcing steel and the concrete strength class. Reinforcement of ductility class A is not permitted in design based on plastic analysis according to Eurocode 2. In the left part of Figure 3.20 the plastic rotation capacity is increasing with increasing x_u/d-ratio, since the capacity is governed by the ultimate steel strain and the section fails due to rupture of the tensile reinforcement. In the right part of the figure the plastic rotation capacity is decreasing with increasing x_u/d-ratio, since a failure here is caused by crushing of the concrete. Estimation of $\theta_{pl,d}$ according to the figure gives a conservative value and any positive effect of confining reinforcement is neglected. For concrete strength classes between C55/67 and C80/95 linear interpolation should be used (CEN 2004).

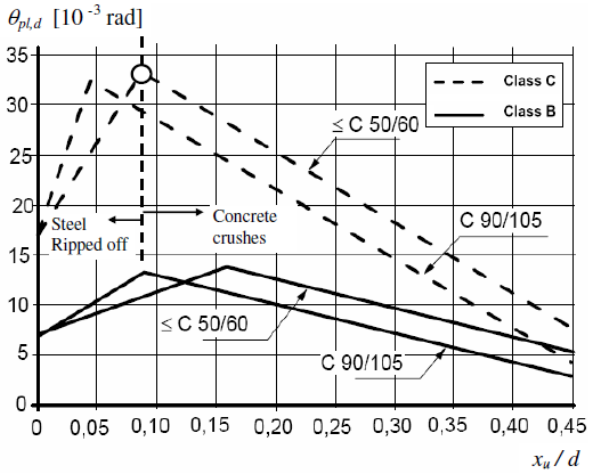

Figure 3.20 Design value of plastic rotation capacity for reinforced concrete section, according Eurocode 2. For concrete classes B and C with shear slenderness λ=3 (CEN 2004).

Figure 3.20 is valid for reinforced concrete members with a shear slenderness value equal to 3. If that is not the case, the design value of plastic rotation capacity should be multiplied with a modification factor (CEN 2004). The plastic rotation capacity is then determined as

$$\theta_{pl,d} = k_\lambda \theta_{pl,d_f} \tag{3.18}$$

where: θ_{pl,d_f} = Plastic rotation capacity according to Figure 3.20

k_λ = Modification factor that considers shear slenderness

λ = Shear slenderness

The modification factor k_λ and the shear slenderness λ can be determined as

$$k_\lambda = \sqrt{\frac{\lambda}{3}} \tag{3.19}$$

$$\lambda = \frac{x_0}{d} \tag{3.20}$$

where: x_0 = Distance from support section to zero moment section in the span

3.6 Cumulative plastic failure

In order to understand how a cumulative plastic failure occurs, a two span beam shown in Figure 3.21 is studied. A plastic hinge with a plastic rotation θ_s is formed over the middle support, when both spans are loaded to their maximum capacity. However, if the right side span is unloaded, the support moment decreases and the response of the support section becomes elastic. Since the load in the left span remains, the maximum moment in the span increases due to equilibrium and a plastic hinge with plastic rotation θ_f is formed in the left span. A new loading at the right span will change the moment distribution back again to its original shape, where plasticity occurs at the support instead of in the left span. A renewed cycle of unloading and reloading gives additional plastic rotations in the support and span. Each such cycle contributes to a permanent plastic rotation and deformation (Lorentsen 1990).

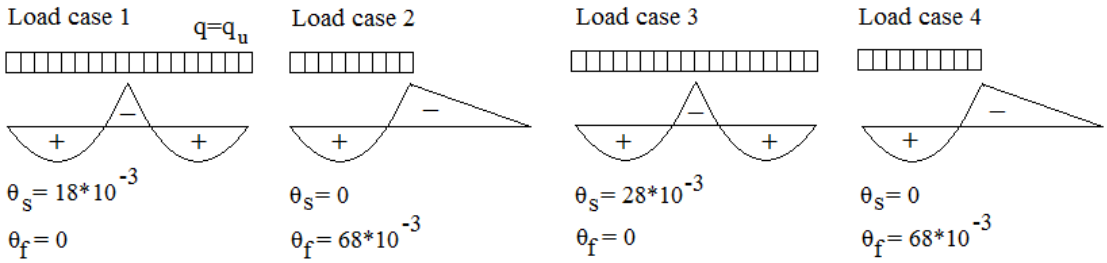

Figure 3.21 Unloading and reloading of the right span give increased rotation in the plastic hinges over span and in the left span. The values of the plastic rotations are determined for a distributed load of 38kN/m and a span of 6m (Lorentsen 1990).

At each unloading an elastic return occurs and at each reloading an elastic increment takes place, followed by a plastic contribution as shown in Figure 3.22. Each load cycle contributes to a plastic deformation and after a certain number of load cycles the beam will collapse, as a consequence of the total imposed plastic rotation and the plastic rotation capacity is reached. This phenomenon is called cumulative plastic failure and can take place even for a low number of load cycles. To resist cumulative plastic failure formation of a plastic hinge should be avoided, while the other span is unloaded and reloaded over the time (Hillerborg 1971).

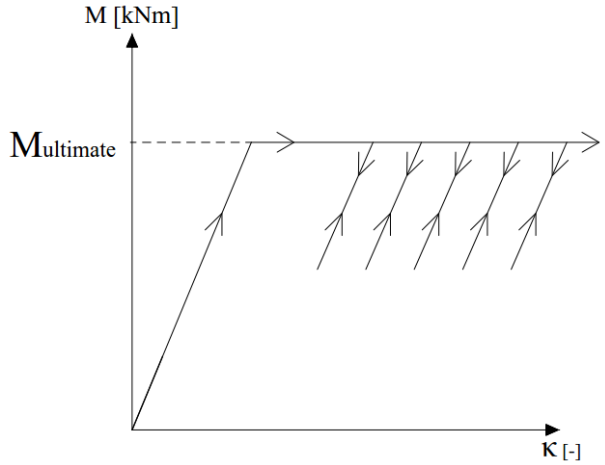

Figure 3.22 Progressive increase of plastic rotation in case of cumulative plastic failure at support (Hillerborg 1971).

4 Analytical analysis

A damaged concrete structure needs to be investigated in detail to find out the cause of the damage and the possible influence on the remaining structural capacity, as it is described in Chapter 2. In this project, a two span continuous beam subjected to uniformly distributed load was studied as an example to determine the influence of overloading on the remaining capacity. This investigation was first carried out by using analytical analysis, which is presented in this chapter.

When a damaged component is discovered in a structure, it is firstly of interest to estimate the current condition. An important parameter that is helpful in structural assessment and easy to measure on site is the deflection, which is related to other essential parameters, for example plastic rotation. Another sign of a damaged structure that may be observed on site is crack pattern and crack width. However, it would be difficult to use as a parameter to determine the magnitude of any overloading. The reason for this is further explained in Section 4.2 and that is why crack width was not used as a parameter in this study.

When the condition of a structure is studied in order to determine whether it was subjected to a past overloading, a forensic engineering investigation is needed. Such investigation also helps to assess the magnitude of the overloading. Having the suspicion confirmed, the future remaining capacity and current condition of the structure may be analysed using the structural assessment approach.

4.1 PART 1: Response of a beam for predefined load steps

4.1.1 Approach

In order to implement forensic engineering and structural assessment in this work, it was important to understand the material, sectional and global behaviour of the reinforced concrete members at different loading phases. Of this reason an example of a structural member was selected, which in this work was a two span continuous beam with a uniformly distributed load. To understand the response at various phases, the study was conducted by first assuming a quasi-permanent load that acts on the beam in the service stage and then assuming an overload that causes yielding of reinforcement but without collapse of the member. Knowing the loading magnitudes at different phases in advance was essential to examine and explain the structural response.

In these studies, five different phases of loading were defined:

- Phase 1: quasi-permanent load,
- Phase 2: overloading, load of a magnitude higher than the yield load,
- Phase 3: unloading, the additional load from Phase 2 is removed and the beam is subjected to load that corresponds to Phase 1,
- Phase 4: back to overloading, load of the same magnitude as in Phase 2,
- Phase 5: load that corresponds to the capacity of the beam.

The beam which was used in order to conduct analytical analysis was placed on three supports, named respectively A, B and C. The analysed beam is symmetrical which means that the two spans are equally long, see Figure 4.1.

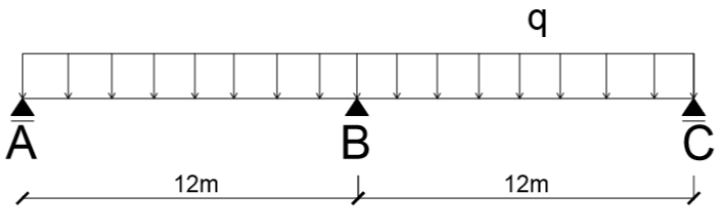

Figure 4.1 Model of the analysed beam and support notations.

The assumed reinforcement arrangement is shown in Figure 4.2.

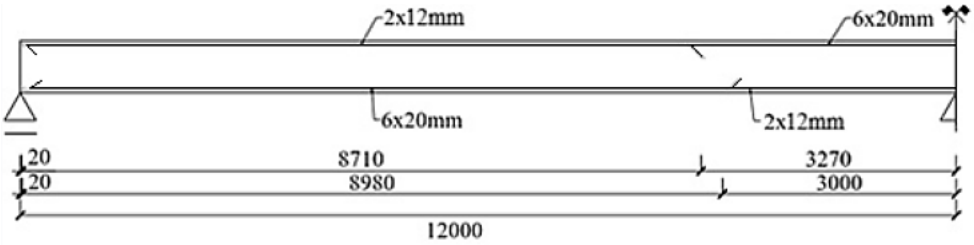

Figure 4.2 Reinforcement arrangement, dimensions in mm.

In the analytical analysis the mean concrete strength and the characteristic steel strength were assumed. This was to avoid differences in results while comparing Part 1 where the loading is known with Part 2, which concerns assessment of a damaged overloaded beam with unknown loading. Part 2 is presented in Section 4.2 and mean values had to be used in the assessment, since they correspond more to what can be expected in reality.

The calculations concerned short term response of the beam since long term effects have small effects on the load-carrying capacity. The main beam properties used in this work are presented in Table 4.1.

Table 4.1 Beam characteristics and assumed properties of concrete and reinforcing steel.

Beam characteristics	
Span l_s [m]	12
Height of the beam h [m]	0.7
Width b [m]	0.3
Sectional gross concrete area A_c [m^2]	0.21
Concrete	
Strength class	C30/37
Mean concrete compressive strength f_{cm} [MPa]	38
Mean concrete tensile strength f_{ctm} [MPa]	2.9

Density of reinforced concrete ρ_c [kN/m^3]	25
Modulus of elasticity of concrete E_c [GPa]	33
Ultimate concrete compressive strain ε_{ccu}	$3.5 \cdot 10^{-3}$
Reinforcing steel	
Characteristic tensile steel strength f_{yk} [MPa]	500
Modulus of elasticity of steel E_{sm} [GPa]	200
Steel yielding strain ε_y	$2.5 \cdot 10^{-3}$
Ultimate steel tensile strain ε_{suk}	0.05

4.1.2 Phase 1

The beam in Phase 1 was subjected to uniformly distributed quasi-permanent load. Since the load was known, it was possible to determine parameters such as moment distribution and deflection. According to theory, with increase of load some parts of the beam start to crack and the sectional response of these sections changes from linear to non-linear. The load that creates the first crack depends on the cracking moments of the sections and the moment distribution along the beam at this stage. When the beam starts to crack, the response of the cracking section is still close to the behaviour in state I. This is due to the tension stiffening effect and its contribution decreases while the load is further increased. It was assumed that the quasi-permanent load is much greater than the load that creates the first crack and thus the tension stiffening effect was disregarded in the beam analysis for the quasi-permanent load. Thus in this phase the sectional model for state II was used. Theoretically, the deformed shapes of the spans should still fit together above the middle support according to the continuity condition presented as

$$\Theta_{1,sup,left} + \Theta_{1,sup,right} = 0 \tag{4.1}$$

where: $\Theta_{1,sup,left}$ = Support rotation at the middle support B on its left side, [rad]

$\Theta_{1,sup,right}$ = Support rotation at the middle support B on its right side, [rad]

The assumed relation between the moment and its corresponding curvature in the span section and the support section is shown in Figure 4.3.

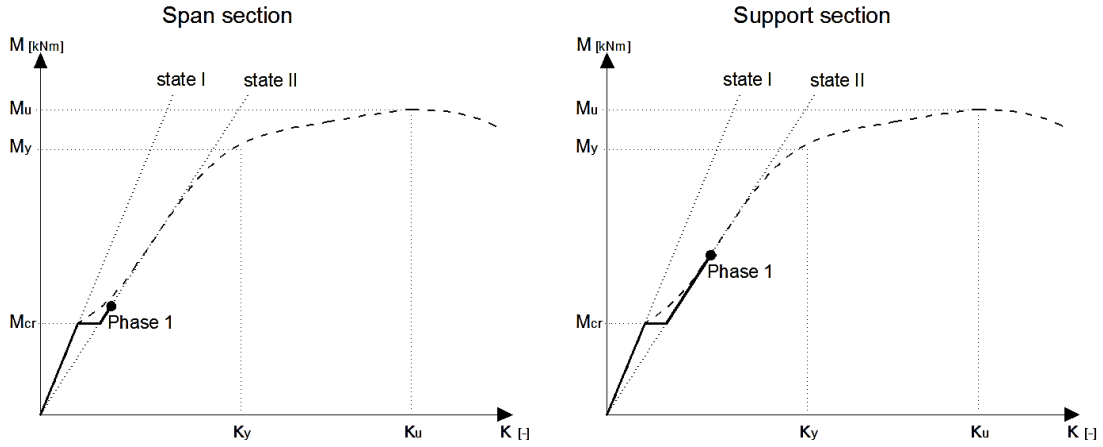

Figure 4.3 Assumed sectional responses of critical sections in Phase 1.The dotted line indicates the real response while the solid line indicates the simplification implemented in the analysis.

The load that was used in the analysis in Phase 1 corresponds to the quasi-permanent load combination and with an assumed value as given in expression (4.2). A quasi-permanent load corresponds to the time average of the load in the service state. When the load is further increased it reaches its characteristic value. However, in this work the overloading is associated with yielding of the middle support B section. The assumed value of the characteristic load presented in expression (4.3) was therefore exceeded. In order to see how the beam behaves also at the serviceability limit state the moment and deflection in Phase 1 was also calculated for the characteristic load, see Appendix A Section A.5.

$$q_1 = 9.243 \text{ kN/m} \tag{4.2}$$

$$q_{characteristic} = 11.590 \text{ kN/m} \tag{4.3}$$

The curvature along the span κ_1 was determined using moment of inertia corresponding to the sectional model for the cracked state, state II. The curvature was calculated as

$$\kappa_1(x) = \frac{M_{1.x}(x)}{E_c \cdot I_{.II.span}} \tag{4.4}$$

where:
κ_1 = Curvature for span in Phase 1
$M_{1.x}$ = Moment in section x in Phase 1
$I_{II.span}$ = Moment of inertia in state II for support section

The curvature of sections in the support region was determined similarly. The statically indeterminate support moment was determined by taking into consideration the fact that the beam and the load are symmetrical and that there are no plastic rotations over the middle support B, calculated as

$$\theta_{1.sup.left} = \frac{\int_0^{l_s} \kappa_1(x) \cdot x dx}{l_s} = 0 \tag{4.5}$$

where: κ_1 = Curvature along the span in Phase 1

The deflection along the span was determined as

$$f_{1.span}(x) = \theta_{1.A} \cdot x - \int_0^x \int_0^x \kappa_1(x) dx dx \tag{4.6}$$

where: $f_{1.span}$ = Deflection in a section in Phase 1
κ_1 = Curvature in a section in Phase 1
$\theta_{1.A}$ = Rotation at support A in Phase 1

The calculations carried out for Phase 1 can be found in Appendix A Section A.5.

4.1.3 Phase 2

The study in Part 1 was based on the assumption that the magnitude of overloading is known in advance and this load was assumed to be higher than the load that causes yielding of the reinforcement. Firstly, to be able to implement this assumption into the analysis, the yielding load $q_{y.sup}$ was determined using equation (4.7). This expression is only valid if the stiffness along the beam in the cracked state is constant. Next the load q_{ult}, corresponding to formation of a collapse mechanism was determined, by taking into consideration cross sectional capacity of the critical sections at mid support and in the spans, see equation (4.8). Thus the moment that corresponds to the overload in Phase 2 could be chosen in the interval between the yielding and ultimate moments.

$$M_{y.sup} = \frac{q_{y.sup} \cdot l_s^{\,2}}{8} \tag{4.7}$$

$$M_{u.span} = \frac{\left(\frac{q_{ult} \cdot l_s}{2} - \frac{M_{u.sup}}{l_s}\right)^2}{2q_{ult}} \tag{4.8}$$

where: $q_{y.sup}$ = Load that creates yielding of the support section
$M_{y.sup}$ = Yielding moment of support section
q_{ult} = Load that corresponds to a collapse mechanism of the beam
$M_{u.sup}$ = Moment capacity of the support section
$M_{u.span}$ = Moment capacity of the critical section in the span

For the studied beam the yielding load was chosen as $q_{y.sup}$=31.083 kN/m. The ultimate load was determined as q_{ult} =47.526 kN/m. The overload was then chosen as q_2=35.430 kN/m, which means that 26% of the available interval was used for overloading.

Due to overloading the sectional response of the beam changes to state III as it is indicated in Figure 4.4. The top branch of the moment-curvature relation has an inclination but the ultimate capacity of the section is close to its yielding moment. This branch could in plastic analysis be simplified to a horizontal top branch.

However, since both the yielding and the ultimate moment were calculated in this project, this idealisation was not used and instead a value for the moment related to the overloading was chosen between these two markings. The moment-curvature relation between the yielding moment and the ultimate moment was assumed to be linear and a moment in Phase 2 was chosen in this interval.

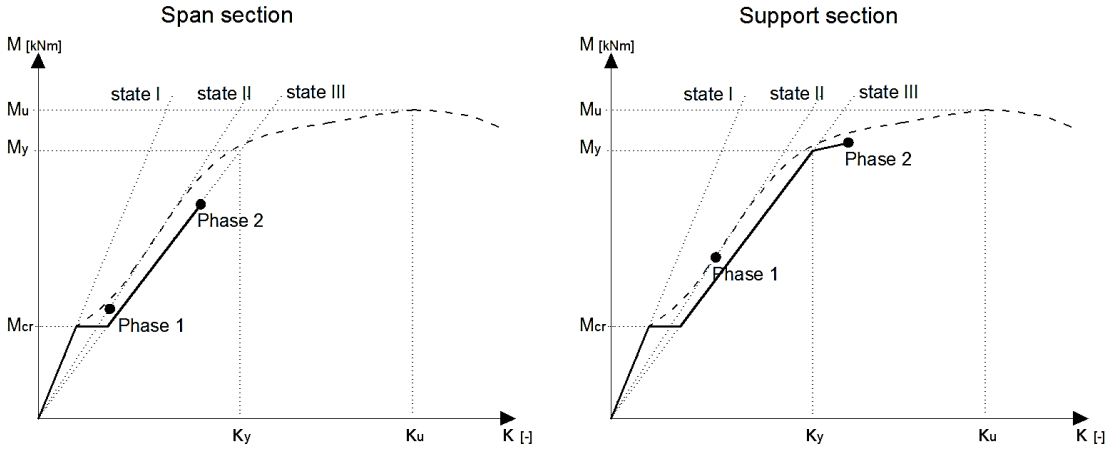

Figure 4.4 *Assumed sectional responses of the critical sections in Phase 2. The dotted line indicates the real response while the solid line indicates the simplification implemented in the analysis.*

To conduct the analysis a new stiffness was determined that could describe the sectional response in state III. It was assumed that there is a significant influence of plastic concrete strain on the sectional response and that the sectional model for state III is needed. To characterise the sectional response a simplified bilinear moment-curvature relationship was used, according to the approach presented in Section 3.5.2. Hence, the bending moment and the corresponding curvature were determined accurately using a model for state III for the states when yielding is reached and when the section fails. These points were then connected by straight lines. The curvature of the support section when yielding starts was determined according to (4.12). The slope of the first branch of the moment-curvature relation corresponds to the stiffness of the section before yielding and was determined according to (4.13). This stiffness is referred to as the stiffness based on the state III model.

$$\kappa_{y.sup} = \frac{\varepsilon_{cc.y.sup}}{x_{y.sup}} \tag{4.12}$$

$$EI_{sup} = \frac{M_{y.sup}}{\kappa_{y.sup}} \tag{4.13}$$

where: $\kappa_{y.sup}$ = Curvature of support section when yielding starts

$\varepsilon_{cc.y.sup}$ = Maximum concrete strain in support section when yielding starts

EI_{sup} = Stiffness of support section that corresponds to state III

It would be reasonable in Phase 2 to assume the stiffness according to state II for the span region since this part has not reached yielding. However, it is still recommended to use the stiffness based on the state III model after yielding is reached in any section of the beam. This is due to the fact that the sectional response gradually changes from

state II to state III and the concrete already shows some plastic response before yielding of the reinforcement occurs in any section of the beam. For a small overloading above the yield load it can be justified to assume the stiffness based on the state II model. However, for higher overloading there will normally be significant influence of plastic concrete strain. For the studied beam in Phase 2 the stiffness based on the state III model was assumed although only a small overloading was assumed. The curvature in Phase 2 for section in the support region was determined as in (4.14) and for sections in the span region as in (4.15).

$$\kappa_{2.sup}(x) = \frac{M_{2.x}(x)}{EI_{sup}} \tag{4.14}$$

$$\kappa_{2.span}(x) = \frac{M_{2.x}(x)}{EI_{span}} \tag{4.15}$$

where: $\kappa_{2.sup}$ = Curvature of section in support region in Phase 2

$\kappa_{2.span}$ = Curvature of section in span region in Phase 2

$M_{2.x}$ = Moment in a section in Phase 2

EI_{span} = Stiffness of span section that corresponds to state III

In Phase 2, a plastic hinge forms over the middle support B due to yielding of the reinforcement in this section. The increase of load that causes the plastic rotation of this hinge results also in higher elastic deformations in the span. It was assumed in the analytical analysis that the plastic deformations were concentrated to the plastic hinge. However, in reality there exists a plastic region that is extended within a distance from the middle support, which creates some plastic deformation outside the support section. The total plastic rotation over the middle support B was in Phase 2 equal to the sum of plastic rotations on both sides of the support and is defined as

$$\Theta_{2,sup,left} + \Theta_{2,sup,right} = \Theta_{pl} \tag{4.16}$$

where: $\Theta_{2,sup,left}$ = Plastic rotation over the middle support B on its left side, [rad]

$\Theta_{2,sup,right}$ = Plastic rotation over the middle support B on its right side, [rad]

The plastic rotation over the middle support B on its one side was calculated as

$$\theta_{2.sup.left} = \frac{\int_0^{l_s} \kappa_2(x) \cdot x dx}{l_s} \tag{4.17}$$

where: κ_2 = Curvature of a section in Phase 2

The deflection along the span was determined as

$$f_{2.span}(x) = \theta_{2.A} \cdot x - \int_0^x \int_0^x \kappa_2(x) dx dx \tag{4.18}$$

where: $f_{2.span}$ = Deflection along the span in Phase 2

$\theta_{2.A}$ = Rotation at support A in Phase 2

A parameter called plastic rotation capacity $\Theta_{pl.u}$ was also determined in order to check that the plastic rotations are below this capacity. A design value of the plastic rotation capacity can be estimated according to SS-EN-1992-1-1 and Figure 3.20 in Section 3.5.4 (CEN 2004).

One of other methods that exist to determine plastic rotation capacity $\Theta_{pl.u}$ is the ABC-method, which takes other effects into consideration, such as presence of stirrups in the analysed region and the bond properties between concrete and reinforcement (Lorentsen 1990). The method presented in Eurocode 2 proposes a design value of the plastic rotation capacity $\Theta_{pl.d}$, while the ABC-method provides a mean value. What is common for both these methods is that they take into consideration the *x/d*-ratio of the analysed section and the ductility of the reinforcing steel. The ABC-method was used in this project to make it possible to compare the results of the analytical analysis and the numerical analysis since the beam was analysed assuming mean values of material properties in both types of analysis.

The calculated plastic rotation capacities for the studied beam according to both these methods are presented in Table 4.2 and the detailed calculations can be found in Appendix A Section A.10.

Table 4.2 Comparison of the two methods used to determine the plastic rotation capacity $\Theta_{pl,u}$

Method	Plastic rotation capacity $\Theta_{pl,u}$ [rad] for double-sided plastic hinge
Eurocode 2	0.013 (design value)
ABC-Method	0.039 (mean value)

Detailed calculations for Phase 2 can be found in Appendix A Section A.6.

4.1.4 Phase 3

In Phase 3 the overloading was removed and the beam was again subjected to only the quasi-permanent load of the same magnitude as in Phase 1. Phase 3 is especially interesting due to the changes in moment distribution and deflection. During unloading, the sectional response was assumed to follow the model for state II ignoring any tension stiffening effect. When the beam is unloaded, the elastically deformed span tends to return to the same deflection as in Phase 1. However, that is actually not possible. Since plastic rotation has already developed over the support B, the formed plastic hinge will remain. This means that the formed plastic region will be in conflict with the span that has experienced only elastic deformations and would be able to go back to its initial deflection, if no plastic hinge was there. However, the plastic rotation of the hinge now becomes a new boundary condition that the end rotation of the span must satisfy. This will cause a restraint in the support section and will in fact result in an additional moment, distributed linearly along the beam. This

moment is in this work referred to as restraint moment $M_{restraint}$. The described process is presented in Figure 4.5.

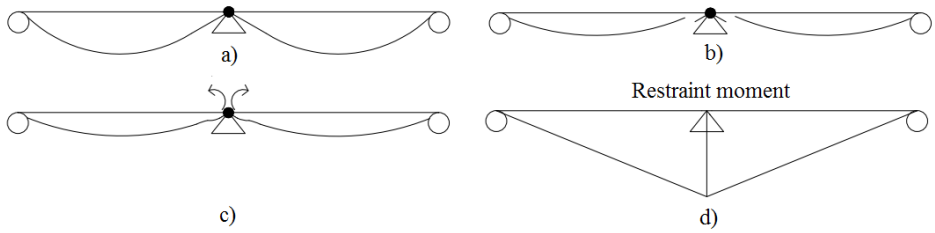

Figure 4.5 *Formation of restraint moment when load is decreases from Phase 2 to Phase 3 a) overloaded beam in Phase 2 with a plastic hinge b) unloaded beam with new boundary condition c) restraint moment occur in the connection between elastic part and plastic hinge d) restraint moment.*

The restraint moment corresponds to the moment needed to fit the elastic part of the beam to the plastic part. Another way to understand this phenomenon is to consider the beam without the outer supports A and C[1]. The created plastic rotation in Phase 2 over the middle support B, see Figure 4.6.a, results in stiff rotations of the beam as presented in Figure 4.6.b. However, since there are supports A and C, the span cannot deflect in this shape. This means that certain forces acting on the beam at supports A and C are needed to prevent this stiff rotation, see Figure 4.6.c, so that the deflected shape of the beam can look like in Figure 4.6.d instead. These forces result in this additional restraint moment $M_{restraint}$ that occurs in Phase 3, see Figure 4.6.e, and this changes the initial moment distribution.

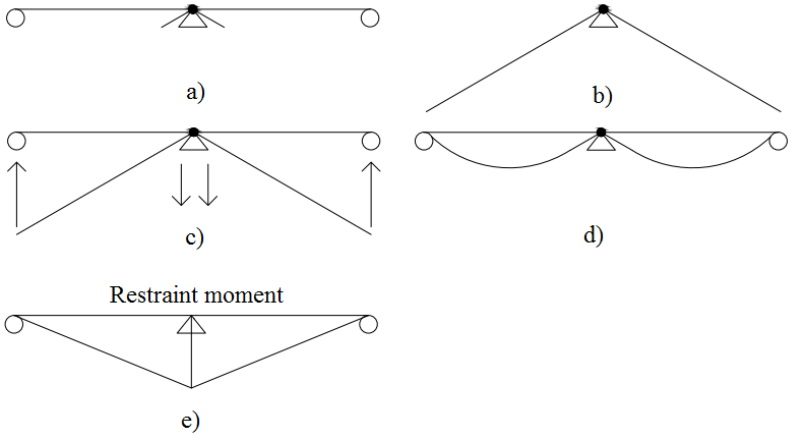

Figure 4.6 *Alternative explanation of the restraint moment a) beam with a plastic hinge b) stiff rotation of the beam without supports A and C c) restraint forces are needed to place the ends of the beam back to the supports d) supports A and C are again applied e) restraint moment.*

The additional moment $M_{restraint}$ changes the shape of the moment diagram along the beam. Due to its occurrence, the support moment is decreased and the span moment increases. This shows how the process of overloading and unloading changes the moment distribution in Phase 3 compared to Phase 1. The changed moment

[1] Mario Plos (Associate professor, Chalmers University of Technology) Meeting 05-04-2016

distribution along the beam results in a changed deflected shape of the beam. The deflection along the span is higher in Phase 3 in comparison to Phase 1, but lower than in Phase 2. This is directly related to the presence of the restraint moment $M_{restraint}$. Furthermore, the plastic hinge developed during Phase 2 remains in Phase 3 and it is assumed that the plastic rotation is equal to the plastic rotation in Phase 2, because the moment is not sufficiently high to change the plastic deformation[1].

In Phase 3 the beam was analysed using the stiffness according to the model for state II. The support moment was determined by iteration such that the end rotation of the span could be obtained as similar as possible to the plastic rotation in Phase 2. The curvature of sections in the support region and the expression for the end rotation at support B are presented in (4.19) and (4.20). The curvature for sections in the span regions was obtained similarly using the moment of inertia for span sections in state II.

$$\kappa_{3.sup} = \frac{M_{3.x}(x)}{EI_{II.sup}} \tag{4.19}$$

$$\theta_{3.sup.left} = \frac{\int_0^{l_s} \kappa_3(x) \cdot x dx}{l_s} \tag{4.20}$$

where:
- $\kappa_{3.sup}$ = Curvature of section in support region in Phase 3
- $M_{3.x}$ = Moment in a section in Phase 3
- $EI_{II.sup}$ = Stiffness of support section in state II
- $\theta_{3.sup.left}$ = Plastic rotation over the middle support B on its left side in Phase 3
- κ_3 = Curvature of a section in Phase 3

The deflection along the span was determined as

$$f_{3.span}(x) = \theta_{3.A} \cdot x - \int_0^x \int_0^x \kappa_3(x) dx dx \tag{4.21}$$

where:
- $f_{3.span}$ = Deflection in a section in Phase 3
- $\theta_{3.A}$ = Rotation at support A in Phase 3

The restraint moment $M_{restraint.sup}$ over the middle support was determined as the difference between the moment over the middle support B in Phase 1 and the support moment over the middle support B in Phase 3, see (4.22).

$$M_{restraint.sup} = M_{3.sup} - M_{1.sup} = 72.574 \text{ kNm} \tag{4.22}$$

where:
- $M_{restraint.sup}$ = Restraint moment in the support section B
- $M_{3.sup}$ = Moment in the support section B in Phase 3
- $M_{1.sup}$ = Moment in the support section B in Phase 1

[1] Björn Engström (Professor, Chalmers University of Technology) Meeting 09-03-2016

Figure 4.7 shows the assumed relations between moment and curvature of the critical section in Phase 3.

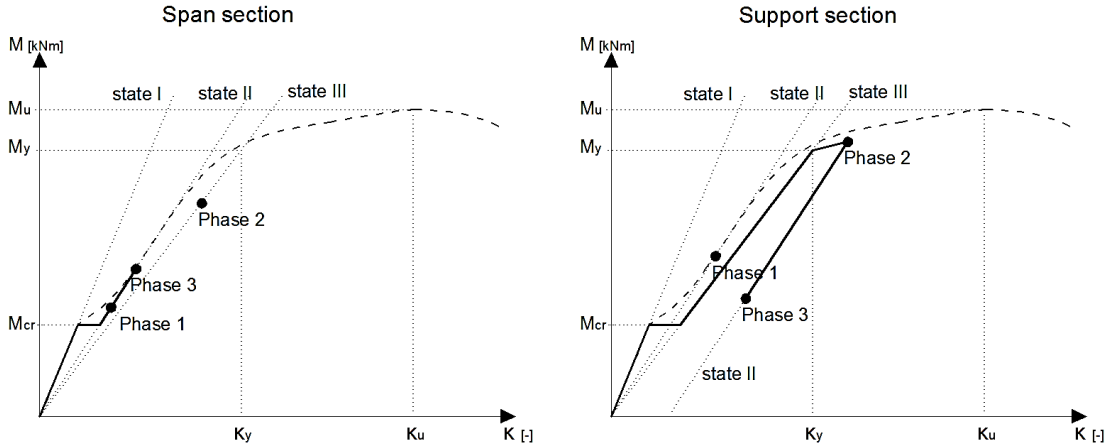

Figure 4.7 *Assumed sectional responses of the critical section in Phase 3. The dotted line indicates the real response while the solid line indicates the simplification implemented in the analysis.*

Detailed calculations for Phase 3 can be found in Appendix A Section A.7.

4.1.5 Phase 4

In the fourth phase the beam is once again overloaded with the same uniformly distributed load of the same magnitude as in Phase 2. Due to this assumption, it was found that the sections have the same response in this phase as in Phase 2, since both the load and the plastic rotation are the same. The deflection in the span was found to be equal to the deflection in Phase 2, as well as the moment distribution. The restraint moment $M_{restraint}$ disappeared in Phase 4, because the deformations in the support region fit together again. The plastic rotations did not change, since the load is of the same magnitude. As these parameters are the same in both mentioned phases, the response of the beam in Phase 4 is the same as if nothing has happened in the past. It is essential to understand here that this is only the case when the load is uniformly distributed and fixed in space in the same way as the beam was loaded in Phase 2. Such behaviour would most probably not be observed in case of a second overloading that would occur only in one of the spans.

The assumed moment-curvature relations of the critical sections are shown in Figure 4.8.

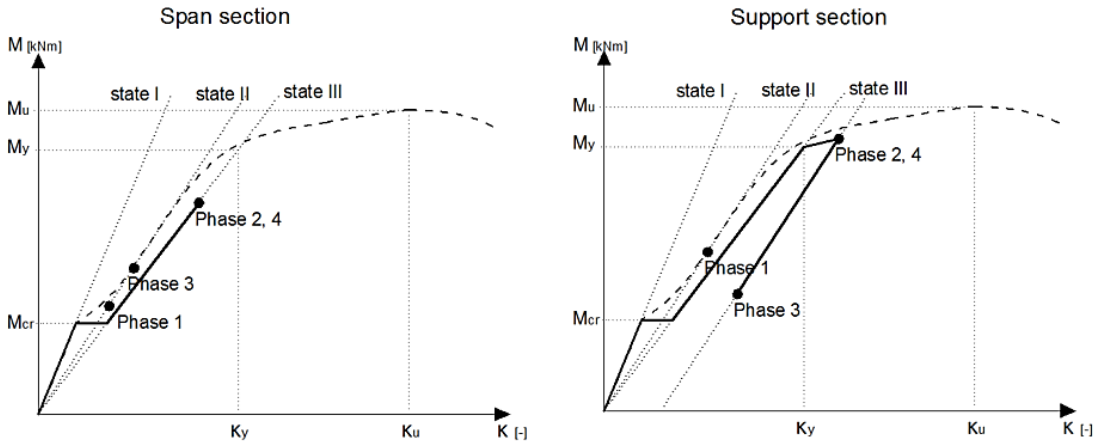

Figure 4.8 *Assumed sectional response of the critical sections in Phase 4. The dotted line indicates the real response while the solid line indicates the simplification implemented in the analysis.*

Phase 4 was analysed with regard to plastic rotation in Phase 2. The value of support moment in Phase 4 was iterated such that the same plastic rotation could be obtained as in Phase 2. The curvature of sections in the support regions was calculated according to (4.24). The stiffness according to the state III model was used. The reason for using the stiffness based on the state III model here is that the beam was analysed for the total load and not only for the load increase. If the beam would be analysed for the load increase only, stiffness according to the state II model should be used, since the plastic deformations has already occurred. The stiffness based on the state III model is explained in Section 3.5.2. The plastic rotation on the left side of the middle support B was determined by (4.25).

$$\kappa_{4.sup}(x) = \frac{M_{4.x}(x)}{"EI_{sup}"} \tag{4.24}$$

$$\theta_{4.sup.left} = \frac{\int_0^{l_s} \kappa_4(x) \cdot x dx}{l_s} \tag{4.25}$$

where:
- $\kappa_{4.sup}$ = Curvature of support sections in Phase 4
- $M_{4.x}$ = Moment in a section in Phase 4
- $"EI_{sup}"$ = Stiffness according to state III model of the support section
- $\theta_{4.sup.left}$ = Plastic rotation over the middle support B on its left side in Phase 4
- κ_4 = Curvature of a section in Phase 4

The deflection along the span was determined as

$$f_{4.span}(x) = \theta_{4.A} \cdot x - \int_0^x \int_0^x \kappa_4(x) dx dx \tag{4.26}$$

where:
- $f_{4.span}$ = Deflection in a section in Phase 4
- $\theta_{4.A}$ = Rotation at support A in Phase 4

Calculations for Phase 4 can be found in Appendix A Section A.8.

4.1.6 Phase 5

Phase 5 concerns loading until a collapse of the beam occurs. Here the load was higher than in all other phases, causing higher moments in the span. All the previous phases were analysed assuming moment-curvature relations with a small inclination of the top branch after yielding. In this phase the maximum moments were assumed to be equal to the moment capacities of the critical sections. Hence, it was assumed that the plastic rotation capacity was sufficient to allow for formation of a collapse mechanism. This approach was implemented into the analysis of the beam to see the influence of the unloading and overloading. As a consequence the deflections in the span were higher in this phase in comparison to the previous ones. The plastic rotation was also increased due to higher load.

The assumed moment-curvature relations of the critical sections are shown in Figure 4.9.

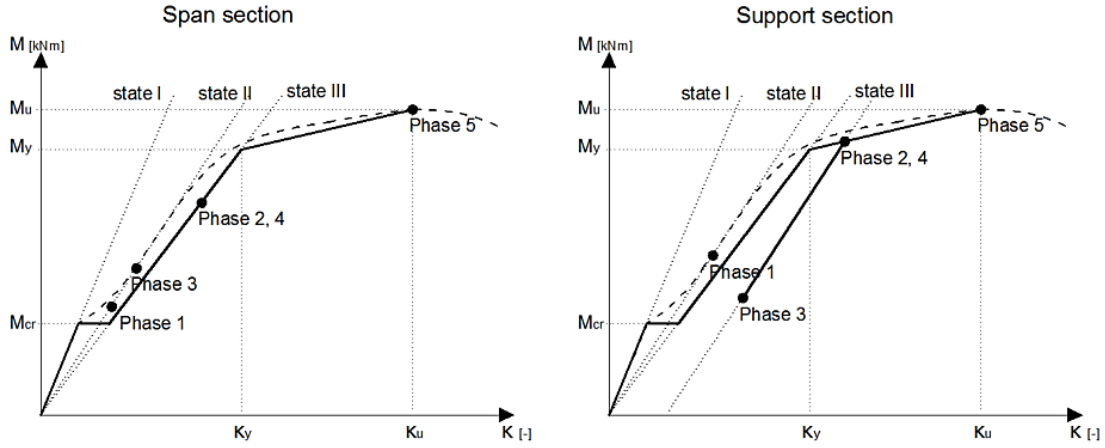

Figure 4.9 *Assumed sectional responses of critical sections in Phase 5. The dotted line indicates the real response while the solid line indicates the simplification implemented in the analysis.*

The analysis was conducted assuming sectional stiffness according to the model for state III for support and span regions respectively. The support moment and the span moment were determined by the moment capacities of the critical sections with respect to concrete strength as well as reinforcement strength and ultimate strains. The curvature of sections in the support region was determined by (4.27). The curvature for sections in the span region was determined similarly. The plastic rotation on one side of the middle support B was according to (4.28).

$$\kappa_{5.sup}(x) = \frac{M_{5.x}(x)}{"EI_{sup}"} \tag{4.27}$$

$$\theta_{5.sup.left} = \frac{\int_0^{l_s} \kappa_5(x) \cdot x dx}{l_s} \tag{4.28}$$

where: $\kappa_{5.sup}$ = Curvature of support sections in Phase 5

$M_{5.x}$ = Moment in a section in Phase 5

$\theta_{5.sup.left}$ = Plastic rotation over the middle support B on its left side in Phase 5

κ_5 = Curvature of a section in Phase 5

The deflection along the span was determined as

$$f_{5.span}(x) = \theta_{5.A} \cdot x - \int_0^x \int_0^x \kappa_5(x) dx dx \tag{4.29}$$

where: $f_{5.span}$ = Deflection in a section in Phase 5

$\theta_{5.A}$ = Rotation at support A in Phase 5

Detailed calculations for Phase 5 can be found in Appendix A Section A.9.

4.1.7 Parameters relationship

The phases described above can also be compared by finding different relationships between various discussed parameters. These relations are presented in Table 4.3.

Table 4.3 Relations between various parameters in the five loading phases.

Phases	Parameters				
	Load q [kN/m^2]	Support moment M_{sup} [kNm]	Max. span moment M_{span} [kNm]	Max. deflection f [mm]	Plastic rotation Θ_{pl} [rad]
Phase 1	q_1	$M_{sup.1}$	$M_{span.1}$	f_1	-
Phase 2	$q_2 > q_1$	$M_{sup.2} > M_{sup.1}$	$M_{span.2} > M_{span.1}$	$f_2 > f_1$	$\Theta_{pl.2}$
Phase 3	$q_3 = q_1$	$M_{sup.3} = M_{sup.1} - M_{restraint.sup}$	$M_{span.3} = M_{span.1} + M_{restraint.span}$	$f_2 > f_3 > f_1$	$\Theta_{pl.3} = \Theta_{pl.2}$
Phase 4	$q_4 = q_2$	$M_{sup.4} = M_{sup.2}$	$M_{span.4} = M_{span.2}$	$f_4 = f_2$	$\Theta_{pl.4} = \Theta_{pl.2}$
Phase 5	$q_5 > q_4$	$M_{sup.5} > M_{sup.2}$	$M_{span.5} > M_{span.2}$	$f_5 > f_2$	$\Theta_{pl.5} > \Theta_{pl.4}$

4.1.8 Results

The analytical analysis was conducted in order to assure that the behaviour of a two span continuous beam, which is subjected to a uniformly distributed load, was understood correctly. Detailed calculations are shown in Appendix A. However the results and their comparisons are also presented in Table 4.4 and Table 4.5.

The first set of results is presented in Table 4.4, which includes the main important parameters concerning Phase 1 and Phase 3. As it is presented, the support moment is lower after unloading in Phase 3, while the span moment is higher. Also, as it can be observed, the deflection *f* in Phase 3 is higher in comparison to the initial phase, Phase 1. A plastic rotation Θ_{pl} remained in Phase 3 is presented in the table after the overloading was removed. The plastic rotations presented in Table 4.4 are the rotations on one side of the middle support B, meaning that the total plastic rotations are of the double magnitudes.

Table 4.4 Results for Phase 1 and Phase 3 in Part 1.

Parameters	Phase 1	Phase 3
q [kN/m]	9.243	9.243
M_{sup} [kNm]	166.374	93.800
M_{span} [kNm]	93.585	122.779
$M_{restraint.sup}$ [kNm]	0	72.574
f [mm]	9.721	15.55
$\Theta_{pl.left}$ [rad]	0	0.002719

Furthermore, the results obtained from the analysis in Phase 2 and Phase 4 are presented in Table 4.5. These two phases are chosen to be compared to each other, since the magnitude of the applied load is the same for both these phases. As it is presented in the table, the magnitudes of support and span moments for both these phases are the same. Also, the deflection *f* and the plastic rotation Θ_{pl} are equal to each other. For detailed calculations the reader is referred to Appendix A.

Table 4.5 Results for Phase 2 and Phase 4 in Part 1.

Parameters	Phase 2	Phase 4
q [kN/m]	35.430	35.430
M_{sup} [kNm]	566.792	566.792
M_{span} [kNm]	358.828	385.828
f [mm]	43.822	43.822
$\Theta_{pl.left}$ [rad]	0.002718	0.002718

A detailed comparison was made between parameters such as moment distribution, restraint moments, plastic rotations and deflections for the analysed phases, what is presented and discussed below.

Moment distribution

The moment distributions along the beam are presented in Figure 4.10. Each line represents the moment distribution for each corresponding phase. As it can be observed, there is a difference between magnitudes of moments for Phase 1 and Phase 3, although the same load is applied. Also, the moments for Phase 2 and Phase 4 cover each other, which means that the moment distributions for these two phases are exactly the same. Furthermore, the moments in the span for Phase 5 are the highest in comparison to all other phases. By plotting the obtained moment distributions for all five phases, an influence of overloading and unloading can be observed, especially by looking at the moments for Phase 1 and Phase 3.

Another thing that can be observed in Figure 4.10, which is also presented by values in Table 4.6, is where maximum span moment occurs. As it can be observed, redistribution of moments takes place when comparing Phase 1 with all the other phases. The section where maximum span moment occurs is the closest to the outer support A for Phase 1. This section with maximum span moment moves away from this support for Phase 2 and 4, even further for Phase 3. Phase 5 corresponds to the ultimate limit state of the studied beam and from this Phase the described distance increases in relation to Phase 4. However it is still somewhat smaller than in Phase 3. For the studied example of beam, the maximum support and span moments are the same in the ultimate limit state, since the moment capacities of the critical sections were chosen to be the same. That the moment capacities were the same resulted in a reinforcement arrangement that gives a constant stiffness along the beam in the cracked state, see Figure 4.2.

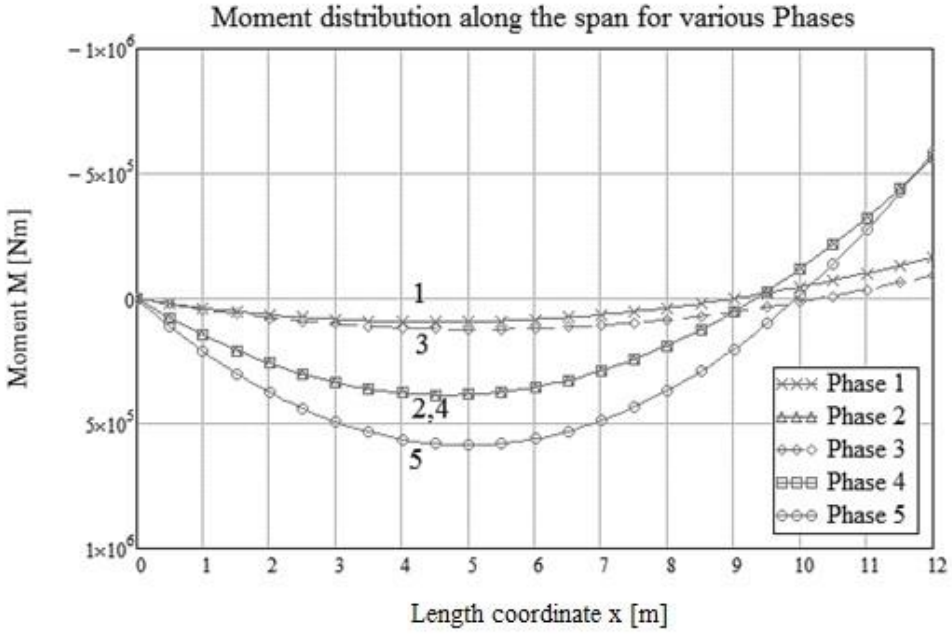

Figure 4.10 Moment distributions along one span of the beam for various loading phases.

Table 4.6 Distance from support A to section where the span moment is maximum.

Phase	x_{span} [m]
Phase 1	4.500
Phase 2	4.667
Phase 3	5.154
Phase 4	4.667
Phase 5	4.971

Deflection distribution

The influence of the temporary overloading can also be seen in the distribution of deflection *f* along the span l_s. These distributions for the different phases are presented in Figure 4.11.The deflection is higher for Phase 3 after overloading in comparison to Phase 1. Also, the deflections are the same for Phase 2 and 4 and they are at their highest in Phase 5.

The section with maximum deflection differs for each of the analysed phases. It is closest to the outer support A for Phase 1. This distance is the highest for Phase 3, smaller for Phase 5 and even smaller for Phase 2 and 4, see Table 4.7. The variation of the maximum deflection section demonstrates the influence of overloading and unloading.

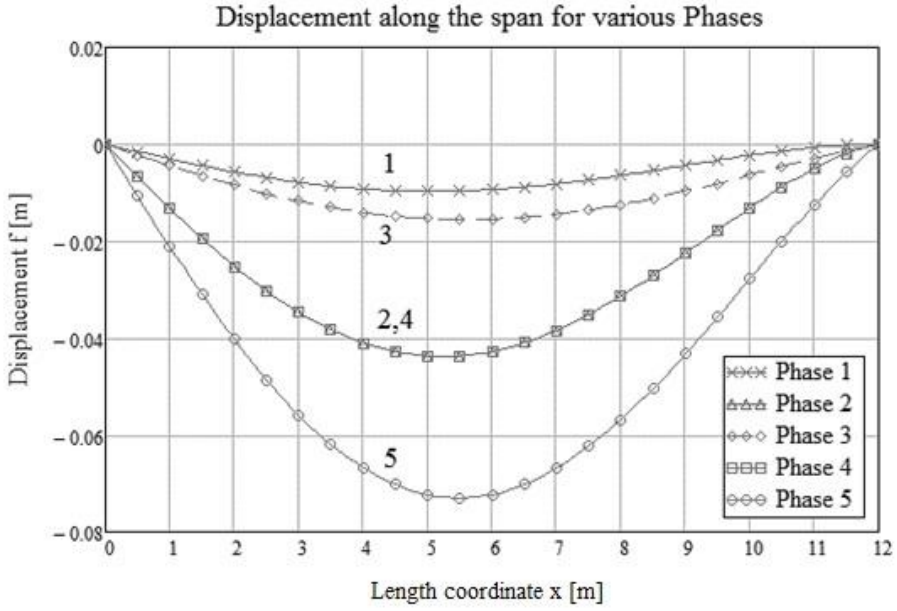

Figure 4.11 Deflection distributions along the span for various loading phases for Part 1.

Table 4.7 Distance from support A to maximum deflection section in the span x_f.

Phase	x_f [m]
Phase 1	5.058
Phase 2	5.232
Phase 3	5.612
Phase 4	5.232
Phase 5	5.487

Plastic rotation

The obtained results showed also the influence of temporary overloading in terms of plastic rotations. The plastic rotations for the five analysed phases are presented in Figure 4.12. As shown in this figure, the plastic rotation is zero for Phase 1. This is obvious, since the reinforcement does not reach yielding at this phase of loading. The plastic rotation that develops in Phase 2 remains during the unloading to Phase 3 and when the structure is reloaded with the same load back to Phase 4, the plastic rotation is still unchanged. The highest plastic rotation in the analysis was obtained in Phase 5, when the collapse occurred. For comparison the plastic rotation capacity was determined according to Eurocode 2 and the ABC-method, see Section 4.1.3. These capacities are indicated in Figure 4.12 with dotted lines. From the figure it appears that the plastic rotation at support B in Phase 5 exceeds the design value given by Eurocode 2. In the further analysis the ultimate load was determined with regard to the limited plastic rotation capacity given by Eurocode 2, see Appendix A Section A.11. This smaller ultimate load was then used in comparison with the ultimate load that was found by the FE analysis, see Section 6.1.1.

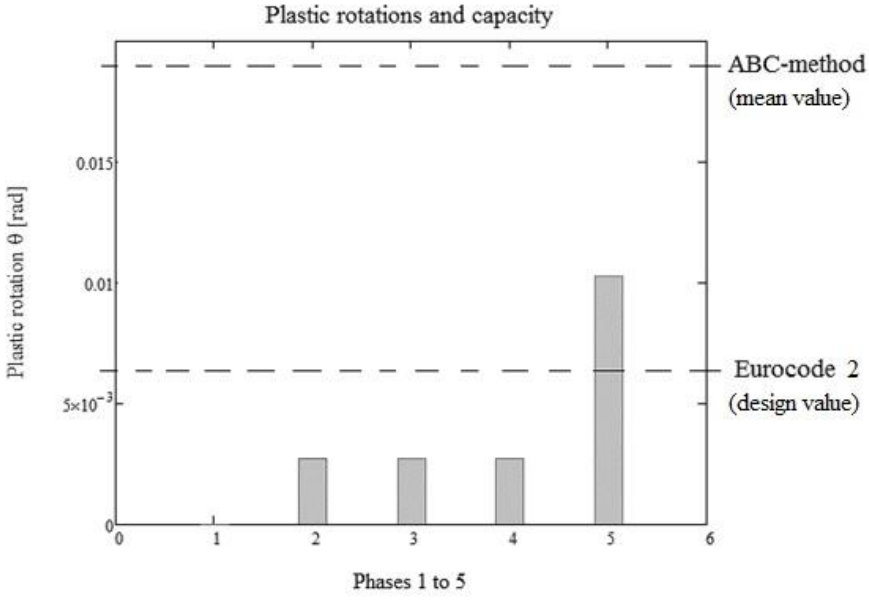

Figure 4.12 Plastic rotations for Phases 1 to 5 indicated by solid bars and the plastic rotation capacities by solid lines.

Restraint moment

As it is described in Section 4.1.3, the studied beam reacts on the temporary overloading by formation of a restraint moment. The obtained difference between the moments in Phase 1 and the moments in Phase 3 is the restraint moment. This restraint moment is plotted in Figure 4.13 and, as it is seen, the moment is highest over the middle support B, indicated in this figure by the point where the length coordinate x is equal to 12m. Furthermore, the figure shows that the restraint moment is of a positive magnitude and, in consequence, contributes to an increased span moment and a decreased support moment in Phase 3, compared with the moments in Phase 1. This is considered to be a correct response, since the plastic rotation developed in Phase 2 is irreversible in Phase 3, which causes conflict between the support section and the span region, see also Figure 4.5.

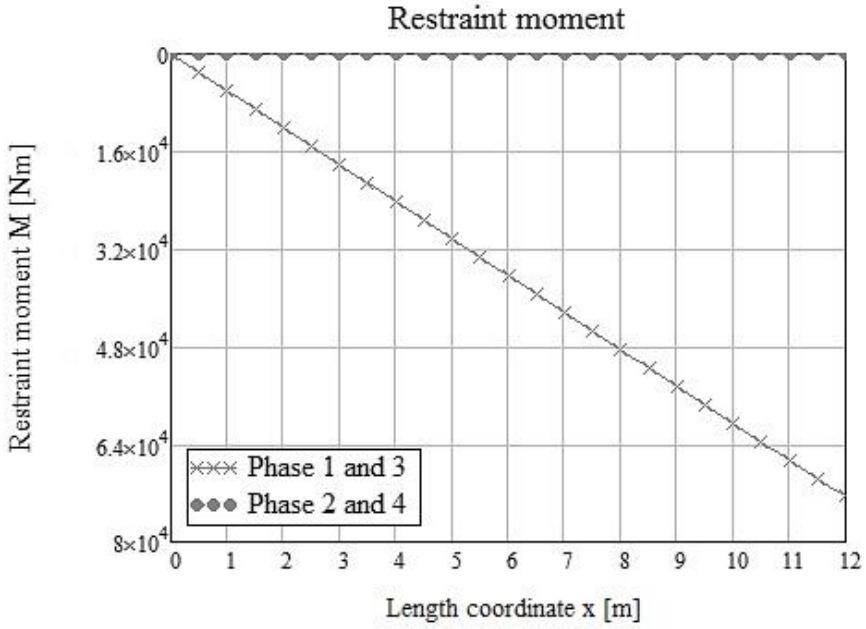

Figure 4.13 Restraint moment developed between Phases 2 and 3 is illustrated. As a comparison the moment difference between Phases 2 and 4 has also been plotted.

Load and deflection

The temporary overloading also influenced the load versus deflection relation. This relationship is shown in Figure 4.14 for all five loading phases. The different phases are indicated by corresponding numbers in the figure. While looking at the deflection in Phase 2 and the curve that corresponds to unloading to Phase 3, an effect of overloading on the beam response can be observed. For all the phases it is the maximum deflection that is shown and due to moment redistribution the maximum deflection occurs in various sections for the different phases. It appears from the figure that the overloading results in a permanent deflection due to plastic deformations. This deflection remains when the beam is unloaded between Phase 2 and Phase 3 and for the same quasi-permanent load, the deflection is higher In Phase 3 than in Phase 1.

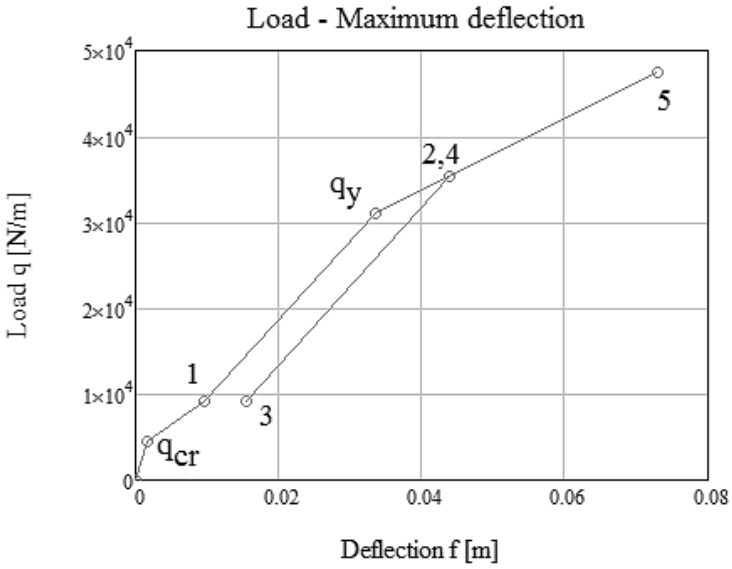

Figure 4.14 Relationship between load and maximum deflection for all loading phases. The numbers indicate the corresponding loading phases and the dots mark the points that have been calculated. Between those points linear relations have been assumed.

4.2 PART 2: Assessment of a damaged beam that has been overloaded in the past

4.2.1 Approach

The behaviour of a two-span continuous beam overloaded with a known uniformly distributed load at different loading phases is described as Part 1 in Section 4.1. This section covers instead the procedure when analysing an existing old beam, which has been overloaded in the past by an unknown distributed load. This case is here referred to as Part 2. This means that the study of the beam began in Phase 3, which is the normal state after overloading where some information could be gathered on site. In Part 2 the past overloading was unknown and a procedure is presented about how to determine this unknown load and its consequences for the future use.

First of all, it is important to verify that the member has been overloaded in the past. Since deflection and crack width are the most reasonable parameters to measure on site, they are most appropriate to use to determine whether an overloading has occurred or not. If the deflection of the member is significantly higher than an estimated deflection for this type of reinforced concrete beam, this is already a sign that the member has been subjected to higher loads than it was meant to carry. The deformation caused by creep and shrinkage must also be considered so the instant deflection caused only by loading can be determined.

Another important parameter is the crack width. It is possible to find the relation between the crack widths observed on site and the plastic rotations, but only if a single crack appears. This may be the case when precast concrete elements are connected to each other across weak joints. However, in a continuous beam that is studied in this work, the connection over the middle support is strong due to high amount of reinforcement in the tensile zone. If a continuous reinforced concrete beam cracks, not only one crack occurs but rather many distributed cracks within a cracked

region. This makes it difficult to find a relation between an observed crack width and the corresponding plastic rotation over the middle support. That is why this parameter may not be used to estimate the magnitude of overloading. The crack width is however still a useful parameter, because it can indicate whether the reinforcement has yielded or not[1]. According to Figure 4.15, there exists a relation between mean crack width and steel stress. The relations in the figure concern single cracks, but can be used approximately also for cracks with normal spacing. For example for a beam made of concrete class C30/37 and 20 mm reinforcement bars of type B500B, a crack width of 1,25 mm indicates that the steel has reached its yield stress, which is equal to 500MPa (Engström 2014). If observed crack widths exceed this value, overloading into the yielding phase in the past can be assumed.

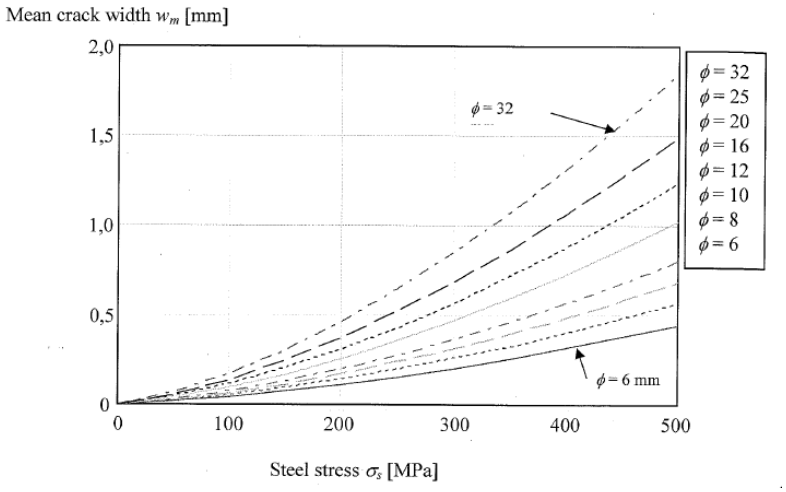

Figure 4.15 Relations between mean crack width and steel stress for single cracks in concrete C30/37 (Engström 2014).

When it is confirmed that the member has been subjected to overload in the past that caused yielding of the reinforcement, an investigation using forensic engineering may begin. In Table 4.8 the loading phases are presented together with the relevant approaches of investigation.

Table 4.8 Various approaches at different phases.

Phase	Approach
Phase 1	Forensic engineering
Phase 2	
Phase 3	Damage discovery
Phase 4	Structural assessment
Phase 5	

[1] Björn Engström (Professor, Chalmers University of Technology) Meeting 13-04-2016

As it can be seen in Table 4.8, the study of an existing beam begins in Phase 3. The current condition of the damaged member is at this phase evaluated. However, to be able to find out what has happened with the beam in the past with regard to loading, a step back to Phase 1 and Phase 2 needs to be taken, which is possible to do using the forensic engineering approach. Next, the future capacity of the beam should be assessed using the structural assessment approach.

As explained in the beginning of this section, the only parameters that can be used to estimate the structural condition of a concrete beam and be measured on site are crack width and deflection. However, as stated above the crack width is not useful in estimation of past overloading and only measurements of the deflection may lead to a solution. Having necessary equipment on site, the deflection of the beam can be measured in many points along the beam. This is very useful in order to plot the deflected shape of the beam on both sides of the support. If the plotted deflection curves on both sides of the middle support do not fit smoothly together, this is a sign of a plastic hinge, see Figure 4.16. Greater number of plotting points increases the accuracy of the deflected shape but as an extra verification the maximum deflection in the span can also be estimated by calculations. The measuring of the deflection along the beam can be performed by special advanced instruments such as Faro Focus 3D. This is a laser scanner equipment used for this type of situations. This instrument measures 976,000 points per second with a ranging error of ±2mm and it is a suitable tool for forensic investigations[1].

In cases when the deflected shapes of the spans do not fit together over the middle support, the plastic rotation can be determined as the angle between the extended tangent lines of the deflection curves at the support section, see Figure 4.16.c.

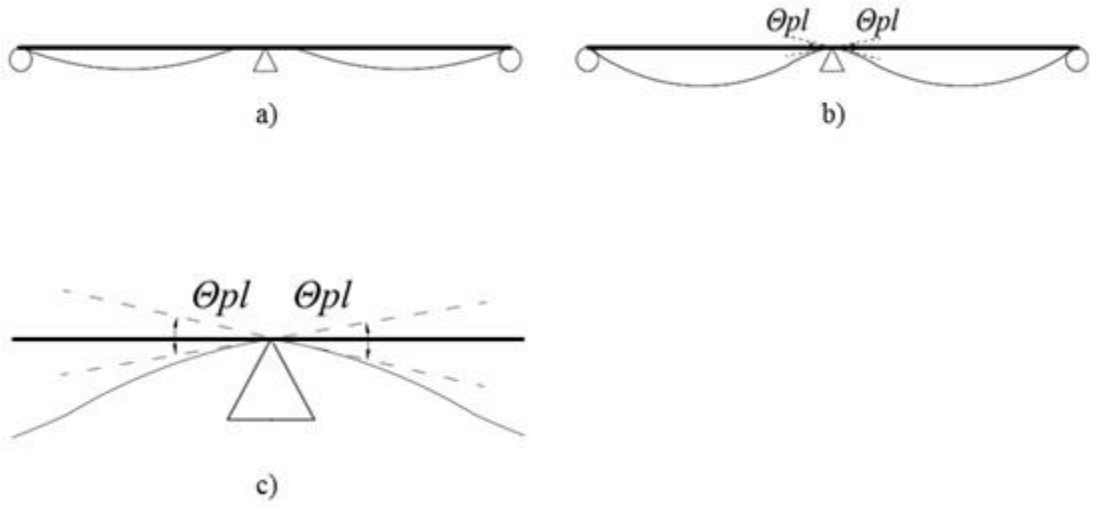

Figure 4.16 Deformation along a two-span continuous beam loaded with a uniformly distributed load, a) deformations fit together, which means no plastic rotations over the middle support b) c) deformations do not fit together as it is indicated by the dotted line, which means that there is a plastic rotation over the middle support.

It is important to note here, that due to the fact that this analysis is based on short term response of the beam, without consideration of long term effects, the total measured

[1] Erik Skansebo (Civilengineer, Norconsult AB) Meeting 23-05-2016

deflection needs to be decreased with an assumed value of a deflection coming from the creep and shrinkage of concrete.

In the studied example of an existing continuous beam, the maximum deflection measured on site and reduced with regard to creep and shrinkage is assumed according to expression (4.30). In expression (4.31) an assumed value of plastic rotation is determined, which is evaluated from the plotted deflection shape. These values are important parameters in the further forensic investigation. It is important to note that the deflections due to creep and shrinkage were not determined by calculation in this work. Since the deformed shape was not measured in reality, the values for the maximum deflection and estimated plastic rotations were just chosen to reasonable values.

$$f_{site} = 18\text{mm} \tag{4.30}$$

$$\Theta_{3.sup.left.measured} = 4 \cdot 10^{-3} \text{ rad} \tag{4.31}$$

Having the plastic rotation estimated from the deformed shape of the beam, other important parameters in Phase 3 can be determined. The moment distribution can be determined by assuming and iterating a moment over the middle support until the plastic rotation in Phase 3 is equal to the observed plastic rotation. Then, the curvature distribution along the span can be determined according to (4.32) and (4.33), for span and support regions respectively. Plastic rotation can be found using (4.34).

$$\kappa_{3.sup}(x) = \frac{M_{3.x}(x)}{E_c \cdot I_{II.sup}} \tag{4.32}$$

$$\kappa_{3.span}(x) = \frac{M_{3.x}(x)}{E_c \cdot I_{II.span}} \tag{4.33}$$

$$\theta_{3.sup.left} = \frac{\int_0^{l_s} \kappa_3(x) \cdot x \cdot dx}{l_s} = 4 \cdot 10^{-3} \tag{4.34}$$

Since the plastic rotation in Phase 3 is estimated by using measured deflections on site, a verification of the estimated plastic rotation is preferred to strengthen this assessment. This verification can be a comparison between the maximum deflection measured on site, reduced with regard to creep and shrinkage, and the maximum deflection calculated for Phase 3, according to (4.36) based on the curvature along the beam from (4.32) and (4.33).

$$f_{3.span}(x) = \theta_{3.A} \cdot x - \int_0^x \int_0^x \kappa_3(x) dx dx \tag{4.36}$$

When the plastic rotation in Phase 3 is known and while taking into consideration the fact that the plastic rotation is the same in Phase 2 and Phase 3, see Section 4.1 for details, the load that has caused the overloading can be found. The support moment that was reached during overloading is higher than the yielding moment. Knowing that, the support moment over the middle support in Phase 2 can be iterated until the

same plastic rotation as in Phase 3 is obtained, taking into consideration the stiffness according to the state III model. The magnitude of the load can be determined by using the bilinear relationship between the moment-curvature, as described in Section 3.5.2. As the moment increases linearly after the yielding moment is reached, and the ultimate load depends on the sectional capacities, the load can be found using the proportions of the moment-curvature relationship. The moment distribution along the beam can be determined according to (4.37). As it is shown in (4.38) and (4.39) the stiffness based on the state III model is used in the calculation of curvature in support and span regions. Equation (4.40) shows how the plastic rotation is calculated for Phase 2, which should agree with the measured plastic rotation in Phase 3.

$$M_{2.x}(x) = \left(\frac{q_2 \cdot l_s}{2} - \frac{M_{2.sup}}{l_s} \right) \cdot x - \frac{q_2 \cdot x^2}{2} \tag{4.37}$$

$$\kappa_{2.sup}(x) = \frac{M_{2.x}(x)}{EI_{sup}} \tag{4.38}$$

$$\kappa_{2.span}(x) = \frac{M_{2.x}(x)}{EI_{span}} \tag{4.39}$$

$$\theta_{2.sup.left} = \frac{\int_0^{l_s} \kappa_2(x) \cdot x \cdot dx}{l_s} = 4 \cdot 10^{-3} \tag{4.40}$$

The damage discovery takes place in Phase 3. The load that acts on the beam in Phase 3 is known, since it is the present load at the discovery stage. However, for Phase 1 it is reasonable to assume that it is the quasi-permanent load related to the previous use of the building. It is possible that the beam is not subjected to the same loads at the phase of discovery, since some of the loads could have been removed. However, in this project it was assumed that the load in Phase 1 can be defined as a quasi-permanent load and that the load in Phase 3 is the same. As described in Section 4.1, there is a difference between the moment distributions in Phase 3 and Phase 1. The support moment was higher in Phase 1 than in Phase 3, and the difference depends on the restraint moment $M_{restraint}$. The restraint moment can be found as the difference between the moments in Phase 1 and the moments in Phase 3.

4.2.2 Results

Also for this part of the study an analytical analysis was conducted and the calculations are presented in Appendix B. The same quasi-permanent load was assumed as in Part 1. However, to obtain some differences in comparison to the study in Part 1 which is presented in Section 4.1, another magnitude of load in Phase 2 respectively Phase 4 was used. This load was still chosen such that yielding of the reinforcement was obtained in the support section in Phase 2. The same amount of reinforcement as well as the same material and cross sectional properties were used as in Part 1 which is presented in Section 4.1. The same type of response of the beam was observed for this part of the analysis as in Part 1, see Table 4.9 and Appendix B for details.

The comparison of parameters obtained for Part 2 shows the same relations as the analysis conducted in Part 1. The deflection for Phase 3 is higher in comparison to the deflection in Phase 1. The restraint moment is higher than the restraint moment in Part 1 in Table 4.4. This agrees with the theory that higher overloading causes larger plastic rotation over the middle support, which prevents the deformation of the span to return to its original shape even more. Hence, the restraint moment that occurs is larger in Part 2 than in Part 1. The results for Phase 2 and Phase 4 are not shown in this section, since they correspond well to the corresponding results in Section 4.1 and Table 4.5.

Table 4.9 Results for Phase 1 and Phase 3 in Part 2.

Parameters	Phase 1	Phase 3
q [kN/m]	9.243	9.243
M_{sup} [kNm]	166.374	59.600
M_{span} [kNm]	93.585	137.908
f [mm]	9.721	18.378
$\Theta_{pl.left}$ [rad]	0	0.004

The moment distributions are shown in Figure 4.17 for all phases in this part of the study, when the load is assumed to be unknown in the beginning.

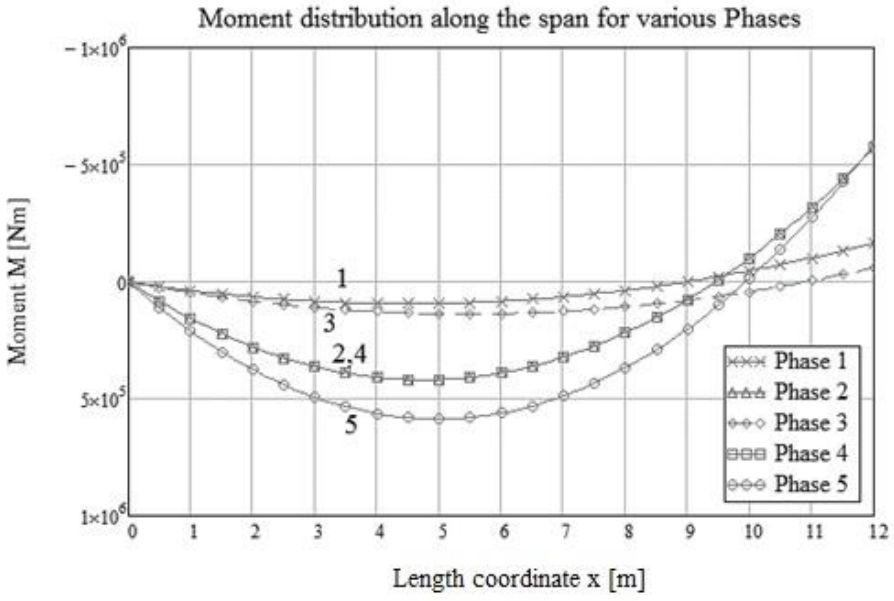

Figure 4.17 Moment distributions along the span for various loading phases in Part 2.

Another result obtained in this part is the load versus deflection relation, see Figure 4.18. As the magnitude of overloading was higher in this analysis in comparison to the example in Part 1, the difference in deflection between Phase 1 and Phase 3 for

the same quasi-permanent load combination was higher in comparison to the corresponding result obtained in Part 1 in Section 4.1.

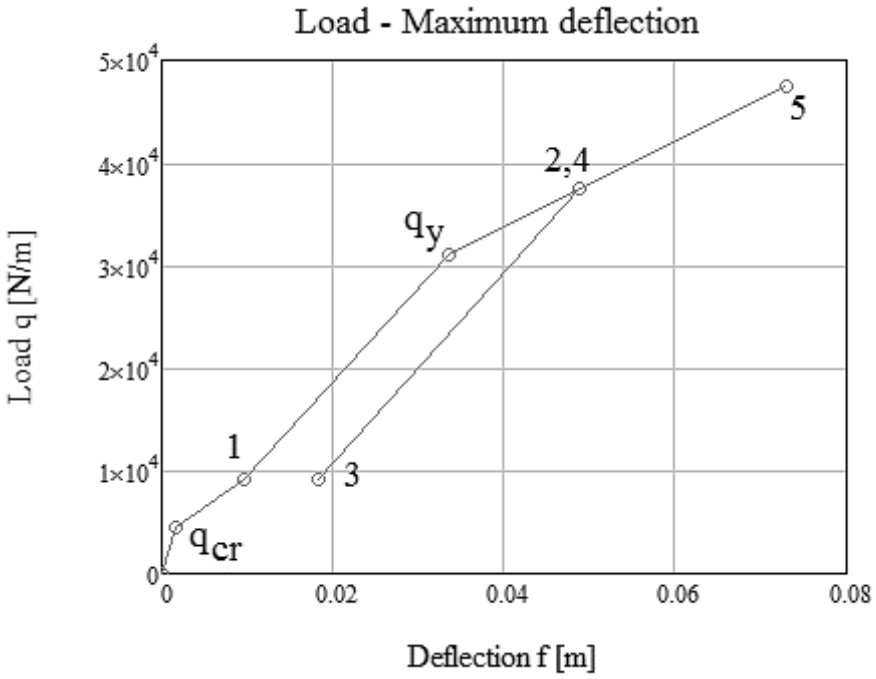

Figure 4.18 Relation between load and maximum deflection for various phases. The numbers indicate the corresponding loading phases and the dots mark the points that have been calculated. Between those points linear relations have been assumed.

5 Numerical analysis using the finite element method

Finite element method (FE method) is a useful tool to analyse structural behaviour on a more advanced level. In this work, this analysis was conducted using a commercial FE program called DIANA TNO (version 9.6) with the help of the processor FX+ for DIANA TNO (version 3.3.0). FE modelling was used in this work to analyse the structural behaviour of a two-span continuous beam with the same properties as in the analytical analysis and also to compare the results from the FE analysis with the results obtained by the analytical method. DIANA TNO was chosen to be the modelling program in this project because it can analyse a beam with consideration of its non-linear behaviour. It was also possible in this program to apply the loading and unloading without any breaks and it is also possible to study the behaviour of the beam in many loading steps.

Firstly, a linear analysis was performed for both plain and reinforced concrete to make sure that the model acts correct. After that, non-linear analysis was conducted.

Furthermore, it was decided that the model should be able to describe bending failure and yielding of reinforcement. Since crack pattern was not needed, beam elements were assumed to be sufficient in the modelling.

The structure was designed as a two-span continuous beam and simply supported, as it is indicated in Figure 5.1. The beam was modelled as 700mm high and 300mm wide, meaning that the modelled beam was of the same geometrical properties as the beam in the analytical analysis.

5.1 Modelling choices

The beam was assumed to be placed on three supports and thus the model is not computationally demanding and no symmetry of the beam was necessary to use. The boundary conditions were modelled according to Figure 5.1. The movement was prevented in the vertical direction in supports A and C, and the translation in support B was fixed in both vertical and horizontal direction.

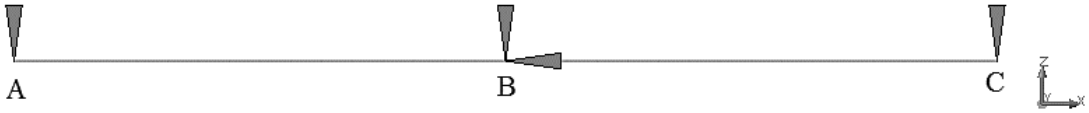

Figure 5.1 Boundary conditions in the modelled beam.

Material properties

Concrete of class C30/37 was used with the same material parameters as in the analytical analysis, see Table 5.1.

Table 5.1 Concrete parameters used as input data in FE analysis.

Concrete compressive mean strength $f_{c,mean}$ [MPa]	38
Tensile strength $f_{t,mean}$ [MPa]	2.9
Modulus of elasticity of concrete E_{cm} [GPa]	33
Poisson ratio for concrete ν	0.2
Concrete density ρ_c [kg/m^3]	2500

Total strain based crack model was used as the material model to describe the material response correctly. Rotating crack orientation was chosen with a mean crack band width of 0.092m, see Appendix C for detailed calculation of this width. Hordijk tensile curve was used with tensile fracture energy G_F of 75 N/m. Also, to describe concrete in compression, Thorenfeldt curve was chosen.

For the reinforcing steel, class B500B was chosen with properties presented in Table 5.2. The steel response was chosen as uni-axial elastic-ideally plastic. Moreover, yield criterion according to von Mises was chosen.

Table 5.2 Reinforcing steel parameters used as input data in FE analysis.

Steel yielding strength f_{yk} [MPa]	500
Modulus of elasticity of steel E_s [GPa]	200
Poisson ratio for steel ν	0.3

Reinforcement modelling

Since the analysis was not based on component level, the reinforcement was modelled as embedded reinforcement, as bars in beam elements, see Figure 5.2. Moreover, no bond-slip relation between the reinforcement and the concrete was applied, meaning that full interaction was assumed between the reinforcement and the concrete.

The same reinforcement amount was used in the modelling as in the analytical analysis, see Chapter 4 and Figure 4.1.

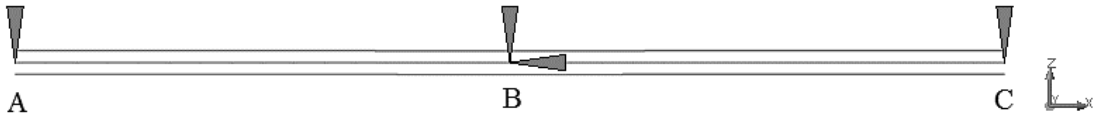

Figure 5.2 Arrangement of reinforcement.

Loading

Both self-weight and variable load were applied as uniformly distributed. The same magnitudes of loads were used in the modelling as in the analytical analysis, see Chapter 4.1 and Appendix A for details.

An essential part in the FE modelling was application of changing loading with consideration to the five loading phases. First of all, the beam was needed to be

loaded until quasi-permanent load combination was reached and then further loaded until yielding of the reinforcement started. To be able to do that, execute blocks were defined in DIANA TNO. The increments for the load to reach Phase 1 were set to 0.05 for 20 steps, such that the entire load could be applied. Next, another uniformly distributed load was applied such that the beam could be loaded little more than the point when yielding of the reinforcement in the middle support section occurred. This load was chosen to 35.43 kN/m. This means that if the load for quasi-permanent load combination was 9.243 kN/m, an additional load of 26.187 kN/m was needed to be applied in order to reach Phase 2. This was done by applying increments of 0.05 for 17 steps. Next, as the beam was supposed to be unloaded, this additional load was removed using increments of -0.05 for 17 steps. Having the beam unloaded, it was loaded again by the same load of 26.187 kN/m, such that the response at the same point before unloading and after reloading could be compared with each other. Lastly, the beam was loaded even more with increments of 0.02 for 50 steps. However, the failure was reached before all the 50 steps were applied and the model stopped at that moment.

The number of iteration steps were set to be 100 for all of the execute blocks that represents the five different phases. Energy convergence norm was chosen in the analysis.

The load that led the sectional response in support B to its plastic response was carefully chosen so that it would correspond to the same load that was used in the analytical analysis, see Chapter 4 and Appendix A. The principle of loading is shown in Figure 5.3.

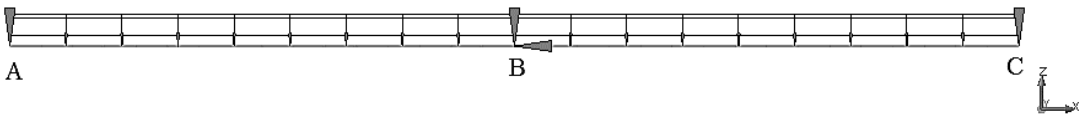

Figure 5.3 Uniformly distributed load along the whole beam.

Mesh

The modelled beam was meshed such that one span was divided into 16 elements, giving 32 elements in total along the beam length, see Figure 5.4. No denser mesh was decided to be needed. It was also considered that the Thorenfeldt curve is based on a test where 300mm long cylindrical elements are used. In FE modelling each element was 750mm. This means that the compressive curve should be adjusted using for example a length scale parameter called "LTHORE". However, since the element size in this work is larger than the mentioned 300mm, the original compressive curve was kept. It was estimated that the adjustment could only give better results in case of smaller element size than 300mm. Thus such modification would not have any significant impact on the results in the modelling.

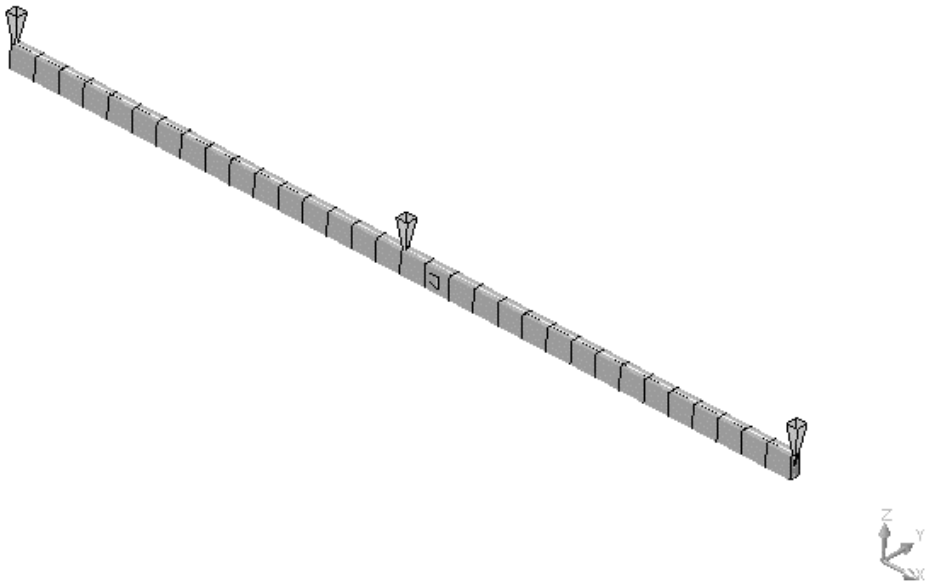

Figure 5.4 Mesh used in the FE modelling.

Integration and iteration method

Two integration points along one element length were used with Gauss integration rule. Moreover, 11 integration points were implemented along the height of one element using Simpson integration rule. This means that the sixth integration point was in the middle of the cross section and the remaining ten integration points were distributed equally towards the top and the bottom of the cross-section. To determine the concrete compressive stress in a section, an integration point at the compressed edge was chosen.

5.2 Output data

The iteration method chosen for this analysis was the BFGS "secant" iteration method, together with the tangential stiffness as a starting option for each new step.

The result from the analysis in DIANA TNO can be presented as an output in DIANA TNO, but it can also be exported as a "Tabulated" file and as a file imported into FX+ for DIANA TNO using "Midas for FX+". In DIANA TNO the obtained results can easily indicate whether the reinforcement has reached yielding or not in the middle support section in Phase 2. However, in this software the data can only be found for the sections where the highest and lowest values appear, for example reinforcement strain and stress in the support. This is considered as a disadvantage if the results obtained in all the sections should be plotted in graphs. In order to determine values for all elements and nodes along the beam and to plot graphs for other important parameters, the software FX+ for DIANA was used. Here can also the results for different load steps be selected and plotted. Although it was the result from the analysis in the DIANA TNO software that was imported into the FX+ for DIANA program, an observation has been made that the imported and "original" results do not always agree with each other. Therefore the result from DIANA TNO was also exported as a "Tabulated" file.

In order to read the result from the "Tabulated" file and create graphs, a script in Matlab was created where parameters like deflection, moment, steel stress and strain, concrete stress and strain, reaction forces and rotations were predefined as output data. To simplify the output data from the "Tabulated" file several files of this type

were created, each with the parameter of interest that was chosen by a predefined function called "result selection". This function explains for the program which parameter to calculate. The first file includes the deflection values for the nodes in the spans for all load steps with the "result selection" according to Table 5.3. It also contains the strain and stress for the reinforcement bars in the top middle part of the beam and in the bottom over the span. The most critical section in the bottom of the span varies depending on whether it is the moment or deflection that is checked. Also the critical section varies when the load changes and in this project the deflection was checked in the node where the highest value was obtained at failure. The second "Tabulated" file was created to determine the moment distribution along both spans for the load steps corresponding to all the five phases. The "result selection" is shown in Table 5.3. In the third "Tabulated file" the reaction forces were presented for the nodes over the three supports. The last file was created to determine the deflection along both spans for the load steps corresponding to all the five phases.

Table 5.3 The selected results in DIANA TNO used to obtain the desired parameters while using the Matlab script.

Parameters	Result selection	Direction
Deflection f [mm]	Displa Total Transl Global	z-direction
Moment M [kNm]	Stress Total Moment Global	y-direction
Reaction forces [N]	Force Reacti Transl Global	z-direction
Stress σ [MPa]	Stress Total Cauchy Local	xx-direction
Strain ε	Strain Total Green Local	xx-direction
Rotation Θ [rad]	Displa Total Rotati Global	x,y,z- direction

5.3 Results

The FE modelling was performed mainly for comparison with the analytical analysis. In this section the result for the overloaded beam analysed in DIANA TNO is presented. As described before, the input data for FE analysis are the same as in the analytical analysis.

The first set of results is presented in Table 5.4. This table contains comparison of the results from Phase 1 and Phase 3. It was decided to compare these results to each other since the applied load in these two phases was the same. An extra check of the loads acting on the beam was done by summing up all the reaction forces acting in the support sections and dividing them by the length of the beam. Therefore the loads presented in Table 5.4 and 5.5 are the exact values that DIANA TNO used during the process of analysis. As it can be seen in Table 5.4, the load q used in each of the discussed phases is the same. As the values show, the support moment obtained in Phase 3 is lower in comparison to the support moment obtained in Phase 1. A reverse effect is obtained in case of comparison of span moments, where the span moment obtained in Phase 3 is of a higher magnitude compared to Phase 1. Also, the maximum deflection for the span section is higher in Phase 3 compared to the initial

phase, Phase 1. With consideration of the fact that the stresses and strains were below the yielding limit in Phase 1 it is understandable that the magnitude of the plastic rotation is equal to zero. Since the analysed beam in Phase 3 was again subjected to the quasi-permanent load after unloading from Phase 2, the developed plastic rotation in Phase 2 should remain. This is why the obtained plastic rotation in Phase 3 is higher than zero.

Table 5.4 Results for Phase 1 and Phase 3.

Parameters	Phase 1	Phase 3
q [kN/m^2]	9.244	9.244
M_{sup} [kNm]	150.900	116.700
M_{span} [kNm]	99.39	112.200
$M_{restraint.sup}$ [kNm]	0	34.2
$M_{restraint.span}$ [kNm]	0	12.81
f [mm]	3.7	14.0
$\Theta_{pl.left}$ [rad]	0	0.001427

Furthermore, a set of results with parameters referred to Phase 2 and Phase 4 is presented in Table 5.5. The parameters in these two phases are compared to each other since the applied load in Phase 2 and Phase 4 is of the same magnitude and distribution. As it can be observed in Table 5.5, all the shown parameters are almost equal to each other. Even though the loading history is different for both these phases, the values are the same as if the beam has not been subjected to any unloading and reloading.

Table 5.5 Results for Phase 2 and Phase 4.

Parameters	Phase 2	Phase 4
q [kN/m^2]	35.433	35.437
M_{sup} [kNm]	588.200	588.300
M_{span} [kNm]	377.300	377.300
$M_{restraint.sup}$ [kNm]	0	0.1
$M_{restraint.span}$ [kNm]	0	0
f [mm]	43.6	43.6
$\Theta_{pl.left}$ [rad]	0.001416	0.001416

The parameters presented in Table 5.4 and Table 5.5 are the main factors which were used for the comparison between the analysed phases. Furthermore in this section, these parameters are discussed in detail.

A general result obtained in FE analysis is the global deformation and an overview of the analysed beam can be seen in Figure 5.5. The beam has deformed in a usual way, where the middle support B has remained on its initial place. The spans have deflected symmetrically in comparison to each other, as a resultant of the uniformly distributed load with a constant magnitude along the beam.

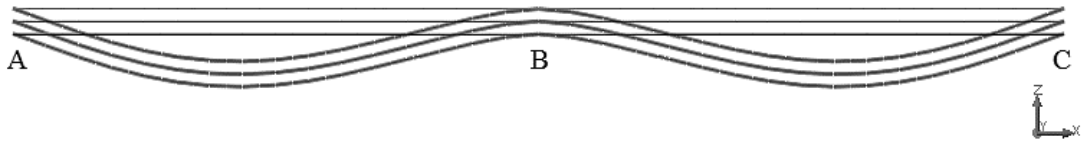

Figure 5.5 Global deformation of the analysed beam in Phase 3.

Moment distribution

The first essential indicator of a change in the structural response during application of the various loading phases is the moment distribution. The obtained moments along the beam are presented in Figure 5.6 for all five phases. As it can be seen, the moments for Phase 2 and 4 are equal to each other. The moments are at their highest in Phase 5. The difference between the moment distribution for Phase 1 and Phase 3 is relatively small but the difference can be seen in Figure 5.6. The support moment for Phase 1 is higher in comparison to Phase 3 while the span moment is lower in Phase 1 when compared to Phase 3. This is the resultant of the overloading and unloading process, under which a restraint moment occurs, described in detail in Section 4.1.3. Figure 5.6 also shows that plastic redistribution of moments occur while yielding of the reinforcement in the middle support B is reached. This can be seen for example by looking at the support moment that does not increase after Phase 4, while the span moment still increases.

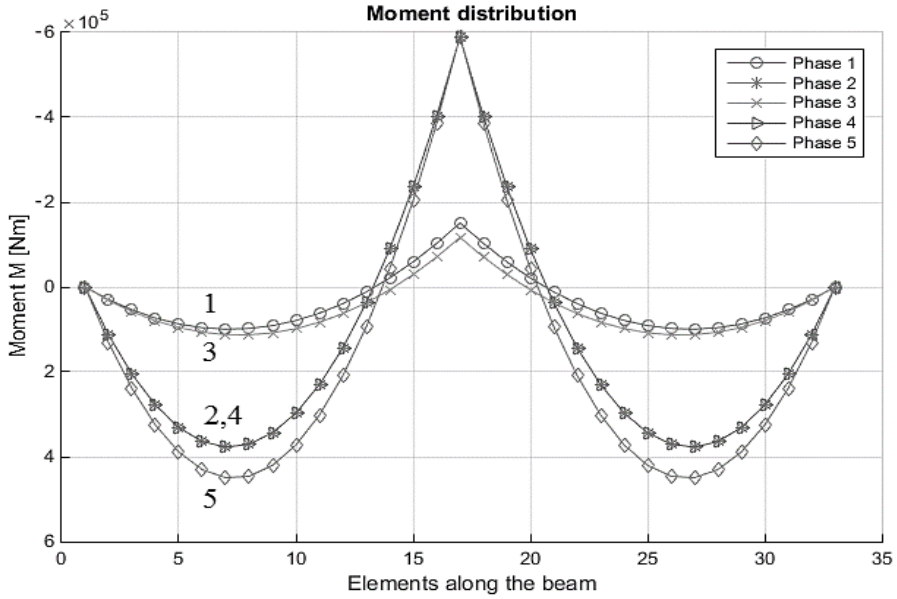

Figure 5.6 Moment distribution along the beam for all five phases.

Restraint moment

The restraint moment and the reason for its occurrence are thoroughly described in Section 4.1.3. The obtained difference in the FE analysis between moment in Phase 1 and Phase 3 is plotted as a moment distribution in Figure 5.7. As it is shown there is no occurrence of restraint moment between Phase 2 and Phase 4, since this moment develops only under unloading process from Phase 2. It can be seen that the restraint moment is at its highest over the middle support B which corresponds to element 16 in Figure 5.7. This moment decreases from the support linearly towards the outer supports A and C, which correspond to element 0 and element 32 respectively. This restraint moment is positive and it contributes to an increased positive value of the support moment and a decreased positive magnitude of moment in the span. It is important to notice, that this restraint moment develops when the beam is unloaded from Phase 2, which is the phase where yielding of the reinforcement in the middle support section occurs. This restraint moment decreases gradually while reloading to Phase 4.

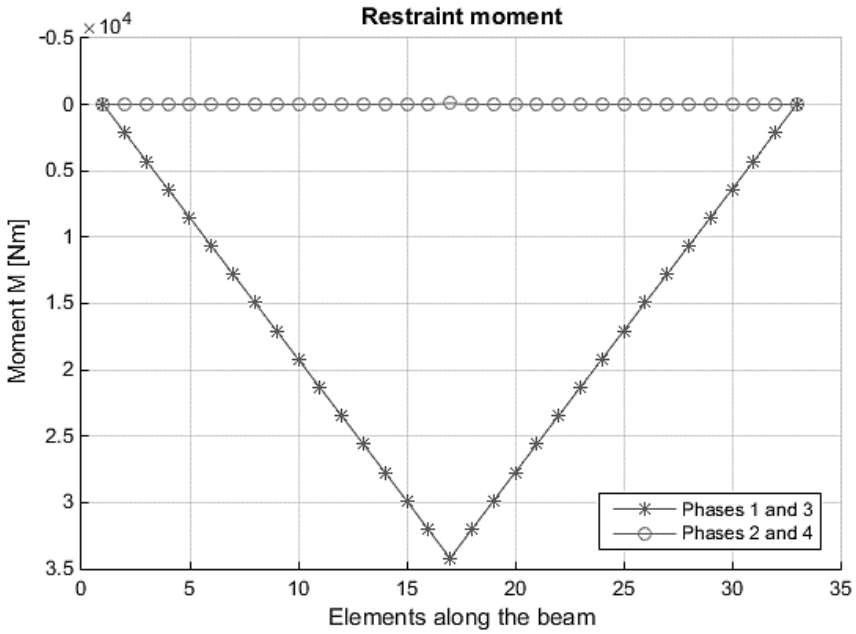

Figure 5.7 Restraint moment along the beam between Phase 1 and 3. As a reference the difference in moment is plotted between Phase 2 and 4.

Deflection distribution

Another important factor that is shown in Figure 5.8 is the deflection distribution along the beam. This distribution indicates the changing sectional and material response under the change of load magnitude. As it is shown, the deflections in Phase 2 and Phase 4 are equal to each other. This is interpreted as no changes in the material and structural response have occurred after the process of overloading and unloading. The deflections are higher in Phase 3 in comparison to Phase 1, which is a result of the temporary overloading in Phase 2. It can be seen that the overloaded beam does not show decreased rigidity in consideration of the applied loads since the deflections in Phase 2 and Phase 4 are the same.

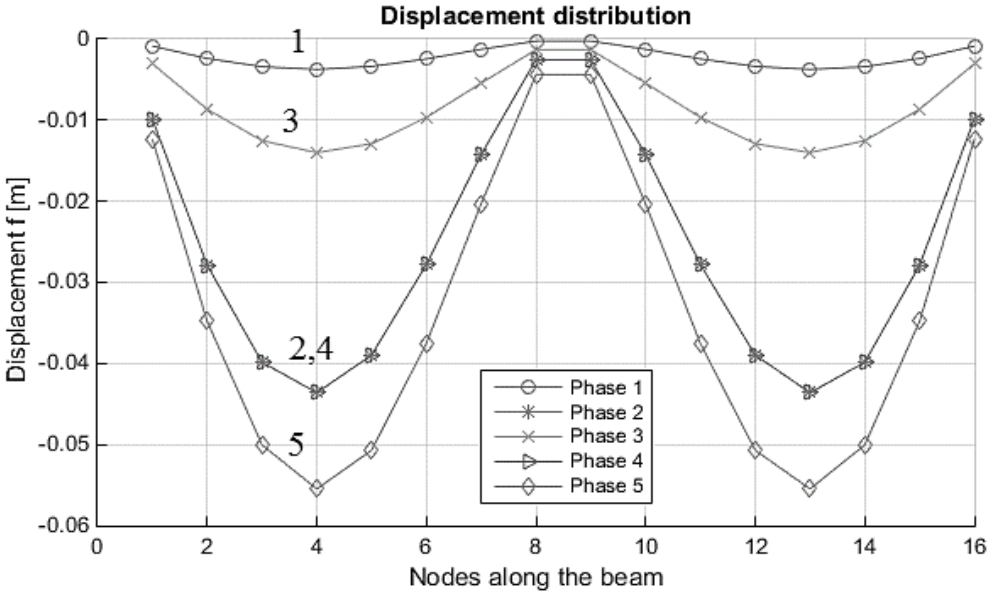

Figure 5.8 Deflection distribution along the beam for all five analysed phases.

Stress and strain for concrete

An important part of the FE analysis was to check if the materials used to model the beam behave in a correct way while subjected to a changing magnitude of load. Stress and strain relations for concrete were checked to assure that the material shows a realistic response while subjected to overloading. The stress was plotted against the strain and the relation between these two parameters is shown in Figure 5.9.a, for the middle support section. The support section was especially of interest due to the fact that it is in this section where a development of plastic rotation occurs while the overloading happens. Concrete is a much stronger material when it is subjected to compression in comparison to tension and Figure 5.9.a shows the material response only for compression. As it is indicated by the graph, the stress reaches its maximum at 38MPa and its corresponding strain is close to 0.0017. It can also be seen that at around 20MPa the curve deviates from a straight line and the concrete behaves non-linearly in the studied section. Around the value of 37 MPa the curve changes direction and it drops until stress of around 13MPa is reached. This change in sectional response indicates the point of unloading. Next the line follows the same path of its drop until the same stress of 37MPa at the same point is reached, which corresponds to both Phase 2 and Phase 4. The difference that can be seen between the point that corresponds to Phase 1 and Phase 3 is the plastic strains that appear under the overloading of the beam. Furthermore, the concrete reaches its maximum strength and the line turns downwards. A drastic decrease of the stress at around 34MPa can be observed, what indicates failure.

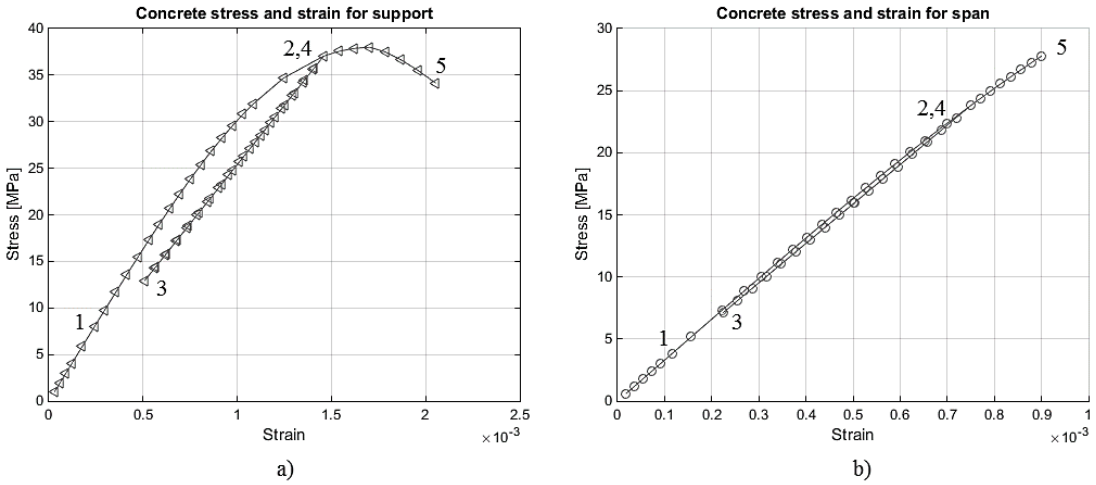

Figure 5.9 Concrete stress and strain for a) support section. b) span section.

Next, stress and strain were similarly checked for the span section. The span section was chosen such as it corresponds to the maximum strain section in the span. The element with highest strain values is different for every loading phase and the section chosen to analyse the span is the one with highest strain at failure. The stress-strain relation is presented in Figure 5.9.b and as it is indicated by the graph, this span section does not reach the maximum concrete strength before the failure of the beam occurs. As it is indicated by the circles that correspond to each obtained stress-strain relation, there is a drop at a stress of around 24MPa. This can be observed by the denser distribution of the mentioned circles along the line in between around 7MPa and 24 MPa. This shows, that due to the unloading, the stress-strain relation drops following the same loading path. While the beam is again loaded, this relation comes back using the same way up to the point of its drop. It can be noticed that the sectional response of the span differs from the one obtained in the support section. This is mainly due to the fact that the compressive zone is not critical in the span section in Phase 2 and thus the concrete is not highly strained. A limit for linear elastic response is often assumed to $0.6 \cdot f_c$ which in this case corresponds to 22.8MPa. As shown in Figure 5.9.b this limit is exceeded at the overloading. The last circle point shows the collapse of the beam. The analysis was load-controlled and to show the stress and strain graphs in a clear way the last failure load step has been deleted. This load step would have shown a drastic increase of strain in comparison to the last load step before failure.

Stress and strain for steel

It is important to check the structural response also by looking at the stresses and strains obtained for the reinforcing steel used in the modelled member. The input model that was used was defined with elastic ideally plastic behaviour of the steel. Firstly, the stress-strain relation of steel was checked for the support section. Since the reinforcement is supposed to yield before the unloading occurs, it is important to see whether this section shows a realistic response to the change in loading. The yielding limit was set to 500MPa in the FE analysis. As it is indicated in Figure 5.10.a, when the yielding of the reinforcement is reached, the curve changes its direction so that the response in that section is non-linear and the curve follows almost horizontal direction with a small inclination. After a while of yielding, the load was removed which is indicated by the drastic drop of the stress. The unloaded section corresponds to a stress of 100MPa and a strain of about 0.004. When the additional load was again

applied, this relation then followed a path in an upwards direction, such as it was parallel to the initial loading line, see Figure 5.10.a. As it is seen, this line reaches the almost horizontal line that indicates yielding. It can be seen that further this relation follows the already began horizontal path until failure is reached. To show clear figures the last load step has been deleted and the last load step shown in the graphs represents the values at the point before failure occurs. This sectional response clearly shows the influence of the temporary overloading and its influence on remaining strains in the reinforcing steel. The space that can be observed in between the points that correspond to Phase 1 and Phase 3 is the indicator of the remaining plastic strains that has developed while the overloading occurred.

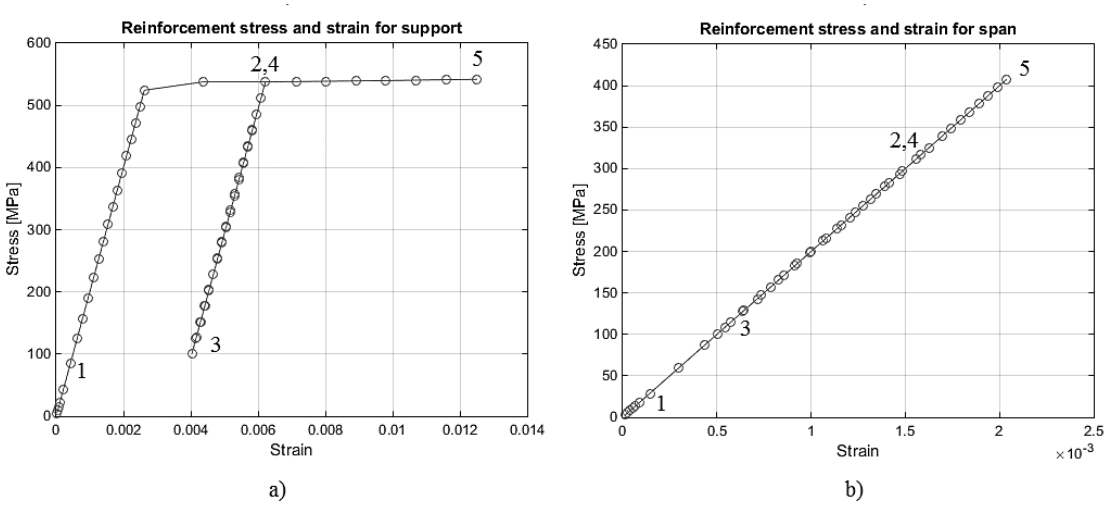

Figure 5.10 Reinforcement stress and strain for a) support section, b) span section.

The stress-strain relation was also checked for the span section, the same section as it is done in case of concrete stresses. As it can be seen in Figure 5.10.b, the stress-strain relation for steel follows a linear relation up until stress of about 340MPa is reached, which corresponds to the point of unloading. When the unloading begins, the curve goes back and follows the same path as in case of the initial loading. As the unloading stops when the quasi-permanent load combination is reached, the dropping of the stress stops as well. When the additional load is again applied, the relation follows the exact same line upwards, see Figure 5.10.b. Furthermore, the relation is still linear while the stress increases until a collapse of the beam occurs. The relation is still linear because the steel stress in span does not reach yielding in the most critical point and failure of the beam occurs when the steel stress is about 410MPa in that section. The structural response is affected by the yielding of reinforcement developed in the middle support, but since the span section does not achieve yielding itself, there are no remaining plastic strains or remaining deformation. The failure of the beam occurs when the concrete crushes and thus the full capacity of the concrete is reached. However the critical span section has not yielded yet and therefore the full capacity of reinforcement is not reached at failure. A more utilized cross-section is when the reinforcement in the span also reaches yielding at failure of the beam, so the cross-section in this project is not designed most effectively.

Plastic rotation

A very important parameter in this work is plastic rotation and how it is influenced by changing magnitude of load. To compare the plastic rotations from the analytical analysis with the ones from FE analysis, this parameter needs to be withdrawn from

the FE analysis. Since the plastic rotation is not a factor that was delivered by the software as a usual output, this parameter was obtained manually with the help of other parameter, which in this work was the deflection of a section of interest. The point where the deflection was measured is shown in Figure 5.11.

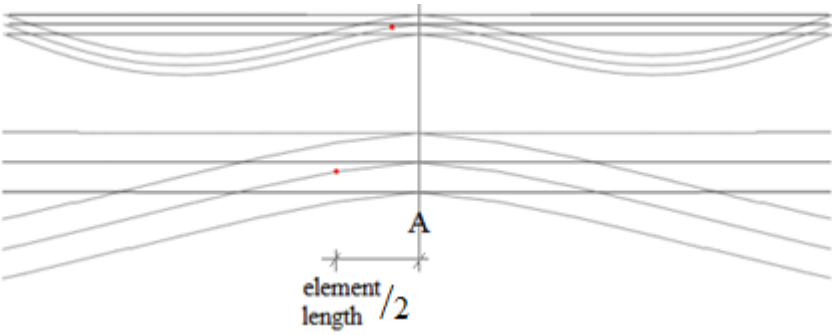

Figure 5.11 Point of deflection measurement to obtain plastic rotation.

The deflection, which was measured in the indicated point in Figure 5.11, was divided with the length of half the element to determine the plastic rotation as

$$\theta_{pl} = \frac{f_{element}}{\frac{l_{element}}{2}} \tag{5.1}$$

According to the assumptions made in the analytical analysis, the rotation over the middle support is zero until yielding of the reinforcement is reached, in case of a two-span continuous beam loaded with a uniformly distributed load. When the mentioned yielding is reached, a plastic rotation over the middle support develops, which is irreversible. However, this may not be directly seen in the numerical analysis. While indeed, once developed plastic rotation remains unchanged under the same or lower distribution and magnitude of load, there is another rotation that may be observed in the numerical analysis and that needs to be taken into account.

During loading, the beam starts to deflect such as a certain rotation of the initially horizontal lines occurs, see Figure 5.5, which corresponds to reinforcement and concrete in the beam. This is an apparent rotation that may not be misunderstood with plastic rotation. This apparent rotation increases until the limit of yielding of the reinforcement is reached and then, if the load is furthermore increased, a development of a plastic rotation starts. The apparent rotation is relatively small, but it is still subtracted from the total rotation when the plastic rotation is determined. It is essential to distinguish, that when the plastic rotation is developed in this symmetric beam the tangent above the middle support B is not equal to zero.

As it is described earlier in this section, when trying to obtain the plastic rotations in the numerical analysis, the rotation over the middle support B was determined by taking into account the deflection, which occurs closest to the middle support B section. This total deflection that is measured in Phase 2 includes the deflections developed under linear and non-linear material response. The obtained rotation, based on this method, is the total rotation in the investigated node. Due to this fact, these total rotations are not the same for Phase 1-3 as it would have been expected. In order to determine the plastic rotations the step that corresponds to the first yielding is taken into account as well as the last step before unloading. The difference in rotations between these steps is considered to be the plastic rotation in Phase 2, while the rest is

just an apparent rotation of the deflected beam. This procedure shows that this method of measuring the plastic is a little bit inaccurate, because it is based on deflection measured at a distance from the middle support B where the actual rotation should occur. To see whether the point where the plastic rotation is determined is in the plastic region or not, the strains in the elements should be studied to determine the extension of the plastic area around the support. This study shows that the nodes within a distance of 0.75-1.0 meter on each side of the middle support correspond to higher strains than the yielding strains in Phase 2 and thus belong to the plastic region.

The described approach on how to obtain the plastic rotation in FE analysis and the difference in the total rotations can be seen in Figure 5.12 below and Figure 5.13. Figure 5.12 indicates the moment and curvature relation for various loading phases and the corresponding rotation for each loading phase.

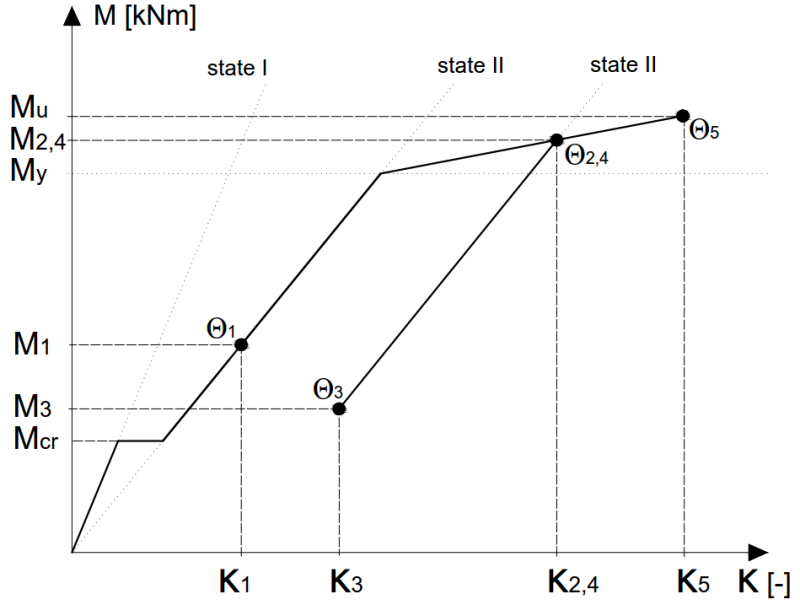

Figure 5.12 Moment-curvature relationship and its corresponding total rotation in the FE analysis for the support section for all five phases.

In Figure 5.13 these total rotations are presented for each loading phase. Phase 1 includes only the discussed apparent rotation, since no yielding occurs here. When the load increases so that the reinforcement starts to yield the difference in rotation at this point and the rotation in Phase 2 is determined as a plastic rotation. The rest of the total rotation in Phase 2 is the apparent rotation. While the beam is unloaded to Phase 3, which corresponds to the quasi-permanent load combination, the total rotation is decreased with the same apparent rotation as in Phase 1. The apparent rotation is therefore decreased in comparison to Phase 2, while the plastic rotation is still unchanged, see Figure 5.13.

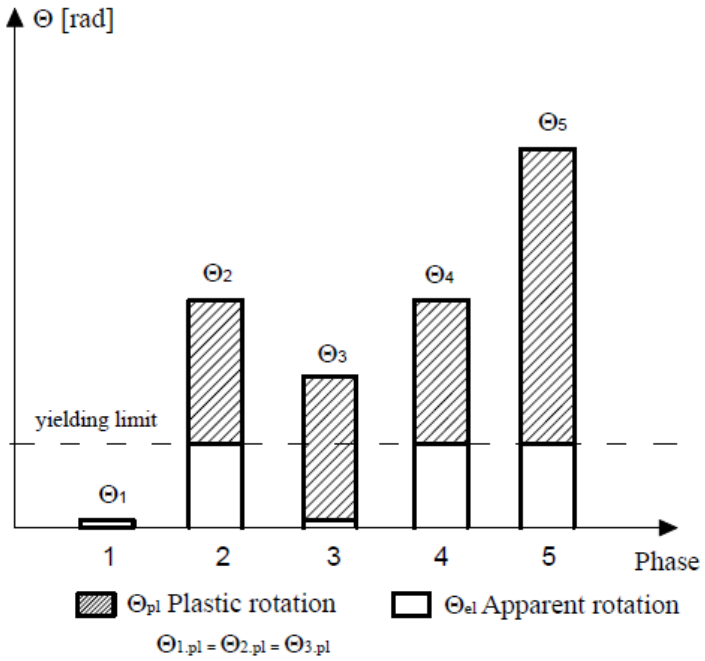

Figure 5.13 Principle of relation between the plastic rotation and the apparent rotation in FE analysis for all loading phases.

The results of the plastic and apparent rotations obtained in the FE analysis are presented in Table 5.6, where the deflections are determined at a distance of half an element length from the middle support.

Table 5.6 Deflection and plastic rotation at a distance of half an element length from the middle support B.

Phase	Deflection f [mm]	Apparent rotation on left side Θ_{left} [rad]	Plastic rotation on left side Θ [rad]
Phase 1	0.12	0.000309	0.000000
Phase 2	1.29	0.002016	0.001416
Phase 3	0.65	0.000309	0.001427
Phase 4	1.29	0.002016	0.001416
Phase 5	2.20	0.002016	0.0038373

As it can be seen in Table 5.6 the plastic rotation that develops during Phase 2 has the same magnitude for Phase 4. Furthermore, this rotation is the same for Phase 3 and thus remains during unloading of the beam. The plastic rotation is at its highest in Phase 5.

6 Evaluation of results

6.1 Residual load carrying capacity

6.1.1 Comparison between FE-analysis and analytical analysis

In order to evaluate the current condition of a structure, structural assessment should be used. Structural assessment can be conducted in consideration of current and future loads and it may be initiated when there is a suspicion of loss of capacity or when there will be a change of loads in the future. In this work, this investigation approach was used while analysing the overloaded two-span continuous beam. In order to estimate the influence of temporary overloading at various loading phases, structural assessment was needed. Such approach helped to understand material behaviour and structural response of the beam when the load was increased, decreased and then increased again until the maximum capacity was reached.

The analysis was conducted using analytical and FE analyse. Having the current capacity assessed, an investigation of the response on future loads was initiated. Failure under loading is one of the aspects considered in structural assessment and it is related to the ultimate limit state, achievement of maximum capacity, formation of a mechanism, high deformation or concerns about increased loads. Thus the evaluation of results in this work is mainly conducted with consideration of common structural parameters, such as moment distribution, deformation and plastic rotation.

The results obtained through analytical and FE analyses showed differences in magnitudes of the analysed parameters. The results of the analytical analysis and numerical analysis are summarised in Tables 6.1 to 6.5. It should be noticed that the values presented in Table 6.5 from the analytical analysis are the new values limited by the plastic rotation capacity determined by Eurocode 2, see Section A.11 in Appendix A.

Table 6.1 Comparison of parameters obtained for analytical and numerical analyse for Phase 1.

Parameter	Phase 1	
	Analytical analysis	Numerical analysis
q [kN/m2]	9.243	9.244
M_{sup} [kNm]	166.374	150.900
M_{span} [kNm]	93.585	99.390
θ_{pl} [rad]	0	0
f [mm]	9.721	3.700

Table 6.2 Comparison of parameters obtained for analytical and numerical analyse for Phase 2.

Parameter	Phase 2	
	Analytical analysis	Numerical analysis
q [kN/m2]	35.430	35.433
M_{sup} [kNm]	566.792	588.200
M_{span} [kNm]	385.828	377.300
θ_{pl} [rad]	0.002718	0.0014160
f [mm]	43.822	43.600

Table 6.3 Comparison of parameters obtained for analytical and numerical analyse for Phase 3.

Parameter	Phase 3	
	Analytical analysis	Numerical analysis
q [kN/m2]	9.243	9.244
M_{sup} [kNm]	93.800	116.700
M_{span} [kNm]	122.779	112.200
θ_{pl} [rad]	0.002719	0.001427
f [mm]	15.550	14.000
$M_{restraint,\ sup}$ [kNm]	72.574	34.200
$M_{restraint,\ span}$ [kNm]	29.194	12.810

Table 6.4 Comparison of parameters obtained for analytical and numerical analyse for Phase 4.

Parameter	Phase 4	
	Analytical analysis	Numerical analysis
q [kN/m2]	35.430	35.437
M_{sup} [kNm]	566.792	588.300
M_{span} [kNm]	385.828	377.300
θ_{pl} [rad]	0.002718	0.001416
f [mm]	43.822	43.600

Table 6.5 Comparison of parameters obtained for analytical and numerical analyse for Phase 5 with limited plastic rotation by the value from Eurocode 2.

Parameter	Phase 5	
	Analytical analysis	Numerical analysis
q [kN/m2]	42.05	39.75
M_{sup} [kNm]	587.105	590.200
M_{span} [kNm]	491.810	449.400
θ_{pl} [rad]	0.006505	0.0038370
f [mm]	59.01	55.50

First of all, difference in moment distributions was observed. For Phase 1, the support moment was higher and span moment lower in the analytical analysis in comparison to the numerical method. A reverse relation was observed in the rest of the loading phases, Phase 2 to 4, where the support moment was lower and the span moment higher in the analytical analysis when compared to FE analysis. This may indicate a pattern between the two methods that were used in this work. Due to the various moment distributions obtained in the analytical and FE analyse, the deflection varied as well. The obtained deflections were similar to each other in these two methods for Phase 2, 3 and 4, however they were slightly higher in the analytical analysis in comparison to the numerical analysis. This is directly dependent on the moment distribution obtained when using the two analyses. Also, plastic rotations that were obtained were almost twice higher for the analytical analysis when compared to the FE modelling.

The differences in the results obtained by the two methods may have various reasons. However, the main reason may be a difference in stiffness distribution and stiffness

variation along the beam. The cracking developed much earlier over the middle support in comparison to span section. This means that in Phase 1 the stiffness in span section was close to the stiffness that corresponds to uncracked state, while the stiffness over the middle support was at this phase much lower. A stiffness variation observed in the two methods was an influence on the overall results.

The stiffness variations along one span for both analytical and numerical analyses are presented in Figure 6.1. As illustrated in this figure the stiffness from the analytical analysis is constant along the beam while the stiffness from the numerical analysis varies. The stiffness in DIANA TNO is determined by studying the eleven integration points along the height of the beam. All the integration points with a negative stress value belong to the compressive zone and in this way the height of the compressive zone could be estimated. From the compressive zone height the moment of inertia could be calculated and thus the stiffness. As it is seen in this figure, the stiffness distribution in the FE model is the same for Phase 2, 3 and 4 while the Phase 5 is fully cracked, except in the region where the moment is zero.

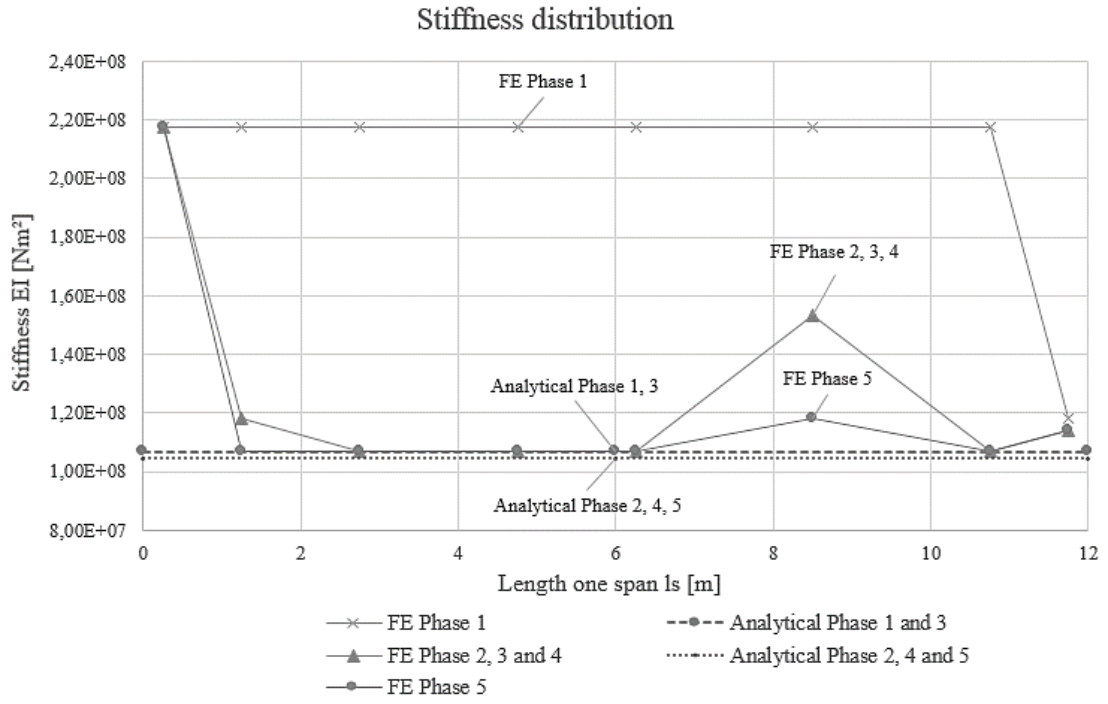

Figure 6.1 Stiffness distribution along half of the beam for all five phases both in analytical and numerical analysis.

A significant influence on the obtained results at early phases in both analyses is the effect of tension stiffening, which is neglected in the analytical analysis. This is especially seen in Phase 1. The stiffness that was used in the analytical analysis is the stiffness that corresponds to cracked state (state II) which means that the beam was assumed to be fully cracked. This stiffness was of a lower magnitude in comparison to the stiffness for uncracked state (state I). However, in case of FE analysis a stiffness variation appeared as it is indicated in Figure 6.1. In the analytical analysis, an idealised model was used after the cracking moment was reached which neglected the effect of tension stiffening. A moment-curvature diagram for the middle support section is shown in Figure 6.2 for both analytical and FE analyses and it includes all the analysed phases. The software used in the FE analysis considered a model where a state in between state I and state II was assumed. Since the used quasi-permanent load

was above the cracking load for the discussed section, there was still some contribution of concrete between its cracked sections. It means that the concrete helped to distribute the forces that were transferred through the steel bars and the response of the sections was closer to the model in state I. Thus the beam was not fully cracked in the FE analysis in Phase 1 as it was assumed in the analytical analysis.

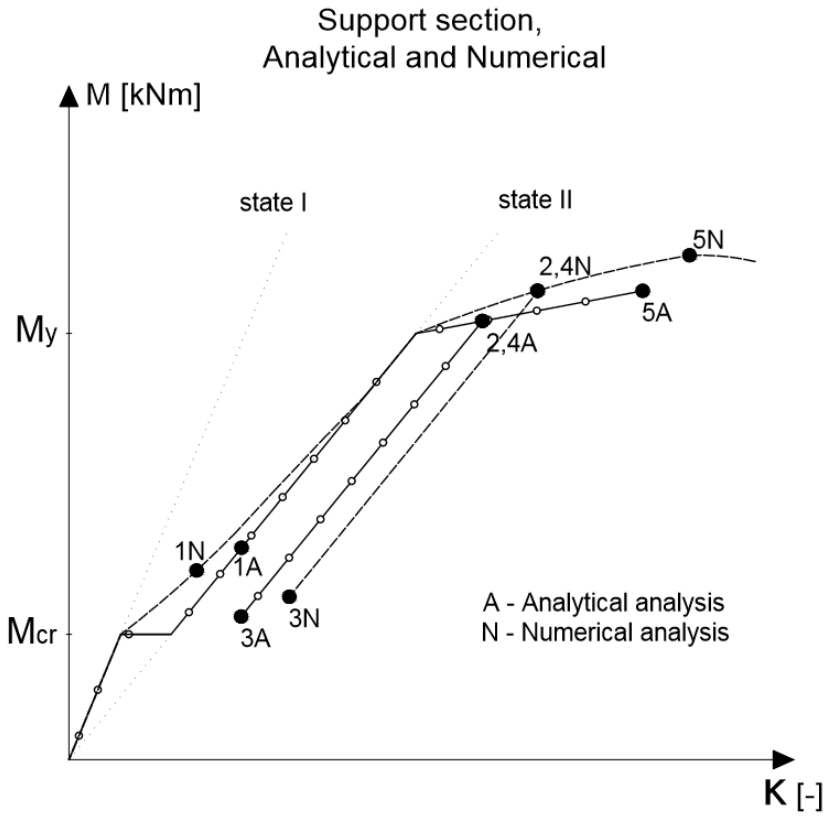

Figure 6.2 Difference between moment-curvature relations for the middle support section for analytical and numerical method for all analysed phases.

Another reason for the obtained differences between the analytical and FE analyses may be associated with the methods accuracy. The model that was used in the FE analysis should correspond more to the real behaviour of the analysed beam. However, the interaction between concrete and steel that was modelled as full may have an influence on tension stiffening and on the overall stiffness of the span and support section. Furthermore, while looking at the plastic rotations some simplifications were implemented in both methods used in this work. The analytical analysis contains assumptions regarding plastic region, which is simplified to a plastic hinge where all the plastic deformations take place in one point. The method used to obtain the plastic rotations in the numerical analysis may also have some uncertainties. It may be inaccurate to use a certain distance from the middle support to read the rotation values. Also, the plastic rotations were determined in FE analysis by looking at the strains and their corresponding deformations. Since the rotations were determined from the deflections of the section in the span close to the support, it was necessary to distinguish the deflections that occurred before the yielding of the reinforcement started, introducing plastic deflections in the section. Such approach helped to compare the results obtained through FE analysis with each other at various loading phases and to the results obtained by the analytical analysis.

Temporary overloading of a structure can result in a failure but if an unloading occurs before failure takes place some other effects may occur. The structural assessment of the beam showed presence of a restraint moment that occurs while the overloading is removed. This was shown by both the analytical and FE method. However, a difference between magnitudes of the restraint moment was observed for these two methods. The obtained restraint moment in the analytical analysis was more than double the magnitude of the corresponding moment in the FE analysis. This may be a resultant of the inaccuracy of the method proposed in the analytical approach where simplifications in the stiffness were made. Also, the obtained support moment in Phase 3 in the FE analysis was higher in comparison to the corresponding moment in the analytical analysis, what is directly connected to the obtained variation of the restraint moment.

As it has already been discussed, the beam in the numerical analysis had a different stiffness ratio than in the analytical analysis, especially in early phases where the stiffness varied along the beam, as shown in Figure 6.1 and Figure 6.2. However, in the model in DIANA TNO the support section was stiffer in comparison to the constant stiffness that was assumed in the analytical analysis. The numerical analysis showed smaller values of deformation and plastic rotation compared with the values from the analytical analysis. This may also be a sign that could strengthen the assumption of stiffness difference between the two methods. The plastic rotation from the numerical method was half the size of the values from the analytical methods. This agrees also with the magnitudes of the restraint moment which was also almost half the size of the value from the analytical method. This corresponds well to the assumption made in the analytical analysis that a plastic rotation creates a permanent angle which does not return under unloading and thus creates a restraint moment. It seems that the higher the plastic rotation and permanent angle is, the higher force is required to force the deformation to return to its original shape what creates higher restraint moment.

In the FE analysis the beam collapsed before the reinforcement in the span reached yielding. Therefore full plastic redistribution of the moments did not occur and the beam reached failure earlier. In the analytical method the capacity was limited by the plastic rotation capacity and therefore the plastic rotation at collapse was set to be equal to the plastic rotation capacity according to Eurocode 2, and full redistribution did not take place in this beam either. This occurred also in the numerical analysis where the beam reached failure for a lower load than it was estimated in the analytical analysis in case of full plastic redistribution. This shows that in the FE analysis the sectional response was limited by the ultimate concrete strain. A suggested reason for why full plastic redistribution did not take place in the FE model is that the plastic rotation capacity was reached before the full capacity of the beam was utilised, although the plastic rotation in FE model was below the plastic rotation capacity estimated by Eurocode 2. In a numerical analysis other aspects could be considered that influence the plastic rotation and the collapse, for example shear cracking which could increase the plastic rotation even more. However, this effect was not included in the output values determined in this project for plastic rotation from the numerical analysis. In another case the values of the plastic rotations could have been higher. It was shown in the analytical analysis that if the plastic rotation was set to be equal to the plastic rotation capacity, the value of load at failure was almost equal to the corresponding value in FE analysis. If full plastic redistribution was assumed in the analytical analysis, the magnitude of load at failure was higher than the respective

value in FE analysis. In this work, in the analytical analysis the plastic rotation was limited by the capacity given by Eurocode 2, which covers design values. The ABC-method was also introduced in this work due to the fact that mean values were used in the analytical analysis. However, the plastic rotation was in this work not limited by this method, since the plastic rotation capacity obtained by Eurocode 2 is on the safe side. A more correct way could have been to use values of plastic rotation capacity in between the values determined by Eurocode 2 and the ABC-method.

In further comparison of the two methods used in this work, yielding moments were compared to each other. In analytical and numerical methods the yielding moments were almost equal to each other, as shown in Table 6.6. The yielding load differs slightly when compared to each other. These results indicate that the yielding occurred at the same loading step for both analyses. Also, the moment in Phase 2 in the numerical analysis was slightly higher which can indicate that the beam in the numerical approach experienced more yielding than the beam in the analytical analysis.

Table 6.6 Yielding moment with corresponding load for both methods.

	Numerical analysis, (DIANA TNO)	Analytical analysis
$q_{y.sup}$ [kN/m]	31.01	31.08
$M_{y,sup}$ [kNm]	550.940	559.492

6.1.2 Comparison with reference beam using FEM

To compare the capacity of the beam when it is subjected to the process of overloading and unloading with a beam that is loaded gradually up to its failure, an FE analysis was conducted also for the case when temporary overloading of a two-span continuous beam does not occur. The result that was obtained through such analysis is a reference result and it is used to see if the response of a temporary overloaded beam deviates from a beam that was not subjected to temporary overloading.

The analysis of the beam without any temporary overloading was conducted with the same modelling choices as it is described in Section 5.1, with the only exception in case of loading. The same magnitudes of applied load were used with the exception of Phase 3 and Phase 4, which correspond to the process of unloading and reloading. Thus this beam was analysed in Phase 1, Phase 2 and Phase 5, a stage until failure occurs.

Figure 6.3 illustrates a relationship between the load and its corresponding deflection in the span section with the highest deflection in Phase 5. As the figure shows, the curve that corresponds to overloading follows exactly the same path as the original reference curve. Although the beam was unloaded between Phase 2 and Phase 3 the section reached the failure for the same load as it would not have been temporary overloaded before, what is indicated in Figure 6.3.

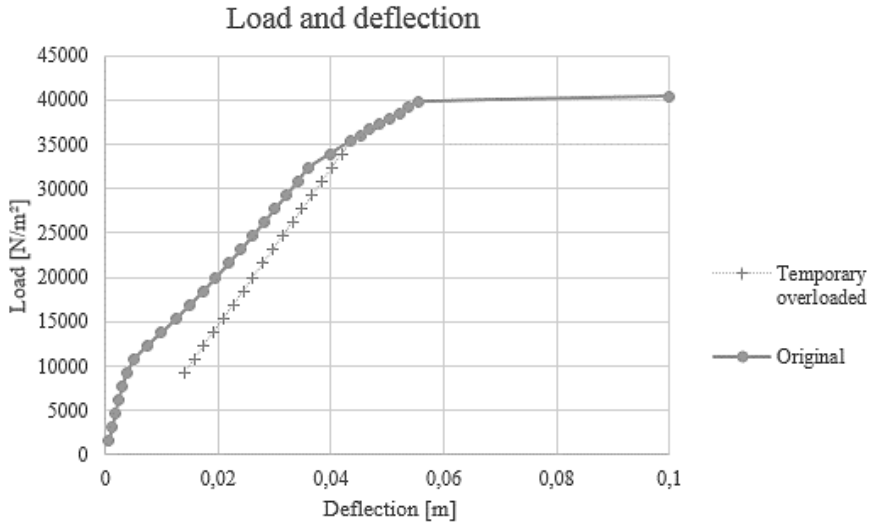

Figure 6.3 Load on the beam vs deflection of the section in the span that had the highest value at failure.

The same pattern was obtained while considering the moment distribution along the length of the beam, what is shown in Figure 6.4. Since Phase 1 and 2 had the same structural response in both analyses because the temporary overloading had not occurred yet, the important comparison was to plot Phase 2 and 5 for the original analysis together with Phase 4 and 5 for the temporary overloaded beam. As seen in Figure 6.4 the moment distribution is still unchanged in these phases although the beam was overloaded in the past.

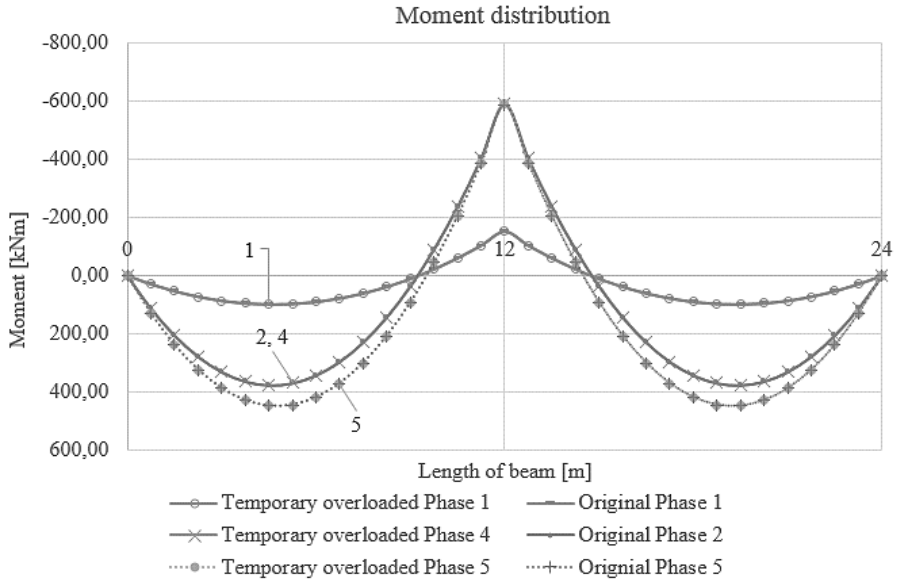

Figure 6.4 Moment distribution along the beam for reference beam and temporarily overloaded beam. Number 12 and 24 shows the length of the spans.

Another parameter that indicates the influence of overloading on the material response and structural response of the beam is plastic rotation. The plastic rotation was estimated in the same way as described in Section 5.1 Figure 6.5 shows how the plastic rotations in Phase 4 and Phase 5 for the overloaded beam agree with that of the

original reference. There is some difference between these two results in Phase 5, however all the values before this failure step are exactly the same and thus an assumption has been made that there is no difference in plastic rotation capacity of the beam when the beam has been temporarily overloaded or not.

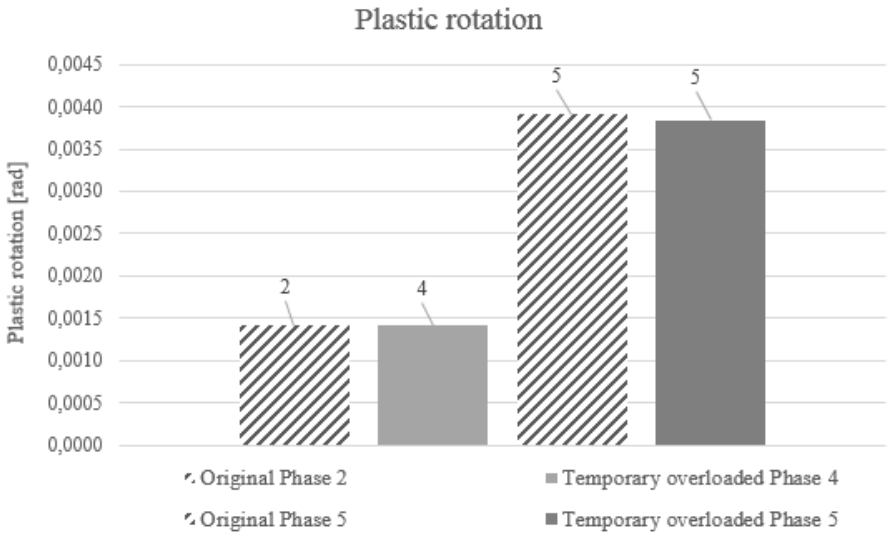

Figure 6.5 Plastic rotation for the temporary overloaded beam and the original beam.

All these three comparisons presented above indicate that the residual load carrying capacity is not influenced by the applied overloading in this work. It is assumed that these comparisons are sufficient to show the response to overloading and if more parameters would have been presented they would have followed the same pattern.

Furthermore, as it is described in Section 3.6 the plastic rotations may cumulate while the load cases are changed during the loading and unloading. It has to be emphasised that in this work only distributed, fixed in space load was applied on the beam during the entire process of overloading and unloading. However, in reality it is seldom that any added or removed loads are distributed with fixed position. Usually an additional load may occur such as heavy machinery, considered in fact as a moving and concentrated load. Such load distribution could lead to other results than presented in this work in case of fixed distributed loads. Also, it has to be considered that in this project only a symmetric statically indeterminate beam was considered what may affect the obtained results significantly.

6.2 Damage investigation of a structure

The results showed that an existing concrete structure with significant crack widths and deflection should further be investigated. The analysis of the beam in Section 4.2 showed that the problem of how to determine the past overloading should be further studied. The procedure proposed in Section 4.2 is possible to apply when a two-span continuous beam overloaded with a uniformly, fixed distributed load is analysed. Moreover, to be able to apply this procedure a magnitude of plastic rotations should first be determined. It is estimated in this work that this is possible to be done by plotting the deflected shape of the beam that is measured on site. However, this approach has not been checked in this work on site and thus not proven to be possible to carry out. There are also many uncertainties considering the long terms effects such

as creep and shrinkage and their influence on the total deformation measured on site. Also, a good access to the deflected beam is a demand to be able to perform the measuring in a correct way and for this approach to be applicable.

As the literature survey as well as the analytical analysis showed, deflection is a factor that can lead to determination of plastic rotations and thus to the uniformly distributed and fixed load applied on the two-span continuous beam. It was estimated that the deflected shape of the beam may be used to determine plastic rotation over the middle support. Measuring the deflected shape was assumed in the analysis to be possible. It has been decided that the maximum deflection in the span may be used as an extra verification while assessing the overloading magnitude. This can be done by calculating the maximum deflection for the estimated overloading. This deflection should be compared with the maximum deflection measured on site. It is also important to take long term effects into consideration while using measured deflection. Using the maximum deflection does not give an exact value of plastic rotation and can instead be treated as a verification of the result to see how reliable the plastic rotation determined from the deflected shape is.

As the results obtained in the analysis of Part 1 and Part 2 showed, an temporary overloading changes the moment distribution after the overload is removed. If the same load case is again applied on the member after unloading, the plastic rotation is still of the same magnitude. This is especially important since, as it was assumed in this work, the structural assessment is associated with Phase 3 which corresponds to the stage after the overloading is removed. It means that if a structural assessment is to be carried out when a suspicion of past overloading exists, the initial moment distribution does not occur anymore due to the presence of the restraint moment. However, based on the results it was concluded that if the overloading defined by the forensic engineering approach will again be applied on the member in the future, its capacity will remain unchanged and the restraint moment will disappear, as it is shown in this work.

Forensic investigation seems to be a scientific field with an increasing importance in structural engineering. Forensic engineering will probably be more commonly used in the future so that reuse of old structures will be possible to a larger extent. This would be more effective with regard to the environment, construction- and material costs. Hopefully forensic investigation and reasonable determination of damage causes will reduce the risk of insufficient safety.

7 Summary

7.1 Conclusions

Based on the conducted literature study, analytical and numerical analyses and the discussion, the following conclusions were drawn:

- Overloading into the yielding phase of a two-span continuous beam with a uniformly distributed and fixed load does not decrease the load-carrying capacity, if the same case of overloading is applied in the future. This is under the assumption that the load-carrying capacity of the beam is determined by the moment capacities of critical sections.
- Temporary overloading into the yielding phase of a two-span continuous beam changes the moment distribution in the service state by formation of a restraint moment over the middle support. This leads to a decreased moment over the middle support and an increased moment in the span.
- The restraint moment increases with the magnitude of overloading.
- The plastic rotation that develops over the middle support under overloading is irreversible, which means that it remains while the overloading is removed.
- The procedure proposed in this work on how to determine a past overloading is valid only for statically indeterminate two-span continuous beams, loaded by a uniformly distributed and fixed load. The procedure can be applied once the plastic rotation is determined from a plotted deflected shape of the beam, measured on site.

7.2 Further work

Possible improvements of the analysis of overloaded structures and further studies in this field are for instance:

- Considering long term effects such as creep and shrinkage in the analysis and study their influence in case of temporary overloading of a beam.
- Analysing a three-span continuous beam. Since a two-span continuous beam is a simple case, a three-span continuous beam would be more representative for cases with a higher number of spans.
- Modelling a beam with shell elements and using more complex geometries, loads and modelling choices.
- Modelling an overloaded slab by using shell elements to analyse the response in two directions, firstly just by modelling one field and furthermore by modelling higher amount of fields in two directions. The presence and magnitude of restraint moments when the member has a two-way response could be investigated. A slab model could also be compared to a case in reality with regard to crack pattern, where this can be investigated on site.
- Using other load cases than a uniformly distributed and fixed load to study the influence of unloading and reloading when the load is not always uniformly distributed over the beam length. Especially cumulative plastic failure could be analysed, which happens when load is removed only from some parts of structural member.

- Experimental studies and measurements could be performed to see whether the deflected shape of a beam can really be plotted and used to determine plastic rotations.

8 References

ACI Comittee 224, 2007. Causes , Evaluation , and Repair of Cracks in Concrete Structures.

Acker, A. Van et al., 2012. *Design of precast concrete structures against accidental actions*, Swizerland: fib, International Federation of Structural Concrete.

Aikivuori, A.M., Lacasse, M.A. & Vainer, D.J., 1999. Critical loss of performance - What fails before durability. *Durability of Building Materials and Components 8, Vols 1-4, Proceedings*.

Banville, M.H., 2008. Structural Assessment and Repair of Concrete Structures. *Interface*. Available at: www.rci-online.org.

Bluey Technologies, Evaluating Cracking in Concrete Evaluating Cracking In Concrete. *Bluey Technologies Pty Ltd*, p.10.

Campbell, P., 2001. *Learning from Construction Failures: Applied Forensic Engineering* C. Peter, ed., New York: Whittles Publishing Services.

Chen, W.-F., 2007. *Plasticity in Reinforced Concrete*, Fort Lauderdale: Ross, J.

Concrete Society, 1992. *Non-structural cracks in concrete* Third edit. R. E. Lavery, ed., Kalgoorlie: The Concrete Society.

Douglas, J., Ransom, B. & Ransom, W., 2007. Understanding building failures. *Construction*.

Engström, B., 2015. *Design and analysis of continuous beams and columns* Edition 20., Göteborg: Chalmers University of Technology, Division of Structural Engineering, Concrete Structures.

Engström, B., 2014. *Restraint cracking of reinforced concrete structures* Edition 20., Göteborg: Chalmers University of Technology, Division of Structural Engineering, Concrete Structures.

Engström, B., 2011. *Bärande konstruktioner del 1* Edition 11., Göteborg: Chalmers University of Technology, Division of Structural Engineering

Gilbert, R.., 2001. Shrinkage, Cracking and Deflection - the Serviceability of Concrete Structures. *Electronic Journal of Structural Engineering*, 1(1).

Gold, C. a & Martin, a J., 1999. Refurbishment of concrete buildings: Structural & services options 8/99.

Greenberg, T., 2015. Forensic Engineers - The Unsung Superhero. *The University of Texas at Austin*. Available at: https://sites.utexas.edu/civ-eng-comm/2015/10/15/forensic-engineers-the-unsung-superhero/ [Accessed January 25, 2016].

Hillerborg, A., 1971. Experimentellt studium av tillväxtflytbrott hos armerade betongbalkar.

Holický, M. et al., 2013. *Basics for assessment of existing structures* 1st ed., Czech Republic: Klokner Institute, Czech Technical University of Prague.

IAEA, I.A.E.A., 2002. Guidebook on non-destructive testing of concrete structures. *Training Course Series*, 17(17).

Interval, V., 2012. Concrete Cracks : An Overview of Types of Cracking / Deterioration and Their Implications Table of Contents. *Overview of Types and Causes*.

Johansson, R. & Antona, B., 2011. Crack Control of Concrete Structures Subjected to Restraint Forces. *Chalmers University of Technology, Master Thesis. Division of Structural Engineering*.

Kattilakoski, J., 2013. CRACK CONTROL OF CONCRETE STRUCTURES IN SPECIAL CASES. , (March).

Lim, S., 2013. Redistribution of force concentrations in reinforced concrete cantilever slab using 3D non-linear FE analyses. *Chalmers University of Technology, Master Thesis. Division of Structural Engineering*.

Lindelöf, A. & Walhelm, B., 2014. Moment distribution and cumulative plastic rotation in reinforced concrete slabs subjected to concentrated forces. *Chalmers University of Technology*.

Lorentsen, M., 1990. *Betonghandbok konstruktion* K. Cederwall, M. Lorentsen, & L. Östlund, eds., Örebro: AB Svensk Byggtjänst.

Marková, J., 2010. Reliability Assessment of Existing Concrete Bridges. *Journal of Konbin*, 14-15(-1). Available at: http://www.degruyter.com/view/j/jok.2010.14-15.issue--1/v10040-008-0169-5/v10040-008-0169-5.xml.

Mehndi, S.M., Khan, M.A. & Ahmad, S., 2014. CAUSES AND EVALUATION OF CRACKS IN. *International Journal of Technical Research and Applications*, 2(5).

Nguee, C.S., 2006. Case Studies on Forensic Stuctural Engineering.

Noon, R.K., 2001. *Forensic Engineering Investigation*, Florida: CRC Press LLC.

Plos, M. et al., 2004. *Evaluering av bärförmåga hos broar med hjälp av förfinade analysmetoder. Ett samarbetprojekt mellan LTH, LTU och Chalmers*,

Rücker, P.W., Hille, D.F. & Rohrmann, D.R., 2006. *F08a. Guildeline for the Assessment of Existing Structures*, Berlin.

Spellman, F.R. & Bieber, R.M., 2012. *Environmental Health and Science Desk Reference*, United Kingdom: Government Institutes.

Stuart, M., 2012. *Structural Concrete Textbook on behaviour, design and performance* Second edi., Swizerland: fib, International Federation of Structural Concrete.

Suprenant, B.B.A. & Basham, K.D., 1993. Evaluating cracks in concrete walls.

Sustainable Bridges, 2007a. Guideline for Inspection and Condition Assessment. *Assessment*.

Sustainable Bridges, 2007b. Guideline for Load and Resistance. *Sustainable Bridges*.

TSO, 2007. *Inspection manual for highway structures* Volume 1., London: The Stationery Office, TSO.

Urs, N. et al., 2015. Residual Life Assessment of Concrete Structures-A Review. *International Journal of Engineering and Technical Research (IJETR).*, (3).

Wilby, C.B., 1983. *Structural Concrete: Materials; Mix Design; Plain, Reinforced and Prestressed concrete; Design Tables*, United Kingdom: Butterworth & Co.

Appendix A: Analytical analysis PART 1

PART 1

In this part all the loads are known and the calculations describe the material response from Phase 1 to Phase 5, considered as the phase until failure occurs. This is to show the structural behavior of a two span continous beam under uniformly distributed load, when it is loaded to service load, yielding, subjected to overloding, unloaded, reloaded and finally failure.

A.1 BEAM PROPERTIES

Analysis of a two span continous beam

$kN := newton \cdot 10^3$ $MN := newton \cdot 10^6$ $MPa := Pa \cdot 10^6$ $GPa := Pa \cdot 10^9$

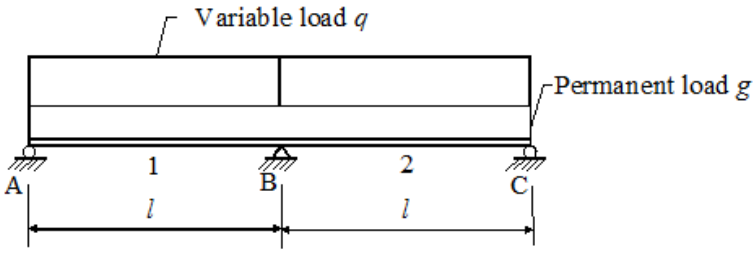

Load case : Variable load in both spans

Input data:

Span length:

$l_s := 12m$

Cross section

Concrete gross section:

$b := 0.30 \cdot m$ $h := 0.700 \cdot m$

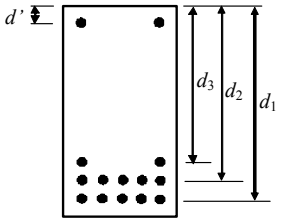

$A_c := b \cdot h$ $A_c = 0.21\ m^2$

$x_c := \frac{h}{2}$ $x_c = 0.35\ m$

$I_c := \frac{b \cdot h^3}{12}$ $I_c = 8.575 \times 10^{-3}\ m^4$

Reinforcement:

$\phi'_s := 12mm$ $\phi_s := 20mm$ $c'_c := 30mm$ $c_c := 30mm$

$A'_{s.si} := \left(\frac{\phi'_s}{2}\right)^2 \cdot \pi = 113.097 \cdot mm^2$ $A_{s.si} := \left(\frac{\phi_s}{2}\right)^2 \cdot \pi = 314.159 \cdot mm^2$

Section in field:

Assuming 1 layer of reinforcement

$A_{s1.span} := 6 \cdot A_{s.si}$ $d_{1.span} := h - c_c - \frac{\phi_s}{2} = 0.66\,m$

$A'_{s.span} := 2 \cdot A'_{s.si} = 2.262 \times 10^{-4}\,m^2$ $d'_{span} := c'_c + \frac{\phi'_s}{2} = 0.036\,m$

Section at support:

The section is defined upside down. Assuming 2 layers of reinforcement in the tensile zone and one layer in the compressive zone

$A_{s1.sup} := 6 \cdot A_{s.si}$ $d_{1.sup} := h - c_c - \frac{\phi_s}{2} = 0.66\,m$

$A_{s2.sup} := 0 \cdot A_{s.si}$ $d_{2.sup} := h - c_c - \frac{\phi_s}{2} - 20mm = 0.64\,m$

$A'_{s.sup} := 2 \cdot A'_{s.si}$ $d'_{sup} := c'_c + \frac{\phi'_s}{2} = 0.036\,m$

Material proporties in the service state

Concrete C30/37

$f_{cmean} := 38 \cdot MPa$

$f_{ctk0.05} := 2.0MPa$ $f_{ctm} := 2.9 \cdot MPa$ $f_{ctk0.095} := 3.8 \cdot MPa$

$E_c := 33 \cdot GPa$

$g_c := 25 \frac{kN}{m^3}$ density of concrete

$\varepsilon_{cu} := 3.5 \cdot 10^{-3}$ ultimate concrete strain

Mean values are used since Part 2 is considering a measured value and not design values. Also, short term is considered since the deflection in Part 2 is decreased by the assumed deflection caused by creep.

Reinforcement steel B500B

$f_{yk} := 500 \cdot MPa \qquad f_{uk} := 540MPa \qquad E_{sm} := 200 \cdot GPa$

$\varepsilon_{sy} := \frac{f_{yk}}{E_{sm}} = 2.5 \times 10^{-3}$ yielding steel strain

$\varepsilon_{suk} := 0.05$ ultimate steel strain

Modular ratio: short term response: $\alpha := \frac{E_{sm}}{E_c} \qquad \alpha = 6.061$

Load

Load assumption: since the analysed beam is not a real case study, the applied load is chosen as distributed uniformly fixed and as a reasonable value.

Quasi-permanent combination (SLS):

$q_1 := 9.243 \frac{kN}{m}$ The load is chosen so that it corresponds to FE modelling

Characteristic load combination (SLS):

$q_{1.ch} := 11.59 \frac{kN}{m}$

Overloaded plastic load combination:

$q_2 := 35.43 \frac{kN}{m}$ Same as in FEM

SECTIONAL CONSTANTS IN UNCRACKED STATE (STATE I), SHORT TERM RESPONSE

Uncracked section (state I model), short term response:
Support:

$$A_{I.sup} := A_c + (\alpha - 1) \cdot \left(A_{s1.sup} + A_{s2.sup} + A'_{s.sup}\right) = 0.221\,m^2$$

$$x_{I.sup} := \frac{A_c \cdot \frac{h}{2} + (\alpha - 1) \cdot \left(A_{s1.sup} \cdot d_{1.sup} + A_{s2.sup} \cdot d_{2.sup} + A'_{s.sup} \cdot d'_{sup}\right)}{A_{I.sup}} = 0.362\,m$$

$$I_{I.sup} := \frac{b \cdot h^3}{12} + b \cdot h \cdot \left(\frac{h}{2} - x_{I.sup}\right)^2 + (\alpha - 1) \cdot A_{s1.sup} \cdot \left(d_{1.sup} - x_{I.sup}\right)^2 \ldots = 9.574 \times 10^{-3}\,m^4$$
$$+ (\alpha - 1) \cdot A_{s2.sup} \cdot \left(d_{2.sup} - x_{I.sup}\right)^2 \ldots$$
$$+ (\alpha - 1) \cdot A'_{s.sup} \cdot \left(x_{I.sup} - d'_{sup}\right)^2$$

Flexural rigidity for support at state I:

$$EI_{I.sup} := E_c \cdot I_{I.sup} = 315.941 \cdot MN \cdot m^2$$

Span:

Moment of inertia at state I:

$$A_{I.span} := A_c + (\alpha - 1) \cdot \left(A_{s1.span} + A'_{s.span}\right) = 0.221\,m^2$$

$$x_{I.span} := \frac{A_c \cdot \frac{h}{2} + (\alpha - 1) \cdot \left(A_{s1.span} \cdot d_{1.span} + A'_{s.span} \cdot d'_{span}\right)}{A_{I.span}} = 0.362\,m$$

$$I_{I.span} := \frac{b \cdot h^3}{12} + b \cdot h \cdot \left(\frac{h}{2} - x_{I.span}\right)^2 + (\alpha - 1) \cdot A_{s1.span} \cdot \left(d_{1.span} - x_{I.span}\right)^2 \ldots = 9.574 \times 10^{-3}\,m^4$$
$$+ (\alpha - 1) \cdot A'_{s.span} \cdot \left(x_{I.span} - d'_{span}\right)^2$$

Flexural rigidity for support at state I:

$$EI_{I.span} := E_c \cdot I_{I.span} = 315.941 \cdot MN \cdot m^2$$

SECTIONAL CONSTANTS IN CRACKED STATE (STATE II), SHORT TERM RESPONSE

Cracked section (state II model), short term response:

Span:

Assuming a value of the compressive zone :

$$x_{II.span} := 0.18m$$

$$x_{II.span} := \text{root}\left[\frac{b \cdot x_{II.span}^2}{2} \ldots + (\alpha - 1) \cdot A'_{s.span}\left(x_{II.span} - d'_{span}\right) - \alpha \cdot A_{s1.span} \cdot \left(d_{1.span} - x_{II.span}\right), x_{II.span}\right]$$

$$x_{II.span} = 0.187\,m$$

Moment of inertia at state II:

$$I_{II.span} := \frac{b \cdot x_{II.span}^{3}}{3} + (\alpha - 1) \cdot A'_{s.span} \cdot \left(x_{II.span} - d'_{span}\right)^2 + \alpha \cdot A_{s1.span} \cdot \left(d_{1.span} - x_{II.span}\right)^2$$

$$I_{II.span} = 3.236 \times 10^{-3}\, m^4$$

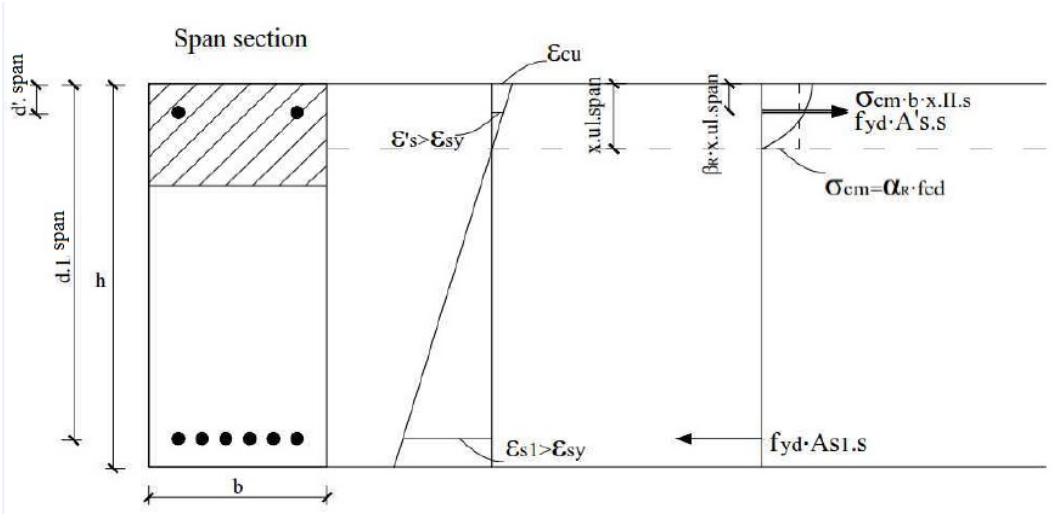

Flexural rigidity: $EI_{II.span} := E_c \cdot I_{II.span}$ $EI_{II.span} = 106.784 \cdot MN \cdot m^2$

Support:

Assuming a value:

$$x_{II.sup} := 0.18 \cdot m$$

$$x_{II.sup} := \text{root}\left[\frac{b \cdot x_{II.sup}^{2}}{2} + (\alpha - 1) \cdot A'_{s.sup} \cdot \left(x_{II.sup} - d'_{sup}\right) - \alpha \cdot A_{s1.sup} \cdot \left(d_{1.sup} - x_{II.sup}\right) + -\alpha \cdot A_{s2.sup} \cdot \left(d_{2.sup} - x_{II.sup}\right) \cdots, x_{II.sup}\right]$$

$$x_{II.sup} = 0.187\, m$$

Moment of inertia at state II:

$$I_{II.sup} := \frac{b \cdot x_{II.sup}^{3}}{3} + (\alpha - 1) \cdot A'_{s.sup} \cdot \left(x_{II.sup} - d'_{sup}\right)^2 + \alpha \cdot A_{s1.sup} \cdot \left(d_{1.sup} - x_{II.sup}\right)^2 \cdots + \alpha \cdot A_{s2.sup} \cdot \left(d_{2.sup} - x_{II.sup}\right)^2$$

$$I_{II.sup} = 3.236 \times 10^{-3}\, m^4$$

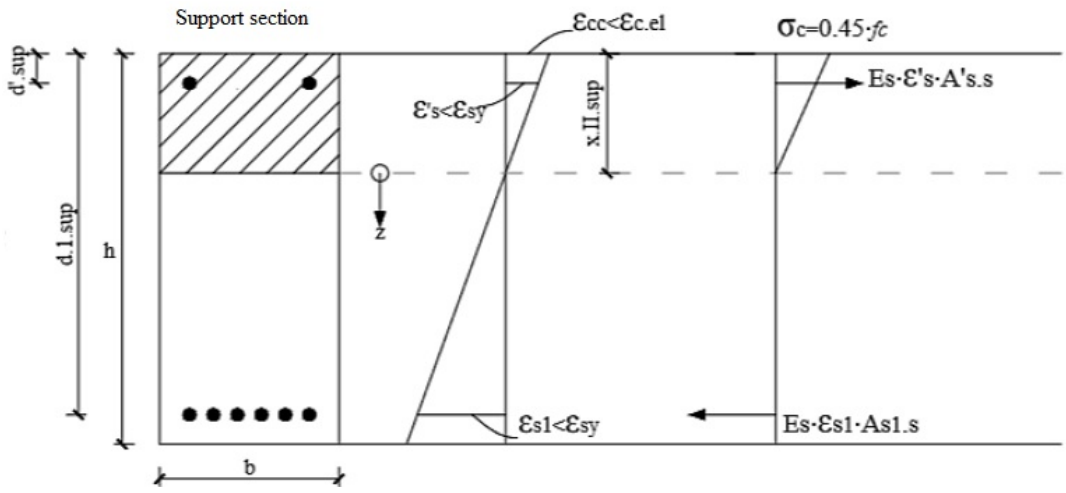

Flexural rigidity: $EI_{II.sup} := E_c \cdot I_{II.sup}$ $EI_{II.sup} = 106.784 \cdot MN \cdot m^2$

Stiffness ratio, cracked section, short term response:

$$\frac{EI_{II.sup}}{EI_{II.span}} = 1$$ The stiffness is constant along the beam.

A.2 CRACKING PHASE

Cracking moment:

For uncracked stage the reinforcement could be neglected. However in these calculations the reinforcement is considered

$$M_{cr.sup} := \frac{f_{ctm} \cdot I_{I.sup}}{h - x_{I.sup}} = 82.088 \cdot kN \cdot m$$

$$M_{cr.span} := \frac{f_{ctm} \cdot I_{I.span}}{h - x_{I.span}} = 82.088 \cdot kN \cdot m$$

Cracking load for support section:

$$q_{cr.sup} := \frac{8 \cdot M_{cr.sup}}{l_s^{\,2}} = 4.56 \cdot \frac{kN}{m}$$

Cracking load for span section:

$$q_{cr.span} := \frac{\left(128 \cdot M_{cr.span}\right)}{9 \cdot l_s^{\,2}} = 8.107 \cdot \frac{kN}{m}$$

The values are below the quasi-permanent load. The quasi-permanent load corresponds to state II response both in span and in the support.

$$R_{cr.A} := \frac{q_{cr.sup} \cdot l_s}{2} - \frac{M_{cr.sup}}{l_s} \qquad x := 0 \cdot m, 0.1 \cdot m .. l_s$$

$M_{cr.x}(x) := R_{cr.A} \cdot x - \frac{q_{cr.sup} \cdot x^2}{2}$ Expression for the moment along the beam

Curvature in span region, cracked state (state II):

$$\kappa_{cr.span.I}(x) := \frac{M_{cr.x}(x)}{EI_{I.span}}$$ Assumed fully cracked

Curvature at support region, cracked state (state II):

$$\kappa_{cr.sup.I}(x) := \frac{M_{cr.x}(x)}{EI_{I.sup}}$$

$\kappa_{cr}(x) := \text{if}\left(M_{cr.x}(x) \geq 0, \kappa_{cr.span.I}(x), \kappa_{cr.sup.I}(x)\right)$ Expression for the curvature along the beam

Support rotation at support A:

$$\theta_{cr.A} := \frac{\int_0^{l_s} \kappa_{cr}(x)\cdot\left(l_s - x\right) dx}{l_s}$$

$$\theta_{cr.A} = 5.196 \times 10^{-4}$$

Section with rotation equal to 0 and thus the maximum deflection in the span:

Assuming a value of the distance from the outer support where maximum deflection might occure:

$$x_{cr.f} := 5\cdot m$$

$$x_{cr.f} := \text{root}\left(\int_0^{x_{cr.f}} \kappa_{cr}(x)\, dx - \theta_{cr.A}, x_{cr.f}\right)$$

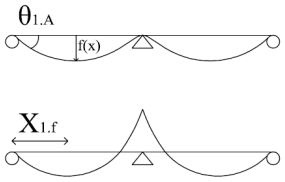

$$x_{cr.f} = 5.058\,m$$

Maximum deflection:

$$f_{cr} := \theta_{cr.A}\cdot x_{cr.f} - \int_0^{x_{cr.f}} \kappa_{cr}(x)\cdot\left(x_{cr.f} - x\right) dx$$

$$f_{cr} = 1.621\cdot mm$$

Expression of the deflection in span:

$$f_{cr.span}(x) := \theta_{cr.A}\cdot x - \int_0^x \int_0^x \kappa_{cr}(x)\, dx\, dx$$

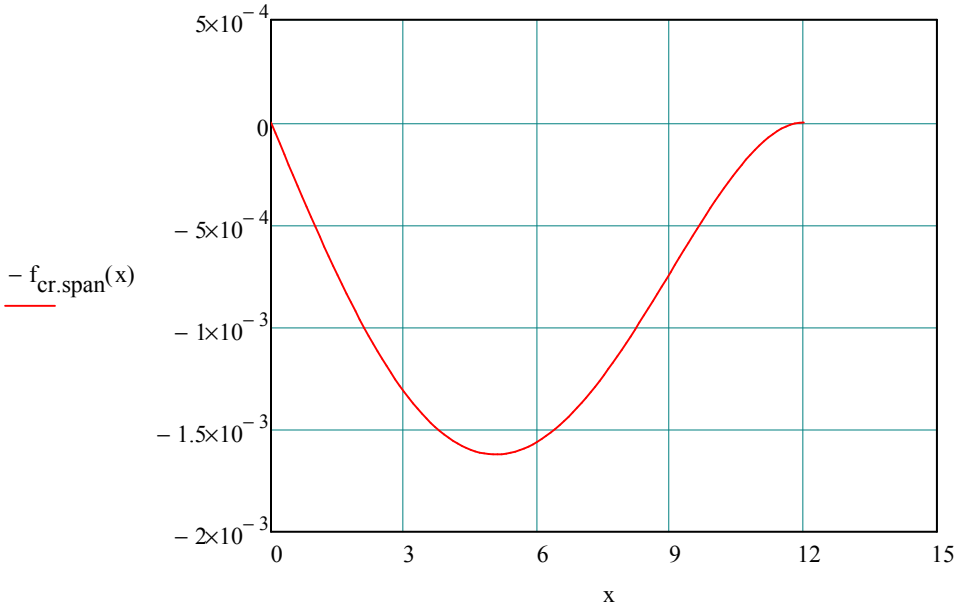

A.3 YIELDING PHASE

Values of yielding moments for the support and span section are needed in order to secure that the chosen load that would result is plastic deflection causes overloading.

Support:

Assuming that the concrete strain is lower than ultimate concrete strain εcc<εcu:

Sum of yielding forces:

$$F_{sy.total.sup} := f_{yk}\cdot\left(A_{s1.sup} + A_{s2.sup}\right) = 942.478\cdot kN$$

Assuming a value of compressive zone in yielding:

$$x_{y.sup} := 0.1935m$$

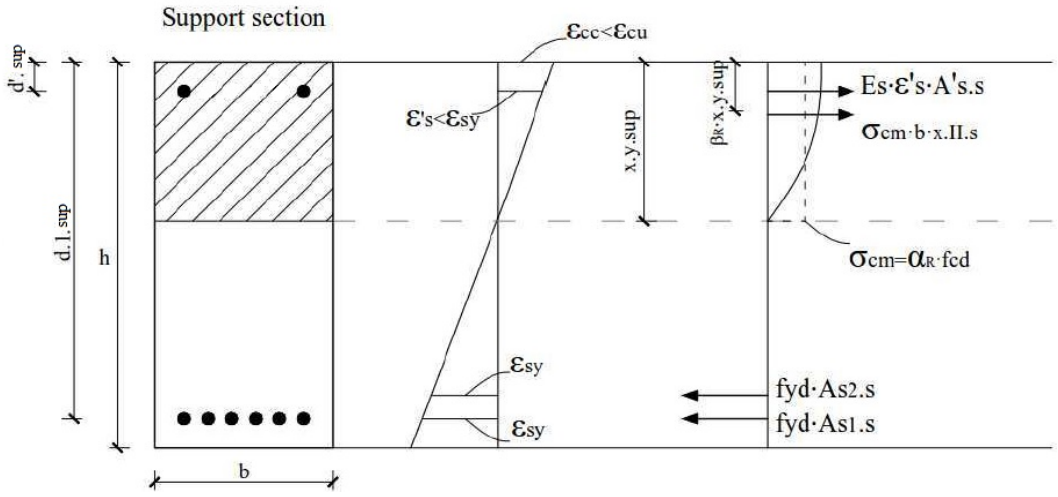

$$\varepsilon_{cc.y.sup} := \frac{x_{y.sup}\cdot\varepsilon_{sy}}{d_{1.sup} - x_{y.sup}} = 1.037\times 10^{-3}$$

Concrete strain at the phase of tensile reinforcement yielding

$$\varepsilon'_{s.y.sup} := \frac{\left(x_{y.sup} - d'_{sup}\right)\cdot\varepsilon_{cc.y.sup}}{x_{y.sup}} = 8.441\times 10^{-4}$$

Steel strain of the reinforcement in the compressive zone at the phase of tensile reinforcement yielding

$$\varepsilon'_{s.y.sup} > \varepsilon_{sy} = 0$$

Check if the reinforcement in the compression zone yields

The strain for the steel in tensile zone is calculated for one layer of reinforcement.

$\alpha_{R.y} := 0.41$

$F'_{s.y.sup} := \varepsilon'_{s.y.sup} \cdot E_{sm} \cdot A'_{s.sup} = 38.184 \cdot kN$

$F_{c.y.sup} := f_{cmean} \cdot \alpha_{R.y} \cdot x_{y.sup} \cdot b = 904.419 \cdot kN$

$F'_{s.y.sup} + F_{c.y.sup} = 942.603 \cdot kN$

Almost the same as the sum of yielding forces in the tensile zone means that the assumed depth of compression zone in yielding (xy) is correct.

$\beta_{R.y} := 0.35$

$M_{y.sup} := F_{c.y.sup} \cdot \left(d_{1.sup} - \beta_{R.y} \cdot x_{y.sup}\right) \ldots + F'_{s.y.sup} \cdot \left(d_{1.sup} - d'_{sup}\right) - f_{yk} \cdot A_{s2.sup} \cdot \left(d_{1.sup} - d_{2.sup}\right) = 559.492 \cdot kN \cdot m$

Span:

Assuming εcc<εcu:

Sum of yielding forces:

$F_{sy.total.span} := f_{yk} \cdot \left(A_{s1.span}\right) = 942.478 \cdot kN$

Assuming a value:

$x_{y.span} := 0.1935m$

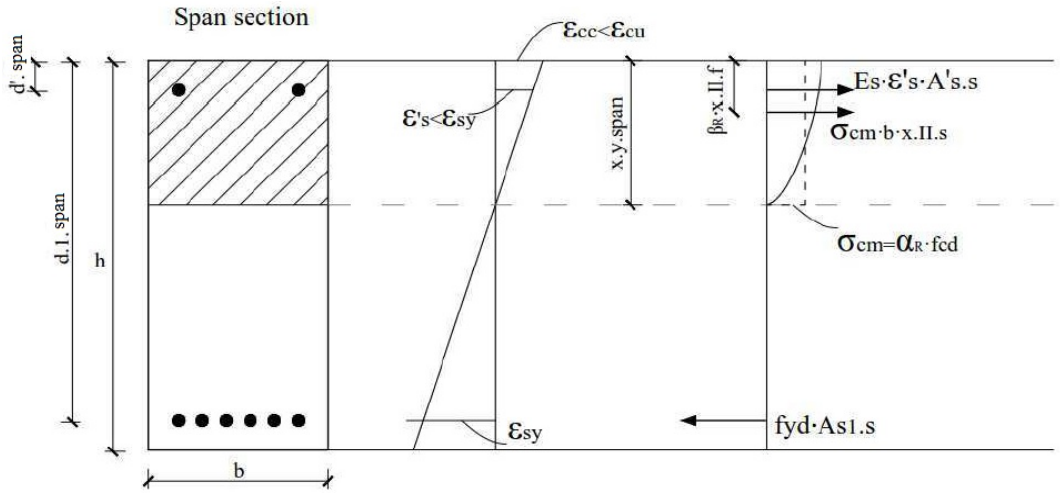

$$\varepsilon_{cc.y.span} := \frac{x_{y.span} \cdot \varepsilon_{sy}}{\left(d_{1.span} - x_{y.span}\right)} = 1.037 \times 10^{-3}$$

Concrete strain at the phase when reinforcement in tensile zone yields

$$\varepsilon'_{s.y.span} := \frac{\left(x_{y.span} - d'_{span}\right) \cdot \varepsilon_{cc.y.span}}{x_{y.span}} = 8.441 \times 10^{-4}$$

Steel strain of the reinforcement in the compressive zone

$$\alpha_{R.y.span} := 0.41$$

$\varepsilon'_{s.y.span} > \varepsilon_{sy} = 0$ Check if the reinforcement in the compression zone yields

$$F'_{s.y.span} := \varepsilon'_{s.y.span} \cdot E_{sm} \cdot A'_{s.span} = 38.184 \cdot kN$$

$$F_{c.y.span} := f_{cmean} \cdot \alpha_{R.y.span} \cdot x_{y.span} \cdot b = 904.419 \cdot kN$$

$F'_{s.y.span} + F_{c.y.span} = 942.603 \cdot kN$ Almost the same as the sum of yielding forces in the tensile zone means that the assumed depth of compression zone in yielding (xy) is correct.

$$\beta_{R.y.span} := 0.35$$

$$M_{y.span} := F_{c.y.span} \cdot \left(d_{1.span} - \beta_{R.y.span} \cdot x_{y.span}\right) + F'_{s.y.span} \cdot \left(d_{1.span} - d'_{span}\right) = 559.492 \cdot kN \cdot m$$

Load at first yielding:

$$q_{y.sup} := \frac{M_{y.sup} \cdot 8}{l_s^2} = 31.083 \cdot \frac{kN}{m}$$

For stiffness constant along the beam

$$R_{y.A} := \frac{q_{y.sup} \cdot l_s}{2} - \frac{M_{y.sup}}{l_s} = 139.873 \cdot kN \qquad x := 0 \cdot m, 0.1 \cdot m .. l_s$$

$$M_{y.x}(x) := R_{y.A} \cdot x - \frac{q_{y.sup} \cdot x^2}{2}$$

Expression for moment along the beam

Yielding curvature in support region:

$$\kappa_{y.sup} := \frac{\varepsilon_{cc.y.sup}}{x_{y.sup}} = 5.359 \times 10^{-3} \frac{1}{m}$$

Stiffness support:

$$EI_{sup} := \frac{M_{y.sup}}{\kappa_{y.sup}} = 1.044 \times 10^{8} \cdot N \cdot m^2$$

Yielding curvature in span region:

$$\kappa_{y.span} := \frac{\varepsilon_{cc.y.span}}{x_{y.span}} = 5.359 \times 10^{-3} \frac{1}{m}$$

Stiffness span:

$$EI_{span} := \frac{M_{y.span}}{\kappa_{y.span}} = 1.044 \times 10^{8} \cdot N \cdot m^2$$

$$\kappa_{y.sup.x}(x) := \frac{M_{y.x}(x)}{EI_{sup}}$$

$$\kappa_{y.span.x}(x) := \frac{M_{y.x}(x)}{EI_{span}}$$

For safety reasons, it is better to assume state III for both support and span region. The deformations will be due to this assumption overestimated, but it is a safe assumption. It is not clear when the response changes from state II to state III, and since concrete shows some plastic response before the yielding moment is reached, this is a safe assumption.

Expression for the curvature along the beam

$$\kappa_y(x) := \text{if}\left(M_{y.x}(x) \geq 0, \kappa_{y.span.x}(x), \kappa_{y.sup.x}(x)\right)$$

Deflection at span when yielding at support:

Support rotation at support A:

$$\theta_{y.A} := \frac{\int_0^{l_s} \kappa_y(x)\cdot\left(l_s - x\right) dx}{l_s}$$

$$\theta_{y.A} = 0.011$$

Section with rotation equal to 0 and thus the maximum deflection in the span:

Assuming a value of the distance from the outer support where maximum deflection might occure:

$$x_{y.f} := 5\cdot m$$

$$x_{y.f} := \text{root}\left(\int_0^{x_{y.f}} \kappa_y(x)\, dx - \theta_{y.A}, x_{y.f}\right)$$

$$x_{y.f} = 5.058\,m$$

Maximum deflection at yielding:

$$f_y := \theta_{y.A}\cdot x_{y.f} - \int_0^{x_{y.f}} \kappa_y(x)\cdot\left(x_{y.f} - x\right) dx$$

$$f_y = 33.437\cdot mm$$

Expression of the deflection in span 1:

$$f_{y.span}(x) := \theta_{y.A} \cdot x - \int_0^x \int_0^x \kappa_y(x)\, dx\, dx$$

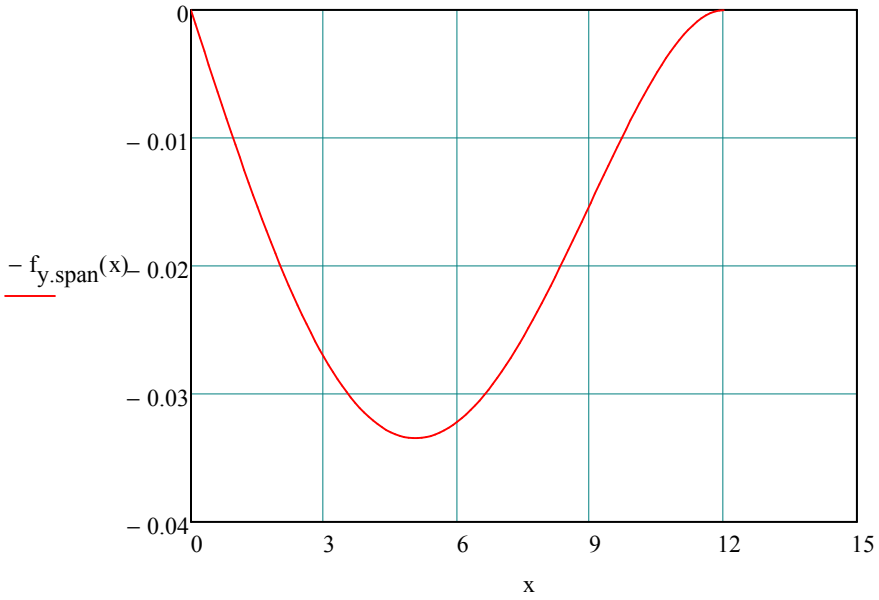

A.4 ULTIMATE PHASE

Ultimate moments:

The ultimate limit moments Mul are equal to the moment capacity Mrd of the considered cross sections. The sectional response is considered at state III. Ultimate moments are a special case of state III.

Moment capacity in the support section B

$\alpha_{R.ul} := 0.81$

$\beta_{R.ul} := 0.416$

Assuming yielding, where the steel strains are higher than the steel yield strain :
εs' , εs2 > εsy

Assuming a value of compression zone in the ultimate limit state:

$x_{ul.sup} := 0.1m$

$x_{ul.sup} := \text{root}\left(f_{yk} \cdot A_{s1.sup} + f_{yk} \cdot A_{s2.sup} - f_{yk} \cdot A'_{s.sup} - \alpha_{R.ul} \cdot f_{cmean} \cdot b \cdot x_{ul.sup}, x_{ul.sup}\right)$

$x_{ul.sup} = 0.09 \cdot m$

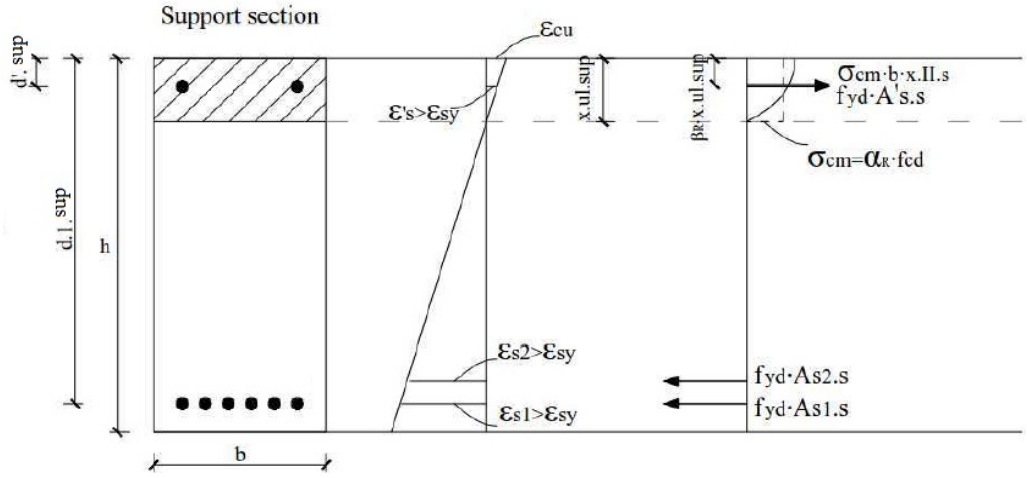

$\varepsilon_{sy} = 2.5 \times 10^{-3}$

$\varepsilon_{s1.sup} := \dfrac{\left(d_{1.sup} - x_{ul.sup}\right) \cdot \varepsilon_{cu}}{x_{ul.sup}} = 0.022$

$\varepsilon_{s1.sup} > \varepsilon_{sy} = 1$ YES!

In case if the condition above is not fullfiled, the full steel yield stress (fyd) may not be used in the calculations of moments. In such situation, the calculated steel strain that is lower then the yield strain should be used, multiplied with the concrete modulus of elasticity as steel stress $\varepsilon_{s2.sup} \cdot E_{sm}$.

$$\varepsilon'_{s.sup} := \frac{\left(x_{ul.sup} - d'_{sup}\right)\cdot\varepsilon_{cu}}{x_{ul.sup}} = 2.097\times 10^{-3} \qquad \varepsilon_{sy} = 2.5\times 10^{-3}$$

$$\varepsilon'_{s.sup} > \varepsilon_{sy} = 0$$

New assumption of x when compressive reinforcement is not yielding:

$$x_{ul.sup} := 0.1m$$

$$x_{ul.sup} := root\left[\begin{matrix}\left(f_{yk}\cdot A_{s1.sup}\right) \cdots \\ +\left(f_{yk}\cdot A_{s2.sup}\right) - \left(\varepsilon'_{s.sup}\cdot E_{sm}\cdot A'_{s.sup}\right) - \left(\alpha_{R.ul}\cdot f_{cmean}\cdot b\cdot x_{ul.sup}\right)\end{matrix}, x_{ul.sup}\right]$$

$$x_{ul.sup} = 0.092\cdot m$$

$$\varepsilon_{sy} = 2.5\times 10^{-3}$$

$$\varepsilon_{s1.sup.new} := \frac{\left(d_{1.sup} - x_{ul.sup}\right)\cdot\varepsilon_{cu}}{x_{ul.sup}} = 0.022$$

$$\varepsilon_{s1.sup.new} > \varepsilon_{sy} = 1 \qquad \text{YES!}$$

$$\varepsilon'_{s.sup.new} := \frac{\left(x_{ul.sup} - d'_{sup}\right)\cdot\varepsilon_{cu}}{x_{ul.sup}} = 2.127\times 10^{-3}$$

$$\varepsilon'_{s.sup} > \varepsilon_{sy} = 0$$

$$M_{ul.sup} := \alpha_{R.ul}\cdot f_{cmean}\cdot b\cdot x_{ul.sup}\cdot\left(d_{1.sup} - \beta_{R.ul}\cdot x_{ul.sup}\right) \cdots + \varepsilon'_{s.sup.new}\cdot E_{sm}\cdot A'_{s.sup}\cdot\left(d_{1.sup} - d'_{sup}\right) - f_{yk}\cdot A_{s2.sup}\cdot\left(d_{1.sup} - d_{2.sup}\right)$$

$$M_{ul.sup} = 587.105\cdot kN\cdot m \qquad M_{y.sup} = 559.492\cdot kN\cdot m$$

Moment capacity in the span section B

Assuming yielding εs' > εsy

Assuming a value of compressive zone in the span section:

$x_{ul.span} := 0.1m$

$x_{ul.span} := root\left(f_{yk} \cdot A_{s1.span} - \alpha_{R.ul} \cdot f_{cmean} \cdot b \cdot x_{ul.span} - f_{yk} \cdot A'_{s.span}, x_{ul.span}\right)$

$x_{ul.span} = 0.09\,m$

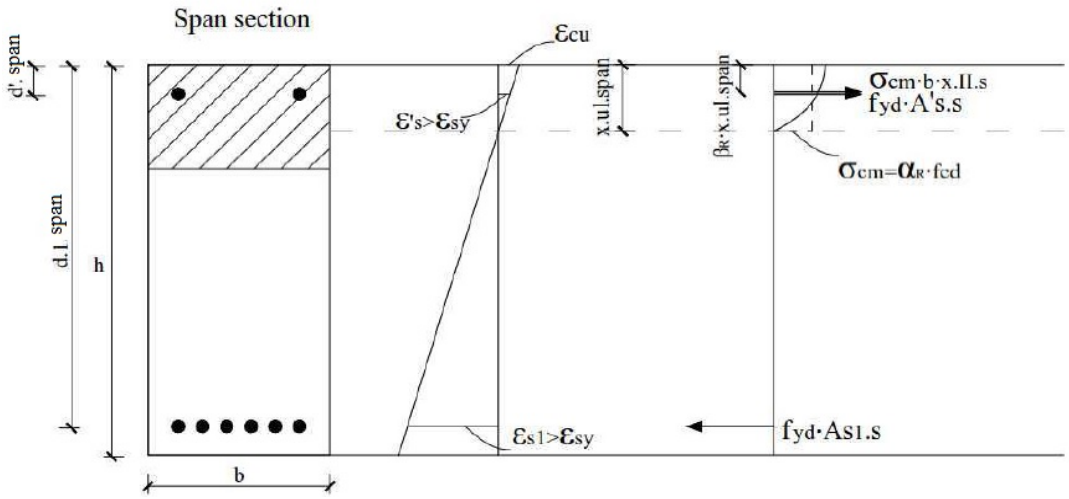

$$\varepsilon_{s1.span} := \frac{\left(d_{1.span} - x_{ul.span}\right) \cdot \varepsilon_{cu}}{x_{ul.span}} = 0.022$$

$\varepsilon_{s1.span} > \varepsilon_{sy} = 1$ YES!

$$\varepsilon'_{s.span} := \frac{\left(x_{ul.span} - d'_{span}\right) \cdot \varepsilon_{cu}}{x_{ul.span}} = 2.097 \times 10^{-3}$$

$\varepsilon'_{s.span} > \varepsilon_{sy} = 0$ YES!

New assumption x when compressive reinforcement not yielding:

$x_{ul.span} := 0.1m$

$x_{ul.span} := root\left(f_{yk} \cdot A_{s1.span} - \alpha_{R.ul} \cdot f_{cmean} \cdot b \cdot x_{ul.span} - \varepsilon'_{s.span} \cdot E_{sm} \cdot A'_{s.span}, x_{ul.span}\right)$

$x_{ul.span} = 0.092\,m$

$$\varepsilon_{s1.span.new} := \frac{\left(d_{1.span} - x_{ul.span}\right)\cdot\varepsilon_{cu}}{x_{ul.span}} = 0.022$$

$\varepsilon_{s1.span.new} > \varepsilon_{sy} = 1$ YES!

$$\varepsilon'_{s.span.new} := \frac{\left(x_{ul.span} - d'_{span}\right)\cdot\varepsilon_{cu}}{x_{ul.span}} = 2.127\times 10^{-3}$$

$\varepsilon'_{s.span.new} > \varepsilon_{sy} = 0$

$$M_{ul.span} := f_{cmean}\cdot\alpha_{R.ul}\cdot x_{ul.span}\cdot b\cdot\left(d_{1.span} - \beta_{R.ul}\cdot x_{ul.span}\right) \ldots + \varepsilon'_{s.span.new}\cdot E_{sm}\cdot A'_{s.span}\cdot\left(d_{1.span} - d'_{span}\right) = 587.105\cdot kN\cdot m$$

$\frac{M_{ul.sup}}{M_{ul.span}} = 1$ $M_{y.span} = 559.492\cdot kN\cdot m$

Maximum design load:

Assuming a value:

$$q_{ult} := 40\,\frac{kN}{m}$$

$$q_{ult} := root\left[\frac{\left[\frac{\left(q_{ult}\cdot l_s\right)}{2} - \frac{M_{ul.sup}}{l_s}\right]^2}{\left(2\cdot q_{ult}\right)} - M_{ul.span}, q_{ult}\right]$$

$q_{ult} = 47.526\cdot\frac{kN}{m}$ Ultimate limit load that corresponds to load in Phase 5

Comparison with other loads used in the analysis:

$q_1 = 9.243\cdot\frac{kN}{m}$ Quasi permanent load combination

$q_{1.ch} = 11.59\cdot\frac{kN}{m}$ Characteristic load combination

$q_2 = 35.43\cdot\frac{kN}{m}$ Overloading, matched with FEM analysis

$q_{y.sup} = 31.083\cdot\frac{kN}{m}$ Load at fisrst yielding

Ductility:

Check if the ductility is sufficient in the support:

$$d_m := \frac{\left(6 \cdot d_{1.sup} + 0 \cdot d_{2.sup}\right)}{6} = 0.66\,m$$

for concrete class C30/37 the ductility must be lower than 0,25:

$$ductility := \frac{x_{ul.sup}}{d_m} = 0.139$$

The ultimate limit moments ratio should be in between 0.5 and 2, then the ductility is considered to be sufficient.

$$\frac{M_{ul.sup}}{M_{ul.span}} = 1$$

Moment distribution for quasi-permanent load combination, short term response:

Support moment according to linear elastic analysis assuming constant stiffness along the span:

$$M_{1.el} := \frac{q_1 \cdot l_s^{\,2}}{8} \qquad q_1 = 9.243 \cdot \frac{kN}{m}$$

$$M_{1.el} = 166.374 \cdot kN \cdot m$$

Support moment according to nonlinear analysis, considering cracking but neglecting small influence of tension stiffening:

Assumption of support moment to fullfil the continuity condition where the rotations on both sides of the middle support B are equal to each other, what means that together they give zero, θb1=-θb.2=0

Assuming a value: $M_{1.sup} := 166.374 kN \cdot m$

$$R_{1.A} := \frac{q_1 \cdot l_s}{2} - \frac{M_{1.sup}}{l_s} \qquad R_{1.A} = 41.593 \cdot kN \qquad x := 0 \cdot m, 0.1 \cdot m .. l_s$$

$M_{1.x}(x) := R_{1.A} \cdot x - \frac{q_1 \cdot x^{2}}{2}$ Expression for the moment along the beam

Curvature in span region, cracked state (state II):

$\kappa_{1.span.II}(x) := \frac{M_{1.x}(x)}{E_c \cdot I_{II.span}}$ Assumed fully cracked

Curvature at support region, cracked state (state II):

$$\kappa_{1.sup.II}(x) := \frac{M_{1.x}(x)}{E_c \cdot I_{II.sup}}$$

$\kappa_1(x) := \text{if}\left(M_{1.x}(x) \geq 0, \kappa_{1.span.II}(x), \kappa_{1.sup.II}(x)\right)$ Expression for the curvature along the beam

Support rotation at B, towards span 1:

$$\theta_{1.sup.left} := \frac{\int_0^{l_s} \kappa_1(x)\cdot x\,dx}{l_s}$$

$\theta_{1.sup.left} = 0$ The rotation is almost zero. The continuity condition is thus fullfiled.

$x_s := 0$

$x_{1.span} := Maximize(M_{1.x}, x_s) = 4.5\,m$ The distance from the outer support to the maximum span moment in the beam

$M_{1.span} := M_{1.x}(Maximize(M_{1.x}, x_s)) = 93.585\cdot kN\cdot m$ The maximum span moment in the beam

$M_{1.x}(l_s) = -166.374\cdot kN\cdot m$ Corresponds to support moment at support B, OK!

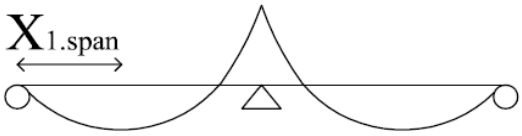

Deflection assuming fully cracked beam:

The maximum deflection can be estimated by calculating the support rotation at support A (outer support). Since the beam is analysed in cracked state (state II) this is an apparent deflection.

Support rotation at support A:

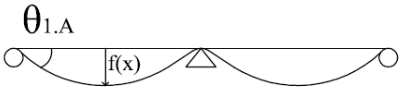

$$\theta_{1.A} := \frac{\int_0^{l_s} \kappa_1(x)\cdot(l_s - x)\,dx}{l_s}$$

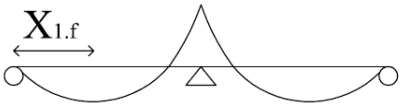

$\theta_{1.A} = 3.116\times 10^{-3}$

Section with rotation equal to 0 and thus the maximum deflection in the span:

Assuming a value of the distance from the outer support where maximum deflection might occure:

$x_{1.f} := 5\cdot m$

$$x_{1.f} := root\left(\int_0^{x_{1.f}} \kappa_1(x)\,dx - \theta_{1.A}, x_{1.f}\right) \qquad x_{1.f} = 5.058\,m$$

Maximum deflection:

$$f_1 := \theta_{1.A} \cdot x_{1.f} - \int_0^{x_{1.f}} \kappa_1(x) \cdot (x_{1.f} - x)\, dx$$

$$f_1 = 9.721 \cdot mm$$

Expression of the deflection in span:

$$f_{1.span}(x) := \theta_{1.A} \cdot x - \int_0^x \int_0^x \kappa_1(x)\, dx\, dx$$

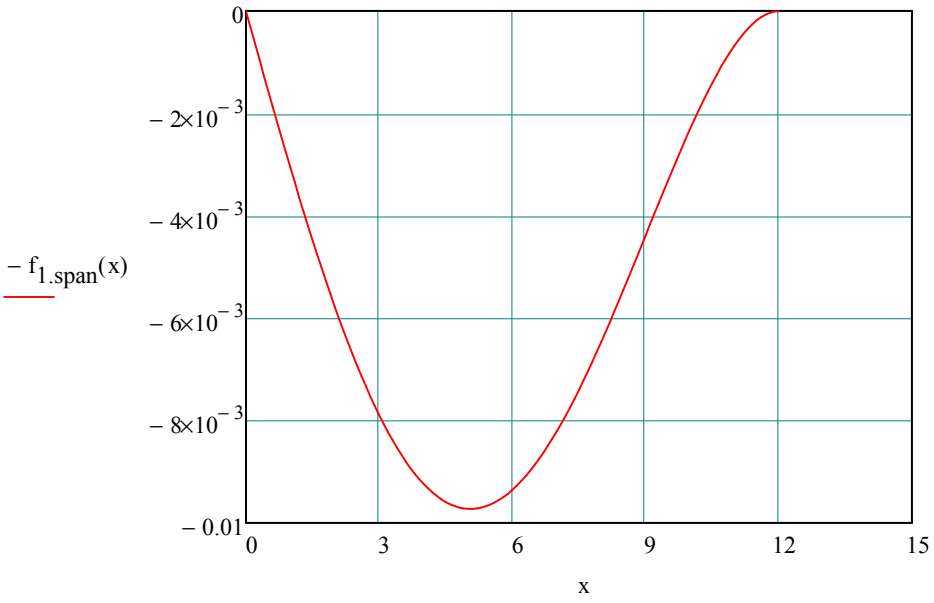

Moment distribution for characteristic- load combination, short term response:

Calculation of moments and deflection for characteristic-load combination is conducted since this combination is a starting point for overloading in practice. In practise, this load combination should not be exceed.

Support moment according to linear elastic analysis assuming constant stiffness along the span:

$$M_{1.ch.el} := \frac{q_{1.ch} \cdot l_s^{\,2}}{8} \qquad q_{1.ch} = 11.59 \cdot \frac{kN}{m}$$

$$M_{1.ch.el} = 208.62 \cdot kN \cdot m$$

Support moment according to nonlinear analysis, considering cracking but neglecting small influence of tension stiffening:

Assumption of support moment to fullfil the continuity condition where the rotations on both sides of the middle support B are equal to each other, what means that together they give zero, θb1=-θb.2=0

Assuming a value: $M_{1.ch.sup} := 208.62\,kN\cdot m$

$$R_{1.ch.A} := \frac{q_{1.ch}\cdot l_s}{2} - \frac{M_{1.ch.sup}}{l_s} = 52.155\cdot kN \qquad x := 0\cdot m, 0.1\cdot m .. l_s$$

$$M_{1.ch.x}(x) := R_{1.ch.A}\cdot x - \frac{q_{1.ch}\cdot x^2}{2}$$ Expression for the moment along the beam

Curvature in span region, cracked state (state II):

$$\kappa_{1.ch.span.II}(x) := \frac{M_{1.ch.x}(x)}{E_c\cdot I_{II.span}}$$ Assumed fully cracked

Curvature at support region, cracked state (state II):

$$\kappa_{1.ch.sup.II}(x) := \frac{M_{1.ch.x}(x)}{E_c\cdot I_{II.sup}}$$

Expression for the curvature along the beam

$$\kappa_{1.ch}(x) := \text{if}\left(M_{1.ch.x}(x) \geq 0, \kappa_{1.ch.span.II}(x), \kappa_{1.ch.sup.II}(x)\right)$$

Support rotation at B, towards span 1:

$$\theta_{1.ch.sup.left} := \frac{\int_0^{l_s} \kappa_{1.ch}(x)\cdot x\,dx}{l_s}$$

$\theta_{1.ch.sup.left} = 0$ The rotation is zero. The continuity condition is thus fullfiled.

$x_s := 0$

$x_{1.ch.span} := \text{Maximize}\left(M_{1.x}, x_s\right) = 4.5\,m$ The distance from the outer support to the maximum span moment in the beam

The maximum span moment in the beam

$$M_{1.ch.span} := M_{1.ch.x}\left(\text{Maximize}\left(M_{1.ch.x}, x_s\right)\right) = 117.349\cdot kN\cdot m$$

$M_{1.ch.x}(l_s) = -208.62 \cdot kN \cdot m$ Corresponds to support moment at support B, OK!

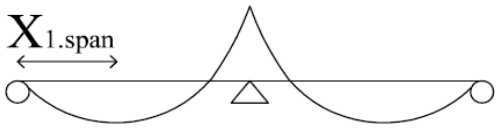

Deflection assuming fully cracked beam:

The maximum deflection can be estimated by calculating the support rotation at support A (outer support). Since the beam is analysed in cracked state (state II) this is an apparent deflection.

Support rotation at support A:

$$\theta_{1.ch.A} := \frac{\int_0^{l_s} \kappa_{1.ch}(x) \cdot (l_s - x)\, dx}{l_s}$$

$$\theta_{1.ch.A} = 3.907 \times 10^{-3}$$

Section with rotation equal to 0 and thus the maximum deflection in the span:

Assuming a value of the distance from the outer support where maximum deflection might occure:

$$x_{1.ch.f} := 5 \cdot m$$

$$x_{1.ch.f} := \text{root}\left(\int_0^{x_{1.f}} \kappa_1(x)\, dx - \theta_{1.A}, x_{1.f}\right)$$

$$x_{1.ch.f} = 5.058\, m$$

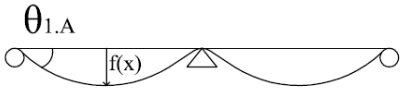

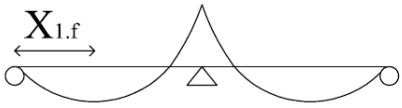

Maximum deflection:

$$f_{1ch} := \theta_{1.ch.A} \cdot x_{1.ch.f} - \int_0^{x_{1.ch.f}} \kappa_{1.ch}(x) \cdot \left(x_{1.ch.f} - x\right) dx$$

$$f_{1ch} = 12.19 \cdot mm$$

Expression of the deflection in span:

$$f_{1.ch.span}(x) := \theta_{1.ch.A} \cdot x - \int_0^x \int_0^x \kappa_{1.ch}(x)\, dx\, dx$$

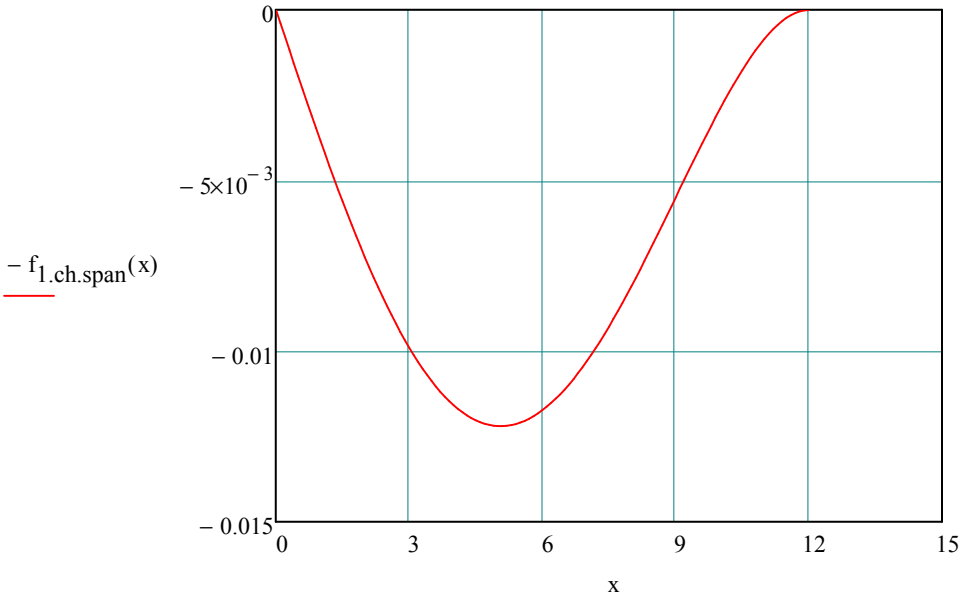

Moment distribution for combination that corresponds to overloading higher than yielding load, short term response:

Support moment according to nonlinear analysis, considering cracking but neglecting small influence of tension stiffening:

Assumption of support moment is the yielding moment:
The moment that corresponds to the overloading load is higher than the yieding moment My. Since the relation between the curvature and moment is assumed as bilinear with an increased branch after yielding moment My is reached, the moment that corresponds to overloading is determined from linear ralation between ultimate moment Mu and yielding moment My.

Relation between the difference between Mu and My, and the difference between qu and qy:

$$M_{uy} := \frac{M_{ul.sup}}{kN\cdot m} - \frac{M_{y.sup}}{kN\cdot m} = 27.614$$ The difference between ultimate and yielding moment over the support

$$q_{uy} := \frac{q_{ult}}{\frac{kN}{m}} - \frac{q_{y.sup}}{\frac{kN}{m}} = 16.444$$ The difference between ultimate and yielding load

$$Relation := \frac{M_{uy}}{q_{uy}} = 1.679$$ Tangent between M and q

$$atan(Relation) = 59.227\cdot deg$$ Angle

The difference between q2 and qy:

$$q_{2y} := \frac{q_2}{\frac{kN}{m}} - \frac{q_{y.sup}}{\frac{kN}{m}} = 4.347$$

The difference between moments M2 and My:

$$M_{2y} := \tan(atan(Relation))\cdot q_{2y} = 7.3$$

The magnitude of support moment at Phase2:

$$M_{2.sup} := M_{y.sup} + M_{2y}\cdot kN\cdot m = 566.792\cdot kN\cdot m \qquad M_{y.sup} = 559.492\cdot kN\cdot m$$

$$R_{2.A} := \frac{q_2 \cdot l_s}{2} - \frac{M_{2.sup}}{l_s} \qquad R_{2.A} = 165.347 \cdot kN \qquad x := 0 \cdot m, 0.1 \cdot m .. l_s$$

$$M_{2.x}(x) := R_{2.A} \cdot x - \frac{q_2 \cdot x^2}{2}$$ Expression for the moment along the beam

$x_s := 0$

$x_{2.span} := \text{Maximize}(M_{2.x}, x_s) = 4.667\,m$ The distance from the outer support to the maximum span moment in the beam

$M_{2.span} := M_{2.x}(\text{Maximize}(M_{2.x}, x_s)) = 385.828 \cdot kN \cdot m$ The maximum span moment in the beam

$M_{2.x}(l_s) = -566.792 \cdot kN \cdot m$ Corresponds to the support moment, OK!

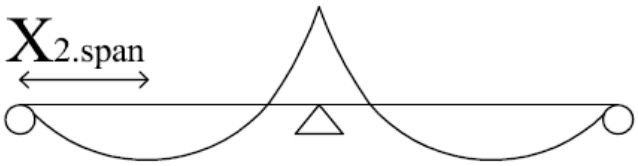

Field moment is lower than yield moment. So at q2 (overloading load) there is only yielding over support, thus no failure of the whole beam.

$M_{2.span} < M_{y.span} = 1$

Support:

Ultimate curvature support:

$$\kappa_{u.sup} := \frac{\varepsilon_{cu}}{x_{ul.sup}} = 0.038 \frac{1}{m}$$

Yielding curvature support:

$$\kappa_{y.sup} := \frac{\varepsilon_{cc.y.sup}}{x_{y.sup}} = 5.359 \times 10^{-3} \frac{1}{m}$$

Stiffness support:

$$EI_{sup} := \frac{M_{y.sup}}{\kappa_{y.sup}} = 1.044 \times 10^{8} \cdot N \cdot m^2$$

Span:

Ultimate curvature span:

$$\kappa_{u.span} := \frac{\varepsilon_{cu}}{x_{ul.span}} = 0.038\,\frac{1}{m}$$

Yielding curvature span:

$$\kappa_{y.span} := \frac{\varepsilon_{cc.y.span}}{x_{y.span}} = 5.359 \times 10^{-3}\,\frac{1}{m}$$

Stiffness span:

$$EI_{span} := \frac{M_{y.span}}{\kappa_{y.span}} = 1.044 \times 10^{8}\cdot N\cdot m^{2}$$

It would be reasonable in this case to assume stiffness in state II for curvature in span region. However, it is recomanded to use stiffness at state III after yielding in a section of the beam starts. This is due to the fact that it is difficult to define when the response changes from state II to state III exactly, since before yielding occurs the concrete already shows some plastic response. This is thus an assumption on safe side.

$$\kappa_{2.sup}(x) := \frac{M_{2.x}(x)}{EI_{sup}} \qquad \kappa_{2.span}(x) := \frac{M_{2.x}(x)}{EI_{span}}$$

Expression for the curvature along the beam

$$\kappa_2(x) := \text{if}\left(M_{2.x}(x) \geq 0, \kappa_{2.span}(x), \kappa_{2.sup}(x)\right)$$

Plastic rotation

$$l_{2.o} := 2\cdot\frac{R_{2.A}}{q_2} = 9.334\,m$$

$$l_{2.b} := l_s - l_{2.o} = 2.666\,m$$

$$z_{2.c} := l_{2.b}\cdot\frac{\frac{l_{2.o}}{3} + \frac{l_{2.b}}{4}}{\frac{l_{2.o}}{2} + \frac{l_{2.b}}{3}} = 1.813\,m$$

$$\theta_{2.sup.left} := \frac{\int_0^{l_s} \kappa_2(x)\cdot x\,dx}{l_s} = 2.718\times 10^{-3}$$

The rotation is checked by other method:

$$\theta_{2.sup.left} := \frac{\left[\frac{2}{3}\cdot\frac{M_{2.span}}{EI_{span}}\cdot l_{2.o}\cdot\frac{l_{2.o}}{2} - \frac{q_2}{2\cdot EI_{sup}}\cdot\left(l_{2.o}\cdot\frac{l_{2.b}^{2}}{2} + \frac{l_{2.b}^{3}}{3}\right)\cdot\left(l_{2.o} + z_{2.c}\right)\right]}{l_s} = 2.718\times 10^{-3}$$

Deflection:

The maximum deflection can be estimated by calculating the support rotation at support A (outer support). Since the beam is analyzed in cracked state (state II) this is an elastic deflection (reversible in theory).

Support rotation at support A:

$$\theta_{2.A} := \frac{\int_0^{l_s} \kappa_2(x)\cdot\left(l_s - x\right)dx}{l_s}$$

$$\theta_{2.A} = 0.014$$

Assuming a value of the distance from the outer support where maximum deflection might occure:

$$x_{2.f} := 5\cdot m$$

$$x_{2.f} := root\left(\int_0^{x_{2.f}} \kappa_2(x)\,dx - \theta_{2.A}, x_{2.f}\right)$$

$$x_{2.f} = 5.232\,m$$

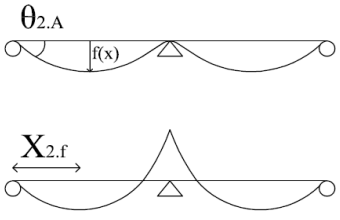

$$f_2 := \theta_{2.A} \cdot x_{2.f} - \int_0^{x_{2.f}} \kappa_2(x) \cdot \left(x_{2.f} - x\right) dx$$

$$f_2 = 43.822 \cdot mm$$

Deflection in span 1:

$$f_{2.span}(x) := \theta_{2.A} \cdot x - \int_0^x \int_0^x \kappa_2(x)\, dx\, dx$$

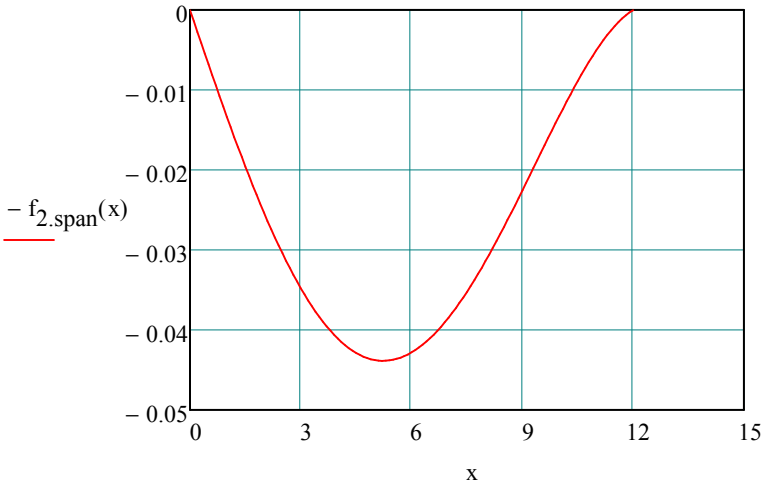

Moment distribution, short term response:

The analysis is based on state II model.

Support moment according to nonlinear analysis, considering cracking but neglecting small influence of tension stiffening:

The same load as in Phase 1 applies:

$$q_3 := q_1 = 9.243 \cdot \frac{kN}{m}$$

Assuming a value until the plastic rotation is equal to the plastic rotation in Phase 2:

$$M_{3.sup} := 93.8kN \cdot m$$

$$R_{3.A} := \frac{q_3 \cdot l_s}{2} - \frac{M_{3.sup}}{l_s} \qquad R_{3.A} = 47.641 \cdot kN \qquad x := 0 \cdot m, 0.1 \cdot m .. l_s$$

$$M_{3.x}(x) := R_{3.A} \cdot x - \frac{q_3 \cdot x^2}{2}$$ Expression for the moment along the beam

$$x_s := 0$$

$$x_{3.span} := \text{Maximize}\left(M_{3.x}, x_s\right) = 5.154\,m$$ The distance from the outer support to the maximum span moment in the beam

$$M_{3.span} := M_{3.x}\left(\text{Maximize}\left(M_{3.x}, x_s\right)\right) = 122.779 \cdot kN \cdot m$$ The maximum span moment in the beam

$$M_{3.x}\left(l_s\right) = -93.8 \cdot kN \cdot m$$ Corresponds to the support moment, OK!

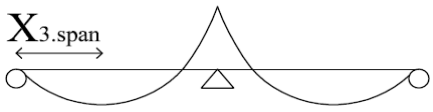

Curvature at field, cracked:

$$\kappa_{3.span.II}(x) := \frac{M_{3.x}(x)}{E_c \cdot I_{II.span}}$$ Assumed fully cracked

Curvature at support, cracked:

$$\kappa_{3.sup.II}(x) := \frac{M_{3.x}(x)}{E_c \cdot I_{II.sup}}$$

$$EI_{II.sup} = 106.784 \cdot MPa \cdot m^4$$

$$E_c \cdot I_{II.sup} = 106.784 \cdot MPa \cdot m^4$$

Expression for the curvature along the beam

$$\kappa_3(x) := \text{if}\left(M_{3.x}(x) \geq 0, \kappa_{3.span.II}(x), \kappa_{3.sup.II}(x)\right)$$

Plastic rotation

Discontinuity condition: θ.sup3a+θ.sup3b=θ.sup2

Plastic rotation at Phase 3 should be equal to plastic rotation at Phase 2:

$$\theta_{3.sup.left} := \frac{\int_0^{l_s} \kappa_3(x)\cdot x\,dx}{l_s} = 2.719\times 10^{-3}$$

$$\theta_{3.sup.left} + \theta_{3.sup.left} = 5.437\times 10^{-3}$$

Comparison with Phase 2:

$$\theta_{2.sup.left} = 2.718\times 10^{-3}$$

$$\theta_{2.sup.left}\cdot 2 = 5.437\times 10^{-3}$$

The discontinuity condition is fullfiled when these are equal to each other. Looking just for one side since the beam is symmetric

Check by other method:

$$l_{3.o} := 2\cdot\frac{R_{3.A}}{q_1} = 10.309\,\text{m}$$

$$l_{3.b} := l_s - l_{3.o} = 1.691\,\text{m}$$

$$z_{3.c} := l_{3.b}\cdot\frac{\frac{l_{3.o}}{3}+\frac{l_{3.b}}{4}}{\frac{l_{3.o}}{2}+\frac{l_{3.b}}{3}} = 1.141\,\text{m}$$

$$\theta_{3.sup.left} := \frac{\left[\frac{2}{3}\cdot\frac{M_{3.span}}{EI_{II.span}}\cdot l_{3.o}\cdot\frac{l_{3.o}}{2} - \frac{q_1}{2\cdot EI_{II.sup}}\cdot\left(l_{3.o}\cdot\frac{l_{3.b}^{2}}{2}+\frac{l_{3.b}^{3}}{3}\right)\cdot\left(l_{3.o}+z_{3.c}\right)\right]}{l_s} = 2.719\times 10^{-3}$$

Restraint moment:

Support: Field:

$M_{1.sup} = 166.374 \cdot kN \cdot m$ $M_{1.span} = 93.585 \cdot kN \cdot m$

$M_{3.sup} = 93.8 \cdot kN \cdot m$ $M_{3.span} = 122.779 \cdot kN \cdot m$

$M_{restraint.sup} := M_{3.sup} - M_{1.sup} = -72.574 \cdot kN \cdot m$ The result is decreased moment over support

$M_{restraint.span} := M_{3.span} - M_{1.span} = 29.194 \cdot kN \cdot m$ The result is increased moment over span

The restraint moment :

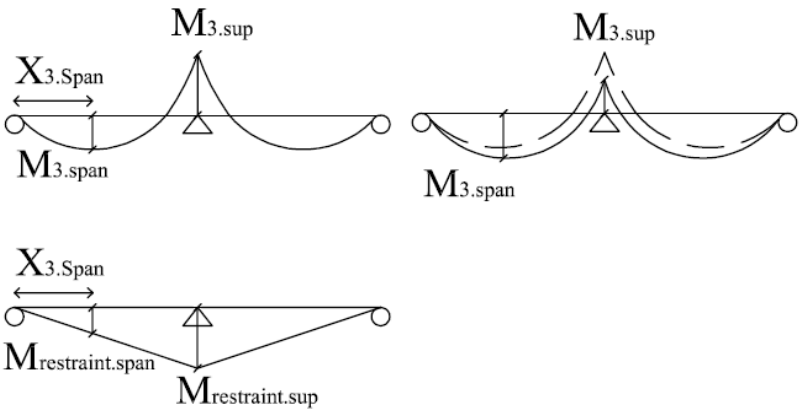

Deflection assuming fully cracked beam:

The maximum deflection can be estimated by calculating the support rotation at support A (outer support). Since the beam is analyzed in cracked state (state II) this is an apparent deflection.

Support rotation at support A:

$$\theta_{3.A} := \frac{\int_0^{l_s} \kappa_3(x) \cdot (l_s - x)\, dx}{l_s}$$

$\theta_{3.A} = 4.475 \times 10^{-3}$

Section with rotation equal to 0 and thus the maximum deflection in the span:

Assuming a value of the distance from the outer support where maximum deflection might occure:

$x_{3.f} := 5 \cdot m$

$x_{3.f} := \text{root}\left(\int_0^{x_{3.f}} \kappa_3(x)\,dx - \theta_{3.A}, x_{3.f}\right)$

$x_{3.f} = 5.612\,m$

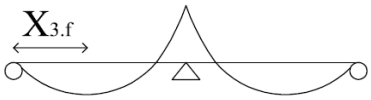

Maximum deflection:

$f_3 := \theta_{3.A} \cdot x_{3.f} - \int_0^{x_{3.f}} \kappa_3(x) \cdot (x_{3.f} - x)\,dx$

$f_3 = 15.55 \cdot mm$

Deflection in span 1:

$f_{3.span}(x) := \theta_{3.A} \cdot x - \int_0^x \int_0^x \kappa_3(x)\,dx\,dx$

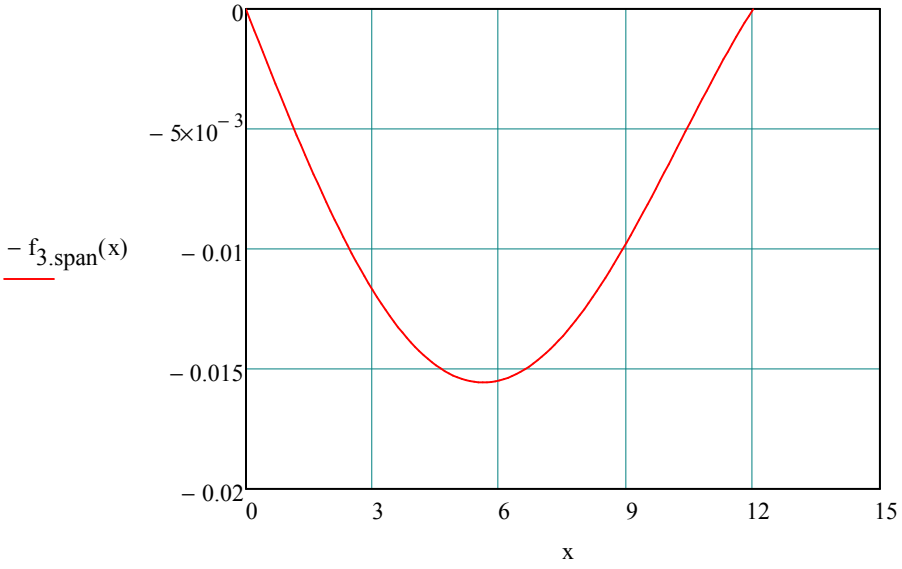

Moment distribution for overloading, short term respons:

Support moment according to nonlinear analysis, considering cracking but neglecting small influence of tension stiffening:

$q_4 := q_2$

Assuming the same value as in Phase 2 $M_{4.sup} := 566.792\,kN\cdot m$ $M_{2.sup} = 566.792\cdot kN\cdot m$

$R_{4.A} := \frac{q_4\cdot l_s}{2} - \frac{M_{4.sup}}{l_s}$ $R_{4.A} = 165.347\cdot kN$ $x := 0\cdot m, 0.1\cdot m .. l_s$

Expression for the moment along the beam

$M_{4.x}(x) := R_{4.A}\cdot x - \frac{q_4\cdot x^2}{2}$

$x_s := 0$

$x_{4.span} := \text{Maximize}(M_{4.x}, x_s) = 4.667\,m$ The distance from the outer support to the maximum span moment in the beam

$M_{4.span} := M_{4.x}(\text{Maximize}(M_{4.x}, x_s)) = 385.828\cdot kN\cdot m$ The maximum span moment in the beam

$M_{4.x}(l_s) = -566.792\cdot kN\cdot m$ Corresponds to the support moment, OK!

$M_{2.span} = 385.828\cdot kN\cdot m$

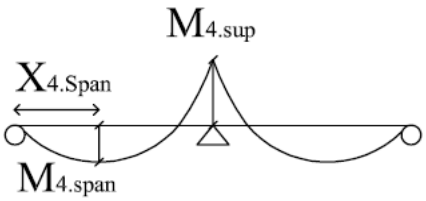

Curvature:

$\kappa_{4.sup}(x) := \frac{M_{4.x}(x)}{EI_{sup}}$ $\kappa_{4.span}(x) := \frac{M_{4.x}(x)}{EI_{span}}$

Expression for the curvature along the beam

$$\kappa_4(x) := \text{if}\left(M_{4.x}(x) \geq 0, \kappa_{4.span}(x), \kappa_{4.sup}(x)\right)$$

Plastic rotation

$$l_{4.o} := 2 \cdot \frac{R_{4.A}}{q_2} = 9.334\,\text{m}$$

$$l_{4.b} := l_s - l_{4.o} = 2.666\,\text{m}$$

$$z_{4.c} := l_{4.b} \cdot \frac{\frac{l_{4.o}}{3} + \frac{l_{4.b}}{4}}{\frac{l_{4.o}}{2} + \frac{l_{4.b}}{3}} = 1.813\,\text{m}$$

$$\theta_{4.sup.left} := \frac{\int_0^{l_s} \kappa_4(x) \cdot x\,dx}{l_s} = 2.718 \times 10^{-3}$$ Phase 4

$$\theta_{2.sup.left} = 2.718 \times 10^{-3}$$ Phase 2

$$\theta_{4.sup.left} := \frac{\left[\frac{2}{3} \cdot \frac{M_{4.span}}{EI_{span}} \cdot l_{4.o} \cdot \frac{l_{4.o}}{2} - \frac{q_4}{2 \cdot EI_{sup}} \cdot \left(l_{4.o} \cdot \frac{l_{4.b}^{\,2}}{2} + \frac{l_{4.b}^{\,3}}{3}\right) \cdot \left(l_{4.o} + z_{4.c}\right)\right]}{l_s} = 2.718 \times 10^{-3}$$

Deflection:

The maximum deflection can be estimated by calculating the support rotation at support A (outer support). Since the beam is analyzed in cracked state (state II) this is an apparent rotation.

Support rotation at support A:

$$\theta_{4.A} := \frac{\int_0^{l_s} \kappa_4(x) \cdot \left(l_s - x\right) dx}{l_s}$$

$$\theta_{4.A} = 0.014$$

Assuming a value of the distance from the outer support where maximum deflection might occure:

$x_{4.f} := 5 \cdot m$

$x_{4.f} := \text{root}\left(\int_0^{x_{4.f}} \kappa_4(x)\,dx - \theta_{4.A}, x_{4.f}\right)$

$x_{4.f} = 5.232\,m$

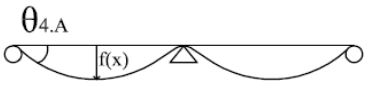

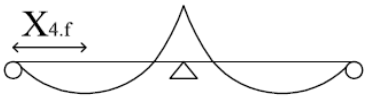

Maximum deflection:

$f_4 := \theta_{4.A} \cdot x_{4.f} - \int_0^{x_{4.f}} \kappa_4(x) \cdot (x_{4.f} - x)\,dx$

$f_4 = 43.822 \cdot mm$

Deflection in span 1:

$f_{4.span}(x) := \theta_{4.A} \cdot x - \int_0^x \int_0^x \kappa_4(x)\,dx\,dx$

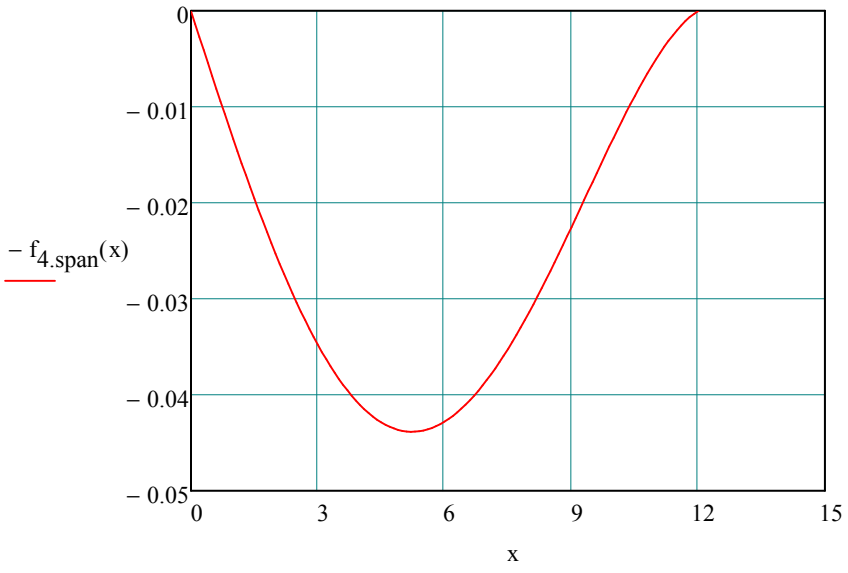

A.9 PHASE 5

The analysis is performed at state III model.

$q_5 := q_{ult} = 47.526 \cdot \frac{kN}{m}$ Ultimate load

$M_{5.sup} := M_{ul.sup} = 587.105 \cdot kN \cdot m$ Ultimate support moment $M_{y.sup} = 559.492 \cdot kN \cdot m$

$M_{5.span} := M_{ul.span} = 587.105 \cdot kN \cdot m$ Ultimate span moment $M_{y.span} = 559.492 \cdot kN \cdot m$

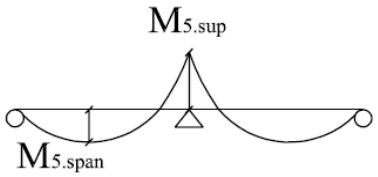

Plastic rotation in ultimate limit state

$$R_{5.A} := \frac{(q_5 \cdot l_s)}{2} - \frac{M_{5.sup}}{l_s} = 236.233 \cdot kN$$

$$l_{5.o} := 2 \cdot \frac{R_{5.A}}{q_5} = 9.941\,m$$

$$l_{5.b} := l_s - l_{5.o} = 2.059\,m$$

$$z_{5.c} := l_{5.b} \cdot \frac{\frac{l_{5.o}}{3} + \frac{l_{5.b}}{4}}{\frac{l_{5.o}}{2} + \frac{l_{5.b}}{3}} = 1.393\,m$$

$$\theta_{5.sup.left} := \frac{\left[\frac{2}{3} \cdot \frac{M_{5.span}}{EI_{span}} \cdot l_{5.o} \cdot \frac{l_{5.o}}{2} - \frac{q_5}{2 \cdot EI_{sup}} \cdot \left(l_{5.o} \cdot \frac{l_{5.b}^{\,2}}{2} + \frac{l_{5.b}^{\,3}}{3}\right) \cdot (l_{5.o} + z_{5.c})\right]}{l_s} = 0.01$$

$x := 0 \cdot m, 0.1 \cdot m .. l_s$

Expression for the moment along the beam

$$M_{5.x}(x) := R_{5.A} \cdot x - \frac{q_5 \cdot x^2}{2}$$

$x_s = 0$

$x_{5.span} := \text{Maximize}\left(M_{5.x}, x_s\right) = 4.971\,\text{m}$

$M_{5.x}\left(l_s\right) = -587.105 \cdot \text{kN} \cdot \text{m}$ Corresponds to support moment, OK!

Curvature at span:

$$\kappa_{5.span}(x) := \frac{M_{5.x}(x)}{EI_{span}}$$

Curvature at support:

$$\kappa_{5.sup}(x) := \frac{M_{5.x}(x)}{EI_{sup}}$$

Expression for curvature along the span:

$$\kappa_5(x) := \text{if}\left(M_{5.x}(x) \geq 0, \kappa_{5.span}(x), \kappa_{5.sup}(x)\right)$$

$$\theta_{5.sup.left} := \frac{\int_0^{l_s} \kappa_5(x) \cdot x \, dx}{l_s} = 0.01$$

$\theta_{5.sup} := 2 \cdot \theta_{5.sup.left} = 0.021$

Deflection:

The maximum deflection can be estimated by calculating the support rotation at support A (outer support).

Support rotation at support A:

$$\theta_{5.A} := \frac{\int_0^{l_s} \kappa_5(x)\cdot\left(l_s - x\right) dx}{l_s}$$

$$\theta_{5.A} = 0.022$$

Section with rotation equal to 0 and thus the maximum deflection in the span:

Assuming a value of the distance from the outer support where maximum deflection might occure:

$$x_{5.f} := 5\cdot m$$

$$x_{5.f} := \text{root}\left(\int_0^{x_{5.f}} \kappa_5(x)\, dx - \theta_{5.A}, x_{5.f}\right)$$

$$x_{5.f} = 5.487\,m$$

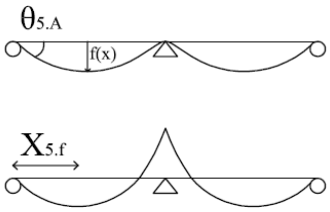

Maximum deflection:

$$f_5 := \theta_{5.A} \cdot x_{5.f} - \int_0^{x_{5.f}} \kappa_5(x) \cdot \left(x_{5.f} - x\right) dx$$

$$f_5 = 73.025 \cdot mm$$

Deflection in span:

$$f_{5.span}(x) := \theta_{5.A} \cdot x - \int_0^x \int_0^x \kappa_5(x)\, dx\, dx$$

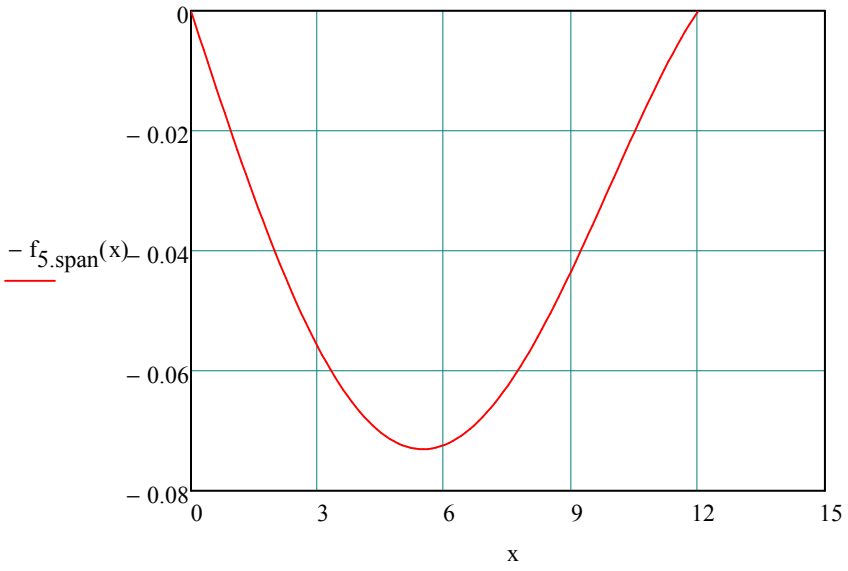

A.10 PLASTIC ROTATION CAPACITY

According to Eurocode 2:

$\text{ductility} = 0.139$

Reinforcement B500B, concrete C30/37

Plastic rotation capacity from the graph in Eurocode 2:

$\theta pl_d := 0.013$

Shear Slenderness:

$l_{5.b} = 2.059\,\text{m}$ Support moment region

$d_m = 0.66\,\text{m}$ Effective depth

$\lambda_s := \frac{l_{5.b}}{d_m} = 3.12$

Condition to fullfil:

$\lambda_s > 3 = 1$ OK!

Modification factor:

$k_{\lambda.s} := \sqrt{\frac{\lambda_s}{3}} = 1.02$

Modified capacity:

$\theta pl_{d.EC} := \theta pl_d \cdot k_{\lambda.s} = 0.013$

Plastic rotation capacity based on Eurocode 2 is determined as total plastic rotation capacity, what means that both sides are included in this value.

According to Betonghandbok:

$f_{yk} = 500 \cdot \text{MPa}$ Mean value of the tensile strength for steel

$f_{cmean} = 38 \cdot \text{MPa}$ Mean value of the compressive strength for concrete C30/37

The calculation is performed without consideration to stirrups.
This is because there are no stirrups in FE modelling. There are stirrups in such beam in reality.

$$\omega_{bal} := 0.8 \cdot \frac{\left(3.5 \cdot 10^{-3}\right)}{3.5 \cdot 10^{-3} + \frac{f_{yk}}{E_{sm}}} = 0.467$$

$$\omega_s := \frac{\left(A_{s1.sup} + A_{s2.sup}\right) \cdot f_{yk}}{b \cdot d_m \cdot f_{cmean}} = 0.125$$

$$\omega'_s := \frac{A'_{s.sup} \cdot f_{yk}}{b \cdot d_m \cdot f_{cmean}} = 0.015$$

$\omega_v := 0$ No consideration of stirrups

$\omega_{s.1} := 0$ No consideration of stirrups

$$A_\theta := 1 - 1.4 \cdot \frac{\omega_s}{\omega_{bal}} = 0.624$$

The minimum value of A.θ that is allowed is 0.05

$A_{\theta.m} := 0.05$

$l_{5.b} = 2.059\,m$ Length from the support to the point where moment is zero along the beam

$B_\theta := 1.0$ For KS600 (page 106 BHB)

$$C_\theta := 10 \cdot \frac{l_{5.b}}{d_m} = 31.195$$

The maximum value of C.θ that is allowed is 45

$C_{\theta.m} := 45$

A*B should be lower than 1.7:

$A_\theta \cdot B_\theta = 0.624$

The plastic moment capacity on both side of the middle support:

$$\theta_{pl.d.ABC} := 2\left(A_\theta \cdot B_\theta \cdot C_\theta \cdot 10^{-3}\right) = 0.039$$

$\theta_{5.sup} = 0.021$ The support rotation in ultimate state

A.11 PLASTIC ROTATION LIMITATION

The analysis is performed at state III model.

Ultimate load

Load iteration until plastic rotation is equal to the plastic rotation in Eurocode 2.

$q_{5.new} := 42.05 \frac{kN}{m}$ $q_{ult} = 47.526 \cdot \frac{kN}{m}$

$M_{5.sup} := M_{ul.sup} = 587.105 \cdot kN \cdot m$ Ultimate support moment $M_{y.sup} = 559.492 \cdot kN \cdot m$

$M_{5.span} := M_{ul.span} = 587.105 \cdot kN \cdot m$ Ultimate span moment $M_{y.span} = 559.492 \cdot kN \cdot m$

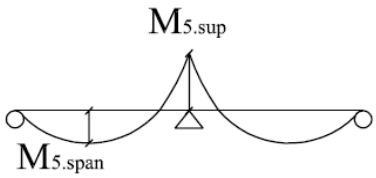

Plastic rotation in ultimate limit state

$$R_{5.A.new} := \frac{(q_{5.new} \cdot l_s)}{2} - \frac{M_{5.sup}}{l_s} = 203.375 \cdot kN$$

$$l_{5.o.new} := 2 \cdot \frac{R_{5.A.new}}{q_{5.new}} = 9.673\,m$$

$$l_{5.b.new} := l_s - l_{5.o.new} = 2.327\,m$$

$$z_{5.c.new} := l_{5.b.new} \cdot \frac{\frac{l_{5.o.new}}{3} + \frac{l_{5.b.new}}{4}}{\frac{l_{5.o.new}}{2} + \frac{l_{5.b.new}}{3}} = 1.578\,m$$

$x := 0 \cdot m, 0.1 \cdot m .. l_s$

Expression for the moment along the beam

$$M_{5.new.x}(x) := R_{5.A.new} \cdot x - \frac{q_{5.new} \cdot x^2}{2}$$

$x_s = 0$

$x_{5.span.new} := \text{Maximize}\left(M_{5.x}, x_s\right) = 4.971\,\text{m}$

$M_{5.new.x}\left(l_s\right) = -587.105 \cdot \text{kN} \cdot \text{m}$ Corresponds to support moment, OK!

$M_{5.span.new} := M_{5.new.x}\left(\text{Maximize}\left(M_{5.new.x}, x_s\right)\right) = 491.81 \cdot \text{kN} \cdot \text{m}$

Curvature at span:

$$\kappa_{5.span.new}(x) := \frac{M_{5.new.x}(x)}{EI_{span}}$$

Curvature at support:

$$\kappa_{5.sup.new}(x) := \frac{M_{5.new.x}(x)}{EI_{sup}}$$

Expression for curvature along the span:

$$\kappa_{5.new}(x) := \text{if}\left(M_{5.new.x}(x) \geq 0, \kappa_{5.span.new}(x), \kappa_{5.sup.new}(x)\right)$$

$$\theta_{5.sup.left.new} := \frac{\int_0^{l_s} \kappa_{5.new}(x) \cdot x \, dx}{l_s} = 6.505 \times 10^{-3}$$

$\theta_{5.sup.new} := 2 \cdot \theta_{5.sup.left.new} = 0.013$ $\theta pl_{d.EC} := \theta pl_d \cdot k_{\lambda.s} = 0.013$

Load itteration until plastic rotation is equal to plastic rotation in Eurocode 2

Deflection:

The maximum deflection can be estimated by calculating the support rotation at support A (outer support).

Support rotation at support A:

$$\theta_{5.A.new} := \frac{\int_0^{l_s} \kappa_{5.new}(x) \cdot \left(l_s - x\right) dx}{l_s} \qquad \theta_{5.A.new} = 0.018$$

Section with rotation equal to 0 and thus the maximum deflection in the span:

Assuming a value of the distance from the outer support where maximum deflection might occure:

$x_{5.f.new} := 5 \cdot m$

$x_{5.f.new} := \text{root}\left(\int_0^{x_{5.f.new}} \kappa_{5.new}(x)\,dx - \theta_{5.A.new}, x_{5.f.new}\right)$

$x_{5.f.new} = 5.383\,m$

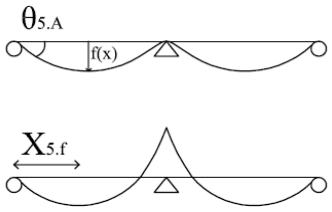

Maximum deflection:

$$f_{5.new} := \theta_{5.A.new} \cdot x_{5.f.new} - \int_0^{x_{5.f.new}} \kappa_{5.new}(x) \cdot \left(x_{5.f.new} - x\right) dx$$

$f_{5.new} = 59.011 \cdot mm$

Deflection in span:

$$f_{5.span.new}(x) := \theta_{5.A.new} \cdot x - \int_0^x \int_0^x \kappa_{5.new}(x)\,dx\,dx$$

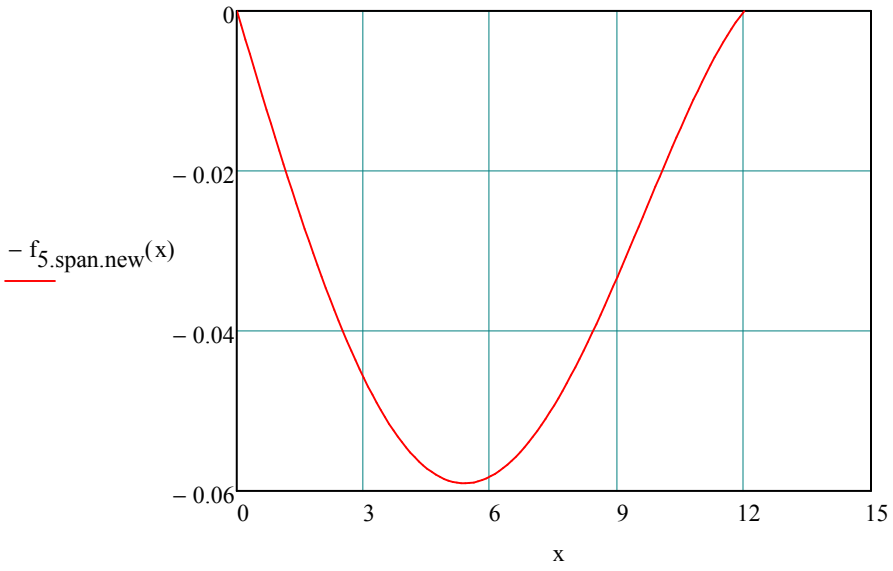

A.12 COMPARISON OF PARAMETERS

Support Moment:

$M_{1.sup} = 166.374 \cdot kN \cdot m$

$M_{2.sup} = 566.792 \cdot kN \cdot m$

$M_{3.sup} = 93.8 \cdot kN \cdot m$

$M_{4.sup} = 566.792 \cdot kN \cdot m$

$M_{5.sup} = 587.105 \cdot kN \cdot m$

Field Moment:

$M_{1.span} = 93.585 \cdot kN \cdot m$ Phase 1

$M_{2.span} = 385.828 \cdot kN \cdot m$ Phase 2

$M_{3.span} = 122.779 \cdot kN \cdot m$ Phase 3

$M_{4.span} = 385.828 \cdot kN \cdot m$ Phase 4

$M_{5.span} = 587.105 \cdot kN \cdot m$ Phase 5

$M_{5.span.new} = 491.81 \cdot kN \cdot m$ Phase 5, plastic rotation limitation

Restraint moment support:

$M_{3.sup} - M_{1.sup} = -72.574 \cdot kN \cdot m$

Restraint moment span:

$M_{3.span} - M_{1.span} = 29.194 \cdot kN \cdot m$

Load:

$q_{cr.sup} = 4.56 \cdot \frac{kN}{m}$ Cracking load for middle support

$q_{cr.span} = 8.107 \cdot \frac{kN}{m}$ Cracking load for span

$q_1 = 9.243 \cdot \frac{kN}{m}$ Phase 1, Service load quasi-permanent

$q_{1.ch} = 11.59 \cdot \frac{kN}{m}$ Characteristic load

$q_{y.sup} = 31.083 \cdot \frac{kN}{m}$ Yielding load for support

$q_2 = 35.43 \cdot \frac{kN}{m}$ Phase 2, Overload

$q_3 = 9.243 \cdot \frac{kN}{m}$ Phase 3, Service load quasi-permanent

$q_4 = 35.43 \cdot \frac{kN}{m}$ Phase 4, Overload

$q_{5.new} = 42.05 \cdot \frac{kN}{m}$ Ultimate load, with plastic rotation limitation

Plastic rotation:

$\theta_{1.sup.left} = 0$ Phase 1 No rotations at this Phase

$\theta_{2.sup.left} = 2.718 \times 10^{-3}$ Phase 2

$\theta_{3.sup.left} = 2.719 \times 10^{-3}$ Phase 3

$\theta_{4.sup.left} = 2.718 \times 10^{-3}$ Phase 4

$\theta_{5.sup.left} = 0.01$ Phase 5

$\theta_{5.sup.left.new} = 6.505 \times 10^{-3}$ Phase 5, plastic rotation limitation

Platic rotation capacity

$\theta pl_{d.EC} = 0.013$ $\theta_{5.sup.left} \cdot 2 = 0.021$ For both sides

$\theta_{pl.d.ABC} = 0.039$

Deflection:

$f_1 = 9.721 \cdot mm$ Phase 1

$f_y = 33.437 \cdot mm$ Yielding at supoprt

$f_2 = 43.822 \cdot mm$ Phase 2

$f_3 = 15.55 \cdot mm$ Phase 3

$f_4 = 43.822 \cdot mm$ Phase 4

$f_5 = 0.073\,m$ Phase 5

$f_{5.new} = 59.011 \cdot mm$ Phase 5, with plastic rotation limitation

Maximum deflection section:

$x_{1.f} = 5.058\,m$

$x_{2.f} = 5.232\,m$

$x_{3.f} = 5.612\,m$

$x_{4.f} = 5.232\,m$

$x_{5.f} = 5.487\,m$

Maximum moment section:

$x_{1.span} = 4.5\,m$

$x_{2.span} = 4.667\,m$

$x_{3.span} = 5.154\,m$

$x_{4.span} = 4.667\,m$

$x_{5.span} = 4.971\,m$

Stiffeness distribution along halv the beam:

$$EI_{Phase1}(x) := if\left(M_{1.x}(x) > 0, E_c \cdot I_{II.span}, E_c \cdot I_{II.sup}\right)$$

$$EI_{Phase2}(x) := if\left(M_{2.x}(x) > 0, EI_{span}, EI_{sup}\right)$$

$$EI_{Phase3}(x) := if\left(M_{3.x}(x) > 0, E_c \cdot I_{II.span}, E_c \cdot I_{II.sup}\right)$$

$$EI_{Phase4}(x) := if\left(M_{4.x}(x) > 0, EI_{span}, EI_{sup}\right)$$

$$EI_{Phase5}(x) := if\left(M_{5.x}(x) > 0, EI_{span}, EI_{sup}\right)$$

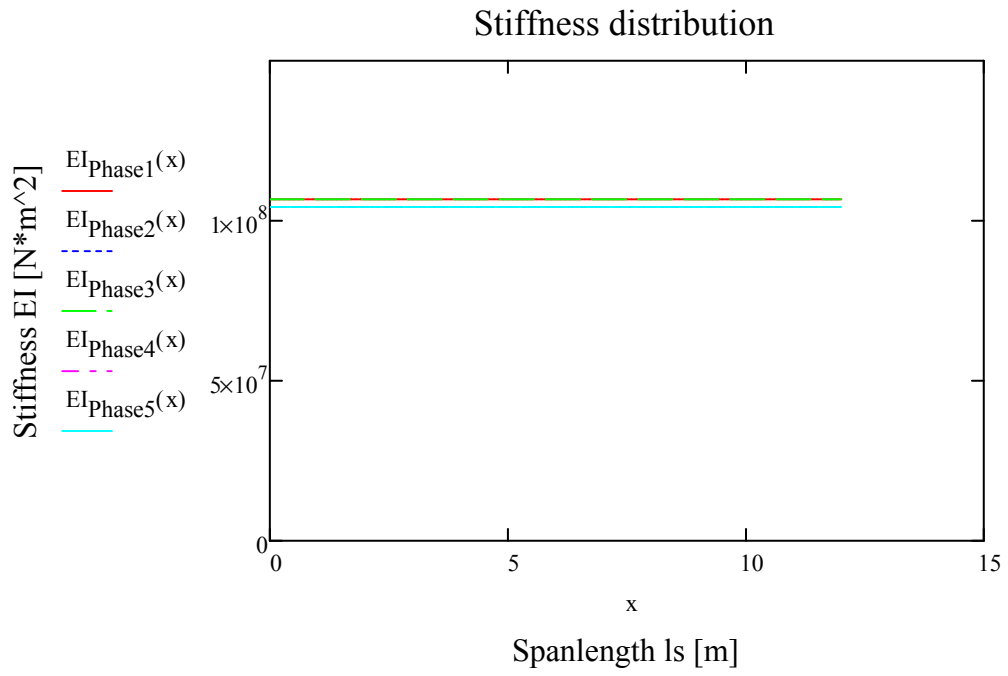
Stiffness distribution
Stiffness EI [N*m^2]
EIPhase1(x)
EIPhase2(x)
EIPhase3(x)
EIPhase4(x)
EIPhase5(x)
1×10^8
5×10^7
0
0
5
10
15
x
Spanlength ls [m]

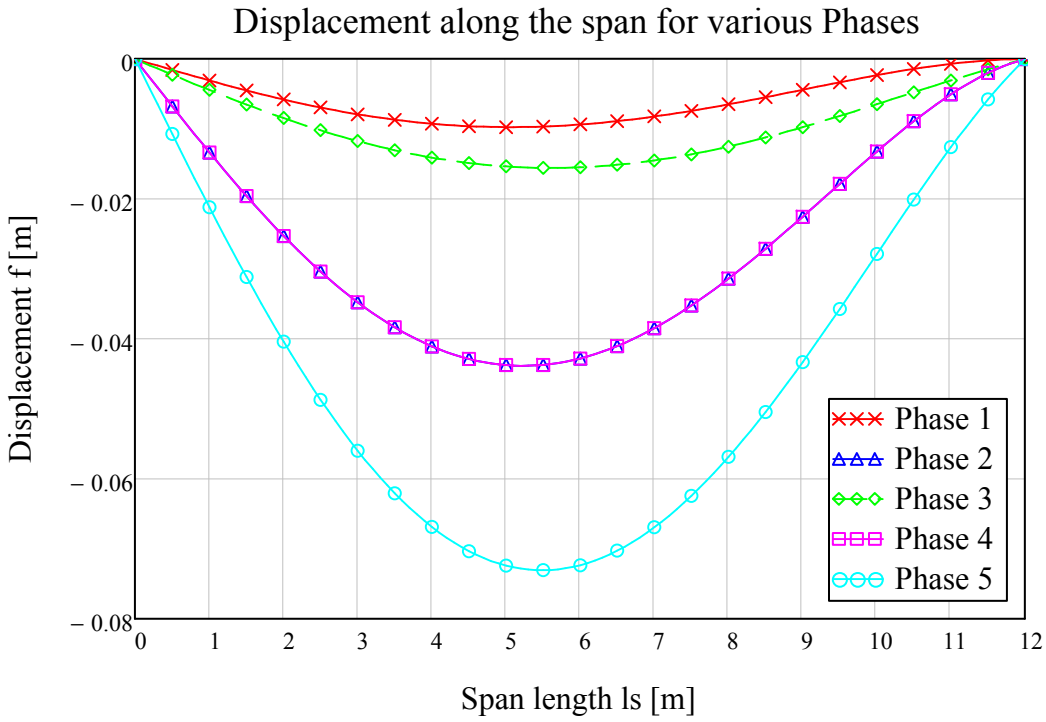
Displacement along the span for various Phases
Displacement f [m]
0
– 0.02
– 0.04
– 0.06
– 0.08
0
1
2
3
4
5
6
7
8
9
10
11
12
Phase 1
Phase 2
Phase 3
Phase 4
Phase 5
Span length ls [m]

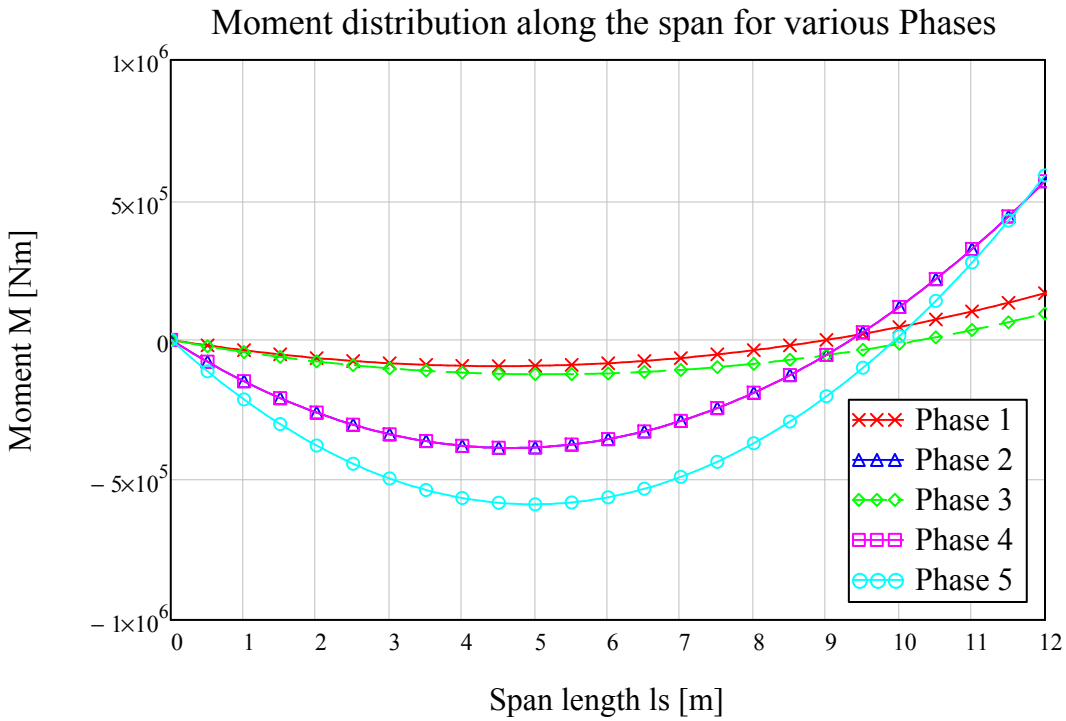

$M_{restraint1.3}(x) := M_{3.x}(x) - M_{1.x}(x)$ Difference in moment between Phase 1 and 3

$M_{restraint2.4}(x) := M_{4.x}(x) - M_{2.x}(x)$ Difference in moment between Phase 2 and 4

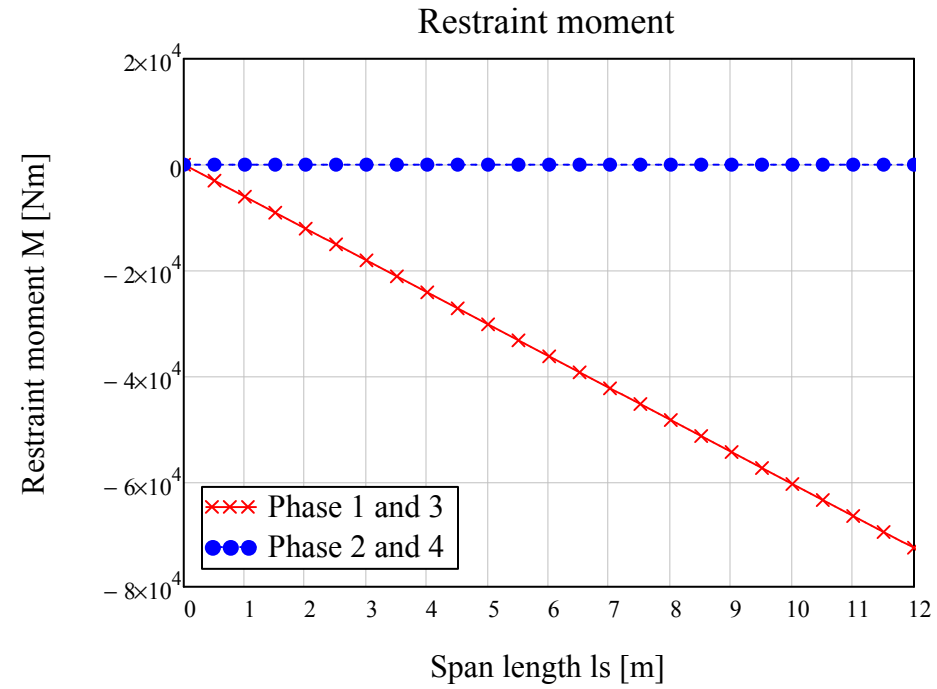
Restraint moment
Restraint moment M [Nm]
2×10^4
0
– 2×10^4
– 4×10^4
– 6×10^4
– 8×10^4
0 1 2 3 4 5 6 7 8 9 10 11 12
Phase 1 and 3
Phase 2 and 4
Span length ls [m]

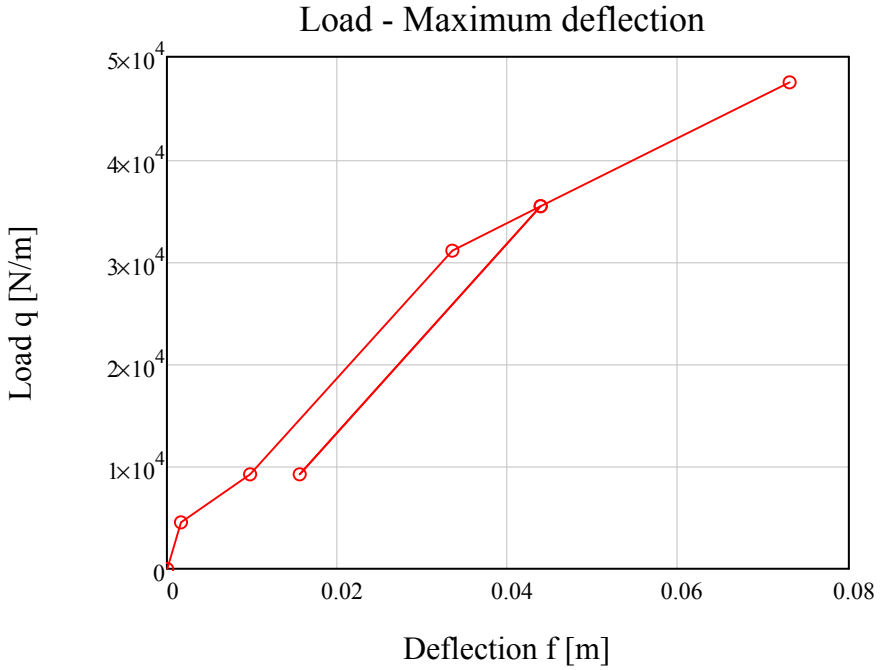
Load - Maximum deflection
Load q [N/m]
5×10^4
4×10^4
3×10^4
2×10^4
1×10^4
0
0 0.02 0.04 0.06 0.08
Deflection f [m]

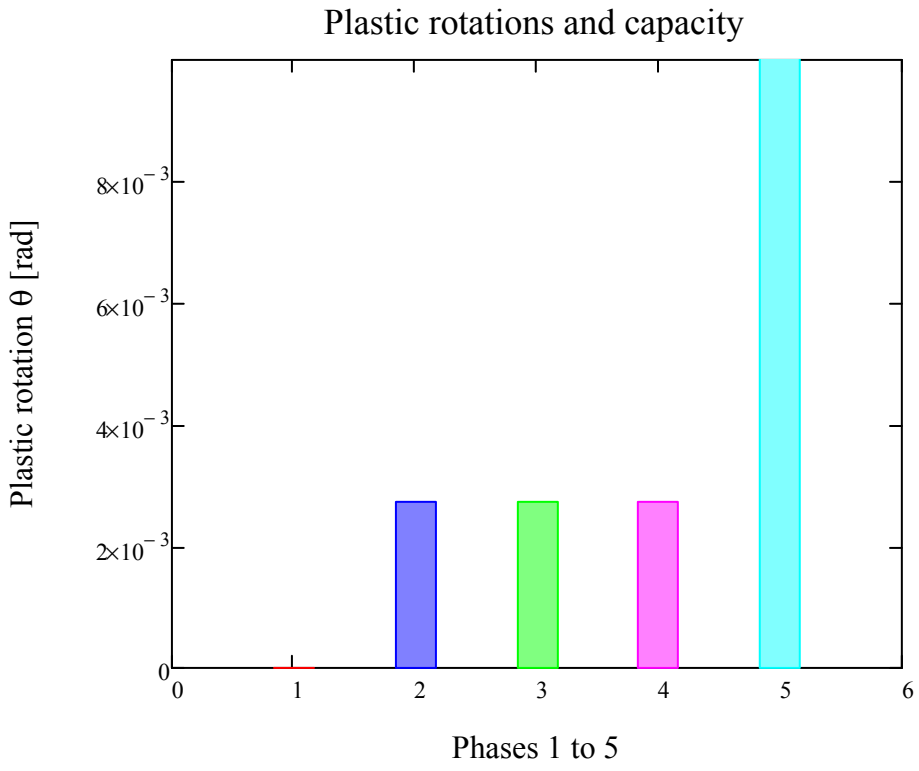
Plastic rotations and capacity
Plastic rotation θ [rad]
8×10⁻³
6×10⁻³
4×10⁻³
2×10⁻³
0
0
1
2
3
4
5
6
Phases 1 to 5

Appendix B: Analytical analysis PART 2

PART 2

In this part a damage structure is found in Phase 3. The deflection in this phase is measured along a whole span and the load acting on the structure is also easly decided. What load has caused the overloading and how this influences the response of the beam is shown in these calculations.

B.1 BEAM PROPERTIES

Analysis of a two span continous beam

$kN := newton \cdot 10^3$ $MN := newton \cdot 10^6$ $MPa := Pa \cdot 10^6$ $GPa := Pa \cdot 10^9$

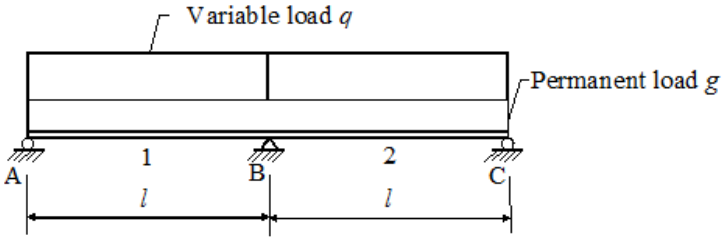

Load case : Variable load in both spans

Input data:

Span length:

$l_s := 12m$

Cross section

Concrete gross section:

$b := 0.30 \cdot m$ $h := 0.700 \cdot m$

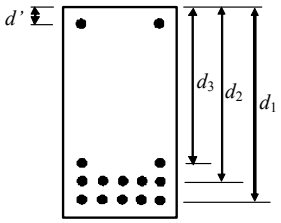

$A_c := b \cdot h$ $A_c = 0.21\ m^2$

$x_c := \frac{h}{2}$ $x_c = 0.35\ m$

$I_c := \frac{b \cdot h^3}{12}$ $I_c = 8.575 \times 10^{-3}\ m^4$

Reinforcement:

$\phi'_s := 12mm$ $\phi_s := 20mm$ $c'_c := 30mm$ $c_c := 30mm$

$A'_{s.si} := \left(\frac{\phi'_s}{2}\right)^2 \cdot \pi = 113.097 \cdot mm^2$ $A_{s.si} := \left(\frac{\phi_s}{2}\right)^2 \cdot \pi = 314.159 \cdot mm^2$

Section in field:

Assuming 1 layer of reinforcement

$A_{s1.span} := 6 \cdot A_{s.si}$ $d_{1.span} := h - c_c - \frac{\phi_s}{2} = 0.66\,m$

$A'_{s.span} := 2 \cdot A'_{s.si} = 2.262 \times 10^{-4}\,m^2$ $d'_{span} := c'_c + \frac{\phi'_s}{2} = 0.036\,m$

Section at support:

The section is defined upside down. Assuming 2 layers of reinforcement in the tensile zone and one layer in the compressive zone

$A_{s1.sup} := 6 \cdot A_{s.si}$ $d_{1.sup} := h - c_c - \frac{\phi_s}{2} = 0.66\,m$

$A_{s2.sup} := 0 \cdot A_{s.si}$ $d_{2.sup} := h - c_c - \frac{\phi_s}{2} - 20mm = 0.64\,m$

$A'_{s.sup} := 2 \cdot A'_{s.si}$ $d'_{sup} := c'_c + \frac{\phi'_s}{2} = 0.036\,m$

Material properties in the service state

Concrete C30/37

$f_{cmean} := 38 \cdot MPa$

$f_{ctk0.05} := 2.0MPa$ $f_{ctm} := 2.9 \cdot MPa$ $f_{ctk0.095} := 3.8 \cdot MPa$

$E_c := 33 \cdot GPa$

$g_c := 25 \frac{kN}{m^3}$ density of concrete

$\varepsilon_{cu} := 3.5 \cdot 10^{-3}$ ultimate concrete strain

Mean values are used in Part 2 since Part 2 is considering a measured value and not design values. Also, short term is considered since the deflection in Part 2 is decreased by the assumed deflection caused by creep.

Reinforcement steel B500B

$f_{yk} := 500 \cdot MPa \quad f_{uk} := 540 MPa \quad E_{sm} := 200 \cdot GPa$

$\varepsilon_{sy} := \frac{f_{yk}}{E_{sm}} = 2.5 \times 10^{-3}$ yielding steel strain

$\varepsilon_{suk} := 0.05$ ultimate steel strain

Modular ratio: short term response: $\alpha := \frac{E_{sm}}{E_c} \quad \alpha = 6.061$

Load

Load assumption: the applied load is a reasonably chosen value and is applied as uniformly distributed.

Quasi-permanent combination (SLS):

$q_3 := 9.243 \frac{kN}{m}$ The load is chosen so that it corresponds to FE modelling

Characteristic load combination (SLS):

$q_{3.ch} := 11.59 \frac{kN}{m}$

SECTIONAL CONSTANTS IN CRACKED STATE, SHORT TERM RESPONSE

Cracked section has been chosen because the main point of interest in this investigation is the point just before and after yielding moment occurence My. Only the stage when the structural response changes from linear to nonlinear and thus to plasticity is of interest.

Cracked section, short term response:

Span:

Assuming a value of the compressive zone:

$x_{II.span} := 0.18m$

$$x_{II.span} := root\left[\frac{b \cdot x_{II.span}^{2}}{2} + (\alpha - 1) \cdot A'_{s.span}\left(x_{II.span} - d'_{span}\right) - \alpha \cdot A_{s1.span} \cdot \left(d_{1.span} - x_{II.span}\right), x_{II.span}\right]$$

$x_{II.span} = 0.187\,m$

Moment of inertia:

$$I_{II.span} := \frac{b \cdot x_{II.span}^{3}}{3} + (\alpha - 1) \cdot A'_{s.span} \cdot \left(x_{II.span} - d'_{span}\right)^2 + \alpha \cdot A_{s1.span} \cdot \left(d_{1.span} - x_{II.span}\right)^2$$

$$I_{II.span} = 3.236 \times 10^{-3}\, m^4$$

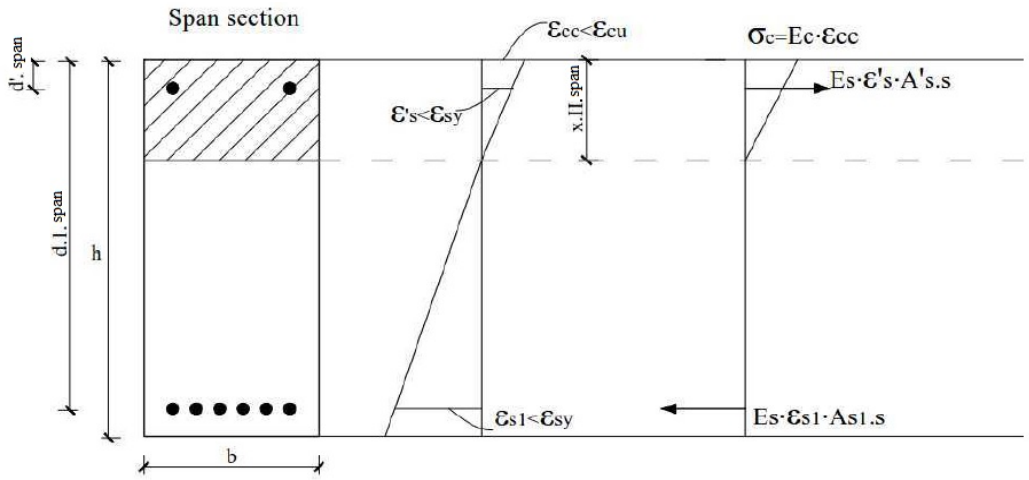

Flexural rigidity: $EI_{II.span} := E_c \cdot I_{II.span}$ $EI_{II.span} = 106.784 \cdot MN \cdot m^2$

Support:

Assuming a value:

$$x_{II.sup} := 0.18 \cdot m$$

$$x_{II.sup} := \text{root}\left[\frac{b \cdot x_{II.sup}^{2}}{2} + (\alpha - 1) \cdot A'_{s.sup} \cdot \left(x_{II.sup} - d'_{sup}\right) - \alpha \cdot A_{s1.sup} \cdot \left(d_{1.sup} - x_{II.sup}\right) \cdots + -\alpha \cdot A_{s2.sup} \cdot \left(d_{2.sup} - x_{II.sup}\right), x_{II.sup}\right]$$

$$x_{II.sup} = 0.187\, m$$

Moment of inertia:

$$I_{II.sup} := \frac{b \cdot x_{II.sup}^{3}}{3} + (\alpha - 1) \cdot A'_{s.sup} \cdot \left(x_{II.sup} - d'_{sup}\right)^2 + \alpha \cdot A_{s1.sup} \cdot \left(d_{1.sup} - x_{II.sup}\right)^2 \cdots + \alpha \cdot A_{s2.sup} \cdot \left(d_{2.sup} - x_{II.sup}\right)^2$$

$$I_{II.sup} = 3.236 \times 10^{-3}\, m^4$$

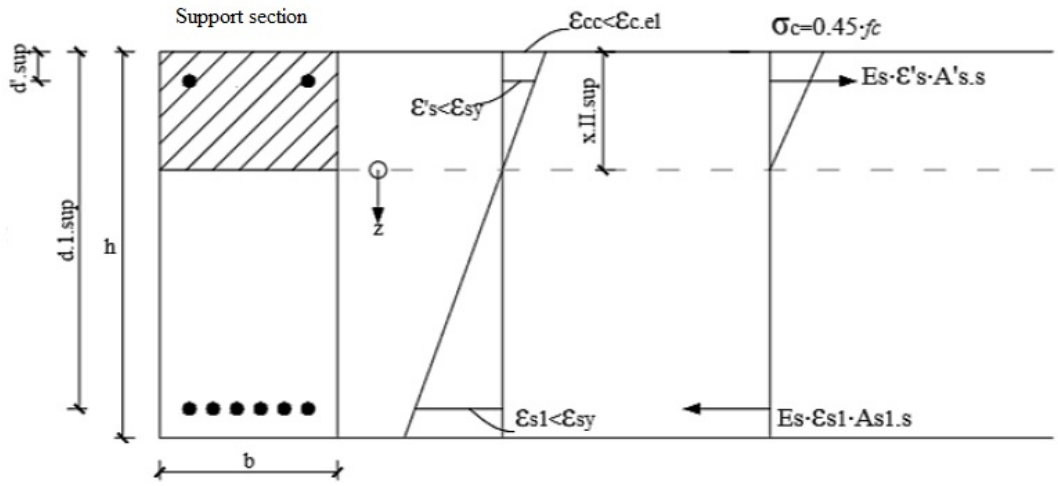

Flexural rigidity: $EI_{II.sup} := E_c \cdot I_{II.sup}$ $EI_{II.sup} = 106.784 \cdot MN \cdot m^2$

Stiffness ratio, cracked section, short term response:

$$\frac{EI_{II.sup}}{EI_{II.span}} = 1$$

The ratio is higher than 1.The stiffness is not constant along the beam

B.2 YIELDING, CRACKING AND ULTIMATE MOMENTS

Calculations of yielding moments, cracking moments and ultimate moments are carried out in PART 1. Since the analysed beam in PART 2 is of the same proporties and is subjected to the same loads, these moments are the same for both parts, PART 1 and PART 2.
The yielding moments and ultimate moments are presented below:

Cracking moments

$M_{cr.sup} := 82.088\,kN\cdot m$

$M_{cr.span} := 82.088\,kN\cdot m$

Yielding moments

$M_{y.sup} := 559.492\,kN\cdot m$

$M_{y.span} := 559.492\,kN\cdot m$

Ultimate moment

$M_{ul.sup} := 587.105\,kN\cdot m$

$M_{ul.span} := 587.105\,kN\cdot m$

Cracking load:

$q_{cr.sup} := 4.56\,\frac{kN}{m}$

$q_{cr.span} := 8.107\,\frac{kN}{m}$

Curvature at yielding:

$\kappa_{y.sup} := 5.359\cdot 10^{-3}\cdot\frac{1}{m}$

$\kappa_{y.span} := 5.359\cdot 10^{-3}\cdot\frac{1}{m}$

$q_{y.sup} := \frac{M_{y.sup}\cdot 8}{l_s^{\,2}} = 31.083\cdot\frac{kN}{m}$

Ultimate load:

$q_{ult} := 47.526\,\frac{kN}{m}$

Service load in discovered phase:

$q_3 = 9.243\cdot\frac{kN}{m}$

Max Deflection at Cracking load:

$f_{cr} := 1.621\,mm$

$f_y := 33.437\,mm$

Damage discovery

B.3 PHASE 3 - phase of measurements

Deflection along the whole beam:

Usually, investigation of an existing beam starts by an observation on site. Beam deflection is a parameter that can be measured on site, if a sufficient access to the beam is provided. If the measured deflection is significant, it may point out possible overloading in the past.

One option to use the deflected shape of the beam is to measure the deflection of the beam in many points along the span. The only challanging part is the beam-column connection. Hoewever, advanced measuring methods exists nowadays such as lasers, which are able to scan the beam and get information from its inside.

Long term effect, such as creep, has a significant influence on the deflections. Thus, the deflections due to long term effects should be taken away from the measured deflected shape of the beam. This will help to carry out the analysis with consideration to short term response. However, if long term effects are considered in the analysis of a beam from the beginning, these should be included in the deflection.

Measured deflected shape of the beam may be used to determinate the plastic rotation that occurs while the beam is overloaded. The deflected shape of the beam should indicate plastic region over the middle support with higher curvature inclination in comparison to the curvature in the span.

Estimation from a plotted deformation shape, the angle according to the figure above can be determined and defined as the plastic rotation above the middle support.

$\theta_{3.sup.left.measured} := 4 \cdot 10^{-3}$

Since the plastic rotation is assumed to be the same after unloading the determined plastic rotation in Phase 3 is equal to the plastic rotation in Phase 2.
To make an extra check, maximum deflection of the beam may be compared with the maximum deflection obtained through calculations. This maximum deflection from calculations is determined by taking into consideration the plastic rotations, defined by the deflected shape of the beam on site. When the load that causes this plastic rotation is found, maximum deflection can be calculated. This deflection is to be compared with the maximum deflection measured on site.

$f_{site} := 50mm$

Moment distribution:

Support moment according to nonlinear analysis, considering cracking

Assuming a value until the plastic rotation is equal to the measured plastic rotation

$M_{3.sup} := 59.6kN \cdot m$

$R_{3.A} := \frac{q_3 \cdot l_s}{2} - \frac{M_{3.sup}}{l_s}$ $R_{3.A} = 50.491 \cdot kN$ $x := 0 \cdot m, 0.1 \cdot m .. l_s$

$M_{3.x}(x) := R_{3.A} \cdot x - \frac{q_3 \cdot x^2}{2}$ Expression for the moment along the beam

$x_s := 0$

$x_{3.span} := \text{Maximize}(M_{3.x}, x_s) = 5.463\,m$ The distance from the outer support to the maximum span moment in the beam

$M_{3.span} := M_{3.x}(\text{Maximize}(M_{3.x}, x_s)) = 137.908 \cdot kN \cdot m$ The maximum span moment in the beam

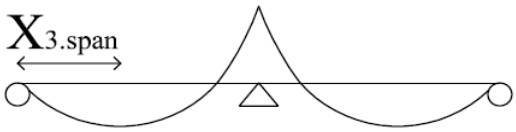

Curvature at field, cracked:

$\kappa_{3.span.II}(x) := \frac{M_{3.x}(x)}{E_c \cdot I_{II.span}}$ Assumed fully cracked

Curvature at support, cracked:

$\kappa_{3.sup.II}(x) := \frac{M_{3.x}(x)}{E_c \cdot I_{II.sup}}$

$\kappa_3(x) := \text{if}(M_{3.x}(x) \geq 0, \kappa_{3.span.II}(x), \kappa_{3.sup.II}(x))$ Expression for the curvature along the beam

Plastic rotation

Continuity condition: θ.sup3a+θ.sup3b=θ.sup2

$$\theta_{3.sup.left} := \frac{\int_0^{l_s} \kappa_3(x)\cdot x\,dx}{l_s} = 4\times 10^{-3}$$

Left side. From measuring in Phase 3

$$\theta_{3.sup.left.measured} = 4\times 10^{-3}$$

$$\theta_{3.sup.left} + \theta_{3.sup.left} = 7.999\times 10^{-3}$$

The continuity condition is fullfiled when these are equal to each other. Looking just for one side since the beam is symmetric

$$l_{3.o} := 2\cdot\frac{R_{3.A}}{q_3} = 10.925\,m$$

$$l_{3.b} := l_s - l_{3.o} = 1.075\,m$$

$$z_{3.c} := l_{3.b}\cdot\frac{\frac{l_{3.o}}{3}+\frac{l_{3.b}}{4}}{\frac{l_{3.o}}{2}+\frac{l_{3.b}}{3}} = 0.722\,m$$

$$\theta_{sup.3} := \frac{\left[\frac{2}{3}\cdot\frac{M_{3.span}}{EI_{II.span}}\cdot l_{3.o}\cdot\frac{l_{3.o}}{2} - \frac{q_3}{2\cdot EI_{II.sup}}\cdot\left(l_{3.o}\cdot\frac{l_{3.b}^{2}}{2}+\frac{l_{3.b}^{3}}{3}\right)\cdot\left(l_{3.o}+z_{3.c}\right)\right]}{l_s} = 4\times 10^{-3}$$

Deflection assuming fully cracked beam:

The maximum deflection can be estimated by calculating the support rotation at support A (outer support).

Support rotation at support A:

$$\theta_{3.A} := \frac{\int_0^{l_s} \kappa_3(x)\cdot\left(l_s - x\right)dx}{l_s}$$

$$\theta_{3.A} = 5.116\times 10^{-3}$$

Section with rotation equal to 0 and thus the maximum deflection in the span:

Assuming a value of the distance from the outer support where maximum deflection might occure:

$x_{3.f} := 5 \cdot m$

$x_{3.f} := \text{root}\left(\int_0^{x_{3.f}} \kappa_3(x)\,dx - \theta_{3.A}, x_{3.f}\right)$

$x_{3.f} = 5.783\,m$

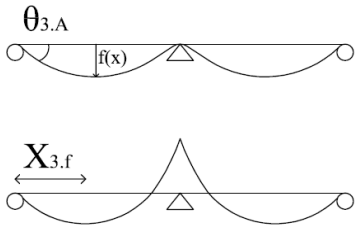

Maximum deflection:

$f_3 := \theta_{3.A} \cdot x_{3.f} - \int_0^{x_{3.f}} \kappa_3(x) \cdot (x_{3.f} - x)\,dx$

$f_3 = 18.378 \cdot mm$

Deflection in span 1:

$f_{3.span}(x) := \theta_{3.A} \cdot x - \int_0^x \int_0^x \kappa_3(x)\,dx\,dx$

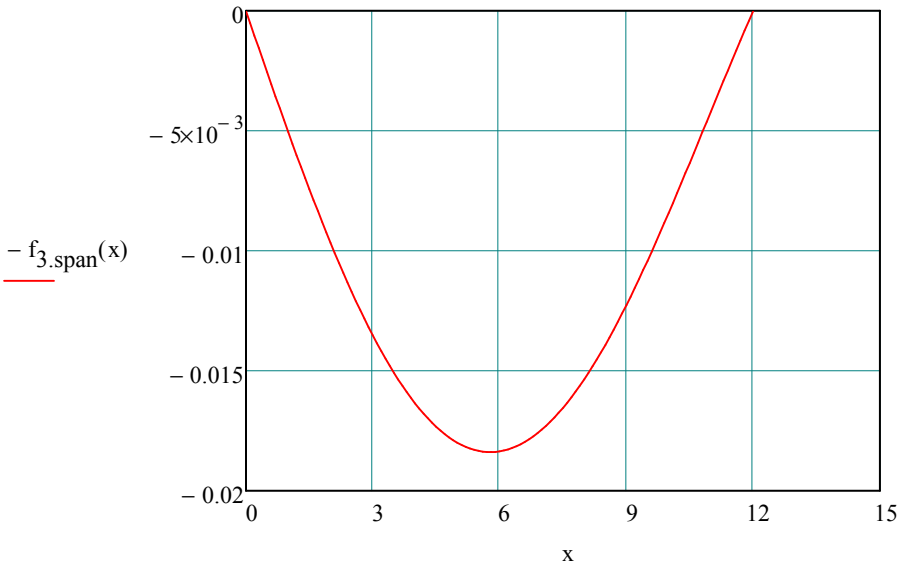

Forensic engineering

B.5 PHASE 2 AND LOAD ITERATION

Determination of overloading that occurs in Phase 2 is conducted in this part.
The plastic rotation at Phase 2 is the same as the plastic rotation at Phase 3.

Stiffness for State III, determined in analysises carried out for PART 1:

$$EI_{sup} := \frac{M_{y.sup}}{\kappa_{y.sup}} = 1.044 \times 10^{8} \cdot N \cdot m^{2}$$

$$EI_{span} := \frac{M_{y.span}}{\kappa_{y.span}} = 1.044 \times 10^{8} \cdot N \cdot m^{2}$$

Support moment according to nonlinear analysis, after yielding has been reached considering average stiffness: When yielding has been reached over the midsupport plastic redistribution occurs and the support moment does not increase further more

The value of overloading is iterated until the plastic rotation at Phase 2 is the same as the plastic rotation at Phase 3.

$$q_2 := 37.48 \frac{kN}{m}$$

Relation between the difference between Mu and My, and the difference between qu and qy:

$$M_{uy} := \frac{M_{ul.sup}}{kN \cdot m} - \frac{M_{y.sup}}{kN \cdot m} = 27.613$$

The difference between ultimate and yielding moment over the support

$$q_{uy} := \frac{q_{ult}}{\frac{kN}{m}} - \frac{q_{y.sup}}{\frac{kN}{m}} = 16.443$$

The difference between ultimate and yielding load

$$Relation := \frac{M_{uy}}{q_{uy}} = 1.679$$

Tangent between M and q

$$atan(Relation) = 59.227 \cdot deg$$

Angle

The difference between q2 and qy:

$$q_{2y} := \frac{q_2}{\frac{kN}{m}} - \frac{q_{y.sup}}{\frac{kN}{m}} = 6.397$$

The difference between moments M2 and My:

$$M_{2y} := \tan(\operatorname{atan}(Relation)) \cdot q_{2y} = 10.743$$

The magnitude of support moment at Phase2:

$$M_{2.sup} := M_{y.sup} + M_{2y} \cdot kN \cdot m = 570.235 \cdot kN \cdot m \qquad M_{y.sup} = 559.492 \cdot kN \cdot m$$

$$R_{2.A} := \frac{q_2 \cdot l_s}{2} - \frac{M_{2.sup}}{l_s} \qquad R_{2.A} = 177.36 \cdot kN \qquad x := 0 \cdot m, 0.1 \cdot m .. l_s$$

$$M_{2.x}(x) := R_{2.A} \cdot x - \frac{q_2 \cdot x^2}{2}$$

Curvature at support:

$$\kappa_{2.sup}(x) := \frac{M_{2.x}(x)}{EI_{sup}}$$

Curvature at span:

$$\kappa_{2.span}(x) := \frac{M_{2.x}(x)}{EI_{span}}$$

$$\kappa_2(x) := \text{if}\left(M_{2.x}(x) \geq 0, \kappa_{2.span}(x), \kappa_{2.sup}(x)\right)$$

Support rotation at B, towards span 1:

$$l_{2.o} := 2 \cdot \frac{R_{2.A}}{q_2} = 9.464\,m$$

$$l_{2.b} := l_s - l_{2.o} = 2.536\,m$$

$$z_c := l_{2.b} \cdot \frac{\frac{l_{2.o}}{3} + \frac{l_{2.b}}{4}}{\frac{l_{2.o}}{2} + \frac{l_{2.b}}{3}} = 1.723\,m$$

$x_s := 0$

$x_{2.span} := \text{Maximize}(M_{2.x}, x_s) = 4.732\,\text{m}$

$M_{2.span} := M_{2.x}(\text{Maximize}(M_{2.x}, x_s)) = 419.647 \cdot \text{kN} \cdot \text{m}$ $\quad M_{y.span} = 559.492 \cdot \text{kN} \cdot \text{m}$

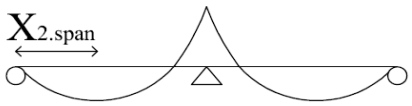

$M_{2.span} < M_{y.span} = 1$ Span moment is less than yield moment in span. Reinforcement is yielding above support, but no collapse takes place.

Plastic rotation on one side of the middle support in case of overloading, that should be almost the same as the measured plastic rotation from the field:

$$\theta_{2.sup.left} := \frac{\int_0^{l_s} \kappa_2(x) \cdot (x)\, dx}{l_s} = 4 \times 10^{-3}$$

Double check with other method:

$$\theta_{2.sup.left} := \frac{\left[\frac{2}{3} \cdot \frac{M_{2.span}}{EI_{span}} \cdot l_{2.o} \cdot \frac{l_{2.o}}{2} - \frac{q_2}{2 \cdot EI_{sup}} \cdot \left(l_{2.o} \cdot \frac{l_{2.b}^{\,2}}{2} + \frac{l_{2.b}^{\,3}}{3} \right) \cdot (l_{2.o} + z_c)\right]}{l_s} = 4 \times 10^{-3}$$

Plastic rotation determined the measuring in Phase 3

$\theta_{3.sup.left.measured} = 4 \times 10^{-3}$

Deflection:

The maximum deflection can be estimated by calculating the support rotation at support A (outer support).

Support rotation at support A:

$$\theta_{2.A} := \frac{\int_0^{l_s} \kappa_2(x)\cdot\left(l_s - x\right) dx}{l_s}$$

$$\theta_{2.A} = 0.015$$

Assuming a value of the distance from the outer support where maximum deflection might occure:

$$x_{2.f} := 5\cdot m$$

$$x_{2.f} := \text{root}\left(\int_0^{x_{2.f}} \kappa_2(x)\, dx - \theta_{2.A}, x_{2.f}\right)$$

$$x_{2.f} = 5.293\,m$$

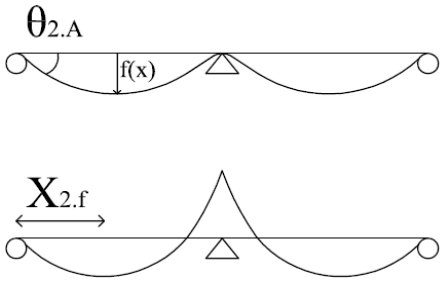

Maximum deflection:

$$f_2 := \theta_{2.A}\cdot x_{2.f} - \int_0^{x_{2.f}} \kappa_2(x)\cdot\left(x_{2.f} - x\right) dx$$

$$f_2 = 48.747\cdot mm$$

Deflection in span 1:

$$f_{2.span}(x) := \theta_{2.A} \cdot x - \int_0^x \int_0^x \kappa_2(x)\, dx\, dx$$

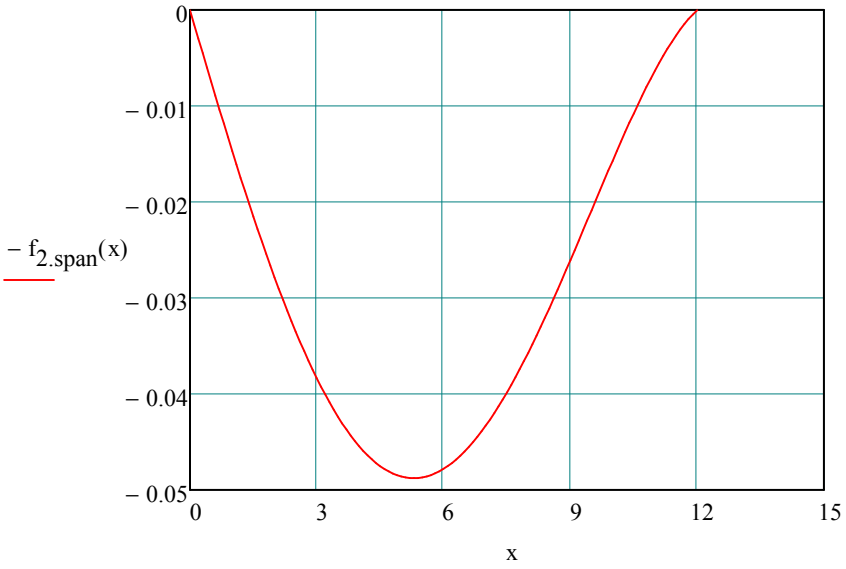

Assuming that q1=q3

$q_1 := q_3 = 9.243 \cdot \frac{kN}{m}$

Moment distribution for characteristic load combination, short term response:

Support moment according to linear elastic analysis assuming constant stiffness along the span:

$M_{1.el} := \frac{q_1 \cdot l_s^2}{8}$ $q_1 = 9.243 \cdot \frac{kN}{m}$

$M_{1.el} = 166.374 \cdot kN \cdot m$

Support moment according to nonlinear analysis, considering cracking but neglecting small influence of tension stiffening:

Assumption of support moment to fullfil the continuity condition where the rotations on both sides of the middle support are eual to each other and together they give zero θb1=-θb.2=0

Assuming a value: $M_{1.sup} := 166.374 kN \cdot m$

$R_{1.A} := \frac{q_1 \cdot l_s}{2} - \frac{M_{1.sup}}{l_s}$ $R_{1.A} = 41.593 \cdot kN$ $x := 0 \cdot m, 0.1 \cdot m .. l_s$

$M_{1.x}(x) := R_{1.A} \cdot x - \frac{q_1 \cdot x^2}{2}$ Expression for the moment along the beam

Curvature at field, cracked:

$\kappa_{1.span.II}(x) := \frac{M_{1.x}(x)}{E_c \cdot I_{II.span}}$ Assumed fully cracked

Curvature at support, cracked: $I_{II.span} = 3.236 \times 10^{-3} m^4$

$\kappa_{1.sup.II}(x) := \frac{M_{1.x}(x)}{E_c \cdot I_{II.sup}}$

$\kappa_1(x) := \text{if}\left(M_{1.x}(x) \geq 0, \kappa_{1.span.II}(x), \kappa_{1.sup.II}(x)\right)$ Expression for the curvature along the beam

Support rotation at B, towards span 1:

$$\theta_{1.sup.left} := \frac{\int_0^{l_s} \kappa_1(x)\cdot x\,dx}{l_s}$$

$\theta_{1.sup.left} = 0$ The rotation is zero. The continuity condition is thus fullfiled.

$x_s := 0$

$x_{1.span} := \text{Maximize}(M_{1.x}, x_s) = 4.5\,m$ The distance from the outer support to the maximum span moment in the beam

$M_{1.span} := M_{1.x}(\text{Maximize}(M_{1.x}, x_s)) = 93.585\cdot kN\cdot m$ The maximum span moment in the beam

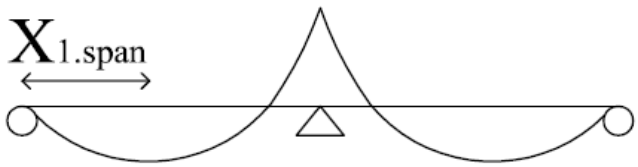

Deflection assuming fully cracked beam:

The maximum deflection can be estimated by calculating the support rotation at support A (outer support).

Support rotation at support A:

$$\theta_{1.A} := \frac{\int_0^{l_s} \kappa_1(x)\cdot(l_s - x)\,dx}{l_s}$$

$\theta_{1.A} = 3.116\times 10^{-3}$

Section with rotation equal to 0 and thus the maximum deflection in the span:

Assuming a value of the distance from the outer support where maximum deflection might occure:

$x_{1.f} := 5 \cdot m$

$x_{1.f} := \text{root}\left(\int_0^{x_{1.f}} \kappa_1(x)\,dx - \theta_{1.A}, x_{1.f}\right)$

$x_{1.f} = 5.058\,m$

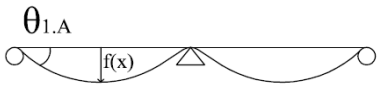

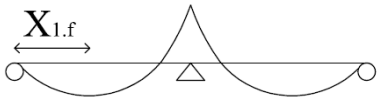

Maximum deflection:

$f_1 := \theta_{1.A} \cdot x_{1.f} - \int_0^{x_{1.f}} \kappa_1(x) \cdot (x_{1.f} - x)\,dx$

$f_1 = 9.721 \cdot mm$

Expression of the deflection in span 1:

$f_{1.span}(x) := \theta_{1.A} \cdot x - \int_0^x \int_0^x \kappa_1(x)\,dx\,dx$

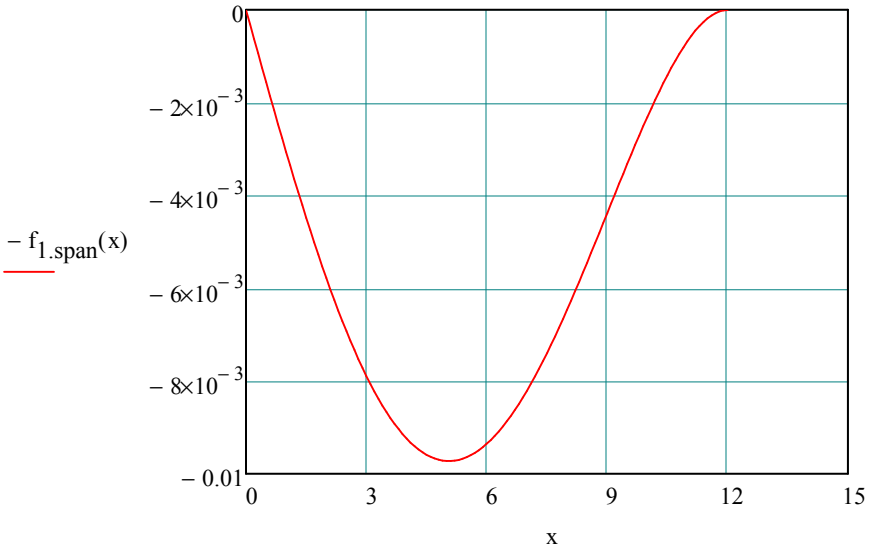

Restraint moment:

Support:

$M_{1.sup} = 166.374 \cdot kN \cdot m$

$M_{3.sup} = 59.6 \cdot kN \cdot m$

Span:

$M_{1.span} = 93.585 \cdot kN \cdot m$

$M_{3.span} = 137.908 \cdot kN \cdot m$

$M_{restraint.sup} := M_{3.sup} - M_{1.sup} = -106.774 \cdot kN \cdot m$ Moment over support decreses

$M_{restraint.span} := M_{3.span} - M_{1.span} = 44.323 \cdot kN \cdot m$ Moment in span increases

The restraint moment is larger at support than at field, illustrated in the figure to the right

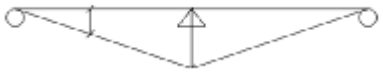

Structural assessment

B.7 PHASE 4

Moment distribution for overloaded plastic combination, short term response:

Support moment according to nonlinear analysis, considering cracking but neglecting small influence of tension stiffening:

The magnitude of load at Phase 4 is the same as in Phase 2.

$q_4 := q_2 = 37.48 \cdot \frac{kN}{m}$

Assumption of support moment equal to the one in Phase 2

$M_{4.sup} := M_{2.sup} = 570.235 \cdot kN \cdot m \qquad M_{y.sup} = 559.492 \cdot kN \cdot m$

$R_{4.A} := \frac{q_4 \cdot l_s}{2} - \frac{M_{4.sup}}{l_s} \qquad R_{4.A} = 177.36 \cdot kN \qquad x := 0 \cdot m, 0.1 \cdot m .. l_s$

$M_{4.x}(x) := R_{4.A} \cdot x - \frac{q_4 \cdot x^2}{2}$ Expression for the moment along the beam

$x_s := 0$

$x_{4.span} := \text{Maximize}(M_{4.x}, x_s) = 4.732\,m$ The distance from the outer support to the maximum span moment in the beam

$M_{4.span} := M_{4.x}(\text{Maximize}(M_{4.x}, x_s)) = 419.647 \cdot kN \cdot m$ The maximum span moment in the beam

$M_{2.span} = 419.647 \cdot kN \cdot m$

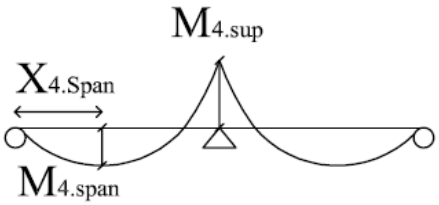

Curvature:

$$\kappa_{4.sup}(x) := \frac{M_{4.x}(x)}{EI_{sup}} \qquad \kappa_{4.span}(x) := \frac{M_{4.x}(x)}{EI_{span}}$$

Expression for the curvature along the beam

$$\kappa_4(x) := \text{if}\left(M_{4.x}(x) \geq 0, \kappa_{4.span}(x), \kappa_{4.sup}(x)\right)$$

Plastic rotation

$$l_{4.o} := 2 \cdot \frac{R_{4.A}}{q_2} = 9.464\,\text{m}$$

$$l_{4.b} := l_s - l_{4.o} = 2.536\,\text{m}$$

$$z_{4.c} := l_{4.b} \cdot \frac{\frac{l_{4.o}}{3} + \frac{l_{4.b}}{4}}{\frac{l_{4.o}}{2} + \frac{l_{4.b}}{3}} = 1.723\,\text{m}$$

$$\theta_{4.sup.left} := \frac{\int_0^{l_s} \kappa_4(x) \cdot x\,dx}{l_s} = 4 \times 10^{-3}$$ Phase 4

$$\theta_{2.sup.left} = 4 \times 10^{-3}$$ Phase 2

Check by other method:

$$\theta_{4.sup.left} := \frac{\left[\frac{2}{3} \cdot \frac{M_{4.span}}{EI_{span}} \cdot l_{4.o} \cdot \frac{l_{4.o}}{2} - \frac{q_2}{2 \cdot EI_{sup}} \cdot \left(l_{4.o} \cdot \frac{l_{4.b}^2}{2} + \frac{l_{4.b}^3}{3}\right) \cdot \left(l_{4.o} + z_{4.c}\right)\right]}{l_s} = 4 \times 10^{-3}$$

Deflection:

The maximum deflection can be estimated by calculating the support rotation at support A (outer support).

Support rotation at support A:

$$\theta_{4.A} := \frac{\int_0^{l_s} \kappa_4(x) \cdot \left(l_s - x\right) dx}{l_s}$$

$$\theta_{4.A} = 0.015$$

Assuming a value of the distance from the outer support where maximum deflection might occure:

$x_{4.f} := 5 \cdot m$

$x_{4.f} := \text{root}\left(\int_0^{x_{4.f}} \kappa_4(x)\,dx - \theta_{4.A}, x_{4.f}\right)$

$x_{4.f} = 5.293\,m$

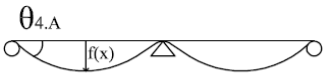

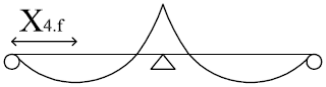

Maximum deflection:

$f_4 := \theta_{4.A} \cdot x_{4.f} - \int_0^{x_{4.f}} \kappa_4(x) \cdot (x_{4.f} - x)\,dx$

$f_4 = 48.747 \cdot mm$ $\quad f_2 = 48.747 \cdot mm$

Deflection in span 1:

$f_{4.span}(x) := \theta_{4.A} \cdot x - \int_0^x \int_0^x \kappa_4(x)\,dx\,dx$

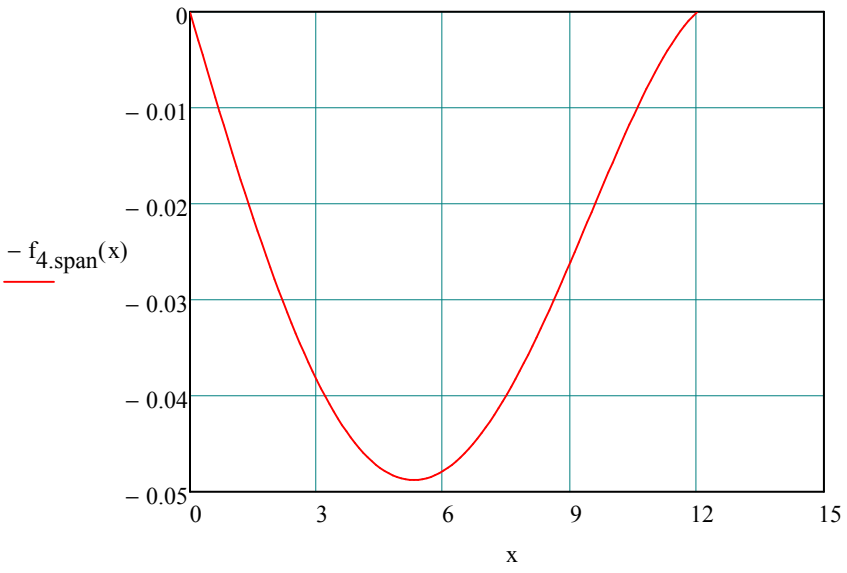

B.8 PHASE 5

Prediction of the load carrying capacity is conducted using structural assessment approach:

The maximum ultimate load and moments are calculated in PART 1.

$q_5 := q_{ult} = 47.526 \cdot \frac{kN}{m}$ Ultimate load

$M_{5.sup} := M_{ul.sup} = 587.105 \cdot kN \cdot m$ Ultimate support moment

$M_{5.span} := M_{ul.span} = 587.105 \cdot kN \cdot m$ Ultimate span moment

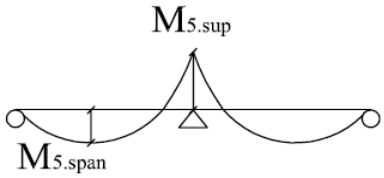

$$R_{5.A} := \frac{(q_5 \cdot l_s)}{2} - \frac{M_{5.sup}}{l_s} = 236.231 \cdot kN$$

$$l_{5.o} := 2 \cdot \frac{R_{5.A}}{q_5} = 9.941\,m$$

$$l_{5.b} := l_s - l_{5.o} = 2.059\,m$$

$$z_{5.c} := l_{5.b} \cdot \frac{\frac{l_{5.o}}{3} + \frac{l_{5.b}}{4}}{\frac{l_{5.o}}{2} + \frac{l_{5.b}}{3}} = 1.393\,m$$

Plastic rotation in ultimate limit state:

$$\theta_{5.sup.left} := \frac{\left[\frac{2}{3} \cdot \frac{M_{5.span}}{EI_{span}} \cdot l_{5.o} \cdot \frac{l_{5.o}}{2} - \frac{q_5}{2 \cdot EI_{sup}} \cdot \left(l_{5.o} \cdot \frac{l_{5.b}^{2}}{2} + \frac{l_{5.b}^{3}}{3}\right) \cdot (l_{5.o} + z_{5.c})\right]}{l_s} = 0.01$$

$x := 0 \cdot m, 0.1 \cdot m .. l_s$

$M_{5.x}(x) := R_{5.A} \cdot x - \frac{q_5 \cdot x^2}{2}$ Expression for the moment along the beam

$x_s = 0$

$x_{5.span} := \text{Maximize}\left(M_{5.x}, x_s\right) = 4.971\,\text{m}$

Curvature at span:

$$\kappa_{5.span}(x) := \frac{M_{5.x}(x)}{EI_{span}}$$

Curvature at support:

$$\kappa_{5.sup}(x) := \frac{M_{5.x}(x)}{EI_{sup}}$$

$\kappa_5(x) := \text{if}\left(M_{5.x}(x) \geq 0, \kappa_{5.span}(x), \kappa_{5.sup}(x)\right)$

$$\theta_{5.sup.left} := \frac{\int_0^{l_s} \kappa_5(x) \cdot x \, dx}{l_s} = 0.01$$

$\theta_{5.sup} := 2 \cdot \theta_{5.sup.left} = 0.021$

Deflection:

The maximum deflection can be estimated by calculating the support rotation at support A (outer support). Since the beam is analyzed in cracked state (state II) this is an elastic deflection (reversible in theory).

Support rotation at support A:

$$\theta_{5.A} := \frac{\int_0^{l_s} \kappa_5(x) \cdot \left(l_s - x\right) dx}{l_s}$$

$\theta_{5.A} = 0.022$

Section with rotation equal to 0 and thus the maximum deflection in the span:

Assuming a value of the distance from the outer support where maximum deflection might occure:

$x_{5.f} := 5 \cdot m$

$x_{5.f} := \text{root}\left(\int_0^{x_{5.f}} \kappa_5(x)\, dx - \theta_{5.A}, x_{5.f} \right)$

$x_{5.f} = 5.487\,m$

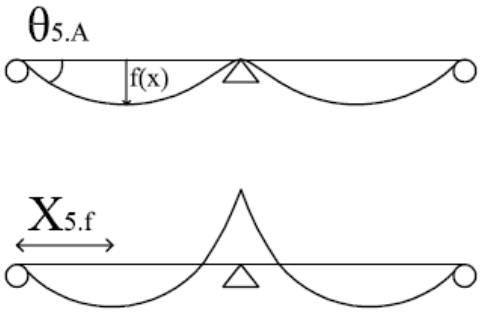

Maximum deflection:

$f_5 := \theta_{5.A} \cdot x_{5.f} - \int_0^{x_{5.f}} \kappa_5(x) \cdot (x_{5.f} - x)\, dx$

$f_5 = 73.023 \cdot mm$

Deflection in span 1:

$f_{5.span}(x) := \theta_{5.A} \cdot x - \int_0^x \int_0^x \kappa_5(x)\, dx\, dx$

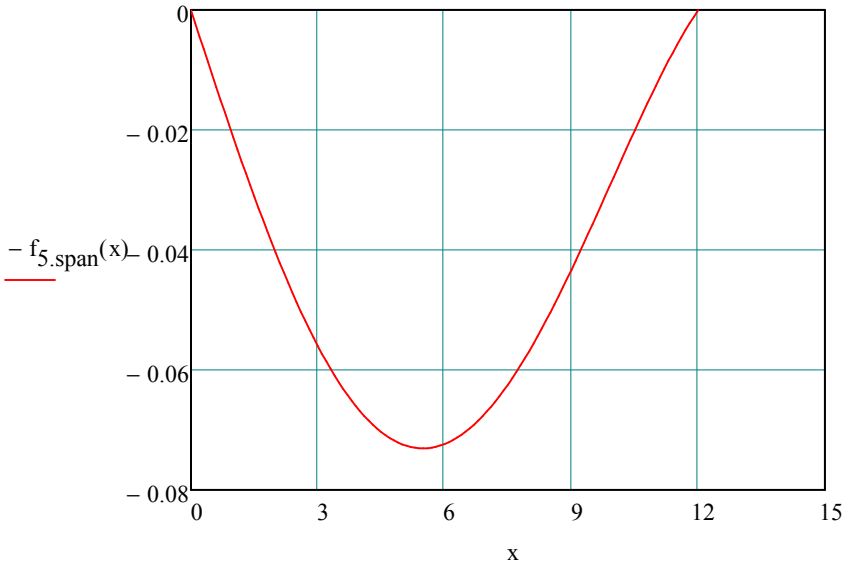

B.9 COMPARISON OF PARAMETERS

Support Moment:

$M_{1.sup} = 166.374 \cdot kN \cdot m$

$M_{2.sup} = 570.235 \cdot kN \cdot m$

$M_{3.sup} = 59.6 \cdot kN \cdot m$

$M_{4.sup} = 570.235 \cdot kN \cdot m$

$M_{5.sup} = 587.105 \cdot kN \cdot m$

Field Moment:

$M_{1.span} = 93.585 \cdot kN \cdot m$ Phase 1

$M_{2.span} = 419.647 \cdot kN \cdot m$ Phase 2

$M_{3.span} = 137.908 \cdot kN \cdot m$ Phase 3

$M_{4.span} = 419.647 \cdot kN \cdot m$ Phase 4

$M_{5.span} = 587.105 \cdot kN \cdot m$ Phase 5

Restraint moment support:

$M_{3.sup} - M_{1.sup} = -106.774 \cdot kN \cdot m$

Restraint moment span:

$M_{3.span} - M_{1.span} = 44.323 \cdot kN \cdot m$

Load:

$q_1 = 9.243 \cdot \frac{kN}{m}$

$q_2 = 37.48 \cdot \frac{kN}{m}$

$q_3 = 9.243 \cdot \frac{kN}{m}$

$q_4 = 37.48 \cdot \frac{kN}{m}$

$q_5 = 47.526 \cdot \frac{kN}{m}$

Plastic rotation:

$\theta_{1.sup.left} = 0$ Phase 1 No rotations at this Phase

$\theta_{2.sup.left} = 4 \times 10^{-3}$ Phase 2

$\theta_{3.sup.left} = 4 \times 10^{-3}$ Phase 3

$\theta_{4.sup.left} = 4 \times 10^{-3}$ Phase 4

$\theta_{5.sup.left} = 0.01$ Phase 5

Deflection:

$f_1 = 9.721 \cdot mm$ Phase 1

$f_2 = 48.747 \cdot mm$ Phase 2

$f_3 = 18.378 \cdot mm$ Phase 3

$f_4 = 48.747 \cdot mm$ Phase 4

$f_5 = 73.023 \cdot mm$ Phase 5

Maximum deflection section:

$x_{1.f} = 5.058\,m$

$x_{2.f} = 5.293\,m$

$x_{3.f} = 5.783\,m$

$x_{4.f} = 5.293\,m$

$x_{5.f} = 5.487\,m$

Maximum moment section:

$x_{1.span} = 4.5\,m$

$x_{2.span} = 4.732\,m$

$x_{3.span} = 5.463\,m$

$x_{4.span} = 4.732\,m$

$x_{5.span} = 4.971\,m$

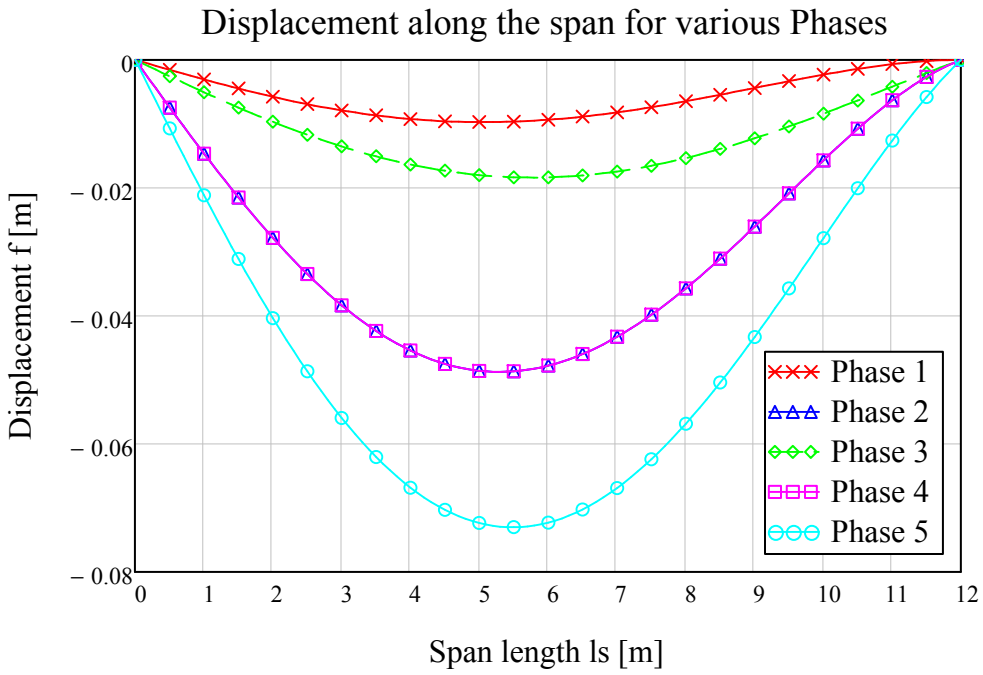
Displacement along the span for various Phases
Displacement f [m]
0
– 0.02
– 0.04
– 0.06
– 0.08
0 1 2 3 4 5 6 7 8 9 10 11 12
Span length ls [m]
Phase 1
Phase 2
Phase 3
Phase 4
Phase 5

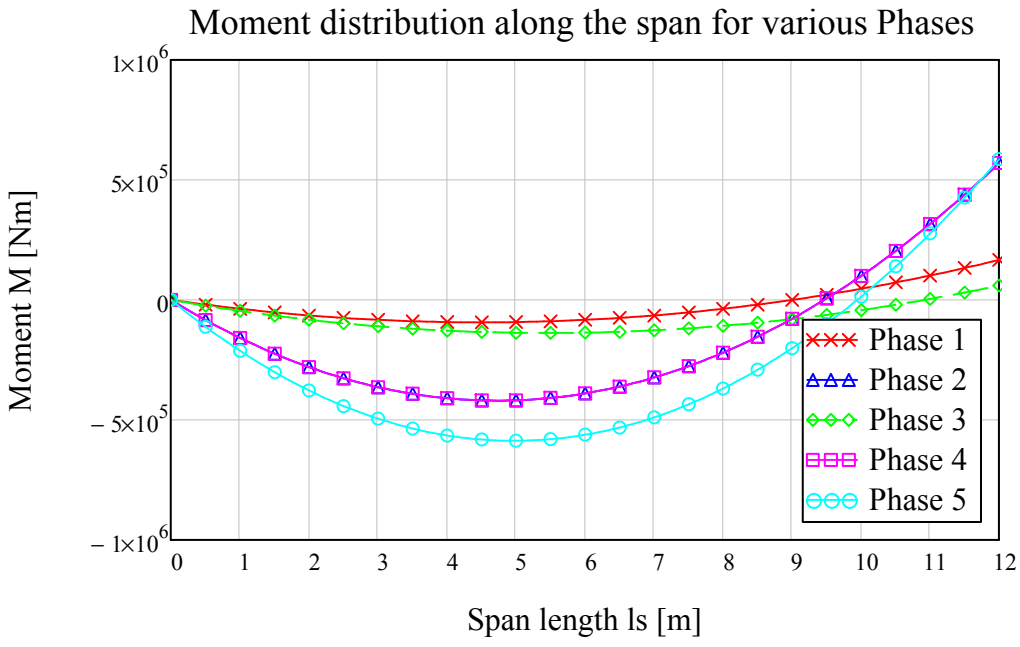
Moment distribution along the span for various Phases
Moment M [Nm]
1×10^6
5×10^5
0
– 5×10^5
– 1×10^6
0 1 2 3 4 5 6 7 8 9 10 11 12
Span length ls [m]
Phase 1
Phase 2
Phase 3
Phase 4
Phase 5

$M_{restraint1.3}(x) := M_{3.x}(x) - M_{1.x}(x)$ Difference in moment between Phase 1 and 3

$M_{restraint2.4}(x) := M_{4.x}(x) - M_{2.x}(x)$ Difference in moment between Phase 2 and 4

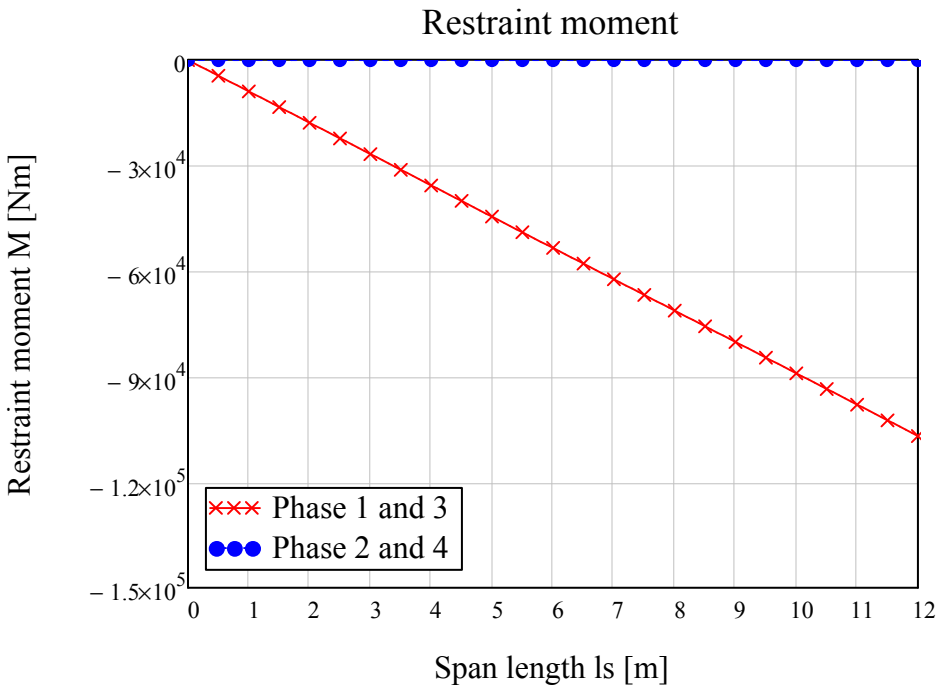

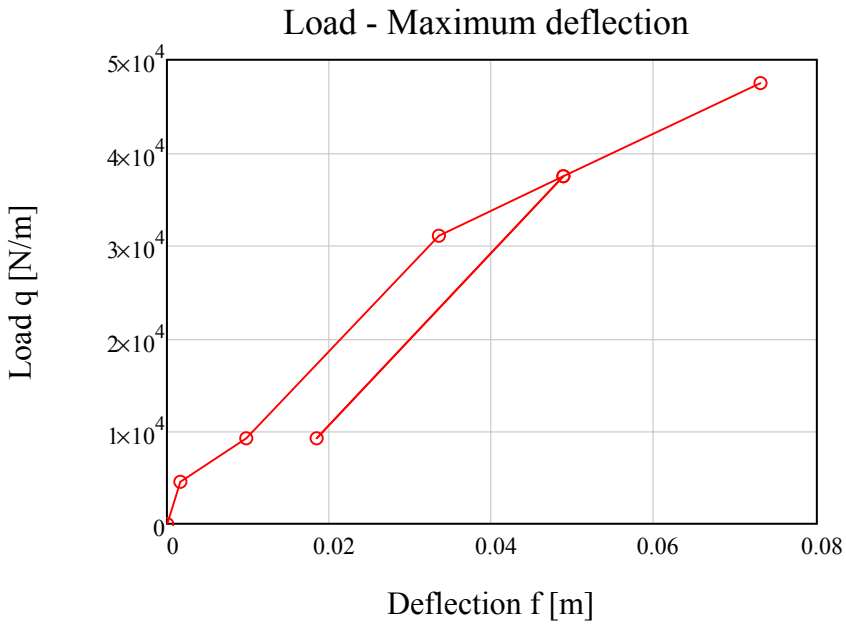

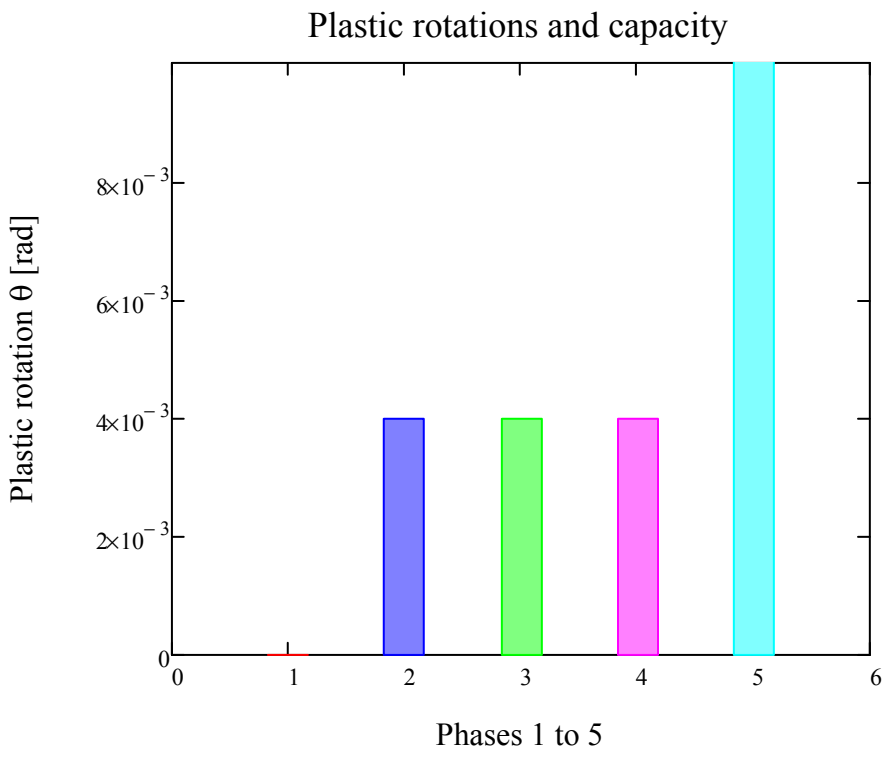
Plastic rotations and capacity
Plastic rotation θ [rad]
8×10⁻³
6×10⁻³
4×10⁻³
2×10⁻³
0
0
1
2
3
4
5
6
Phases 1 to 5

Appendix C: Mean crack spacing and crack band

Linear Elastic Analysis:

Analysis of two span continous beam

$kN := newton \cdot 10^3$ $MN := newton \cdot 10^6$ $MPa := Pa \cdot 10^6$ $GPa := Pa \cdot 10^9$

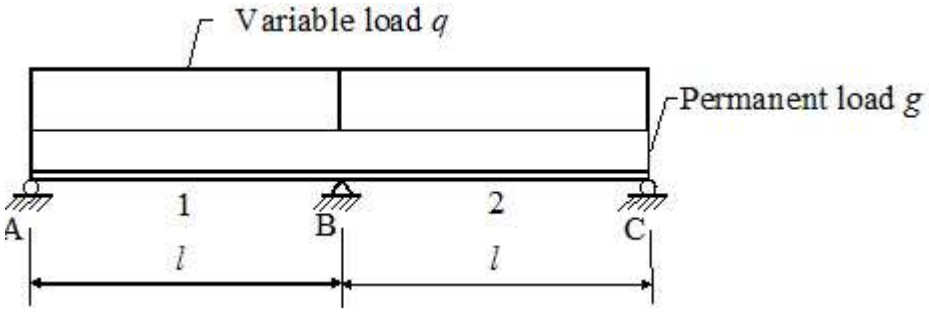

Loads:

Load case: Variable load in both spans

Quasi-permanent load

$q_1 := 9.243 \frac{kN}{m}$

Characteristic load

$q_{1.ch} := 11.59 \frac{kN}{m}$

Overload

$q_2 := 35.43 \frac{kN}{m}$

$l_s := 12m$ Spanlength of beam

$b := 0.30 \cdot m$ Width of cross-section

$h := 0.70 \cdot m$ Height of cross-section

$\varepsilon_{sy} := 2.5 \times 10^{-3}$ Yielding strain of reinforcement

Design moment:

According to Actions on structures and combination of loads

Total load:

$$M_{sup.unreduced} := \frac{(q_1) \cdot l_s^2}{8} = 166.374 \cdot kN \cdot m$$

$$R_1 := \frac{(q_1) \cdot l_s}{2} - \frac{M_{sup.unreduced}}{l_s} = 41.593 \cdot kN$$

$$x_0 := \frac{R_1}{(q_1)} = 4.5\,m$$

$$M_{span} := \frac{9(q_1)\cdot l_s^{\,2}}{128} = 93.585\cdot kN\cdot m$$

Non Linear Analysis:

Analysis of two span continous beam

Maximum crack band width:

$\phi_{eq} := 20mm$

$k_1 := 0.8$ High bond bars

$k_2 := 0.5$ Bending

$k_3 := 3.4$

$k_4 := 0.425$

Reinforcement:

$\phi'_s := 12mm$ $\phi_s := 20mm$ $c'_c := 30mm$ $c_c := 30mm$

$$A'_{s.si} := \left(\frac{\phi'_s}{2}\right)^2\cdot\pi = 113.097\cdot mm^2 \qquad A_{s.si} := \left(\frac{\phi_s}{2}\right)^2\cdot\pi = 314.159\cdot mm^2$$

Section in field:

Assuming 1 layer of reinforcement

$$A_{s1.span} := 6\cdot A_{s.si} \qquad d_{1.span} := h - c_c - \frac{\phi_s}{2} = 0.66\,m$$

$$A'_{s.span} := 2\cdot A'_{s.si} = 2.262\times 10^{-4}\,m^2 \qquad d'_{span} := c'_c + \frac{\phi'_s}{2} = 0.036\,m$$

Section at support:

The section is defined upside down. Assuming 2 layers of reinforcement in the tensile zone and one layer in the compressive zone

$A_{s1.sup} := 6 \cdot A_{s.si}$

$d_{1.sup} := h - c_c - \frac{\phi_s}{2} = 0.66\,m$

$A_{s2.sup} := 0 \cdot A_{s.si}$

$d_{2.sup} := h - c_c - \frac{\phi_s}{2} - 20mm = 0.64\,m$

$A'_{s.sup} := 2 \cdot A'_{s.si}$

$d'_{sup} := c'_c + \frac{\phi'_s}{2} = 0.036\,m$

$d := 0.66m$

$A_{s.sup} := A_{s1.sup}$

$x_{II.span} := 0.187m$

Compressive zone heigth, values from Part 1

$x_{II.support} := 0.187m$

$h_{eff} := \min\left[2.5 \cdot (h - d), \frac{(h - x_{II.support})}{3}, \frac{h}{2}\right] = 0.1\,m$

$2.5 \cdot (h - d) = 0.1\,m$

$\frac{(h - x_{II.support})}{3} = 0.171\,m$

$A_{c.eff} := h_{eff} \cdot b = 0.03 \cdot m^2$

$\rho_{p.eff} := \frac{A_{s.sup}}{A_{c.eff}} = 0.063$

$S_{r.max} := k_3 \cdot 30mm + k_1 \cdot k_2 \cdot k_4 \cdot \frac{\phi_{eq}}{\rho_{p.eff}} = 0.156\,m$

$S_{r.max.max} := \min(S_{r.max}) = 0.156\,m$

$S_{rm} := \frac{S_{r.max.max}}{1.7} = 0.092\,m$

Band crack width

Appendix D: Determination of plastic rotations in the FE-analysis

Temporary overloaded beam

Rotations determination

Node	80	Element length	0,75	Reinforcement element length	0,375

Phase	Load step	Strain ε	Deflection f [m]	Total Rotation Θtot [rad]	Comment	Apparent rotation Θap	Plastic rotation Θpl
	1	0,00002	0,000011	0,0000293			
	2	0,00004	0,000022	0,0000587			
	3	0,00006	0,000033	0,0000880			
	4	0,000084	0,000047	0,0001253			
	5	0,000137	0,000073	0,0001947			
Phase 1	6	0,000232	0,000116	0,0003093		0,0003093	None
	7	0,000363	0,000162	0,0004320			
	8	0,000556	0,000216	0,0005760			
	9	0,000724	0,000267	0,0007120			
	10	0,000883	0,000316	0,0008427			
	11	0,001022	0,00036	0,0009600			
	12	0,001153	0,000402	0,0010720			
	13	0,00128	0,000443	0,0011813			
	14	0,001402	0,000483	0,0012880			
	15	0,001521	0,000522	0,0013920			
	16	0,001642	0,000563	0,0015013			
	17	0,00176	0,000603	0,0016080			
	18	0,001876	0,000642	0,0017120			
	19	0,001988	0,00068	0,0018133			
	20	0,002098	0,000718	0,0019147	Θtot2 - Θpl2	0,0020160	None
	21	0,002212	0,000756	0,0020160	Yielding starts		0,0014160
	22	0,002859	0,001012	0,0026987			
Phase 2	23	0,003535	0,001287	0,0034320	Max, εy at Phase 2		
	24	0,003426	0,00125	0,0033333			
	25	0,003317	0,001213	0,0032347			
	26	0,003209	0,001176	0,0031360			
	27	0,0031	0,001139	0,0030373			
	28	0,002991	0,001102	0,0029387			
	29	0,002882	0,001065	0,0028400			
	30	0,002773	0,001027	0,0027387			
	31	0,002667	0,00099	0,0026400			
	32	0,00256	0,000952	0,0025387			
	33	0,002454	0,000914	0,0024373			
	34	0,002347	0,000876	0,0023360			
	35	0,00224	0,000839	0,0022373			
	36	0,002133	0,000801	0,0021360			
	37	0,002026	0,000764	0,0020373			
	38	0,001919	0,000726	0,0019360			
	39	0,001812	0,000688	0,0018347			
Phase 3	40	0,001705	0,000651	0,0017360	Θap3 = Θap1	0,0003093	0,001427
	41	0,001812	0,000688	0,0018347			
	42	0,00192	0,000726	0,0019360			
	43	0,002028	0,000763	0,0020347			

	44	0,002135	0,000801	0,0021360			
	45	0,002243	0,000838	0,0022347			
	46	0,002351	0,000875	0,0023333			
	47	0,002458	0,000913	0,0024347			
	48	0,002566	0,00095	0,0025333			
	49	0,002673	0,000988	0,0026347			
	50	0,002781	0,001025	0,0027333			
	51	0,002889	0,001063	0,0028347			
	52	0,002996	0,0011	0,0029333			
	53	0,003104	0,001138	0,0030347			
	54	0,003212	0,001175	0,0031333		0,0020160	
	55	0,003319	0,001212	0,0032320	Total plastic rotation for Phase 5		0,0014160
	56	0,003427	0,00125	0,0033333			
Phase 4	57	0,003535	0,001287	0,0034320			
	58	0,003869	0,00142	0,0037867			0,0038373
	59	0,004185	0,001546	0,0041227			
	60	0,004507	0,001674	0,0044640			
	61	0,004828	0,001803	0,0048080			
	62	0,005149	0,001932	0,0051520			
	63	0,005471	0,002062	0,0054987			
Phase 5	64	0,005797	0,002195	0,0058533		0,002016	
Failure	65	0,051278	0,01603	0,0427467			